

Review

A comprehensive review on peptide-bearing biomaterials: From ex situ to in situ self-assembly



Si-Yong Qin^a, Jia-Qi Feng^a, Yin-Jia Cheng^a, Wen-Long Liu^a, Ai-Qing Zhang^a, Lei Wang^{b,*}, Hao Wang^{b,*}, Xian-Zheng Zhang^{c,*}

^a Key Laboratory of Catalysis and Energy Materials Chemistry of Ministry of Education & Hubei Key Laboratory of Catalysis and Materials Science, South-Central Minzu University, Wuhan 430074, PR China

^b CAS Center for Excellence in Nanoscience, CAS Key Laboratory for Biomedical Effects of Nanomaterials and Nanosafety, National Center for Nanoscience and Technology, Beijing 100190, PR China

^c Key Laboratory of Biomedical Polymers of Ministry of Education & Department of Chemistry, Wuhan University, Wuhan 430072, PR China

ARTICLE INFO

Keywords:

Biomaterials
Self-assembling peptide
In situ self-assembly
Disease imaging and therapy
Morphological adaption

ABSTRACT

In the last few decades, we have witnessed the great advances of molecular self-assembly in biomedical applications. Among the building blocks for molecular self-assembly, peptide exhibits several merits such as structural designability, feasible synthetic methodology, and robust self-assembling tendency. Particularly, the excellent biocompatibility, biodegradability and bioactivity bestow peptide-based assemblies with dominant advantages as biological materials. Herein, the state-of-the-art research on peptide self-assembly is reviewed. First, we discuss the representative achievements of *ex situ* peptide self-assembly for cargo delivery carriers, self-deliverable nanomedicines, and tissue engineering materials, which are contributed to the prefabrication of micro/nanoarchitectures in solution. After that, the *in vitro/in vivo* formation of peptide-based nanomaterials is presented, which is nominated as *in situ* peptide self-assembly. The design principle and trigger module of *in situ* peptide self-assembly are summarized, with an emphasis on its biological effects used for disease imaging and therapy. Finally, the combinational modality, *i.e.* integrating *ex situ* construction of peptide self-assemblies for their delivery with *in situ* adaptive transformation of their morphologies to optimize outcomes, is attached, which bridges the gap between *ex situ* and *in situ* peptide self-assembly. We hope this review will provide a panoramic sketch of peptide self-assembly, which is helpful for chemists and material scientists to exploit more biomedical functions from peptide libraries for disease treatments.

1. Introduction

Over the past decades, molecular self-assembly has been widely exploited in various scientific areas such as material science [1–3], catalysis [4–6], energy [7,8], sensor [9], etc. This bottom-up strategy converts individual molecules into a wide variety of sophisticated micro/nanostructures with tailored size and shape. Governed by non-covalent interactions, self-assembly process requires little exogenous energy input, allowing for the facile and green preparation of nanomaterials with superior functions [10]. In particular, the reversibility of non-covalent interactions confers self-assemblies with the ability of responding to external stimuli, making it possible to design smart micro/nanomaterials for biomedical applications. The last few decades have witnessed continuous development of molecular self-assembly, which

provides a feasible path to create functional biomaterials that are applied for medicine, biology and engineering [11–14].

To date, various building blocks such as proteins [15,16], DNA [17–19], and small organic molecules [20–23] have been exploited to fabricate functional biomaterials via molecular self-assembly/aggregation. Among these, peptides and peptide-conjugates (peptide derivatives) have attracted increasing attention due to the intrinsic characteristics that display in three aspects (Fig. 1A). The first is the basic features that include the excellent biocompatibility and biodegradability, structural designability, feasible synthesis, etc [24,25]. The biocompatibility and biodegradability constitute two major criteria for biomaterials, and structural tunability allows for creating countless peptides to precisely encode the structure–function relationship that is often reserved for other molecules. Meanwhile, the peptides can be

* Corresponding authors.

E-mail addresses: wanglei@nanoctr.cn (L. Wang), wanghao@nanoctr.cn (H. Wang), xz-zhang@whu.edu.cn (X.-Z. Zhang).

produced easily in a large scale through the solid-phase peptide synthesis (SPPS). This provides the possibility of further translation into clinical medicines or diagnostic tools. The second is the robust self-assembling ability, facilitating the easy access of supra-architectures. Formation of nanoarchitectures circumvents the low stability and vulnerability to enzyme degradation of individual peptides and prolongs their half-life *in vivo*, accompanying with improved therapeutic effect [26–29]. Furthermore, some new techniques have been established to concurrently synthesize and screen self-assembling peptides to construct nanomaterials [30,31]. The third is the unique biofunctions, which endow peptide-based self-assemblies with dominant advantages in biomedical applications. Various functional peptides such as cell-targeting peptide, cell-penetrating peptide, environment-sensitive peptide, and therapeutic peptide have been discovered/synthesized [25,32], capable of the intelligent and personalized treatments of various diseases.

Since Ghadiri and Zhang respectively used cyclopeptide and linear self-complementary oligopeptide to create nanotubes and macroscopic membrane in the 1990 s [33,34], there has been a flurry of interest in

peptide self-assembly. The earlier research mainly capitalizes on peptide self-assembly strategy to prefabricate nanomaterials in solution for subsequent biomedical applications, which is nominated as *ex situ* peptide self-assembly (Fig. 1B). The resultant peptide nanomaterials benefit the obvious accumulation at lesion sites, showing their great potential for disease treatments. Recently, *in situ* peptide self-assembly has emerged *versus* *ex situ* construction of nanomaterials, which generally occurs *in vitro/in vivo* to generate nano-assemblies [35,36]. Different from the pre-formed nanoparticles, the *in situ* self-assembly starting from individual peptides with small size in living cells can circumvent reticuloendothelial system (RES) trapping. This strategy also allows cargoes to easily pass through blood vessels and deeply penetrate into tumors after their systemic administration [37]. Following this, the subsequent aggregation/assembly induced retention (AIR) effect significantly slows down the diffusion and increases the accumulation and retention of cargoes in the targeted cells/tissues. Specially, the *in situ* formation of nanomaterials usually causes certain biological effects such as destroying the cellular homeostasis, inhibiting the cellular metabolic activity, blocking cell communication, and inducing cell apoptosis, which

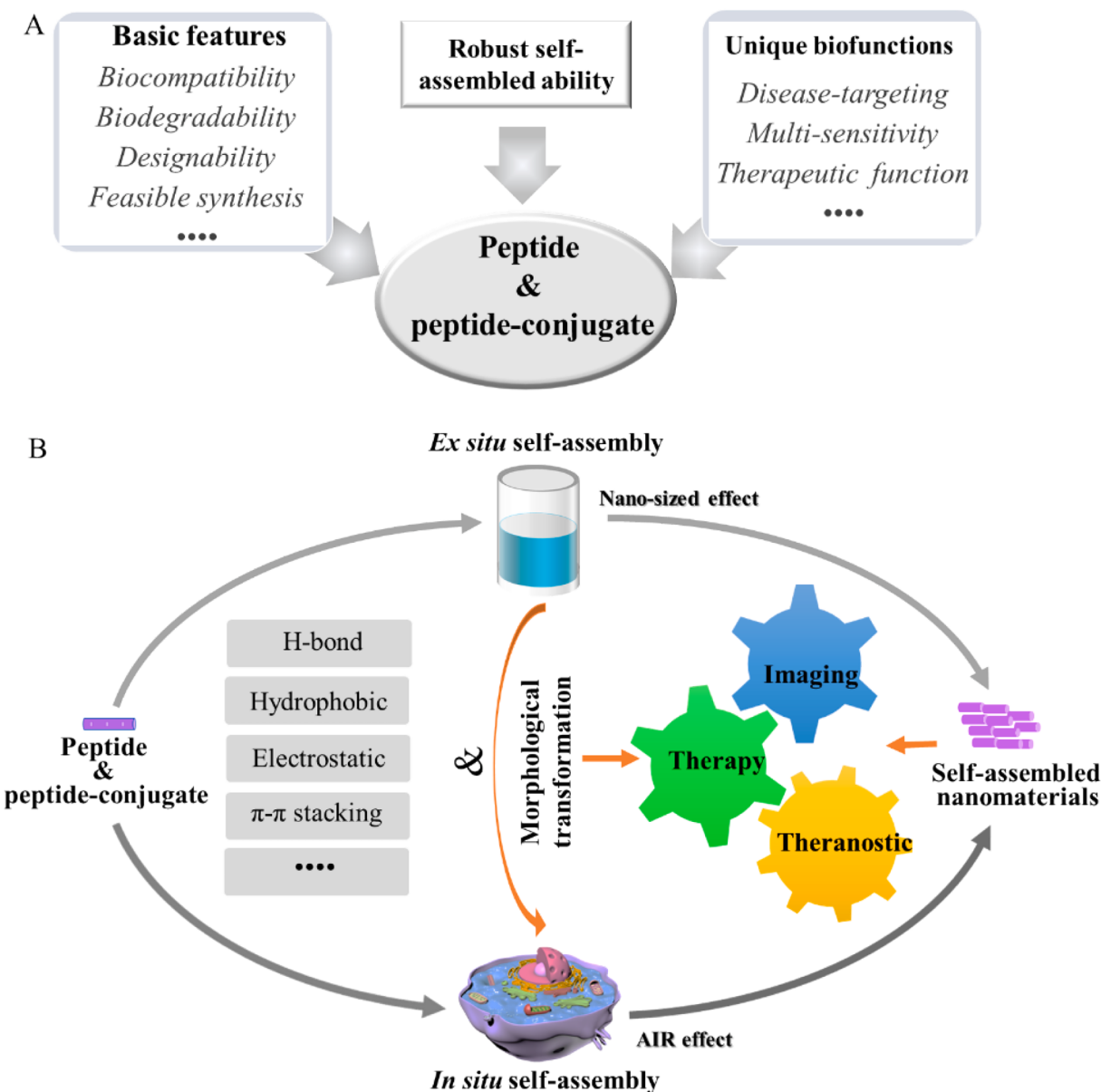


Fig. 1. (A) The merits of peptide and peptide-conjugate as the self-assembling building block to fabricate functional biomaterials. (B) Schematic illustration of peptide-bearing units to construct peptide-based nanomaterials via *Ex situ* and *In situ* peptide self-assembly and their promising applications.

therefore provides a promising methodology for disease diagnosis and targeted therapy [38,39].

Peptide self-assembly has been widely applied as a versatile toolbox to fabricate functional biomaterials for disease treatments, and it has been outlined in various reviews [40–44]. Nevertheless, most reviews focus on the aspects of *ex situ* peptide self-assembly, including peptide structure design, self-assembling strategy, morphology, and relevant functions. Recently, some reviews described the biological effects induced by *in vitro/vivo* peptide self-assembly for disease imaging and therapy [1,45,46]. Nevertheless, most of existing reviews mainly focus on only one modality either *ex situ* or *in situ*, and their applications merely concentrate on a certain field such as drug delivery, regenerative medicine and tissue engineering. It is difficult to systematically learn about peptide self-assembly and extract its overall applications from these published reviews, especially the latest biomedical progress. Therefore, it is necessary to formulate a comprehensive review aiming to teach and guide researchers, in the theory and developing techniques of peptide self-assembly for biomedical applications. On the other hand, *ex situ* self-assembly and *in situ* self-assembly are usually interrelated and sometimes interdependent. It is better to format a review that covers both modalities, especially their combination of *ex situ* and *in situ* self-assembly.

This review systematically introduces the current two modalities of peptide self-assembly, and their applications for disease imaging, therapy and theranostic are highlighted, accordingly. Of note, the integrated modality of combining *ex situ* self-assembly and *in situ* self-assembly is reviewed individually, which involves in re-assembly and morphology transformation to obtain the better outcomes. We explore recent advances in these systems and discuss the relevant applications of peptide self-assemblies.

2. Driving forces of peptide self-assembly

Peptide self-assembly is sophisticated and pertains to an equilibrium thermodynamic process. Self-assembling process is generally

manipulated by various non-covalent interactions including hydrogen bond (H-bond), hydrophobic interaction, π - π stacking, electrostatic interaction, van der Waals force, etc (Fig. 2) [47,48]. For most peptide systems, it is worth pointing out that the cooperativity of multiple interactions rather than relying on one single type is the most efficient pattern to achieve molecular self-assembly. Meanwhile, the kinetic parameters, such as concentration, time, temperature, pH, and counterion, would affect peptide self-assembling process, providing the possibility of further modulating peptide self-assembly via these kinetic factors [49,50]. Herein, we briefly introduce the main non-covalent interactions for peptide self-assembly.

2.1. Hydrogen bond

Peptides, composed of amino acids, contain amide groups in the backbone and carboxyl/amino groups in the side chains, which provide a large number of hydrogen bond-forming sites. Generally, hydrogen bond is essential for peptides to aggregate in aqueous solution. In the typic secondary structures of α -helix and β -sheet conformations for peptide self-assembly, for example, hydrogen bond plays an important role in their formation and stabilization. In 1993, Ghadiri laboratory reported the first cyclopeptide comprised of eight alternative D- and L-amino acid residues, which self-assembled into nanotubes via backbone-backbone hydrogen bond interaction [33]. Meanwhile, hydrogen bond is also applied to tailor the peptide self-assembly in organic solvents. Yan's group reported that the addition of hydrogen-bond forming solvents such as water, ethanol, and DMF would affect the interaction of C = O and N-H in Phe-Phe (FF) dipeptide [51]. The solvent-bridged hydrogen bond promoted a long-range ordered arrangement of FF molecules and resulted in the formation of nanofibers and nanobelts in CH₂Cl₂. Qin and co-workers have emphasized the importance of a trace amount of water to realize the ordered self-assembly of peptide in DMSO, and hydrogen bond played an important role in aligning peptide nanofibers [52].

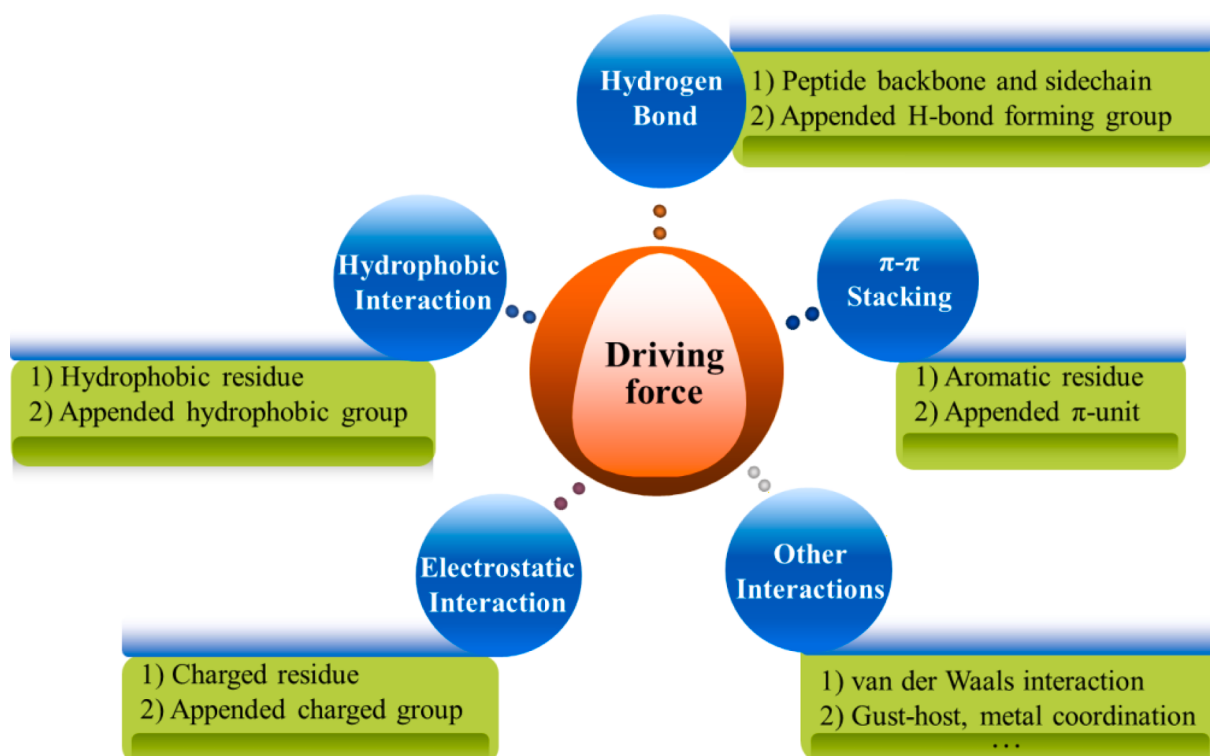


Fig. 2. The main forces to drive peptide self-assembly.

2.2. Hydrophobic interaction

Hydrophobic interaction is a well-documented force to drive the self-assembly of surfactant-like peptide and peptide amphiphile. Surfactant-like peptides consisting of several contiguous hydrophobic amino acids such as Ala, Leu, Val, Phe, etc. and a hydrophilic peptide head could self-assemble into various nanostructures after reaching a certain concentration [53,54]. When dissolved in water, the hydrophobic residues of these peptides are prone to aggregating away from water to minimize their contact with water, and hydrophilic moieties are exposed to the aqueous environment. As a result, the self-assembly of these peptides could be driven by the cooperation of hydrophobic interaction between hydrophobic side chains, hydrogen bond from peptide backbones, etc.

Apart from constructing surfactant-like peptides to capitalize on hydrophobic forces, alkyl tails have been exploited to append to N-terminus, C-terminus and even side chains of peptides to create various peptide amphiphiles for molecular self-assembly. Great strides have been made from the endeavors of Stupp and co-workers, and peptides containing a charged hydrophilic head, a β -sheet forming section, and a hydrophobic alkyl tail were designed [55,56]. In aqueous solution, alkyl tails initiate the hydrophobic collapse, which assist the self-assembly of β -sheet forming domains to form nanostructures. Qin and colleagues employed the hydrophobic interaction to realize ordered self-assembly of peptide amphiphiles in different solvents, and the aligned self-assemblies were applied for the measurement of anisotropic NMR parameters of biomolecules for structural elucidation [57–60].

2.3. π - π stacking

π - π stacking deriving from aromatic rings can also initiate peptide self-assembly. Because of their limited solubility in aqueous solution, aromatic peptides may also contribute to the hydrophobic interaction. Different from the disordered organization for hydrophobic interaction, the aromatic residues are commonly well-organized to participate in π - π stacking. A representative example for π - π stacking guided self-assembly is Phe-Phe, which is derived from the core domain of β -amyloid ($A\beta$) and is critical for amyloid formation [61]. Peptides containing FF segment have been reported to self-assemble into nanostructures with various applications [62,63]. Certainly, tryptophan-bearing peptides and peptide derivatives modified by π -units such as fluorenylmethoxycarbonyl (Fmoc) [64–67], naphthalene [68], pyrene [69], etc. can also be driven by π - π stacking interaction to self-assemble.

2.4. Electrostatic interaction

Interaction between opposite charges is also well-known as one of the driving forces for self-assembly. Peptides containing the oppositely charged residues exhibit the robust electrostatic interaction. Zhang's group pioneered the ionic self-complementary oligopeptides to create macroscopic membrane and functional biomaterials [34,70], in which one of the main driving forces was the Coulombic attraction between opposite charges. In their design, the self-complementary peptides consisted of alternating positively and negatively charged amino acids (e.g. $- + - + - + - +$, $- - + + - + +$, $- - - + + +$, $- - - - + + + +$), which adopted β -sheet or β -strand secondary structures for self-assembly. Apart from the ionic self-complementary oligopeptides, mixing two oppositely charged peptides could also self-assemble into nanofibers via intermolecular electrostatic attraction [71–73].

2.5. Other interactions

Apart from the hydrogen bond, hydrophobic interaction, π - π stacking, and electrostatic interaction mentioned above, van der Waals force is also ubiquitous in self-assembled systems. Comparing with hydrogen bond (~ 10 – 40 kJ mol $^{-1}$) and electrostatic bond (~ 500 kJ mol $^{-1}$), the strength of a typical van der Waals bond is much weaker, with ~ 5 – 10

kJ mol $^{-1}$ [47]. Unlike these double-layer forces, van der Waals forces are usually insensitive to pH and electrolyte concentration, therefore showing a constant attractive presence for peptide self-assembly [74]. Generally, only a few self-assembled systems are mainly governed by van der Waals interaction, but it provides an important contribution to cooperate with other non-covalent interactions and stabilizes the self-assemblies. For example, the van der Waals interaction from alkyl tails in peptide amphiphiles has been shown to be responsible for stabilizing the self-assembled cylindrical nanofibers with other non-covalent interactions [75]. By delicate modification on peptide backbones, some other interactions such as halogen bond [76], host-guest interaction [77,78], cation- π [79], anion- π [80] could also contribute to the peptide self-assembly.

As afore-mentioned, these driving forces are generally interrelated and could not be picked out to separately discuss them. During the self-assembly, moreover, peptides would interact with solvents, and their interaction should also be taken into account. Computer simulation technology such as atomistic molecular dynamics [81] and coarse-grained molecular dynamics [82] may be introduced to further reveal the driving forces of peptide self-assembly.

3. Ex situ peptide self-assembly

3.1. Self-assembled morphology

In order to respond to the sophisticated biological systems, biomaterials should be harnessed with adaptable features. For instance, the lesion sites such as tumor tissues and bacteria-infected sites are observed to possess enhanced permeability and retention (EPR) effect, which involves that nanoparticles with suitable sizes can permeate into tumor tissues through the leaky vasculature and retain for a longer period of time than that of individual small molecules [83]. Along this line, therapeutic agents can be administrated in the nanoscale formulation for effective accumulation at where needed. In recent years, EPR effect has been debated, due to its varied contributions in different tumors. Some researchers proposed a new mechanism of endothelial transcytosis for the entry of nanoparticles into tumors [84]. Notably, in this review we would mainly focus on the preferred accumulating performance of nanoscale architectures in tumors, instead of the mechanism underlying the tumorous accumulation of nanomedicines. Anyway, *ex situ* peptide self-assembly has been regarded as one of the most promising options to create stable nanoarchitectures for cancer research.

To achieve an anticipated supramolecular nanostructure, the peptide structure should be rationally designed according to several critical elements, such as structural amphiphilicity and chemical complementarity. The relationship between peptide structure and the self-assembled morphology can be qualitatively analyzed through the theory in surfactant field [85], according to the formula:

$$P = (V_c/l_c A_0)$$

where V_c and l_c are the volume and length of tail-group, and A_0 is the area of head-group. As a rule of thumb, the amphiphilic peptides aggregate into micelles when the P value lies between $1/3$ and $1/2$, and whose shapes vary gradually from spherical to cylindrical when P is close to $1/2$. For the value of P changing from $1/2$ to 1 , the gradual variation from a cylindrical micelle to a planar bilayer would occur.

By delicate molecular design and encoding peptide sequences, various nanoarchitectures such as nanofiber [86], nanotube [87], nanomicelle [88], nanoribbon [89,90] have been constructed, which can be potentially exploited as cargo delivery carriers, self-deliverable nanomedicines, and tissue engineering materials (Fig. 3). Attributing to the molecular self-assembly, furthermore, aggregated peptides present dense recognition units for multivalent interactions with targeted cells, leading to the boosted biofunctions. Besides, different biofunctions can also be conveniently achieved in one nano-system through the

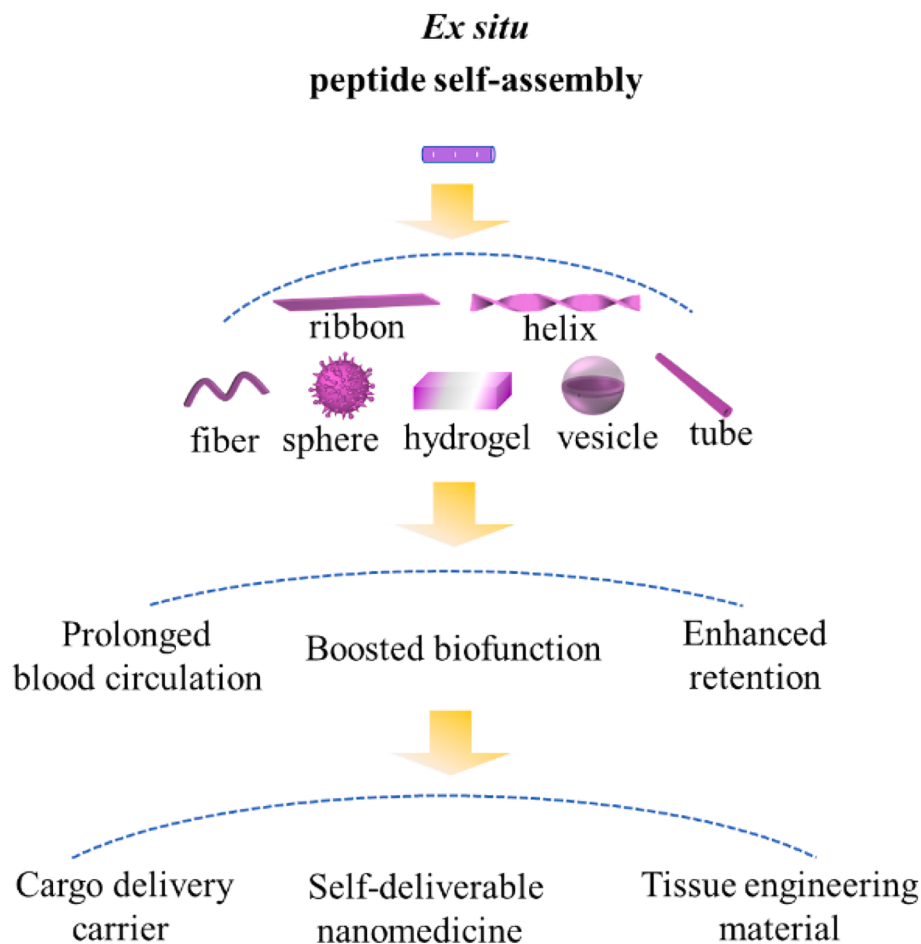


Fig. 3. *Ex situ* peptide self-assembly to construct various nanoarchitectures with promising advantages for different biomedical applications.

supramolecular strategy.

3.2. Applications of *ex situ* self-assembled peptides

3.2.1. Delivering cargo

A main challenge of current agents for disease treatments is the delivering pattern, which determines the drug bioavailability, the quality of imaging/therapy, and even causes side effects. In this respect, intelligent peptide nanocarriers are widely employed to circumvent off-target toxicity and improve the overall efficacy [91]. Through the precise control over peptide self-assembly process, various agents such as imaging/therapeutic drug [92,93], and gene [94,95] can be integrated into smart nanoplates for targeted delivery/on-demand release, which have been reviewed detailedly. In this context, the typical applications of self-assembled peptide nanostructures as nanocarriers to deliver cargoes would be discussed.

3.2.1.1. Chemotherapeutic drug. To address the issues of chemotherapeutic drugs such as poor solubility, non-selective distribution and rapid excretion, nanocarriers self-assembled from peptides and peptide-conjugates have been proposed. To ensure the effective loading on hydrophobic drugs, peptides are generally designed with amphiphilic features. Amphiphilic peptides consisting of a hydrophilic head (composed of Lys, Arg, Asp, Glu, etc.) and a hydrophobic tail (composed of Ala, Leu, Val, Phe, etc.) are the common self-assembling units. Driven by hydrophobic interaction in solution, the hydrophobic segments form a hydrophobic domain encapsulating insoluble drugs. Various amphiphilic peptides such as A₆K₂ [96], and L₆K₄ [97] have been exploited to construct shape-tailored nanoparticles for antitumor drug delivery. In

view of the ionizable feature of amino/carboxyl groups, self-assembled peptide carriers usually exhibit the pH-sensitive drug release behavior [98].

To replenish molecular structures of amphiphilic peptides, several hydrophobic species such as aliphatic tails [99,100], and aromatic groups [101] were employed to cap the hydrophilic peptide heads to investigate their effectiveness of drug delivery. An earlier example reported by Stupp's group showed that self-assembled peptide nanofibers could effectively encapsulate camptothecin (CPT), which improved the drug's solubility by more than 50-fold, resulting in improved antitumor activity *in vitro* and *in vivo* [102]. Recently, bioactive agents such as 1,8-dihydroxy-3-carboxy anthraquinone (Rhein) [103], naproxen [104], and tyroservatide [105] have been connected to peptide chains to construct the peptide-drug conjugates, which will be reviewed in the following section of self-deliverable nanomedicine.

To improve the delivery efficiency and achieve the on-demand drug release, functional peptides such as cancer targeting sequence of arginine-glycine-aspartic acid (RGD) [106], cell penetrating peptide (CPP) [107], mitochondria-targeting group [108], and enzyme-sensitive group [109] have been incorporated into peptide backbones. Zhang's group designed an amphiphilic peptide of V₆K₂GRGDS for anti-tumorous doxorubicin (DOX) delivery [99]. The tumor-targeting sequence of RGD enhanced the drug delivery into integrin over-expressed cancer cells. In acidic cancer cells, the electrostatic repulsion from protonated K residue mediated pH-responsive DOX release for cancer cell killing. Zhao, Qin and Nie, *et al.* used nine arginine (R₉) residues as CPP to improve the cell-penetrating efficiency of DOX (Fig. 4A) [110]. In their design, cholesterol was introduced as the hydrophobic tail to initiate peptide self-assembly and improve the

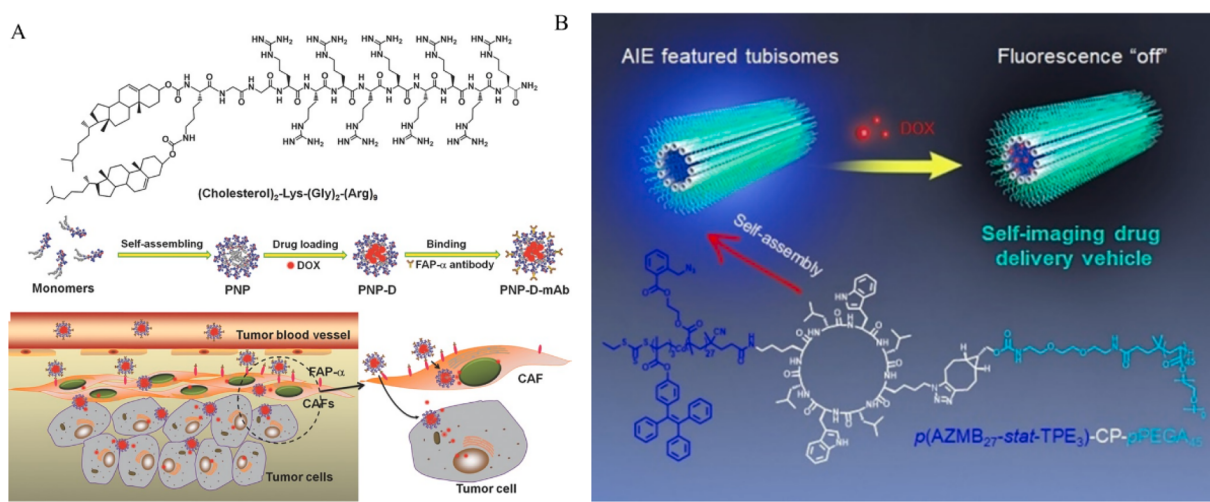


Fig. 4. (A) The molecular structure of (Cholesterol)₂-KG₂R₉ and its proposed self-assembled process to load drug and achieve fibroblast-targeted drug delivery. Reproduced with permission from Ref. [110]. Copyright 2015, Wiley-VCH. (B) Structure of cyclic peptide-based bottlebrush polymer and the schematic illustration of self-assemblies. The fluorescent “On-Off” change mediated by DOX loading was illustrated. Reproduced with permission from Ref. [113]. Copyright 2022, Wiley-VCH.

membrane permeability. To address the nonspecific phagocytosis of positive self-assemblies by RES, mouse monoclonal antibody (mAb) molecule was anchored onto the surface of self-assemblies via electrostatic interaction. At the tumor tissue, mAb-modified nanomedicines targeted human fibroblast activation protein- α (FAP- α , a transmembrane protein overexpressed by cancer-associated fibroblasts, CAFs), accompanying with the detachment of mAb and CPP exposure. Due to the increased drug endocytosis coordinated by CPP and cholesterol, the nanocarrier overcame the tissue barrier and ameliorated the antitumor efficacy. To realize the targeted drug delivery and tumor microenvironment-regulated release, a versatile peptide, consisting of RGD for cancer-targeting, Cys-s-s-Cys that is sensitive to reducing agents, Pro-Val-Gly-Leu-Ile-Gly corresponding to the substrate of matrix metallopeptidase 2 (MMP-2), Ser-Glu-Glu-Asp-Pro for pH-sensitivity, and 41-residue peptide with an α -helix conformation, was developed

for effective delivery of antitumor drug and multi-modal control release [111]. After RGD mediated targeting to tumor cells, the low pH, high levels of DTT and MMP-2 in tumor microenvironment collaboratively stimulated drug release from self-assembled spherical nanoparticles, which dramatically enhanced antitumor effects and reduced the systemic toxicity. To investigate whether enzymes targeted dissociated peptide individuals or nanoarchitectures for the enzyme-induced degradation of self-assemblies, cathepsin B holding both exopeptidase and endopeptidase activities was exploited to degrade the self-assembled peptide nanofibers [112]. Results showed that the enzyme directly acted on the nanofibers instead of dissociated monomers from the self-assemblies. The findings may provide the understanding on designing enzyme-sensitive drug delivery systems.

To monitor the drug release process in living cells, a cyclic peptide-based bottlebrush polymer containing an aggregation-induced emission

Table 1
Summary of peptide-based drug carriers for cancer treatments.

Sequence	Morphology	Cargo	Feature	Applications	Refs
A ₆ K ₂	Vesicle	DOX	Enzyme-triggered morphology-change and drug release	Selectively inhibiting tumor cell growth and showing antibacterial activity	[96]
L ₆ K ₄	Spherical nanoparticle	DOX	Cancer cell-targeted drug delivery and pH-sensitive release	Improved antitumor property comparing with that of free DOX	[97]
V ₆ K ₂ GRGDS	Micelle	DOX	RGD-mediated tumor-targeting and pH- responsive drug release	Specifically delivering DOX into cancerous HeLa cells	[99]
C ₁₈ H ₃₇ -H ₅ R ₇ RGDS	Micelle	Cur	Improved drug aqueous solubility; pH-sensitive property and RGD-mediated tumor targeting	Much higher cancer cell inhibition and lower cytotoxicity towards normal cells than free Cur	[100]
Pyrene-FFRGD	Nanofiber	Cisplatin	RGD-mediated targeting delivery and aggregation-caused-quenching (ACQ)	Selectively delivering and tracking cisplatin in ovarian cancer cell	[101]
C ₁₅ H ₃₁ -A ₄ G ₃ E ₃	Nanofiber	CPT	Improving the CPT aqueous solubility by more than 50-fold	Improved antitumor activity comparing with that of free CPT without carrier	[102]
Rhein-GFFYERGD	Nanofiber	Cisplatin	Dual anticancer drug-based nanomedicine with significant nuclear accumulation property	Efficient cancer cell and tumor inhibition effect	[103]
Npx-D ^D F ^D E ^D Y (^D F: ^D -Phe, ^D E: ^D -Glu, ^D Y: ^D -Tyr) FKFEYYSV	Hydrogel/ Nanofiber Nanofiber	Cisplatin HCPT	Co-assembling with cisplatin to form hydrogel to boost its radiosensitization effect Co-assembling with HCPT to form hydrogel to increasing drug stability and affording sustained release	Enhanced tumor inhibition Better anti-cancer efficacy than that of HCPT	[104] [105]
K(dodecanoic acid) ₂ K (rhodamine)GRGDS	Micelle	CPT	Rhodamine improving the drug loading, self-assembly and fluorescence imaging	Enhanced cytotoxicity in cancer cells in comparing with free CPT and CPT-loaded micelle	[106]
PpIX-KrFxrFxr-PEG ₈ (r: ^D -Arg, Fx: L-cyclohexylalanine)	Micelle	PpIX	Mitochondria and plasma membrane dual-targeting	Single-agent synergistic PDT in mitochondria and plasma membrane	[108]
Nap-FFGPLGLARKRK	Nanofiber	DOX	Cancer-overexpressed MMP7-sensitive drug release	Cancer-targeted drug delivery and selective cancer cell killing	[109]

(AIE) molecule was developed, which self-assembled into cylindrical aggregates with AIE fluorescence (Fig. 4B) [113]. After loading DOX, the fluorescence of aggregates was quenched due to the energy transfer relay (ETR) effect, showing the fluorescence “off” state. Once the DOX release from cylindrical aggregates, the silenced fluorescence was unlocked and realized the in-situ imaging of drug release. Collectively, we summarize the common peptide-based drug carriers for cancer treatments, including the peptide sequence, self-assembled morphology, therapeutic agents, and release mechanism (Table 1).

Supramolecular hydrogels self-assembled from peptides and their derivatives represent another class of highly promising drug delivery systems. Besides the features of common hydrogels with good compatibility and high drug loading capability, peptide hydrogels display the control drug release profiles due to their adjustable mesh size of entangled network, which can be achieved through simply changing the peptide concentration and sequence structure, or introducing physiological stimuli [114,115]. Moreover, the shear thinning feature and appropriate mechanical properties of noncovalent peptide hydrogels are suitable for the injectable therapy, enabling the seamless filling of irregular wound sites left by tumor resection. A plethora of peptide-based hydrogels have been developed to deliver both water-soluble agents and water-insoluble drugs. In one example, MAX8 with the sequence of VKVKVKVVDPPTKVEVKV-NH2 self-assembled into injectable hydrogel to load curcumin for drug delivery [116]. *In vitro* experiments indicated that trapping curcumin within self-assembled fibril network did not impair its bioactivity. Through adjusting the peptide concentration, meanwhile, the release rate and consequent therapeutic efficacy have been conveniently modulated. Zhang’s group developed a self-assembling peptide hydrogel from Fmoc-FFRGDF to deliver antiproliferative 5-fluorouracil (5-Fu) to inhibit the post-operative scar formation [117]. In the filtering surgery of rabbit eye model, the slow release of 5-Fu from hydrogel efficiently inhibited the postoperative inflammation and scleral flap fibrosis. Due to the localized and controlled release of drug from hydrogel, side effects to surrounding ocular tissues have been effectively relieved. Cui’s group reported a peptide bolaamphiphile, in which a hydrophilic peptide segment coupling with an MMP cleavable sequence of PLGVR was proposed as the bridge to connect different hydrophobic groups as two terminals. The yielded peptide self-assembled into supramolecular filament hydrogel, with the PLGVR exposure on the surface to respond to the overexpressed MMP-2. Using anticancer drugs as the hydrophobic terminals, cancer cell-tailored hydrogel degradation and drug release were achievable due to the matched MMP level [118].

3.2.1.2. Gene. Functional DNA and RNA, capable of downregulating/replacing the disorder gene or silencing the expression of unwanted gene, have been widely introduced to cure various diseases, especially human cancers. Nevertheless, the naked DNA/RNA is generally subjected to the quick degradation by nucleases in plasma. The poor cellular targeting and endosome escaping abilities also pose the challenge of their effective delivery in body [119]. Due to this, positively charged peptide self-assemblies have been proposed to condense negative genes. Comparing with lysine, arginine may be more effective to construct gene carriers, because it might improve the interaction of carriers with nucleic acids and negative cell membranes [120]. What’s more, the functional peptides such as the cancer-targeting sequence and nuclear localization sequence bring remarkable advantages for cellular gene delivery. In an early stage, Zhang’s group developed a series of peptide-based gene vectors [121,122]. To optimize the cellular uptake and potentiate the targeted localization of gene in nucleus, VKRKKKP sequence with nuclear localization ability was integrated with the CPP of R₈ to construct the peptide-based gene nanocarrier [123]. This vector exhibited good biocompatibility and excellent transfection activity of up to 4.33×10^9 RLU/mg protein. To further improve the transfection efficacy, they developed a strategy of oxidative polymerization to obtain

disulfide-linked polypeptides for gene delivery. These self-assembled vectors facilitated glutathione (GSH)-induced intracellular gene release and alleviated the polymer degradation-induced cytotoxicity. For example, CPKKKRKVC (CNLSC) was cross-linked with CRRRRRRRRC (CR₈C) to condense plasmid DNA for nuclear import [124]. The incorporation of NLS sequence could decrease the cytotoxicity of vectors and increase their nuclear targeting capability. PolyR₈-NLS (CR₈C: CNLSC = 1:2:1) at a weight ratio of 40 (polypeptide/pGL-3) showed very high transfection efficiency, comparable to linear poly(ethylene imine) (jetPEITM, Polyplus Transfection™).

To efficiently deliver and real-time track therapeutic genes, Xia’s group designed a peptide-AIEgen conjugate to carry and visually monitor the agent delivery into nucleus (Fig. 5A) [125]. The functional peptide was comprised of RGD/DGR for tumor cell targeting, KRRRR motif for gene nuclear localization, and a CPP sequence of RRRR. Capping the C-terminus of peptide with an AIE molecule enhanced the hydrophobicity to initiate self-assembly for gene loading. It also showed the fluorescent feature, facilitating the real-time tracking of nucleus-selective delivery process. As a result of these functions, this nano-system displayed a favorable anti-tumor effect *in vivo*.

In contrast to the common strategy of incorporating hydrophobic lipophilic tails into the terminus of peptides, Li and co-workers found that modifying the side chains of tetralysine with guanidinocarbonylpyrrole (GCP) could effectively enhance the transfection efficacy [126]. The yielded peptide analogue exhibited negligible cytotoxicity, but its transfection efficacy was even better than that of commercial polyethylenimine (PEI). The improved transfection efficacy was attributed to the specific binding interactions between GCP group and DNA/cell membrane. Along this line, they further incorporated the GCP unit into the side chain of a cyclic peptide, and self-assembled nanofibers with positive charge were able to shuttle DNA into cells for gene therapy [127]. Wu and co-workers employed the molecular self-assembly strategy to improve the recognition of phage peptide to bind with targets to potentiate the therapeutic outcomes [128]. The self-assembled brain-specific phage-derived peptide of GYRPVHNIRGHWAPG could target the cerebral endothelial cells, pass through the blood-brain-barrier and thus reach neurons and microglial cells. When used as a carrier, it has demonstrated to be effective and safe for intravenous delivery of the NLC-β-secretase 1 small interfering RNA (siRNA), which down-regulated the BACE1 in the brain without systemic toxicity and inflammation. Very recently, Yang and colleagues connected cholesterol to a transferrin receptor (TfR)-targeted HAIYPRH (T7) peptide to develop a self-assembling gene delivery system for glioma therapy via intranasal administration (Fig. 5B). Self-assembling nanoparticles delivered slit2 siRNA into the lesion site through an olfactory bulb (OB) route and effectively entered glioma cells via the caveolin- and transferrin-dependent pathway (Fig. 5C, D). In the meanwhile, T7-cholesterol (T7-C) acted as an immune adjuvant to mature DCs (Fig. 5E) and loaded slit2 siRNA polarized macrophages from M2 subtype to M1 subtype (Fig. 5F, G). The combination of T7-C and slit2 siRNA increased the proportion of effector T cells for glioma immunotherapy [129].

3.2.1.3. Photosensitizer. Photodynamic therapy (PDT), relying on the cytotoxic reactive oxygen species (ROS) generated by the combination of light source, photosensitizer (PS) and molecular oxygen to kill tumor cells, has attracted extensive research attention in recent years. Because of the minimal invasion, PDT has been used to treat many diseases, such as malignant tumors and inflammatory infections. In the cases of similar drawbacks with chemotherapeutic drugs such as poor solubility and low bioavailability, PSs are also optimized with the employment of carriers to realize the targeted homing and tissue penetration. Peptide-based nanocarriers have been developed as means to overcome delivery barriers and enhance release response at lesion sites, followed by the activation by certain light irradiation to sensitize oxygen to generate ROS.

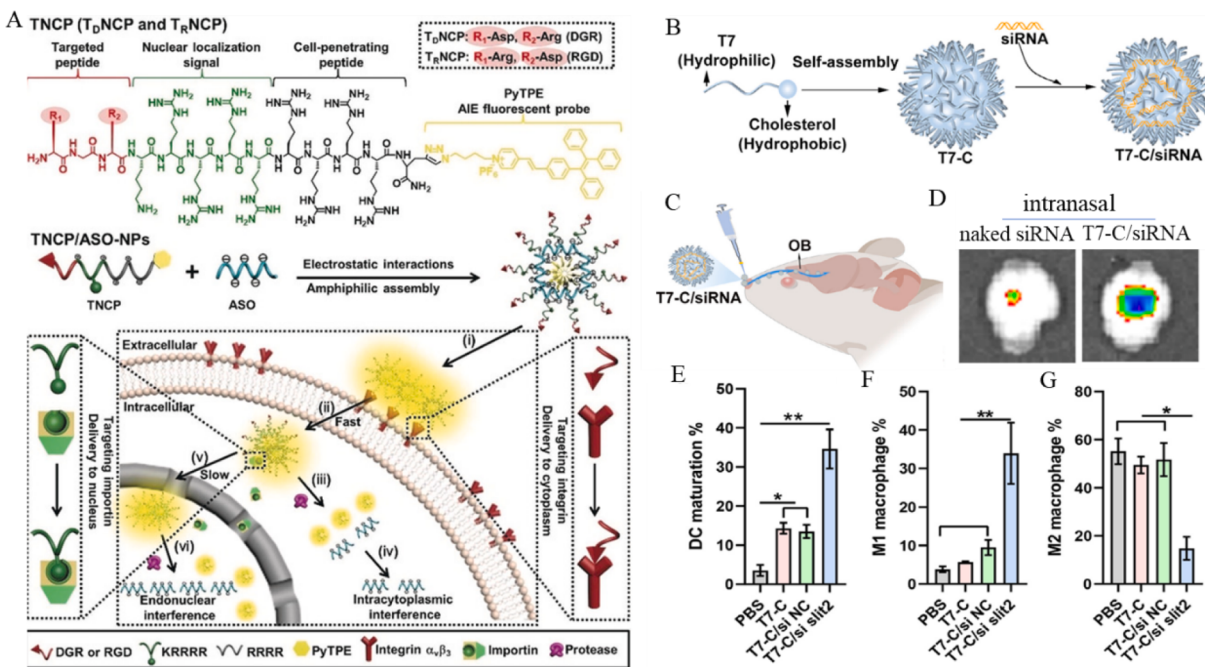


Fig. 5. (A) Structure and function of the peptide-based gene carrier and its co-assembly with single-stranded DNA oligonucleotide (ASO) into nanoparticle for gene delivery. (i) RGD/DGR-mediated targeting to integrin $\alpha_v\beta_3$ on cell membrane; (ii) fast endocytosis into the cytoplasm; (iii) protease-induced partial degradation of complex and ASO release in cytoplasm; (iv) released ASO for intracytoplasmic interference; (v) targeting importin for selective delivery into the nucleus; (vi) protease-induced most release of ASO in the nucleus to elicit endonuclear interference. Reproduced with permission from Ref. [125]. Copyright 2019, Wiley-VCH. (B) Scheme of T7-cholesterol self-assembling into nanoparticle to load siRNA by electrostatic actions. (C) T7-C/siRNA reaching the mouse brain via an OB route. (D) Brain image after the 2 h of intranasal delivery of T7-C/Cy5-siRNA. (E) The percentage of mature dendritic cells (DCs) treated by different modalities. (F, G) The percentage of M1 macrophages and M2 macrophages (detected by flow cytometry) in the tumor microenvironment treated by different modalities. Adapted with permission from Ref. [129]. Copyright 2023 Elsevier.

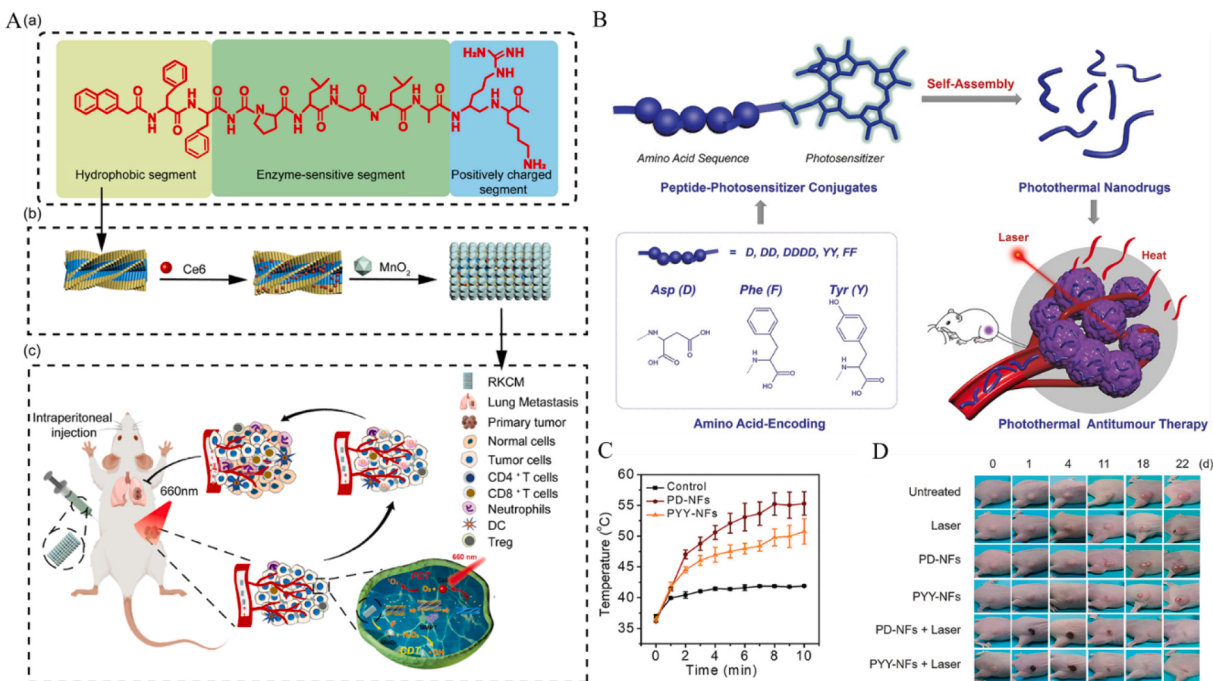


Fig. 6. (A) Self-assembled peptide nanoplatform capable of alleviating tumor hypoxia for highly efficient PDT. (a) Chemical structure of enzyme-sensitive peptide; (b) Schematic illustration of self-assembled peptide fibrils for Ce6 loading and MnO_2 mineralization; (c) In vivo cancer therapeutics mediated by nanocomposite. Reproduced with permission from Ref. [131]. Copyright 2023, American Chemical Society. (B) Illustration of constructing self-assembled photothermal nanodrugs through encoding the type and amount of amino-acid within peptide-photosensitizer conjugates for PTT. (C) Temperature curves of tumor sites treated by different regimens during irradiation ($n = 3$). (D) Photos of mice with different treatments during 22 d observation. Adapted with permission from Ref. [137]. Copyright 2022, Wiley-VCH.

Zhang's group constructed a self-assembled tetra-tail amphiphilic peptide encompassing RGD ligand and cell penetrating R₈ peptide for the encapsulation of porphyrin [130]. The porphyrin-loaded micelle exhibited high phototoxicity towards cancer cells due to the RGD-mediated cancer recognition and R₈-guided membrane penetration. To address the issue that hypoxia in tumor would impair the PDT efficacy, a peptide/Ce6/MnO₂ nanocomposite (RKCM) was fabricated to alleviate tumor hypoxia, so as to ameliorate PDT efficacy (Fig. 6A) [131]. Self-assembled Nap-FFGPLGLARKRK (RK) fibrils encapsulated chlorin e6 (Ce6) in their inner cores, and MnO₂ was mineralized on the surface of fibrils to obtain the nanocomposites. On one hand, Ce6 generated ¹O₂ for PDT under near infrared (NIR) laser irradiation, and MnO₂ catalyzed H₂O₂ to produce O₂, which alleviated hypoxia and potentiated PDT. On the other hand, RKCM released Mn²⁺ ion and catalyzed Fenton-like reaction for CDT. Moreover, RKCM/laser treatment remolded the immunosuppressive tumor microenvironment to recruit more immune cells, which blocked the occurrence of tumor metastasis.

To simplify the complex constructing process of PS carriers, Yan's group proposed a co-assembling strategy to load PSs. Short peptides or an amphiphilic amino acid were introduced and co-assembled with PSs for their delivery [132,133]. The short peptides can be automatically accomplished by the SPPS technique and the amino acid is commercially available, which circumvent the complex constructing process. The formed nanodrugs displayed favorable features, such as tunable nano-size, high loading efficiency, preferable cellular uptake and bio-distribution, as well as on-demand drug release. They further found that a cocktail of small peptide, PS and metal ion could self-assemble into metallo-nanodrugs [134], which exhibited the robust blood circulation and rapidly disassociated in tumor microenvironments by low pH or high GSH. The control drug release guaranteed the efficient and targeted photodynamic ablation towards tumors without side effects. Yu, Mao, Huang, *et al.* combined the host-guest recognition with peptide self-assembly to construct functional nanocarriers for PDT [135]. The recognition between pillar[5]arene bearing ten tri(ethyleneoxide) groups and 4-methylpyridine modified by a peptide was employed to adjust the self-assembled morphologies. 11-Bromo-alkyl group capped G₇CCERGDS peptide self-assembled into fibers in the absence of pillar[5]arene. Once the bromine atom was substituted by 4-methylpyridine, the generated 4-methylpyridine-peptide could act as a guest unit for pillar[5]arene. The yielded host/guest complex self-assembled into sheet-like aggregates. On the other hand, pillar[5]arene bearing ten tri(ethyleneoxide) groups showed thermo-responsive. When the temperature raised to 45 °C, the hydrophilic pillar[5]arene containing ten tri(ethyleneoxide) groups became hydrophobic, and the host/guest complex self-assembled into nanoparticles for drug delivery. Moreover, the oxidized cross-linking of cysteine units on peptide side chain improved the stability of nanomedicine, and endowed it with GSH-sensitive responsiveness. The inherent targeting of peptide and supramolecular strategy greatly boosted the PDT efficiency.

Photothermal therapy (PTT) is an alternative photo-treatment modality. It is associated with hyperthermia generated by photothermal agents under light irradiation. Integrating peptide self-assembly into PTT systems offers the opportunity to engineer the therapeutic outcomes. For example, Yan's group fabricated porphyrin-bearing photothermal nanodots that were formed by peptide-modulated self-assembly [136]. The peptide unit improved the aqueous stability of nanodots and provided a spatial barrier to inhibit their further growth. The formation of stable nanodots totally inhibited the generation of ¹O₂ and fluorescence emission, which therefore led to a high photothermal conversion efficiency for PTT. They further reported an amino acid encoding design to construct supramolecular photothermal nanodrugs for PTT (Fig. 6B) [137]. It was found that the type and amount of amino acid within peptides dominated the self-assembled morphology, stability, energy-conversion pattern, which further determined the therapeutic outcomes. Because of the improved structural stability, self-assembled pheophorbide a-Asp (PD-NFs) and pheophorbide a-Tyr-Tyr (PYY-NFs)

exhibited high photothermal conversion in biological environments (Fig. 6C), which therefore effectively ablated tumors, without tumor recurrence and detectable side effects (Fig. 6D).

3.2.1.4. Multiple therapeutic agents. In recent years, research focus has gradually shifted from monotherapy to combinational therapy to fight cancers, because combinational regimen can sensitize cancer cell to drug, modulate different signaling pathways to induce cell apoptosis, reduce individual drug dose to reduce adverse side effects, and overcome the heterogeneity and multidrug resistance (MDR) of cancers [138,139]. Self-assembled peptides and their derivatives have been proposed to co-deliver different agents for the combinational therapy or synergistic therapy. Zhang's group developed an amphiphilic peptide of (Fmoc)₂KH₇-TAT for drug and gene co-delivery [140]. The self-assembled micelle as a drug carrier exhibited faster DOX release rate at pH 5.0 than that at physiological condition, exerting the tumoricidity triggered drug release. As a gene vector, nano-peptide effectively mediated the transfection of pGL-3 plasmid. The combinational modality resulted in effective tumor inhibition both *in vitro* and *in vivo*. They further used a pH- and enzyme-sensitive peptide derivative of Fmoc-ADDA-H₈R₈-PLGVR-PEG₈ to co-deliver protoporphyrin IX (PpIX) and plasmid DNA (Fig. 7A) [141]. The PLGVR peptide sequence endowed self-assembled nanoparticles with MMP-2 sensitivity, which detached PEG₈ shell and exposed the cationic peptide for drug endocytosis into MMP-2 rich tumor cells. According to the flow cytometry, double-positive cells account for a substantial part of total cells (40.3%), suggesting the effective co-delivery of PpIX and DNA into same cells (Fig. 7B). To achieve the synergism between chemotherapy and gene therapy, this system was exposed to the light irradiation for two times. Before stimulating the phototoxicity of PpIX, a short-time light irradiation was provided to generate ROS to disrupt the endo/lysosomal membranes due to photochemical internalization (PCI) effect. This enhanced the endosomal escape of peptide/PpIX/DNA complex and improved DNA expression. After the gene transfection, a long-time irradiation evoked the phototoxicity of PpIX to achieve PDT (Fig. 7C). To circumvent the drawbacks that co-delivery of multiple agents might impair the bioactivity of each individual agent due to their different physicochemical properties, Lou and colleagues reported an enzyme-sensitive peptide-AIEgen conjugate (FC-PyTPA) to load siRNA, which co-assembled into FCsiRNA-PyTPA complex (Fig. 7D) [142]. After reaching tumor tissue, FCsiRNA-PyTPA was cleaved by extracellular MMP-2 into two parts of FCsiRNA and PyTPA. The former component crossed the cell membrane and suffered from the hydrolysis by cathepsin B (CB) to release self-assembled precursor and Bcl-2 siRNA. The precursor self-assembled into nanofibers and destroyed the lysosomal structure. The latter component of PyTPA entered cells through caveolae-mediated endocytosis to produce ROS under white light irradiation. Attributed to the one-dividing-into-two pattern, the internalization efficiency of each agent was elevated greatly, which further played the individual functions to synergistically inhibit tumor growth. They further developed a caged peptide-AIEgen probe that self-assembled with miR-140 to regulate tumor cell death [143]. In the presence of Cathepsin B (CB), the formed nanoparticle released the cargos of GO203 peptide, miR-140 and PyTPA. The GO203 peptide targeted mucin 1 (MUC1) and downregulated the PD-L1 expression. miR-140 targeted and degraded PD-L1 mRNA for deep downregulation in tumor cells. Meanwhile, PyTPA-mediated PDT induced immunogenic death and activated T cells for effective immunotherapy.

The unique microstructures within hydrogels enable the easy encapsulation of different agents and subsequent control release, so peptide hydrogels show great potential in combinational therapy, especially for some certain tumors. For example, head and neck squamous cell carcinomas (HNSCCs) are common malignant tumors, and their recurrence and poor clinical response require the targeted or combined strategies to potentiate the therapeutic outcomes and improve

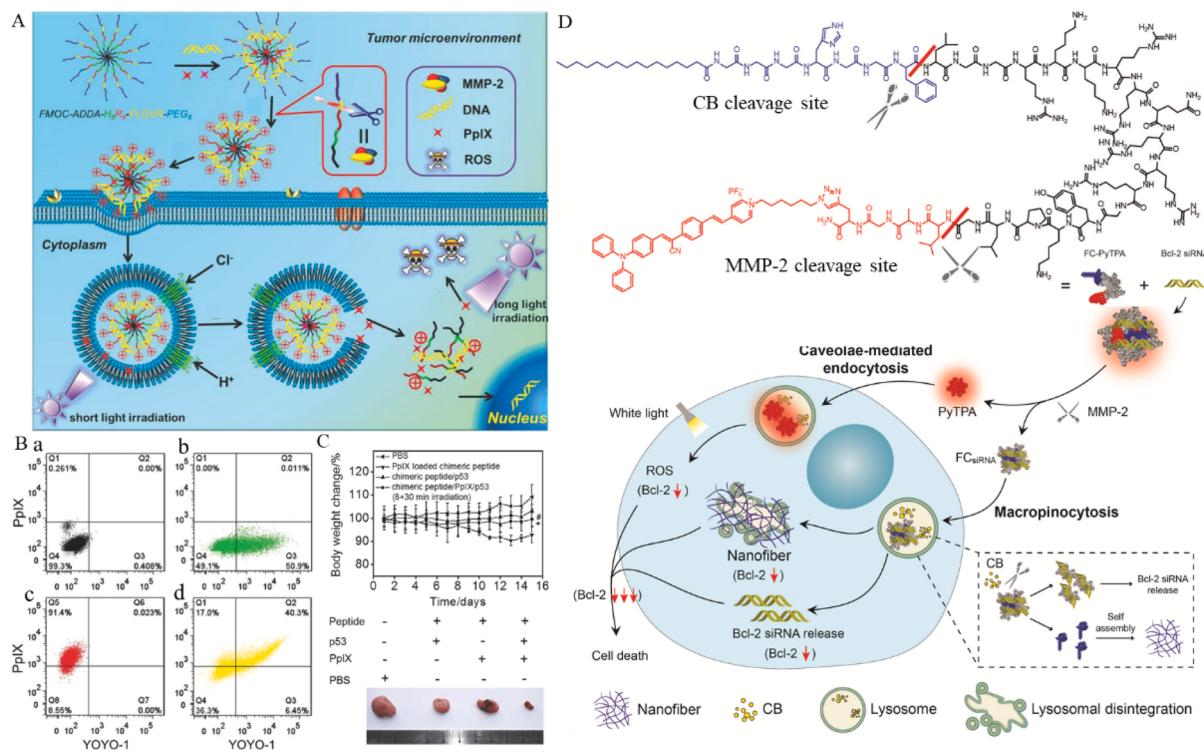


Fig. 7. (A) Schematic diagram of self-assembled Fmoc-ADDA-H₃R₈-PLGVR-PEG₈ to load PpIX and p53 gene for synergistic therapy. (B) Two-color flow cytometry of co-delivered PpIX and gene in SCC-7 cells. (a) The negative control of chimeric peptide; (b) YOYO-1 (green fluorescence) marked peptide/pGL-3 complex; (c) PpIX (red fluorescence) loaded peptide. (d) YOYO-1 marked peptide/PpIX/pGL-3 complex. (C) Weight changes of mice treated with different formulations and their corresponding tumor images at the 15 d post-treatment. Adapted with permission from Ref. [141]. Copyright 215, Wiley-VCH. (D) Schematic diagram of the FC_{siRNA}-PyTPA system with dividing-into-two-part function to play multiple therapeutic functions. Adapted with permission from Ref. [142]. Copyright 2020, Wiley-VCH.

the survival of patients with HNSCC. A peptide hydrogel self-assembled from ac-(RADA)₄-CONH₂ has been exploited as a dual drug-loaded carrier for the treatment of HNSCC [144]. The hydrogel enabled the co-delivery of DOX and curcumin, and drug release rate could be manipulated according to their aqueous solubility. In comparison with the corresponding combination of drug solution, dual drug-loaded hydrogel formulation effectively inhibited the cancer cell growth. Another example for hydrogel-based combination therapy is treating ischemia-reperfusion (I/R)-induced organ injury that generally involves complex pathophysiological process [145]. To address the issue that current therapies mainly target just one pathway (inflammation or cell proliferation), a peptide/heparin hydrogel was developed to co-deliver hepatocyte growth factor (HGF) and TNF- α neutralizing antibody (anti-TNF- α) to promote tissue repair after ischemic injury. In this co-delivered hydrogel platform, the discrepant release kinetics enabled the faster anti-TNF- α release to reduce the inflammatory and tubular apoptosis, and the slower HGF release could promote tubular regeneration after organ injury. Compared with self-assembled peptide or free-drug alone, this sequential dual-drug release relying on peptide hydrogel system showed better efficacy for tissue repair, since it met the different requirements of anti-inflammation and proliferation for the different stages of tissue repair.

3.2.1.5. Others. Apart from the common cargoes including chemotherapeutic drug, gene, and photosensitizer for cancer treatments, self-assembled peptides are also widely studied in other biomedical fields to deliver other agents such as anti-HIV drug [146] ocular drug [147,148], antimalarial agent [149], immunologic adjuvants. A novel peptide-based spherical micelle system was developed to encapsulate resiquimod (R848, FE^R) for melanoma immunotherapy (Fig. 8A) [150]. An amphiphilic peptide of FFVLKTAREYRPAHE with the ability of blocking PD-1/PD-L1 (programmed cell death-1/programmed cell death

ligand-1) axis was screened, which self-assembled into spherical micelles and efficiently encapsulated R848 to activate the suppressed immune microenvironment. After the co-assembly of FE^R with tumor-responsive Gelatin methacryloyl (GelMA), the yielded FE^R/MN could achieve local drug delivery and control release. As shown in Fig. 8B and C, this system down-regulated the PD-1 gene and up-regulated immune factors to achieve the synergistic immunotherapy.

Different from delivering small-molecular drugs, self-assembling peptide has been introduced to transport nano-agents by Zhang and co-workers for tumor therapy (Fig. 8D) [151]. They screened a peptide of HFEYWEERHKKLVFF (named as RT) that could recognize and target the immune checkpoint CD47. It self-assembled into fibrous nano-architectures and trapped Ag₂S quantum dots (QDs) into the fiber inner to achieve the immunotherapy and sonodynamic therapy (SDT). After the tail vein injection of “bead-grafting” nanodrug, this nano-system blocked the CD47/SIRP α axis to elicit immune checkpoint blockade (ICB). Ag₂S QD-mediated SDT produced ROS to destroy tumor cells and release tumor antigens, which promoted the maturation of DCs and further activated the adaptive immune system to eliminate tumor cells. The powerful anti-tumor immune response could act on both primary and distant tumors (Fig. 8E).

3.2.2. Self-deliverable nanomedicine

Common drug delivery systems usually suffer from the aspects of complex carrier synthesis, low drug encapsulation rate, carrier-induced cytotoxicity and immunogenicity, and so on. Drug self-delivery systems have been proposed to overcome these drawbacks, in which the active drugs are designed with nanoscale characteristic to achieve the intracellular delivery without exogenous nanocarriers [152–154]. Many studies show that peptides with certain sequences exhibit therapeutic and imaging functions towards cancer cells and bacteria. Additionally, peptides can self-assemble into various nanomaterials with defined

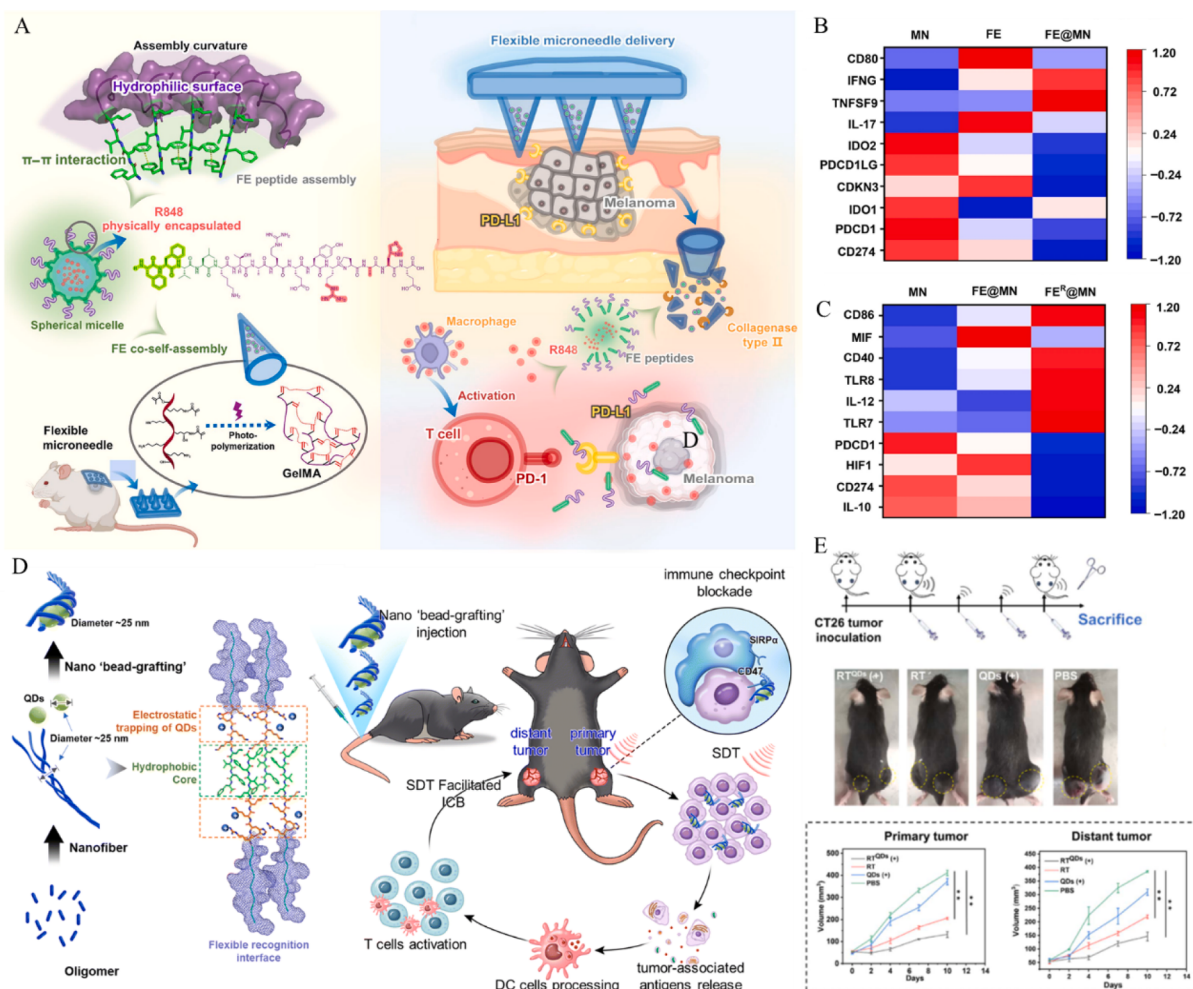


Fig. 8. (A) The illustration of fabricating FE^R@MN and its synergistic immunotherapy mechanism. (B, C) The heatmaps reflecting the alternations of PD-L1-related genes and immune cell activation-associated genes after treated with different formulations, respectively. Adapted with permission from Ref. [150]. Copyright 2022, Elsevier Ltd. (D) Schematic illustration of constructing 'bead-grafting' nanostructures and its anti-tumor therapy via the combination of ICB with SDT. (E) Treatment schedule of bilateral tumors and their therapeutic efficacies reflected by tumor volume. Adapted with permission from Ref. [151]. Copyright 2022, Royal Society of Chemistry.

secondary structures, which can act as the adjuvants to help the imaging and therapy of nanomedicines. In this section, peptide-based self-delivery systems used for cancer cell imaging, cancer therapy, theranostic, antimicrobial agent and immune adjuvant are discussed. Their applications of treating other diseases besides tumors and bacteria are also included.

3.2.2.1. Cancer cell imaging agent. A decline in mortality rates of cancers has been observed over time, which is partly contributed to the improvements of effective diagnosis in their early state. Non-invasive fluorescence-based image technique with high selectivity, real-time reflection and high resolution has been demonstrated to be an effective strategy for cancer diagnosis [155]. Bioinspired fluorescent peptidyl nanoparticles have emerged as a promising fluorescence candidate for effective cancer cell imaging. This was learned from the yellow fluorescent protein (YFP) in which the π - π stacking interaction between tyrosine and phenolate anion of chromophore induces the fluorescent red-shift, and the structure rigidification through Zn(II) coordination enhances the fluorescent signal in green fluorescent mutant protein (GFP). As a consequence, peptides containing continual aromatic side chains have been designed. During the peptide self-assembly, π - π stacking would reduce the excited state energy and increase both the excitation and emission wavelengths, resulting in the amplified

fluorescence signals and red-shifted wavelength for imaging. In contrast to inorganic nanoprobes with concerns of biocompatibility and solubility, and traditional organic fluorophores suffering from the photo-bleaching and broad emission band, self-assembled peptide nanoprobes are biocompatible, photostable, and display narrow emission bandwidth. As for some peptides without intrinsic fluorescence, moreover, their reactable side chains such as amino and carboxyl groups can coordinate with metal ions or react with fluorescent molecules to be equipped with the fluorescent features for imaging.

Zhang and co-workers designed a self-assembled Trp-Phe (WF) dipeptide nanoparticle for targeted cancer cell imaging (Fig. 9A) [156]. After the coordination with Zn(II), WF dipeptide self-assembled into spherical nanoparticles, accompanying with the emission peak shift from original \sim 355 nm to \sim 423 nm. After the incorporation of MUC1 aptamer that can recognize the MUC1 protein that is overexpressed by A549 human carcinoma epithelial cells, the bioinspired dipeptide nanoparticles could target A549 cells for fluorescent imaging. To further red-shift the fluorescent emission wavelength, Qin and co-workers constructed a self-assembled Trp-Phe-Phe-Trp (WFFW) tetrapeptide fluorescent nanoprobe [157]. This nanoprobe displayed photostable and tunable fluorescence signal from 340 nm to 500 nm, and its fluorescent intensity enhanced in comparison to individual WFFW molecule. After the co-assembly with targeted RGDWFFW, the resultant nanoprobe could selectively image the cancer cells, with no need for incorporating

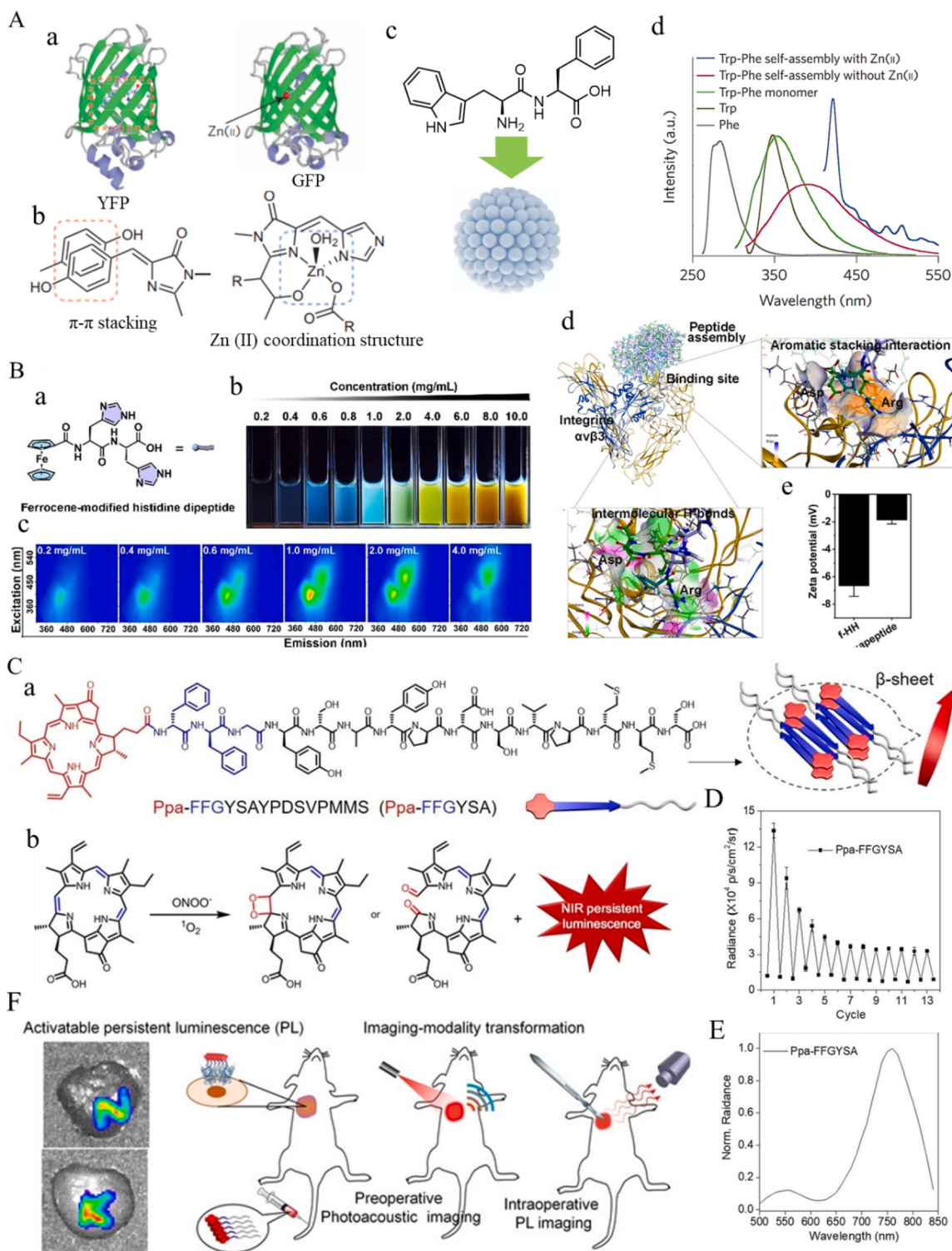


Fig. 9. (A) The fluorescent properties of YFP/GFP and their bioinspired self-assembled Trp-Phe dipeptide nanoparticles for cell fluorescent imaging: a) The structure of YFP and GFP; b) π - π stacking mediated fluorescence red-shift in YFP and Zn(II) coordination mediated fluorescence intensity enhancement in GFP; c) The illustration of Trp-Phe dipeptide self-assembled into fluorescent nanoparticle; d) Fluorescence emission spectra of different groups. Adapted with permission from Ref. [156]. Copyright 2016, Nature Publishing Group. (B) Ratiometric fluorescence of the self-assembled f-HH dipeptide: a) Molecular structure of f-HH dipeptide; b) concentration-dependent fluorescent feature of f-HH dipeptide under 365 nm; c) the contour plot of the f-HH dipeptide with different concentrations; (d) the interaction between integrin $\alpha\beta 3$ and self-assembled peptide, indicating the hydrogen bond interaction and aromatic stacking interaction; and e) Zeta potential of f-HH dipeptide and f-HHGRGD. Reproduced with permission from Ref. [163]. Copyright 2023, American Chemical Society. (C) Chemical structures of Ppa-FFGYSA (a) and Ppa (b) and their relevant properties. (D) PL signal variation of Ppa-FFGYSA with repeated laser irradiation for 13 cycles in PBS. (E) PL spectrum of Ppa-FFGYSA after the addition of peroxynitrite. (F) Schematic illustration of Ppa-FFGYSA for preoperative PA imaging and intraoperative PL image-guided surgery, and the PL images of isolated livers after i.v. injection of Ppa-FFGYSA. Adapted with permission from Ref. [168]. Copyright 2022, Wiley-VCH.

extrinsic fluorescent agents. Following these, based on the combinatorics of aromatic amino acids including tyrosine, phenylalanine and tryptophan, a series of bioinspired fluorescent nanoparticles self-assembled from tyrosine-based peptide [158], tryptophan-based peptide [159,160], and phenylalanine-based peptide [161] have also been developed, with fluorescence signals in the range of 500–600 nm. Kong and co-workers developed different non-fluorescent oligopeptides of Fc-(X)_n (X = F, Y, W, and H; n = 1–3) [162]. These could aggregate into fluorescent nanoparticles and their fluorescence emission wavelength could be tuned in the range of full visible color spectrum by varying aromatic amino acid. It was found that the intermolecular forces could constraint the intramolecular motions of oligopeptide, which blocked the non-radiative conformational relaxation pathway and therefore led to fluorescence emission for imaging. Recently, a ferrocene-modified histidine (f-HH) dipeptide was constructed, which could emit ratiometric fluorescence via an assembly-induced emission (Fig. 9B). The concentration of peptide determined the intensiometric ratio of green to blue fluorescence. After appending GRGD peptide, the yielded hexapeptide could retain the ratiometric fluorescent properties, showing the potential of targeted cancer cell imaging [163].

These studies demonstrated the cancer cell imaging ability of self-assembled peptide nanoparticles. However, tuning the fluorescence of peptide nanoprobe to NIR range is very challenging. The RGD-modified cyclo-[-(D-Ala-L-Glu-D-Ala-L-Trp)₂-] peptide nanoparticle was constructed, which was able to emit NIR fluorescence when excited at 760 nm [164]. Meanwhile, the self-assembled nanoplatform could encapsulate drugs for targeted esophageal cancer therapy and the therapeutic responses could be monitored by the NIR fluorescence. Tamamis, Tan, and Gazit designed a cyclic (L-His-D-His) to coordinate with Zn(II), which emitted both visible and NIR fluorescence under a wide range of excitation wavelengths. Both the visible and NIR fluorescence was imaged in nude mice after the subcutaneous injection of nanoprobe, and the fluorescent signals showed no decay for one week, suggesting the good stability for *in vivo* bio-imaging [165]. Moreover, aromatic cyclo-dipeptides of *cyclo*-FW and *cyclo*-WW could dimerize into QDs, which further served as the self-assembling unit to construct quantum confined nanostructures with photoluminescent properties. By modulating the self-assembly process, the fluorescent emission wavelength can be tuned from the visible region (420 nm) to the NIR region (820 nm) for *in vivo* NIR imaging [166].

Despite these advances, pure peptide-engineered fluorescent nanoprobe are very scarce because of the limited intrinsic optical properties of peptides. As a consequence, fluorescent peptide-conjugate consisting of water-soluble peptide and chromophore has been proposed. A self-assembled peptide nanoprobe capable of responding to the weakly acidic pH in tumor microenvironment was developed [167]. In their design, a fluorescent energy pair (donor and receptor) were harnessed to the side chains of two peptides, and the co-assembly of peptides drove the close of donor and receptor to each other to lock the fluorescence signals. After reaching the acidic tumor microenvironment, the self-assembled nanoparticles quickly dissociated and activated the fluorescence signals. The dissociated small fluorescent components could image heterogeneous tumors due to their enhanced tumor permeability. Ding and co-workers reported a peptide-based porphyrin derivative Ppa-FFGYSAYPDSVPMMs (Ppa-FFGYS), which could persistently emit NIR luminescence for image-guided cancer surgery (Fig. 9C) [168]. Adopting a β -sheet conformation for self-assembly, formed supramolecular probe has been found with enhanced tumor targeting ability, as well as enhanced photoacoustic (PA) and persistent luminescence (PL) signals. Moreover, self-assembled probe showed good cycling stability (Fig. 9D) and long-wavelength PL emission at 760 nm (Fig. 9E), which provided a sufficient operation window and deeper tissue-penetration ability. Originating from the unique molecular structure, probe could realize the light-triggered transformation from PA to PL imaging (Fig. 9F), permitting PL image-guided cancer surgery.

Another strategy is introducing auxiliary units to endow the non-

fluorescent peptide with fluorescent features. As a representative, nonfluorescent alizarin red S (ARS) can strongly bind with the phenylboronic acid moiety to yield the fluorescent signals, which further undergo fluorescent disappearance when encountering targets with higher binding abilities. This means that the phenylboronic acid conjugated peptides are suitable precursors for fabrication of imaging nanoplates. With this foundation, Zhang's group designed a self-assembled B(OH)₂-AEAAELRARARL-OH (named BP) to indirectly detect sialyl Lewis X (sLex)-overexpressed cancer cells, due to the effective recognition of boronic acid group towards sLex [169]. The nonfluorescent BP was pre-coordinated with ARS to obtain BP/ARS with fluorescent feature. Encountering the sLex overexpressed cells, the fluorescence of self-assembled BP/ARS probe switched off due to strong binding induced displacement. Simultaneously, a color change from the orange yellow for BP/ARS to the wine-red of free ARS solution occurred, facilitating the eye-detectable cancer cell identification. Different from the utilization of competition of sLex and ARS with phenylboronic acid moiety, Qin and co-workers found that phenylboronic acid-appended peptide/ARS could respond to Cu (II) due to the stronger binding ability of Cu (II) than BP with ARS. It was found that self-assembled ARS/BP nano-probe enhanced the sensitivity to Cu (II) in comparison with the molecular type of ARS/phenylboronic acid. Due to the high selectivity towards Cu (II), cancer cell targeting, and the nanoscale size effect, the self-assembled indicator has been demonstrated as a promising candidate for Cu (II) imaging in cancer cells *via* fluorescent change [170]. Peptide self-assembly strategy has also been introduced to improve the fluorescent imaging by Wen and co-workers, who developed a NIR-II fluorescent peptide nanoprobe to detect peritoneal metastasis [171]. Relying on a nanochain frame self-assembled from an amphiphilic peptide, NIR-II Ag₂S QDs and targeted RGD peptide were anchored. The yielded NIR-II nanochain probe exhibited higher cancer cell detection capability compared with RGD-functionalized Ag₂S QDs without self-assembled peptide as nano-frame. Guided by NIR-II fluorescent imaging, cytoreductive surgery could be effectively executed.

3.2.2.2. Cancer therapy agent.

Recent studies have shown that some functional peptides can activate cell death in cancers. One typic therapeutic peptide is the (KLAKLAK)₂ (abbreviated KLA) sequence with an α -helix secondary structure (Fig. 10A), which can disrupt mitochondrial and/or plasma membranes and thereafter initiate cell death. To overcome the deficiencies of molecular peptides such as poor cell penetration, rapid *in vivo* degradation and immunogenicity, the self-assembly strategy has first been proposed by Stupp's group to design peptide nanomedicines for cancer therapy. Self-assembly domain containing a hydrophobic alkyl tail and a β -sheet forming sequence was incorporated into therapeutic KLA peptide to promote the self-assembly into nanofibers, which were readily internalized by cancer cells and induced the breast cancer cell death by lysing the plasma and mitochondrial membrane [172]. They further used pegylated peptide amphiphile to co-assemble with the cytolytic KLA peptide, and the yielded nanostructure substantially restrained the degradation of cytolytic KLA by protease trypsin [173]. In an orthotopic breast cancer xenograft model, co-assembled nanostructures significantly inhibited tumor cell proliferation and overall tumor growth. To facilitate the effective recognition of KLA peptide by cancer cells, an innovative pre-targeting strategy depending on the “biotin-avidin” interaction was developed by Zhang's group for tumor cell specific imaging and therapy [174]. The tumor cells were hierarchically modified by transferrin-biotin and FITC-avidin through the effective recognition, enabling the FITC-mediated fluorescence imaging and active capture by biotinylated self-assembled KLA peptide. The released KLA in cancer cell induced mitochondria-dependent apoptosis. They further designed a mitochondria-targeted PpIX-PEG-(KLAKLAK)₂ (designated as PPK), in which PpIX was linked to KLA peptide via a PEG chain [175]. To achieve the highly effective PDT, “dual-stage-light irradiation” strategy was exploited. In detail, a

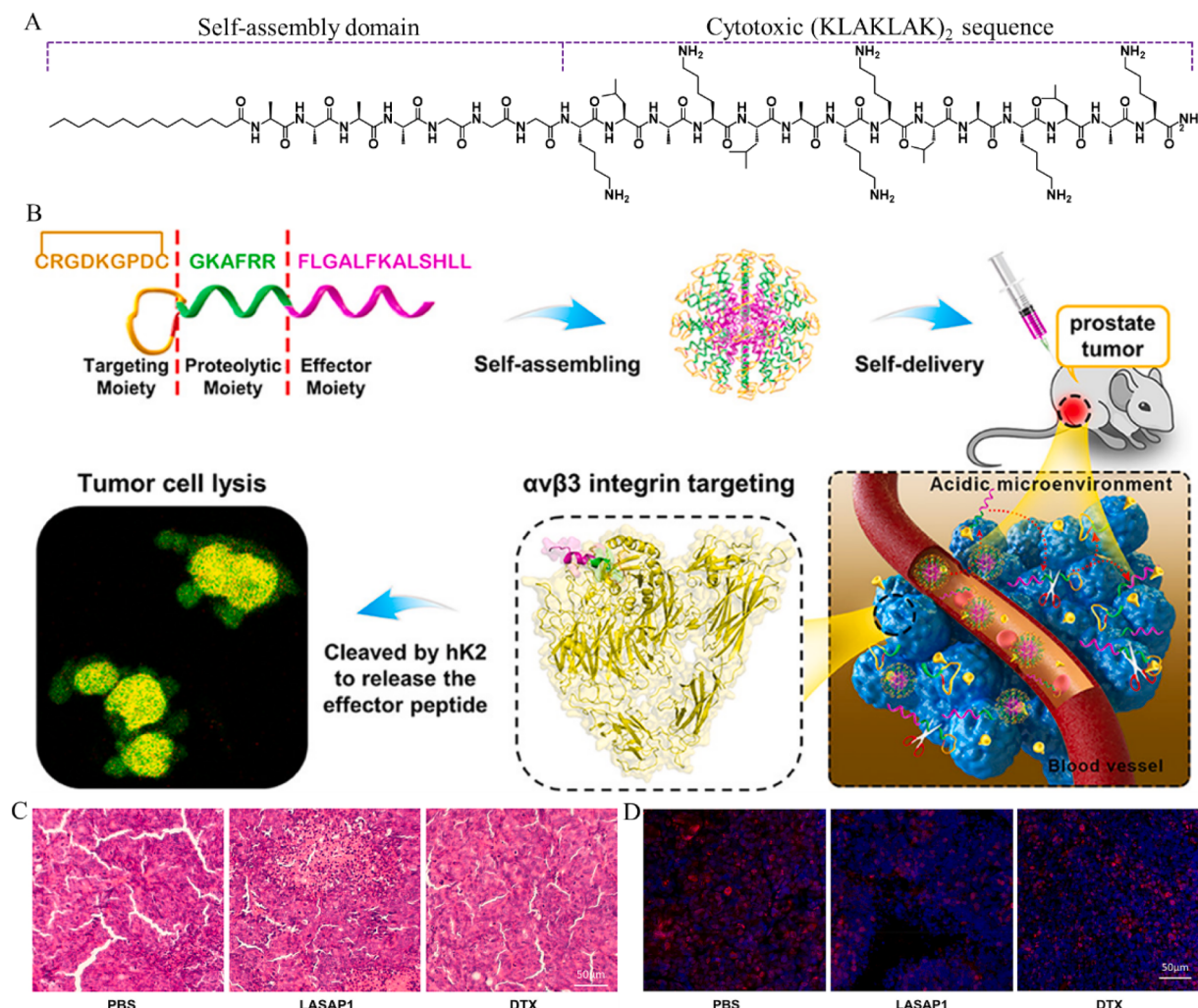


Fig. 10. (A) Chemical structure of KLAK-based peptide amphiphile. (B) Structure of LASAP1, the proposed self-delivering process and its multiple biofunctions. (C) H&E staining of tumor slices from different groups, indicating the apparent necrosis in the LASAP1-treated tumor slice when compared with that treated by PBS and DTX. (D) Ki67 immunofluorescence of different groups, showed less malignant proliferating cells in the LASAP1 treated tumors, blue for nuclei and red for Ki67. Adapted with permission from Ref. [177]. Copyright 2022, American Chemical Society.

short-time light irradiation was first carried out to trigger the PCI effect of PpIX to improve the drug internalization. After the location of drug in mitochondria for KLA-mediated therapy, a long-time irradiation was employed to initiate PDT. Chen and co-workers further used the self-deliverable KLA nanospheres to encapsulate the hydrophobic DOX, which was concurrently modified with tumor recognizing hyaluronic acid (HA) to improve the tumor targeting [176]. Relying on a computer-aided manner, an anticancer peptide of CRGDKGPD**C**GKA**F**RR**L**FLGALFKALSH**L** (1–9 disulfide bond, named as LASAP1) was selected by Luo and colleagues with multiple functions (Fig. 10B) [177]. This peptide self-assembled into spherical nanodrugs and accumulated at the lesion site due to size effect and iRGD targeting. It further disassembled in acidic tumor and suffered from the cleavage by overexpressed hK2 (secreted by prostate tumor cells). The yielded effector peptide of FLGALFKALSH**L** further executed the antitumor function with low systematic toxicity. As a result, the tumor growth in orthotopic prostate cancer mouse model was significantly inhibited, evidenced by the Hematoxylin and eosin (H&E) staining (Fig. 10C) and Ki67 immunofluorescence assays (Fig. 10D).

The tripeptide of tyroservatide (YSV) belongs to a new anticancer drug isolated from the pig spleen. It can interrupt cell cycle and act as a histone deacetylase inhibitor to suppress the activity of histone deacetylase, showing efficient anticancer activity in various cancer cells

[178]. What's more, YSV has been documented with abilities of inhibiting P-glycoprotein (P-gp) efflux pump and down-regulating the mRNA/protein expression of multi-drug resistance gene (MDR1), therefore reversing the MDR in cancer therapy [179]. The lipidation on YSV did not change its anticancer mechanism but could improve its anticancer performance due to the self-assembly [26]. On the one hand, lipidation can increase the membrane permeability of hydrophilic YSV for better cellular uptake. On the other hand, the lipidated YSV could self-assemble and aggregated into nanodrugs, which show improved biostability against proteinase K digestion and enhanced drug retention in tumor tissues. Recently, therapeutic YSV has been applied to combine with other agents for the improved outcomes. To address the poor solubility-induced undesirable circulation of gefitinib (GEF), a clinically approved drug for non-small-cell lung cancer therapy (NSCLC), YSV was exploited to co-assemble with GEF to generate spherical nanoparticles for the enhanced accumulation in tumor tissue [180]. The self-deliverable nanodrug exhibited the clear advantages in cell internalization, selectivity and drug efficacy over the free drugs or GEF/YSV drug mixture. Meanwhile, using a self-assembled FF core as a bridge, PpIX as a photothermal agent was connected with YSV motif to construct rod-like nanodrugs for enhanced cancer chemotherapy [181]. The mild photothermal effect of PpIX sensitized cancer cells to be more susceptible to YSV. With the aid of PA imaging guided mild hyperthermia, notably,

the single one injection achieved 70 % tumor inhibition *in vivo* due to chemo-photothermal therapy, thereby significantly reducing the dose of chemotherapy.

Combining the anticancer activity of therapeutic agents and self-assembly potential of peptides, peptide-drug conjugates with self-deliverable feature have been rationally designed for tumor therapy. Peptide-drug nano-assemblies have been widely investigated with their distinct advantages of simple preparation process and negligible excipient-triggered adverse sides [182]. Comparing with carrier-based nanomedicines that usually have low drug carrying capacity and

batch-to-batch variation of composition in each nanomedicine, self-deliverable peptide prodrugs allow for high and precise drug content because every drug molecule can be quantitatively appended to peptide backbones. Mediated by functional peptides such as cancer cell targeting group [183] and enzyme-sensitive sequence [184,185], active drugs could be delivered into the targeted cells and achieved the on-demand release from nano-systems after their intracellular delivery. Moreover, hydrolyzable bond [186,187], disulfide bond [188,189], and boronic acid-catechol ester [190] are also frequently proposed as the sensitive bridge to fabricate self-assembling drug-peptide conjugates. By delicate

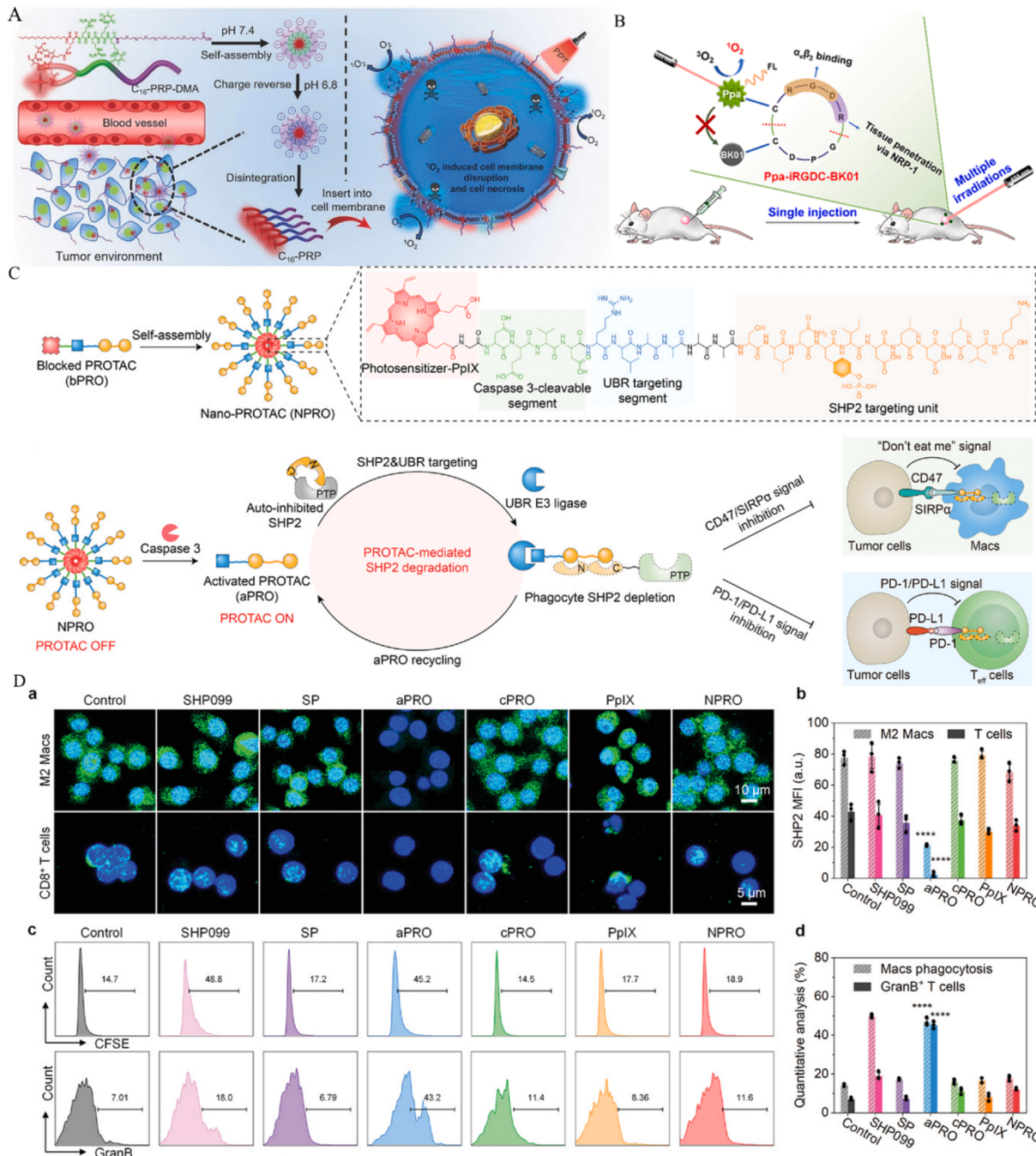


Fig. 11. (A) Cell membrane-targeting PDT with charge reverse feature. Reproduced with permission from Ref. [195]. Copyright 2017, Wiley-VCH. (B) The structure of Ppa-iRGDC-BK01 and schematic illustration of cyclopeptide cleavage and PS release and activation to generate ¹O₂ for the effective tumor eradication. Reproduced with permission from Ref. [197]. Copyright 2020, American Chemical Society. (C) Chemical structure and proposed mechanism of NPRO for cancer photoimmunotherapy. a) CLSM images and b) SHP2 MFIs of M2 Macs and CD8⁺ T cells treated by different formulations. Green: anti-SHP2 antibody, Blue: Hoechst 33342; c) Flow cytometry of Macs phagocytosis and GranB⁺CD8⁺ T cell treated by different formulations; d) the corresponding quantitative data. Adapted with permission from Ref. [198]. Copyright 2023, Wiley-VCH.

design, a series of peptide-based self-deliverable nanodrugs have been developed for cancer therapy. In addition, peptide-drug nano-assemblies provides a route to address the challenges of tumor heterogeneity and multidrug resistance, because of the capability of co-delivering other agents for combinational therapy.

Cui's group conjugated chemotherapeutic CPT to a β -sheet peptide, giving a self-assembling prodrug with a high and unified drug loading of 38 % [191]. Self-assembly of prodrug improved the stabilities of both hydrolysable CPT and biodegradable disulfylbutyrate linker in normal environment. After reaching tumor sites, hydrolytic cleavage of disulfylbutyrate resulted in CPT liberation, providing improved cytotoxic effect in comparing with the insensitive maleimide-linked nanodrug. Using RGDS tetrapeptide as a targeting group, Zhang's group achieved the CPT self-delivery into integrin-overexpressed tumorous cells [192]. Both the *in vitro* and *in vivo* experiments demonstrated that prodrug nanofibers effectively inhibited the growth of integrin-overexpressed tumors. To investigate the structure–activity relationship of peptide-drug conjugates, a series of amphiphilic peptide prodrugs were fabricated via a GSH-responsive linkage for tumor-targeted chemotherapy [183]. It was found that the hydrophobicity/hydrophilicity balance, the drug position and surface charge density affected the self-assembly behavior and the stability of resulted nanostructures. This enables the feasible structure design to improve the anticancer activity. Through engineering the peptide prodrug design, Cui's group achieved a linear, sustainable and rate-controlled drug release from the supramolecular hydrogel over the period of several months [193]. Increasing the hydrophobicity by incorporating an alkyl chain would slow the release rate, whereas incorporating more oppositely charged amino acids could accelerate the dissociation kinetics of the supramolecular nanodrugs.

PSs with reactive groups are also fused with functional peptides for the targeted delivery. In contrast with chemotherapeutic drugs that were generally delivered into cell nucleus for the intercalation into cellular DNA, PSs can be located in cell nucleus, cell membrane and other tissues to exert their functions. Acidity-triggered charge reversal peptide with nuclear localization function was appended to protoporphyrin IX (PpIX), which achieved the tumor-targeted cargo transport and photodynamic therapy in nuclei [194]. When approaching the tumor region, acidity triggered the charge reversal of masked nuclear localization sequence (NLS) peptide, which therefore accelerated the cellular uptake and further nuclear entry of PpIX. Different from the modality of targeting the nuclei, Zhang's group further investigated the PDT towards the cell membrane for tumor treatment (Fig. 11A) [195]. Palmitic acid as a lipophilic component for membrane insertion was conjugated with 2,3-dimethylmaleic anhydride (DMA) modified tetra-peptide sequence (RRKK), which was concurrently appended with PpIX in the side chain and a PEG segment at the C-terminal for molecular self-assembly. Apart from the nanosize effect and charge reverse feature in acidity, self-assembled nanoparticles could insert into the tumor cell membrane for a long-time retention. ROS generated by PpIX directly disrupted cell membrane and rapidly induced cell necrosis. To overcome drug resistance, PpIX-peptide conjugate was programmed to self-assemble into micelles to encapsulate DOX for the synergistic chemo-photodynamic therapy [196]. After the targeting drug delivery, a short laser irradiation induced the PCI effect for lysosome damage and accelerated micelle escape from the endo/lysosomes. Furthermore, ROS generation from PpIX executed the PDT effect while the micelles slowly released DOX in lysosomes. The sustained DOX release prevented drug from being pumped out the cells for synergistic therapy. To avoid the overdose PS administration from the repeated injections prior to each light irradiation, Cho and colleagues developed an injectable single-component peptide depot, so as to effectively eradicate tumor through the one-time injection and subsequent multiple irradiations at intervals (Fig. 11B) [197]. Detailly, the peptide depot was formed by the local injection and self-assembly of peptide monolith, which consisted of a cyclic iRGD, a PS that was activated by the proteolytic/reductive cleavage of the cyclopeptide backbone, and a hydrophilic quencher that

induced intramolecular fluorescence resonance energy transfer (FRET) to lock the PS photoactivity. Due to the dual FRET/self-quenching of PS, the self-assembled depot shielded the photosensitivity and protected it from photobleaching outside the tumor. After the targeted accumulation in tumor region, the tumor-selective proteolytic/reductive cleavage of iRGD cyclopeptide enabled the continued release of PS, which minimized the total drug dose required for multiple-session PDT.

PROTAC (proteolysis targeting chimera), an emerging targeted protein knockdown technology, consists of two covalently linked moieties that bind to the protein of interest (POI) and E3 ligase, respectively. The heterobifunctional structure of PROTAC enables specific and efficient degradation of POI through the intracellular ubiquitin–proteasome system in a persistent and recyclable manner. Recently, peptide-based nano-PROTACs have been demonstrated with some advantages such as chemical flexibility, high biocompatibility, and remarkable bioactivity. Pu's group developed a peptide-based checkpoint nano-PROTACs (NPRO) for targeted degradation of the immunosuppressive signaling protein SHP2 (the Src homology 2 domain-containing phosphatase 2) [198]. NPRO was self-assembled from a blocked PROTAC (bPRO) peptide that consisted of PpIX, caspase-3-cleavable DEVD, RLAA segment capable of targeting UBR E3 ligase, and SHP2 targeting unit of SLNpYIDLDLVK (SP) (Fig. 11C). Under 660 nm photoirradiation, NPRO generated cytotoxic $^1\text{O}_2$ to kill tumor cells, which induced immunogenic cell death and overexpression of caspase-3. The upregulated caspase-3 further cleaved DEVD and released the activated PROTAC (aPRO). aPRO specifically bound to SHP2 and UBR proteins via SLNpYIDLDLVK and RLAA, respectively, leading to persistent and effective degradation of SHP2. In *in vitro* experiments, aPRO induced the high SHP2 degradation in both M2 macrophages (72.8 %) and T cells (95.3 %) (Fig. 11D). The depletion of SHP2 further blocked the immunosuppressive signals of CD47/SIRP α ("Don't eat me") and PD-1/PD-L1, resulting in the increased population of cytotoxic GranB $^+$ CD8 $^+$ T cells (45.2 %) compared to treatment with small-molecule inhibitor of SHP099 (18.9 %). In vivo experiments also showed remarkable antitumor activity and synergistic immunotherapeutic effects of the checkpoint nano-PROTACs through activatable cancer photo-immunotherapy. Aside from immune checkpoint modulation using nano-PROTACs, they also reported a smart nano-PROTAC (SPN_{COX}) targeting COX-1/2, a tumor-expressed immunosuppressive protein, for activatable photo-metabolic cancer immunotherapy [199].

Hydrogel with therapeutic function is another significant modality of self-deliverable medicine. There is a rapid progress in the development of prodrug-based peptide hydrogels [200,201]. For instance, a supramolecular HCPT-FFFK-cyclen hydrogel has been demonstrated to attain the nuclear-targeting anti-tumor therapy *in vitro* and *in vivo* [202]. The introduction of cyclen group was because it not only assisted the entrance of negatively charged HCPT into the nucleus due to its positive charge in tumor environment, but also depleted cellular ATP and therefore reversed ATP-dependent drug efflux to improve the HCPT accumulation.

Therapeutic peptide-based hydrogels have been fabricated to concurrently encapsulate other agents for the combinational therapy. The dual drug-bearing supramolecular hydrogel served as a local therapeutic depot for long-time treatment after a single-dose injection [203]. Covalent conjugation of two CPT units onto the cyclic RGD peptide via a biodegradable disulfanyl-ethyl carbonate linker created a drug-peptide conjugate, which encapsulated DOX/Cur in the core of self-assembled nanotubes for the combination therapy. After the subcutaneous administration of self-assembling solution, the *in situ* gelation in tumor achieved local drug preservation and continuous release, thus inhibiting tumor cell growth, metastasis and recurrence. Meanwhile, the "drug delivered by drug hydrogel" strategy can also be realized though the co-assembly. A drug-peptide conjugate containing nonsteroidal anti-inflammatory drug of naproxen was designed as the cyclooxygenase-2 (COX-2) inhibitor. After co-assembling with the radiosensitizer of cisplatin, the yielded hydrogel inhibited overexpression of COX-2 and

boosted the radiosensitivity of cancer cells against cisplatin to induce apoptosis [104]. Using bioactive peptide as the therapeutic agent, a YSV-derived octapeptide was exploited to co-assemble with HCPT to give supramolecular hydrogel [105]. The formation of co-assembling hydrogel increased the stability of HCPT and afforded sustained drug release. Comparing with HCPT in aqueous solution, HCPT-bearing hydrogel improved the anti-cancer efficacy both *in vitro* and *in vivo*. To overcome the drug resistance of tumor cells, a self-deliverable drug system consisting of covalently linked Taxol and YSV tripeptide has been developed [187]. Triggered by self-hydrolysis of ester bond, Taxol-EYSV disconnected and formed supramolecular hydrogel to co-deliver Taxol and YSV into drug-resistant tumor cells. YSV acted on the histone deacetylase and P-glycoprotein, and the efflux of free Taxol from cells was alleviated. As a result, the combination of Taxol and YSV conquered the drug resistance of tumors.

3.2.2.3. Cancer theranostic agent. The original heterogeneousness and adaptiveness of cancers make most therapeutic modalities be only effective for limited patients. In an attempt to overcome these major hurdles, therapeutic effectiveness should be real-time monitored, so as to timely adjust the therapeutic schedule. Theranostic, integrating the diagnosis purpose into fundamental therapy, is able to intuitively monitor the therapeutic process and evaluate the therapeutic outcomes [204,205]. The feedback information from online diagnosis helps

instantly optimize the therapeutic schedule, which therefore effectively copes with the heterogeneousness and adaptation of cancers. Peptide-based prodrugs with potential self-reporting function have been widely developed [206,207]. Combining with the advantages of self-delivery, several peptide-based nanoplatforms are established for cancer theranostic regimen.

Cui's group used a peptide linker to connect two CPT molecules with a metal-chelating agent of 1,4,7,10-Tetraazacyclododecane-1,4,7,10-tetraacetic acid (DOTA), which associated into tubular supramolecular nanostructures with good biostability. Triggered by intracellular GSH, the nanostructures quickly released CPT to inhibit the growth of tumor spheroids. DOTA as a chelator for metal ions could be potentially used for molecular imaging [208]. Liu and co-workers used the self-deliverable theranostic strategy to record the PDT efficacy [209]. In the designed structure of C₁₆-K(PpIX)GRRRR-AEEA-K(FAM)SDEVDSK (Dabcyl)PEG₈PEG₈, lipophilic palmitic acid contributed to cell membrane-targeting and molecular self-assembly, and the hydrophilic RRRR moiety with positive charge could increase the membrane affinity. The PS of PpIX, 5(6)-carboxyfluorescein (FAM) and 4-(dimethylaminoazo)-benzene-4-carboxylic acid (Dabcyl) as the FRET fluorophore pair were appended to side chains of peptide to elicit the therapeutic and imaging functions, respectively. The hydrophilic PEG₈-PEG₈ prolonged the half-life and enhanced the biocompatibility. Under irradiation, PpIX-induced ROS damaged the cell membrane and activated caspase-3, which further cleaved DEVD peptide and restored the FAM fluorescence to report the

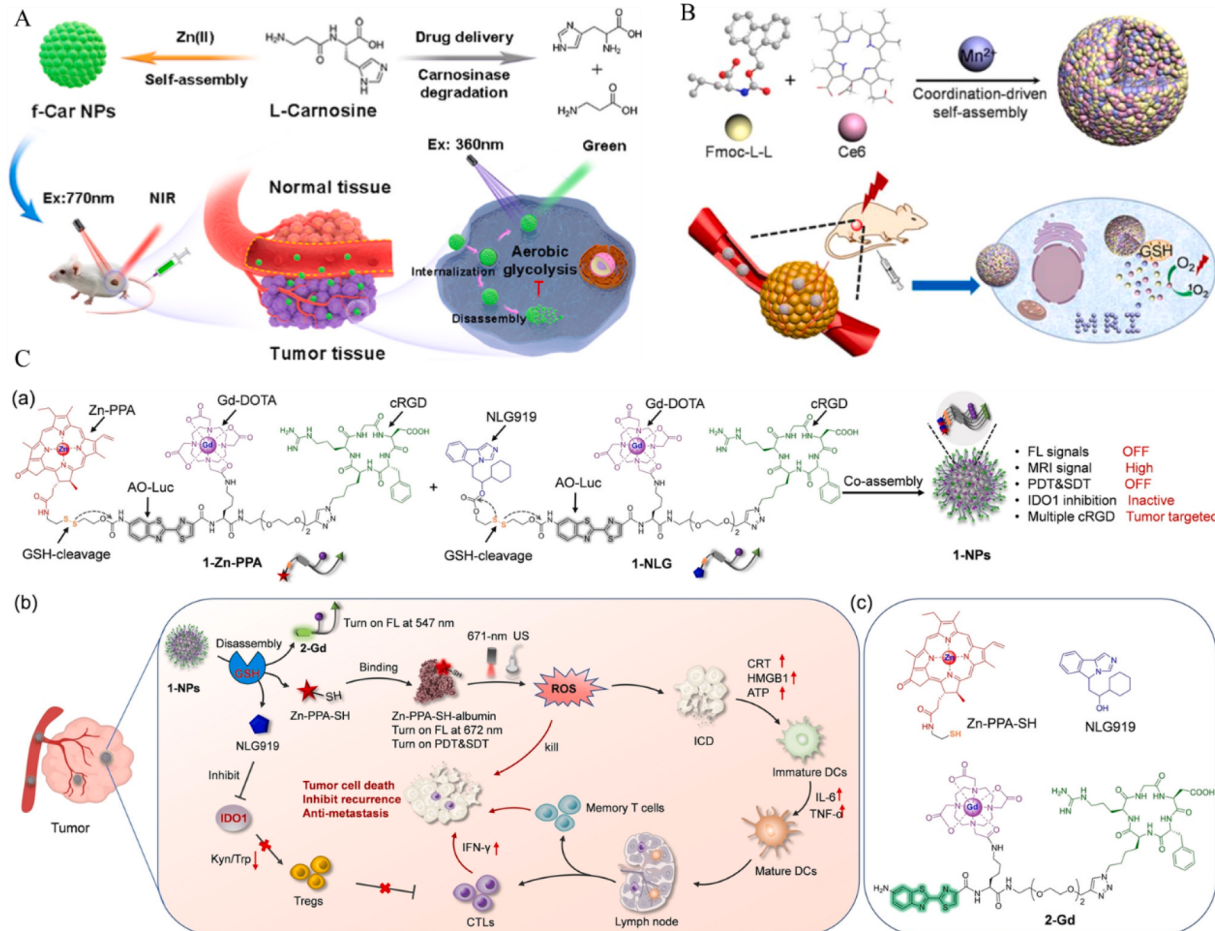


Fig. 12. (A) Anti-tumorous carnosine dipeptide co-assembly with Zn (II) capable of generating fluorescent signal for the cancer theranostic. Reproduced with permission from Ref. [28]. Copyright 2021, American Chemical Society. (B) Mn²⁺-driven co-assembly of Fmoc-L-leucine and Ce6 into supramolecular nanoparticles, facilitating the MRI-guided tumor PDT *in vivo* Reproduced with permission from Ref. [210]. Copyright 2018, American Chemical Society. (C) The co-assembled 1-NPs for GSH-activatable tumor sono-photodynamic immunotherapy. (a) Chemical structures of 1-Zn-PPA and 1-NLG, and the illustration of their co-assembly into 1-NPs; (b) The proposed mechanism of GSH-mediated disassembly of 1-NPs into 2-Gd, Zn-PPA-SH and NLG919, resulting in imaging-guided sono-photodynamic immunotherapy; (c) The chemical structures of released Zn-PPA-SH NLG919 and 2-Gd. Reproduced with permission from Ref. [211]. Copyright 2023, Wiley-VCH.

therapeutic feedback. In another example, a nonfluorescent antitumor dipeptide of carnosine has been found to generate fluorescent nanoparticles through the self-assembly in the presence of Zn (II), showing the cancer theranostic application (Fig. 12A) [28]. The nanoparticles emitted fluorescence signal from the visible to NIR ranges for real-time imaging. Furthermore, the formation of nanoparticle minimized the contact of therapeutic dipeptide with serum and consequently improved the biostability, resulting in high antitumor activity. In another work, coordination driving co-assembly of Fmoc-L-leucine and Mn²⁺ into supramolecular nanoparticles was achieved to encapsulate Ce6 for MRI-guided PDT (Fig. 12B) [210]. The multifunctional theranostic nano-platform could respond to intercellular GSH, and therefore release Ce6 and Mn²⁺ in tumor microenvironment. The binding of Mn²⁺ with GSH depleted intercellular GSH level and decreased the resistance of cells to ROS, leading to improved PDT efficacy. Meanwhile, the generation of GSH/Mn²⁺ complexes prolonged the retention time of Mn²⁺, facilitating the effective MRI-guided tumor PDT.

On the base of the co-assembly of 1-Zn-PPA and 1-NLG shown in Fig. 12C, Liu, Ye and co-workers designed tumor-targeted and redox-activatable nanoparticles (1-NPs) for cooperative sono-photodynamic immunotherapy of tumors [211]. Apart from the same moieties of 1-Zn-PPA and 1-NLG containing a cRGD for tumor-targeting, a hydrophilic Gd-DOTA chelate for MRI, and a hydrophobic amino oxy luciferin (AO-Luc) fluorophore, they were connected with a NIR Zn-chelated pheophorbide of Zn-PPA and an indoleamine 2,3-dioxygenase 1 (IDO1) inhibitor of NLG919 via a GSH-cleavable disulfide bond, respectively. The co-assembled 1-NPs locked the dual FL signals at 547 and 672 nm as well as therapeutic activities of SDT and PDT, but with a high longitudinal relaxivity. Upon the GSH-mediated reduction of disulfide bond, 1-NPs rapidly dissociated and the functional agents of 2-Gd, Zn-PPA-SH and NLG919 were released, which therefore achieved the dual FL emission for imaging, sono-photodynamic therapy and inhibited IDO1 activities that suppressed Tregs expansion and activation.

3.2.2.4. Antibacterial agent. Antibacterial agent is another kind of important biomaterial, which can effectively kill microorganism and inhibit the bacterial infections. As for commonly used antibiotics, bacteria can adapt to the ever-changing environment and therefore develop the corresponding drug-resistance. Peptide-based antibacterial agents exhibit clear advantages over conventional antibiotics. They can slow the emergence of resistance and combat multi-drug resistant bacteria due to their unique membrane disruption killing mechanism [212]. Moreover, antimicrobial peptides display the broad-spectrum antimicrobial properties, and the antibacterial properties of bulk materials can be tailored via changing peptide sequence at molecular level, which allows for the easy determination of the structure/chirality-encoded antimicrobial activity [86,213,214]. Specially, engineering molecular self-assembly to antimicrobial peptides has been well demonstrated to improve their antimicrobial activity, and reduce hemolysis and allergic responses [215,216]. Meanwhile, the yielded peptidyl nano-assemblies accelerate the accumulation process of individual peptides and strengthen their binding avidity with cell membrane. According to the formulations, self-assembled peptide antimicrobial units can be categorized into amphipathic antimicrobial peptides and short amyloid-related peptides.

As for amphipathic antimicrobial peptides, amphiphilicity is one of the typical features, which not only helps peptides interact with the biological membranes, but also enables the molecular self-assembly via certain secondary structure. These peptides typically contain a charged head and a hydrophobic tail, or repeated blocks of hydrophobic and charged residues. Surfactant-like peptides are a representative example and their nano-assemblies have been widely proposed for bacterial inhibition. Chen and co-workers investigated the antibacterial activities of amphiphilic peptides of A₃K, A₆K, and A₉K, and found that their

activities towards both gram-positive and negative bacteria increased significantly along with increasing the hydrophobic tail length [217]. The improved antimicrobial capacity was ascribed to their increased hydrophobicity, which provided stronger hydrophobic affinity with bacterial membrane and therefore more effectively destroyed membrane integrity. Meanwhile, the increased hydrophobicity can provide stronger hydrophobic interaction for self-assembly, resulting in the generation of smaller self-assemblies. The nanostructures with smaller sizes could more readily pass across the bacterial membrane envelope to reach the cell membrane surface for the damage.

To investigate the antibacterial mechanism of self-assembled surfactant-like peptides, self-assembled Ac-A₉K-NH₂ was constructed, which was found to directly bind with the negatively charged bacterial surface, similar with the Ac-A₉K-NH₂ monomers [218]. The following insertion into the bacterial membrane and forming surface nanopores caused the rapid membrane permeabilization. Recently, a panel of amphiphilic peptides consisting of nine-amino acid residues have been reported with potent antibacterial and antibiotic activities (Fig. 13A) [219]. Among these peptides, K3, K4, and K6 exhibited the broad-spectrum antimicrobial activities, and K6 showed the lowest minimal inhibitory concentration (MIC) (Fig. 13B). Comparing with gentamicin, K6 could eliminate the biofilm formation more effectively (Fig. 13C, D). The excellent antibiotic activity was ascribed to its self-assembly into nanoscale structure, which prolonged the *in vivo* half-life and increased the local concentration of peptide drug. A subcutaneous catheter mouse model was established to investigate the *in vivo* therapeutic efficacy of K6 towards an existing polymicrobial biofilm. The skin tissue for K6 treated group (biofilm + K6) recovered effectively at day 6, similar to the noninfected control catheters (mock). But mice treated only with PBS displayed a large number of pus and tissue damage, suggesting the ongoing infection (Fig. 13E).

To modulate their amphiphilicity, some lipid chains are generally appended to the N-terminal (or side chain) of cationic peptides, generating lipopeptide-like antibacterial agents. The lipids segment enables the insertion into bacterial lipid bilayer, while the cationic peptide binds with negatively charged bacterial membrane and leads to its destabilization. Several groups integrated the alkyl chains to antimicrobial peptides, which self-assembled into stable nanostructures for bacterial inhibition [220–223]. Galdiero *et al.* used a nonadecanoic acid appended A₆K peptide to modify an antibacterial WMR peptide (NH₂-WGIR-RILKYGKRS-CONH₂). The generated peptide amphiphile self-assembled into stable nanofibers and showed improved inhibition to biofilm formation when compared to the native WMR peptide without alkylation [215]. Replacing the saturated lipid chains with unsaturated counterparts, Cai and co-workers found the introduction of unsaturated motifs into antimicrobial peptides could significantly decrease the hemolytic activity [224]. This property circumvented the inconsistency that increasing the lipophilicity of saturated fatty acid within amphipathic peptides would concurrently improve the antimicrobial capacity and hemolysis. To understand the antimicrobial mechanism of self-assembled lipopeptides, a series of lipopeptides with the sequence of C_x-G(IKK)_y-NH₂ (C_xG_y, x = 4–12 and y = 2) were designed by attaching different lipid chains to the N-terminus of α -helix-forming peptides [225]. It was found that increasing x (representing the carbon number in the lipid chain, ≤ 10), both of the critical aggregation concentrations (CACs) and MIC decreased, suggesting the increased hydrophobicity and improved antimicrobial activity. Interestingly, the MIC values were significantly lower than the corresponding CACs, indicating that the bacterial membrane disruption was ascribed to the combination of lipid dissolution and membrane-induced aggregation. In detail, C_xG_y with small x exerted the membrane disruption mainly due to monomers for lipid dissolution. But as x increased, C_xG_y underwent membrane-based clustering to form nanoaggregates, which further inserted into the membrane bilayer for structural disruption. To probe the antimicrobial activity of peptide amphiphiles at the supramolecular level, self-assembled micelles, nanofibers, and twisted ribbons were

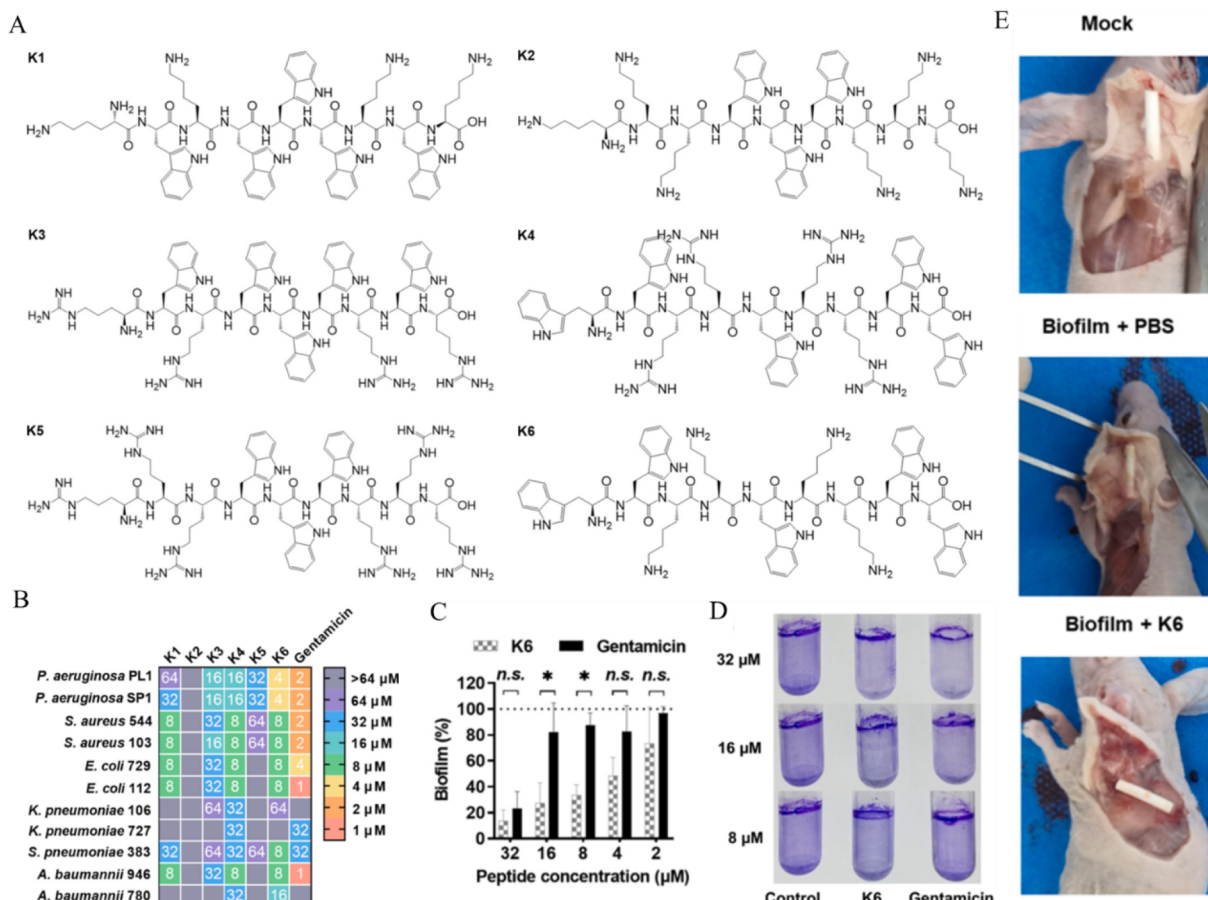


Fig. 13. (A) Chemical structures of peptides K1-K6. (B) MIC values of these peptides against bacteria isolated from clinical infection, and gentamicin used as positive control. K6 and gentamicin eliminating biofilm formation using polystyrene 96-well round-bottom plates (C) and using polystyrene round-bottom tubes (D). (E) Photos of the dorsal skin of mouse treated with K6. Adapted with permission from Ref. [219]. Copyright 2023, the Authors. Published by PNAS. This open access article is distributed under Creative Commons Attribution-NonCommercial-NoDerivatives License 4.0 (CC BY-NC-ND).

constructed and the shape-dependent antibacterial activity was investigated [220]. It was found that micellar nanotherapeutics possessed optimal antimicrobial activity. The probable reason was associated with the hypothesis that the intramolecular cohesion determined their antimicrobial activity, and self-assembled micelles were less stable than nanofibers, leading to the easier disassembly and insertion in the bacteria membrane to cause the cell death. To improve the killing ability of antimicrobial peptides, Zhang's group conjugated PpIX with an antimicrobial KLA peptide to create PPK for effective bacterial inhibition [226]. The positively charged peptide could rapidly bind to microbial cells and disrupt the bacterial membrane. Given a 660 nm light irradiation, PpIX generated the toxic ROS to further kill bacteria. To address the issues that photosensitizer, light source, and local oxygen concentration determine the antimicrobial PDT efficiency, Qin and co-workers developed a combined strategy of chemodynamic therapy (CDT) with peptide-based chemotherapy to combat the bacterial invasion [227]. Linoleic acid hydroperoxide (LAHP) was introduced as the hydrophobic tail and ROS-generating source to connect with an antimicrobial d(KLAK)₂ peptide. Apart from the deactivation of bacterial membrane induced by positive d(KLAK)₂, LAHP group could generate ROS to execute CDT. *In vitro* surface plating method assay result suggested that the combinational strategy possessed improved antibacterial activity. On the mouse skin abscess model infected by *S. aureus*, self-assembled nanomedicine exhibited perfect therapeutic effects without any systemic side effects. Following this, they further programmed the structure of lipopeptides to obtain bifunctional nanotherapeutics, which were applied for melanoma treatment of post-surgical bacterial infection and tumor recurrence [228]. By simply changing the numbers of linoleic

acid (LA) could obtain lipopeptides with significantly different therapeutic activities (Fig. 14A, B). P3-based nanotherapeutics with two LA molecules exhibited good antitumor and antimicrobial activities. In B16F10 tumor bearing BALB/c nude mice with a 95 % tumor resection and methicillin-resistant staphylococcus aureus (MRSA) infection (Fig. 14C), P3-based nanotherapeutics could effectively inhibit melanoma recurrence (Fig. 14D) and promote wound healing (Fig. 14E). Moreover, the nanotherapeutics could eliminate MRSA infection (Fig. 14F, G). The histological staining analysis indicated the ability of P3-based nanotherapeutics for enhancing re-epithelialization and skin appendage formation (Fig. 14H).

Apart from lipid chains, aromatic groups have also been introduced to act as the hydrophobic tail at the N-terminal. n-Butylazobenzene, a photo-sensitive group that can be recognized by β -cyclodextrin (β -CD) to form noncovalent complex and subsequently dissociated by adamantane (Ada) due to the host–guest chemistry, was exploited to adjust the hydrophobicity of tripeptides (*i.e.*, Ala-Gly-Gly-OH and Gly-Gly-Ala-OH) and served as the stimulus-responsive moiety to modulate the antibacterial activity [229]. In response to light irradiation and host–guest interaction, the tripeptide amphiphiles underwent a reversible assembly/disassembly process, accompanying with reversible modulation on bacterial growth and biofilm formation. It was found that the subtlest sequence isomerism of peptides affected their self-assembled morphologies, but their antibacterial and antibiofilm activities were similar. Li and co-workers found a random-coil peptide consisting of repetitive azobenzene and lysine residues self-assembled into spherical nanostructures with poor antibacterial activity (Fig. 15A) [230]. Adding polyoxometalate of H₄SiW₁₂O₄₀ into the peptide solution, co-assembly

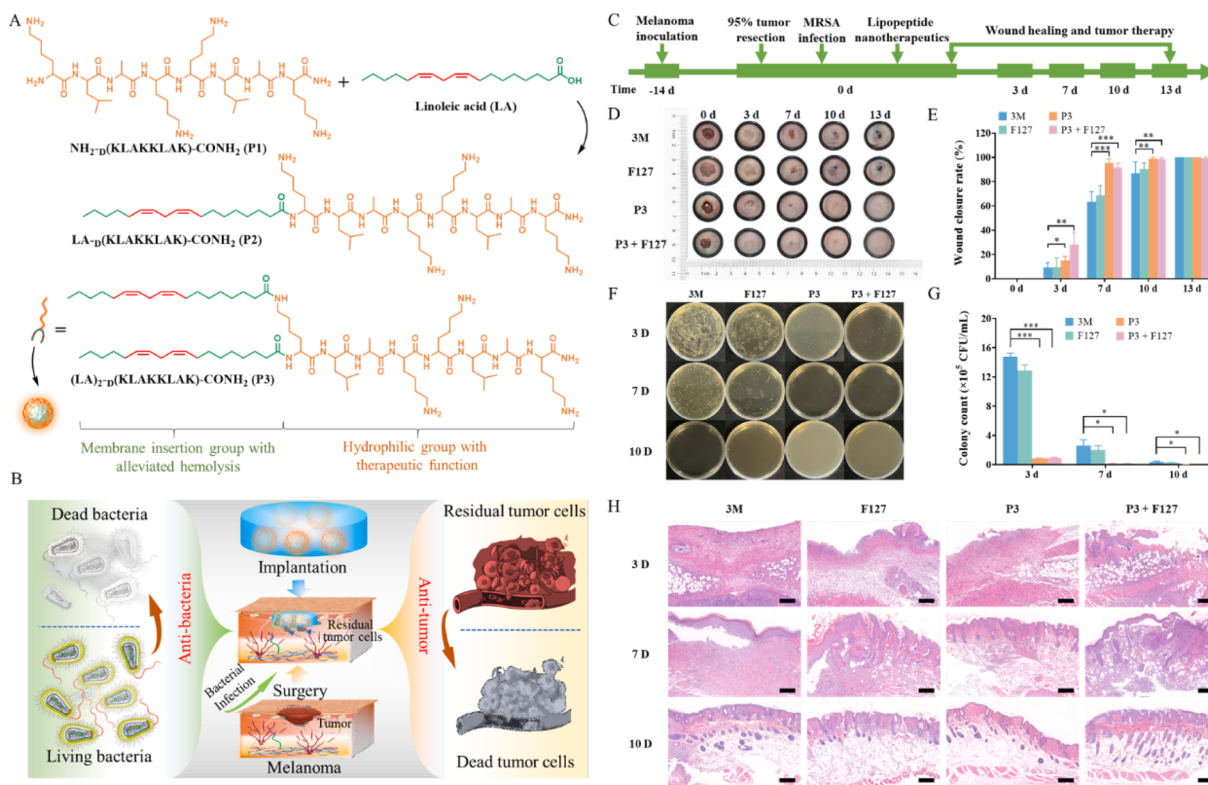


Fig. 14. (A) The molecular structure of programmed lipopeptides. (B) Schematic illustration of P3-based nanotherapeutics to exert the anti-bacterial and anti-tumor functions. (C) Schematic illustration of the experimental schedule for postsurgical wound healing and anti-tumor recurrence. (D) Photographs of mice with 95 % tumor resection and MRSA-infected wounds after the treatment with different formulations for 0, 3, 7, 10, 13 d. (E) Corresponding wound closure rate of mice. (F) Images of bacterial colonies derived from homogenized wound tissues at 3, 7, 10 d. (G) Corresponding statistical data of colonies after therapy. (H) H&E staining images of wounds at 3, 7 and 10 d. Scale bar: 200 μ m. Reproduced with permission from Ref. [228]. Copyright 2023, Elsevier Ltd.

occurred and peptide conformation transformed from a random-coil to a β -sheet state. As a result, nanofibers with the concentrated charge density on their surface were formed. Comparing with pure peptide nanospheres, multivalent nanofibers formed by polyoxometalate and peptide showed enhanced antibacterial efficacy (Fig. 15B), improved drug accumulation in desirable location and resistance to enzymatic degradation.

Inspired by the findings that some classical amyloid proteins and peptides display antimicrobial activity, amyloid-related short peptides have been proposed to fight against bacterial infection. These antibacterial peptides share a high frequency of aromatic phenylalanine, which is regarded as the important role in accelerating and stabilizing the amyloidogenic assemblies. Gazit's group pioneered self-assembled diphenylalanine (FF) motif as the antimicrobial agent [231]. Comparing with the diglycine (GG) that could not self-assemble and individual FF, self-assembled FF has been found to effectively inhibit bacterial growth. In the mechanism investigation, the interaction of self-assembled FF with bacterial membrane resulted in the permeation of outer membrane and concurrent depolarization of inner membrane (Fig. 15C). These upregulated stress response regulons and therefore severely damaged the bacterial integrity (Fig. 15D). In another study, L-type $\text{NH}_2\text{-FF-COOH}$ has been reported with stronger activity against *S. aureus* biofilm relative to the D-form [232]. This opposes what has been observed in some studies that the incorporation of D-amino acids would improve the antibacterial activities because it could improve the proteolytic stability [233]. So more studies should be performed to explicitly link the enantiomer of amino acids to the antibacterial and antbiofilm activity of peptide derivatives.

Peptide-based antibacterial hydrogels have received attention over the past decades, because they can provide a moist environment, fill the irregular wound sites as well as hold the ability to low the risk of

inflammatory responses. Amyloid-related short peptides display excellent hydrogel-forming ability. Moreover, short peptides can be readily synthesized and purified, making antibacterial peptide hydrogels of such cost-effective for large-scale production. Different peptide hydrogels have been demonstrated with potent antimicrobial activities [234–236]. For example, a library of short peptides including Fmoc-D-Phe-D-Phe-CONH₂ (Fmoc-^DP^DF), Fmoc-L-His-D-Phe-D-Phe-CONH₂ (Fmoc-H^DP^DF) and Fmoc-L-Arg-D-Phe-D-Phe-CONH₂ (Fmoc-R^DP^DF) were fabricated, and their hydrogel stability and bactericidal activity were investigated [237]. It was found that these hydrogels exhibited good proteolytic stabilities, but only self-assembled Fmoc-R^DP^DF hydrogel showed excellent bactericidal activities. The bactericidal activity was attributed to the electrostatic interaction between peptide and bacterial membrane components, resulting in cell lysis and death.

A major highlight of hydrogel-based antimicrobial agents was their ability to load other agents for combinational therapy. Wang and co-workers develop a pH-switchable antimicrobial supramolecular hydrogel self-assembled from Ac-Leu-Lys-Phe-Gln-Phe-His-Phe-Asp-NH₂ [238]. This biocompatible hydrogel exhibited pathological acidity-induced broad-spectrum antimicrobial effect. After loading cypate (photothermal agent) and proline (procollagen component) to reduce the excessive inflammatory and improve cellular proliferation, respectively, the antimicrobial hydrogel enabled the rapid and complete eradication of integrated biofilms and rescued the stalled healing in chronic wound. Yan, Wang and co-workers reported a natural antimicrobial peptide of Pro-Phe-Lys-Leu-Ser-Leu-His-Leu-NH₂, which self-assembled in adenosine diphosphate (ADP, capable of inducing platelet aggregation) sodium solution to construct an injectable hydrogel with anti-infection and hemostasis (Fig. 15E). In a rat side wall defect-cecum abrasion model, yielded hydrogel showed excellent anti-adhesion efficacy [239]. Also, the detail design and antimicrobial

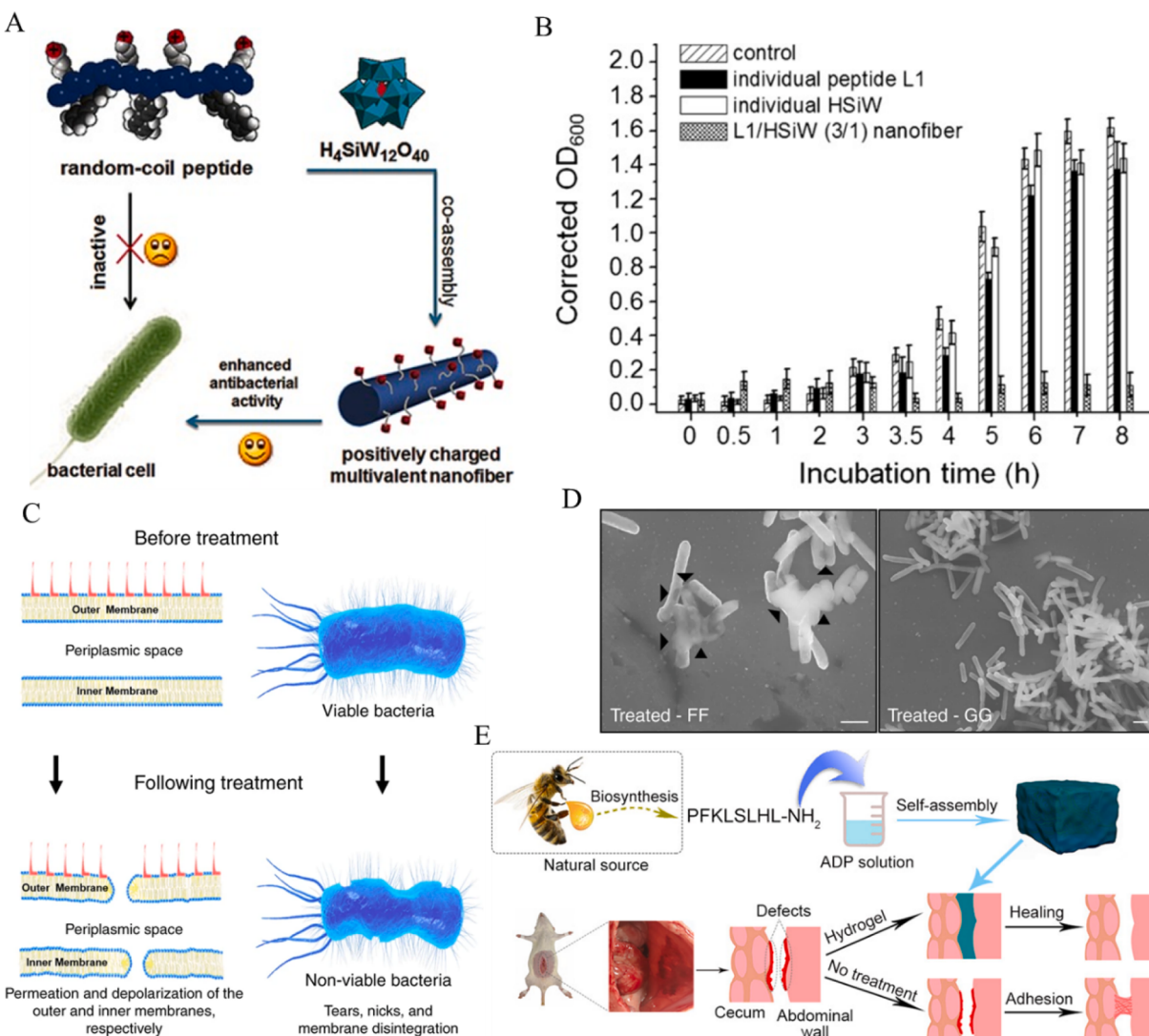


Fig. 15. (A) Polyoxometalate mediated co-assembly with short peptide into well-defined nanofibers for bacterial inhibition. (B) Optical density of *E. coli* after the incubation with different formulations, indicating the highly effective growth inhibition of co-assembled nanofibers. Reproduced with permission from Ref. [230]. Copyright 2016, Wiley-VCH. (C) The proposed antibacterial mechanism of self-assembled FF toward Gram-negative bacteria. FF-bearing nanostructures interacted with the bacterial membrane, leading to the permeation of outer membrane and depolarization of inner membrane. (D) High-resolution SEM images of *E. coli* after treated by FF nanostructures and GG solution. Scale bar: 1 μ m. Adapted with permission from Ref. [231]. Copyright 2017, Springer Nature. (E) Conceptual illustration of constructing peptide-ADP hydrogel and its antiadhesion efficacy in a rat side wall defect-cecum abrasion model. Reproduced with permission from Ref. [239]. Copyright 2022, American Chemical Society.

applications of self-assembled peptides have been reviewed in literatures [240,241].

3.2.2.5. Subunit vaccine/immune adjuvant. Tumor immunotherapy has been widely studied in recent years. As one of the most attractive modalities, tumor vaccine therapy mainly depends on three steps: i) antigen uptake, ii) activating professional antigen-presenting cells (APCs) to elicit T cell responses, iii) effector T cells recognizing tumor cells and eliminating them [242,243]. Despite most peptides eliciting undetectable antibody titers, certain peptides have been found with the ability of eliciting strong antibody responses, which raises the possibility to develop the vaccines and immunotherapies. The key features of peptide-based vaccines were well documented by Skwarczynski and co-workers from the aspects of fast and cost-effective production, clear chemical structure, simple storage condition, easy to develop personalized cancer vaccine, and less likely to induce allergic or autoimmune response [244]. Comparing with molecular immunotherapy, supramolecular nanopeptides display the merits of high immunogenicity, regulated

immune response, and so on [245]. For example, the multivalency of self-assembled peptides enables the repetitive display of epitopes, which therefore improves the affinity with specific receptors to enhance the antibody responses. For cancer immunotherapy, self-assembled supramolecular peptides can function as the vaccines or immune adjuvants.

Self-assembled fibrillar peptides (hydrogels) have been exploited as subunit vaccines or self-adjuvanting vaccines to induce T cell responses. Collier's group reported a peptide consisting of a fibril-forming domain of Q11 (Ac-QQKFQFQQEQQ-Am) and a 17-amino acid OVA peptide (ISQAVHAAHAEINEAGR) with multiple antigenic determinants, which directly elicited high antibody titers with no need for any adjuvants [246]. This response was associated with the covalent binding of the epitope with fibrillizing domain, which self-assembled into long, linear fibrils with the epitope on their surfaces. They further investigated the immunological mechanisms of self-assembling peptide, and found the antibody responses were T cell-dependent [247]. If deleting the T cell-recognizable regions in OVA peptide, immunogenicity would be significantly diminished. Meanwhile, mutating the key self-assembling

residues in Q11 segment could also attenuate the immunogenicity, suggesting that peptide self-assembly played an important role in exerting immune response.

Peptidic nanostructures have also been developed as safe and efficient immune adjuvants to induce a more potent immune response [248,249]. Through interacting with tumor antigens and co-assembly with them for their storage and delivery, peptide-based self-assemblies can prevent rapid antigen degradation, prolong antigen lifetime, assist antigen uptake by targeted cells, and therefore improve the immunogenicity [250]. Luo and colleagues reported a supramolecular hydrogel self-assembled from a D-tetra-peptide, which was simply mixed with antigens for delivery and acted as a novel vaccine adjuvant for enhanced immunotherapy [248]. The injectable vaccines stimulated strong CD8⁺ T-cell response and therefore retarded tumor growth. In another example, a peptide with sequence of Fbp-G^DF^DY^DK(γE)-NH₂ was developed for a protein antigen delivery [251]. The fibril hydrogel formed by peptide and antigen promoted the DC maturation, prolonged the accumulation and retention of antigen in the lymph nodes, and elicited the cytokine secretion.

To optimize the limited efficacy from single-agent immunotherapy, Yang's group reported a tri-functional immunostimulatory supramolecular nanomedicine [252]. Arising from the parallel roles of three functions of indoximod (IND) as IDO inhibitor, DPPA-1 as an antagonist against PD-L1, and an adjuvant of self-assembling G^DF^DY tetrapeptide, the supramolecular nanomedicine could boost the effective immune responses (Fig. 16A, B). Comparing with other formulations, IND-

G^DF^DY-DPPA-1 activated CD8⁺ T cells and CD4⁺ T cells most effectively at the tumor sites, evidenced by the immunohistochemical (IHC) staining of tumor tissues from 4 T1-Luci BALB/c mice (Fig. 16C). Very recently, fluorinated peptide nanovaccine adjuvants containing continuous arginine (R) and fluorinated diphenylalanine peptide (DP) were proposed for enhanced cancer vaccine therapy (Fig. 16D) [253]. Regulating the fluorine (F) amount and R number could modulate the self-assembly performance and antigen-binding affinity. After the screening, 4RDP(F5) has been found with the strongest binding affinity with ovalbumin (OVA, a model antigen). Comparing with the rest of peptides with other R numbers and F amounts, 4RDP(F5) was also most effective to promote DC maturation and antigen's lysosomal escape. As a result, 4RDP(F5)-OVA effectively suppressed the growth of OVA-expressing T lymphoma (EG7-OVA) tumors, resulted from nanovaccine-induced activation of DCs (Fig. 16E).

To enable the reproducible and precise loading of diverse peptide antigens, a generalizable vaccine formulation of peptide antigen-adjuvant conjugates emerged. A nanovaccine of self-assembled peptide-TLR-7/8a conjugate was formed, which effectively activate APCs to promote T-cell immunity [254]. This vaccine platform provided a generalizable strategy to co-deliver any peptide-based tumor antigen and adjuvant with clear molecular structure. To realize the dual features of antigen multivalency from self-assembling vaccines and antigen-specific immune response elicited by adjuvant-antigen conjugates, a series of co-assembled vaccines containing a lipidated human epidermal growth factor receptor 2 (HER2)-derived antigenic peptide with

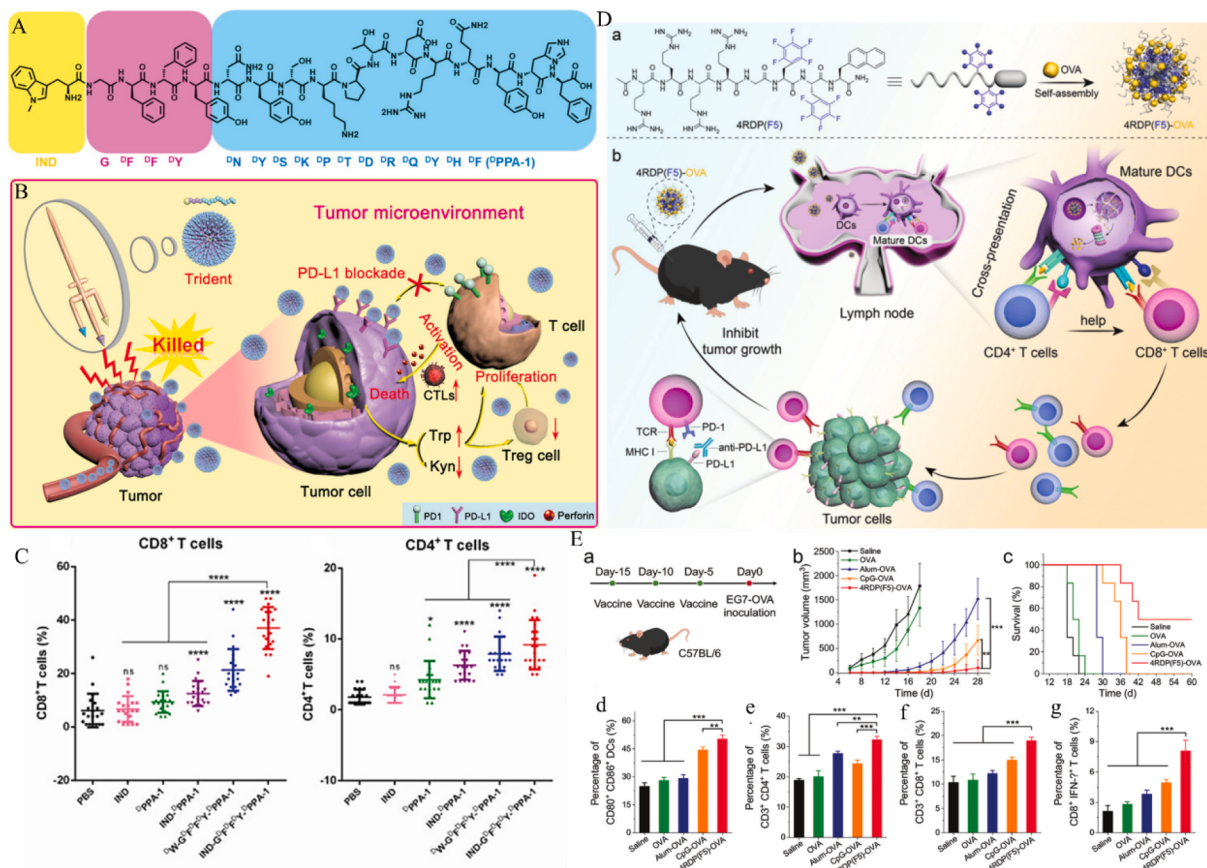


Fig. 16. (A) Structure of the tri-functional IND-G^DF^DY-DPPA-1. (B) Schematic illustration of its anti-tumor mechanism. Self-assembled IND-G^DF^DY-DPPA-1 achieved the tri-function of inhibiting IDO, interfering PD-1/PD-L1 mediated tumor escape, and activating immune response. (C) Statistical analysis from IHC staining of CD8⁺ T cells and CD4⁺ T cells. Adapted with permission from Ref. [252]. Copyright 2021, Wiley-VCH. (D) Self-assembled 4RDP(F5) as an adjuvant to assist OVA for cancer therapy. (a) The forming process of 4RDP(F5)-OVA nanovaccine; (b) Illustration of self-assembled 4RDP(F5)-OVA to inhibit tumor growth. (E) Cancer vaccine therapy evaluation of 4RDP(F5)-OVA. (a) Treatment schedule of nanovaccine in EG7-OVA tumor bearing C57BL/6 mice; (b) Tumor size and (c) survival rate of mice treated by different groups; (d-g) Flow cytometric analysis of mature DCs and T cells. Adapted with permission from Ref. [253]. Copyright 2023, Wiley-VCH.

different lipophilic adjuvants were created as vaccine candidates [255]. The cooperation of antigenic peptide and lipophilic adjuvant elicited a robust immune response.

It has gradually been demonstrated that several factors such as shape, size, surface chemistry and administration route would affect the transport and ultimate immunogenicity of nanomaterials. To ascertain the influence of the dimension on immune responses, helical peptide nanofibers with varying lengths were prepared and their immunogenicity was investigated [256]. In comparison with long nanofibers, short nanofibers were found to be preferentially cross-presented by DCs, and therefore triggered stronger CD8⁺ T-cell responses in mice. The reason that shorter nanofibers triggered stronger immune responses might be ascribed to multiple factors. For instance, shorter nanofibers may possess stronger endosome-escaping ability into the cytosol to increase cross-presentation. Self-assembled nanorod vaccines with an average length of 100–200 nm were also found to be capable of overcoming the limitation caused by the microscale length of cross- β fibrils in vaccinology [257].

3.2.2.6. Treating other diseases. Apart from the typical applications mentioned above, peptide-based nanomedicines have also been exploited to address other diseases such as heparin detection [258], antiviral therapy [259], anti-inflammatory [260,261], liver fibrosis [262] and acute kidney injury [263]. For example, Alzheimer's disease (AD), an important neurodegenerative disease, has seriously affected more than 50 million people worldwide. A proposed mechanism of AD pathogenesis is associated with the mis-aggregation of amyloid- β peptides ($A\beta$) via β -sheet conformation, and FF dipeptide is the core sequence of the mis-aggregation. For this reason, a plenty of research exploited peptide self-assembly to remodel the formation of AD through investigating the self-assembled behavior of FF-containing peptide. In recent years, more and more diagnostic [264,265] and therapeutic platforms [266,267] based on peptide self-assembly have emerged. Photo-oxygenation of $A\beta$ has been demonstrated to efficiently inhibit $A\beta$ aggregation, therefore showing the potential of treating AD. To address the common shortcomings of current PSs with poor blood-brain barrier (BBB) permeability and low selectivity of $A\beta$ photooxygenation, a porphyrin-peptide conjugate (PP-KLVFF) containing KLVFF and an FDA-approved

porphyrin derivative (5-(4-carboxyphenyl)-10,15,20-triphenylporphyrin) was designed to self-assemble into spherical nanostructured PKNPs, which further underwent $A\beta$ -triggered disassembly and suppressed $A\beta$ aggregation through photo-oxygenation (Fig. 17A) [268]. Under light illumination, the excellent photothermal effect of PKNPs effectively improved their BBB permeability. Upon the specific interaction with $A\beta$, PKNPs disassembled and transformed the photothermal activity to photodynamic activity for $A\beta$ photooxygenation. As a result, PKNPs selectively photo-oxygenated $A\beta$ without affecting non-specific proteins. Using transgenic *C. elegans* CL2006 nematode as an AD model, PKNPs decreased $A\beta$ deposition, alleviated $A\beta$ -induced paralysis and motility impairment, and therefore prolonged the life span of AD (Fig. 17B). Shi's group reported a melanocortin 1 receptor (MC1R) peptide agonist of YVLGHFLFDRFG-NH₂, which self-assembled into a fibrous hydrogel to promote skin pigmentation for vitiligo treatment (Fig. 17C) [269]. Comparing with free peptide agonist, self-assembled peptide hydrogel exhibited enhanced biostability, sustained release, and rapid recovery from shear-thinning. After the subcutaneous injection into normal C57BL/6J mice, this peptidyl MC1R agonist hydrogel up-regulated the expression of both tyrosinase and tyrosinase-related protein-1 and 2 (TYRP-1 and TYRP-2), which therefore stimulated melanin synthesis. Masson-Fontana staining showed that the skin treated by hydrogel had the most and richest melanized regions (Fig. 17D), indicating the potential of MC1R agonist hydrogel to promote skin pigmentation.

3.2.3. Tissue engineering material

Apart from the good biocompatibility, desirable biodegradation, feasible design and modification, and biological homology mentioned above, the biological activity confers self-assembled peptide materials with the abilities to interact and communicate with cells and tissues via biomolecular recognition, making them as excellent candidates for tissue engineering materials. For instance, the cell adherable RGD peptide has been well utilized in tissue engineering due to its recognizing binding with integrin overexpressed cells [270–272]. Overall, peptide-based scaffolds have been demonstrated for tissue engineering in literatures [273–275], and herein we discussed the applications of self-assembled peptide hydrogels in the fields of cell culture, promoting

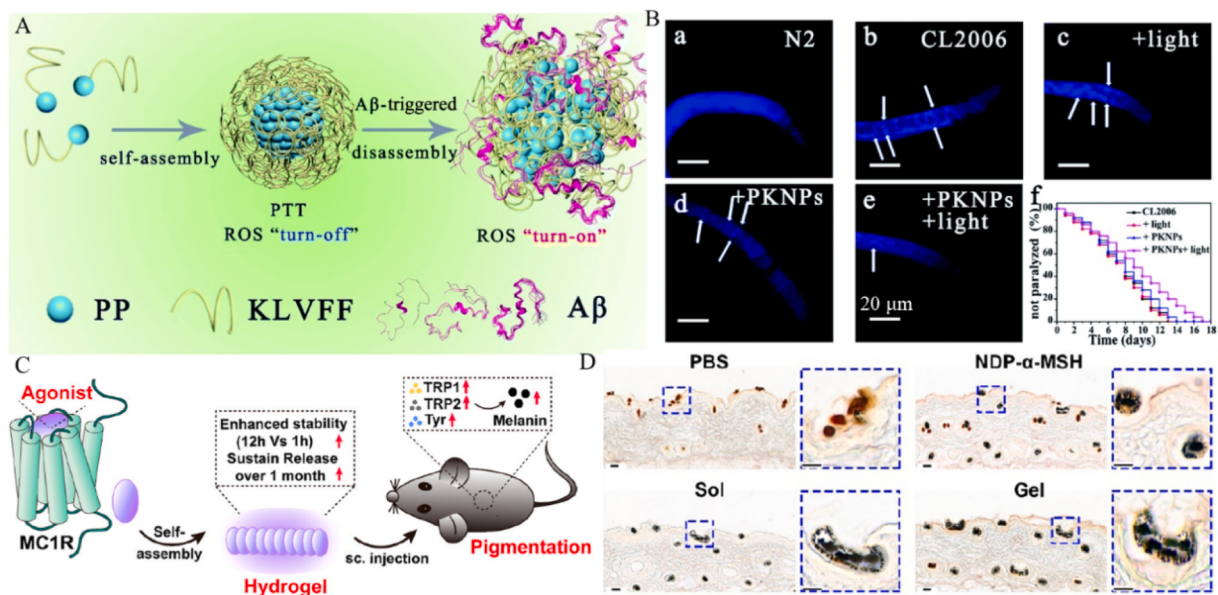


Fig. 17. (A) Illustration of PP-KLVFF self-assembly into PKNPs and $A\beta$ -triggered dis-assembly of PKNPs to initiate photo-oxygenation of $A\beta$. (B) ThS-staining images of $A\beta$ deposits in CL2006 nematodes. White arrows indicating $A\beta$ plaques. (a) Bristol Bristol N2 wild-type strains; (b) untreated; (c) laser irradiation; (d) PKNP; and (e) PKNP & laser irradiation; (f) Survival curves of CL2006 worms treated with different formulations. Reproduced with permission from Ref. [268]. Copyright 2020, Royal Society of Chemistry. (C) Self-assembly of MC1R agonist into an injectable hydrogel and its therapeutic effects in skin pigmentation. (D) Masson-Fontana staining of skin under different treatments. Reproduced with permission from Ref. [269]. Copyright 2023, American Chemical Society.

tissue repairing and regeneration, and remodeling tumor microenvironments.

3.2.3.1. Cell culture scaffolds. To offer an appropriate environment for targeted cells, peptides are generally self-assembled into micro/nano-materials to facilitate cell proliferation, induction, and neo-tissue genesis. In contrast with conventional two dimensional (2D) culture in petri dishes that may change the cell's behavior patterns, three-dimensional (3D) matrices that can mimic their natural behaviors *in vivo* at both phenotypic and genotypic levels, are more suitable for tissue repair and regeneration in their controlled porosities [276,277]. As potent 3D scaffolds, self-assembled peptide hydrogels encompass the following characteristics: i) the easy gelation construction under physiological condition; ii) the high-content water that resembles those of natural tissues; iii) regulatable components to mimic the composition and physicochemical properties of extracellular matrix (ECM); iv) regulatable mechanical properties similar to biological tissues. In an example, self-assembled hydrogels from Fmoc-dipeptides were exploited by Ulijn' group for 3D cell culture [65]. By mixing chondrocyte cells with Fmoc-dipeptide, chondrocytes were observed throughout the hydrogel matrix, and hydrogels supported cell proliferation. Luo and co-workers constructed D-peptide nanofiber scaffold for 3D cell culture. Similar with the L-peptide hydrogels, D-form scaffolds also showed a good biocompatibility, regulatable self-assembling process by external controls, and quick hemostatic feature. Moreover, they were more resistant to proteolytic degradation [278].

Recently, stimulus-responsive peptides have been developed to construct hydrogels for 3D cell culture. An enzymatic Nap-pD-E7 peptide was designed, which aggregated into nanoparticles to anchor mesenchymal stem cells (MSC) and supported them to produce spheroids during the intercellular phosphatase instructed self-assembly [279]. Moreover, MSCs spheroids secreted the growth factors and promoted the neoangiogenesis, and ameliorated heart function. Photo-responsive

peptide hydrogels allow their properties to be remotely controlled. A photo-activated peptide containing 2-nitrobenzyl ester group (NB) was developed to construct photoactivated hydrogel [280]. Fmoc-KDFFF (NB)KK (abbreviated as Fmoc-KDNBK) was designed as a hydrogelator (Fig. 18A), which was photocaged by a positive KK dipeptide whose charge repulsion would prevent the self-assembly in solution. Light irradiation led to the cleavage of NB group, and the removal of KK from Fmoc-KDNBK induced the self-assembly into hydrogel. Because of the spatial and temporal control of light, cells could be mixed with peptide solution to achieve the *in situ* encapsulation for 3D cell culture (Fig. 18B, C). Moreover, the photo-controllable mechanical strength could guide cell spreading on hydrogel surfaces.

Multicellular aggregates, *i.e.*, spheroids, have been well-accepted as 3D cancer models for oncology remodeling *in vitro* [281–284], because of their similarities with human tumors in terms of shape, high cellular density, and chemical environment. 3D spheroid culture is beneficial for potentially understanding tumor cell behaviors, evaluating the aggregation of tumor stem cells, and screening preclinical drugs [285–287]. Self-assembled peptide hydrogels provide suitable 3D environment for tumor cells to form spheroids. The shear-thinning and recoverable behavior of hydrogels facilitate cell loading and spheroid separation. A layer-by-layer bioprinting strategy was proposed to fabricate peptide hydrogel with desirable mechanical property, which could act as a suitable scaffold to generate tumor spheroids [288]. Driven by electrostatic interaction, Fmoc-YD and Fmoc-YK co-assembled into hydrogel after the 3D layer-by-layer printing. Arising from the tunable mechanical strength and suitable degradability, co-assembled fibrillar hydrogel enabled the effective nucleation, growth, and separation of tumor spheroids with size of up to 1 mm. Meanwhile, the growth rate of spheroid could be adjusted by the original cell density in hydrogel. Recently, a biotinylated peptide hydrogel (termed SupraGel) was developed for 3D cell spheroid culture [289]. One D-amino acid was incorporated, with the purpose of decreasing cell-matrix interactions

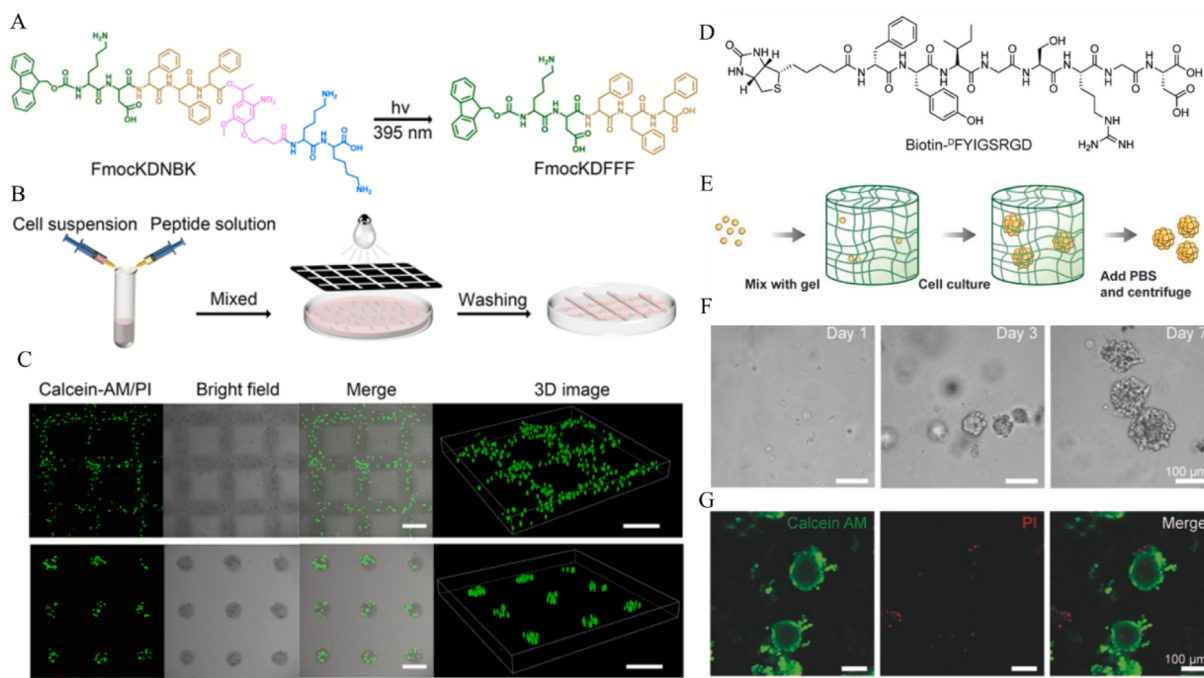


Fig. 18. (A) The photoactivated conversion from Fmoc-KDNBK into Fmoc-KDFFF. (B) Schematic diagram of *in situ* cell encapsulation and subsequent hydrogel photopatterning process. (C) CLSM images of human umbilical vein endothelial cell (HUVEC) cells post-encapsulated in photopatterned Fmoc-KDNBK hydrogel under irradiation. Green fluorescence from calcein-AM representing the live cells. No red fluorescence signal from PI was detected, suggesting the good compatibility of hydrogel. Scale bars: 200 μ m. Reproduced with permission from Ref. [280]. Copyright 2023, American Chemical Society. (D) Structure of the Biotin-D⁰FYIGSRGD. (E) Schematic presentation of cell culture to form spheroid and extracting process. (F) Representative 4 T1 spheroids after different culture times. (G) Live-dead staining of 4 T1 spheroids released from SupraGel after 7 d culture. Scale bars: 100 μ m. Adapted with permission from Ref. [289]. Copyright 2022, Science China Press and Springer-Verlag GmbH Germany, part of Springer Nature.

and facilitating cell spheroid formation (Fig. 18D). After the mixing with SupraGel by gentle vortex, different cells could efficiently form cell spheroids in SupraGel (Fig. 18E). After 7 d cell culture in SupraGel, the average cross-sectional area of 4 T1 spheroids was $11450 \mu\text{m}^2$ (Fig. 18F), and most cells in the spheroids were alive (Fig. 18G). To improve the resistance to proteolytic digestion, D-form peptide hydrogels have been developed for produce tumor spheroids. As an instance, a protease-resistant D-form oligopeptide of Ac-D-Phe-D-Phe-D-Phe-Gly-D-Lys self-assembled into a hydrogel, and HeLa spheroids were well formed in this D-form 3D scaffold [290].

3.2.3.2. Tissue repair and regeneration. Peptides have been widely demonstrated to influence the cell proliferation, migration, and differentiation, which provide the major criteria for tissue repair and regeneration. Through regulating their components to mimic the composition and physicochemical properties of ECM, peptide hydrogels have been developed for the sutureless wound closure [291–293]. In one example, a bioinspired glycopeptide hydrogel self-assembled from β -sheet Q11 peptide-grafted glucomannan was fabricated to imitate the glycoprotein components and ECM fibers to self-accelerate the skin regeneration [294]. The hydrogel directed the polarization of macrophages into M2 phenotype during wound healing process, and therefore promoted wound healing and angiogenesis in the repaired skin tissues. Chu and co-workers also fabricated a series of proangiogenic peptide hydrogels composing of GEETEVTVGLEPG (an angiogenic peptide) and different β -sheet sequences for skin regeneration [295]. The *in vitro* angiogenesis experiments indicated the formation of connected tubes after HUVEC culture on peptide hydrogel surface. New blood vessel growth was observed within 2 weeks after subcutaneous implantation of peptide hydrogels in mice, suggesting the promising function of promoting skin regeneration. By mimicking the structure of platelet-derived growth factors (PDGFs), a self-assembling Nap-FFGVRKKP peptide was designed to simulate the functions of PDGF protein but circumvent the limitations of PDGFs such as poor stability and penetration, and high cost (Fig. 19A) [296]. Similar with PDGF proteins, the self-assembled hydrogel could recognize PDGF receptors (PDGFR) and activate the PDGF signaling

pathway to promote cell proliferation and migration. Using the ionizing radiation-induced injury as a model, self-assembled peptide material showed a good injury repair function. It alleviated the inflammatory response and accelerated skin regeneration.

Recently, coordination chemistry has been employed to construct peptide hydrogels for tissue repair and regeneration. Because GHK tripeptide and copper can accelerate tissue healing, Nap-FFGHK was coordinated with Cu^{2+} to construct supramolecular hydrogel for repairing skin injury (Fig. 19B) [297]. Supramolecular GHK-Cu (Supra GHK-Cu) improved the protease resistance of individual GHK-Cu. Comparing with free GHK-Cu, supra GHK-Cu promoted the collagen deposition, angiogenesis and cell proliferation, which therefore accelerated wound healing more significantly (Fig. 19C, D). According to the H&E staining assay, new skin epithelia, dermis, and appendages were regenerated in the D Supra GHK-Cu treated wound, suggesting the best therapeutic efficacy (Fig. 19E).

Beside promoting the skin regeneration of normal patients, some studies begin to focus on developing self-assembled peptide hydrogels to repair the wound of certain patients. To address the common issues of diabetic wound treatment associating with persistent microbial infection and decreased neovascularization, a self-assembled Fmoc-LFKFF-NH₂ hydrogel was fabricated for diabetic wound treatment [298]. The amyloid-inspired versatile hydrogel elevated the expression of vascular endothelial growth factor A (VEGFA) and hypoxia-inducible factor 1 α (HIF-1 α), and therefore accelerated angiogenesis. Meanwhile, this hydrogel exhibited a broad-spectrum antibacterial activity through a membrane-disruption mechanism, which avoided the bacterial-inflammation and accelerated wound healing. A self-assembling RADA-16I hydrogel scaffold (Ac-RADARADARADARADA-CONH₂) seeded with microvascular cells was injected into rats that suffered from the spinal contusion injury, to evaluate the effect of scaffold vascularization on treating spinal cord injury [299]. Results showed that peptide scaffold containing microvessels not only reduced the inflammation and glial scar formation, but also encouraged axon infiltration into the site of injury.

Short peptides derived from the neuroprotective extracellular

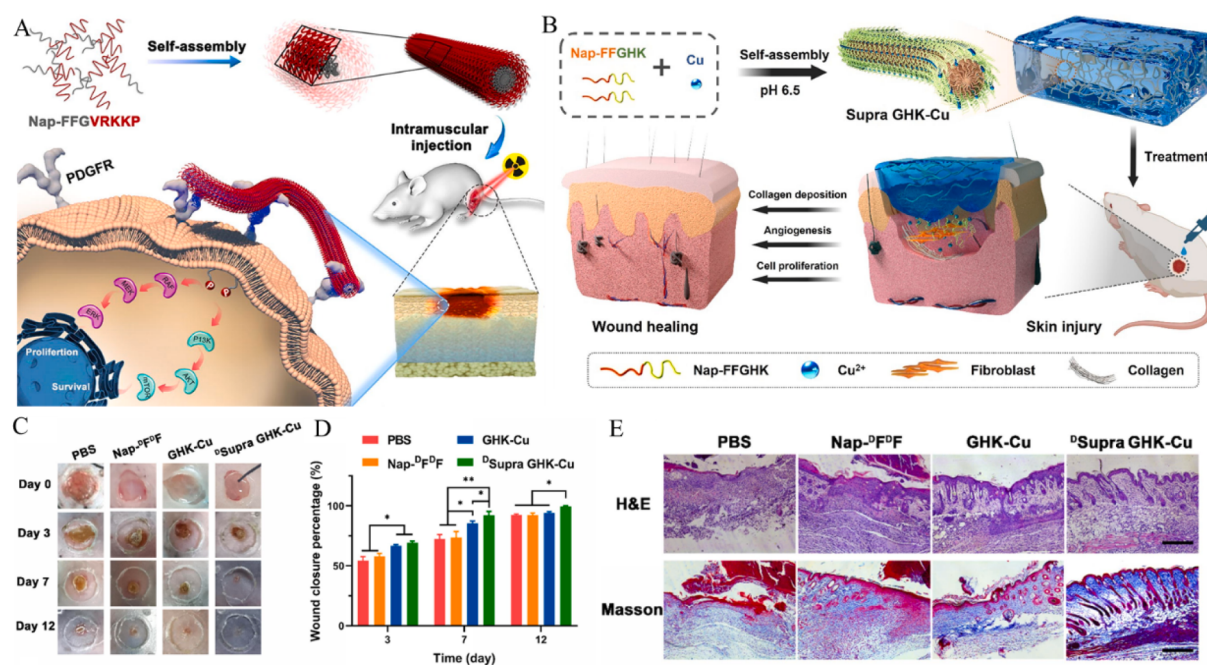


Fig. 19. (A) A self-assembled Nap-FFGVRKKP peptide designed to simulate the function of PDGF proteins for injury repair, Reproduced with permission from Ref. [296]. Copyright 2021, Elsevier Ltd. (B) Nap-FFGHK and Cu^{2+} co-assembling into supramolecular GHK-Cu hydrogel for wound healing. (C) Representative photos of dermal wounds of C57/BL6 mice post-treated with different modalities. (D) Wound closure rate of each group. (E) Representative H&E staining and Masson trichrome images of wound tissues of each group after 12 d treatment. Scale bar: 200 μm . Adapted with permission from Ref. [297]. Copyright 2023, Elsevier Ltd.

glycoprotein ependymin could slow down the side effect of acute glutamate-mediated excitotoxicity (GME) during the traumatic brain injury (TBI) impair, but they suffered from the problem that the easy diffusion away from target sites impaired the therapeutic outcomes [300]. To solve this, self-assembled peptide hydrogels containing an ependymin mimic (a neuroprotective extracellular glycoprotein) were developed to support neuronal survival for TBI impair. The implantable hydrogels could generate a healing microenvironment for neurons and manage the acute pathophysiological sequelae after TBI. In another study, supramolecular nanofibers containing RGD peptides have been identified to augment the therapeutic efficacy of extracellular vesicles (EVs, derived from mesenchymal stem cells (MSC-EVs) and used as a promising cell-free therapy for AKI) in acute kidney injury (AKI) [301]. The peptide hydrogel improved the stability and retention of EVs due to RGD-mediated recognition towards MSC-EVs. The improved EV-loading facilitated the access of microRNA let-7a-5p, which diminished cell apoptosis and increased autophagy levels for kidney repair.

Mechanical cues surrounding cells have been documented to modulate cell behavior and tissue generation. Mechanically dynamic peptide hydrogels offer the models to investigate the influence of mechanical motion on cell behaviors. Two amphiphilic peptides consisting of alternated nonpolar and polar domains self-assembled and cross-linked into hydrogels with well-defined mechanical motion, and the influence of oriented peptide sliding in hydrogel on cell proliferation was probed through the reduction of disulfide bonds [302]. Cleaving the disulfide bonds led to the directional peptide sliding motion along each other, which accelerated the proliferation of incubated cells in the hydrogel via a mechanotransduction mechanism.

3.2.3.3. Remodeling 3D tumor microenvironments. Tumor microenvironment (TME), consisting of various cell types and extra-cellular components, plays an important role in cancer tumorigenesis and progression [303]. Recapitulating TME enables the cancer cell behavior research and the preclinical assessment of anticancer therapeutics. As a key component of TME, tumor ECM shows a strong interdependency with cancer cells. For example, cancer cells would continuously produce fresh excretion and alter the ECM components, which in turn deregulate the signaling within cancer cells to potentiate their invasion [304]. Investigating the physicochemical changes in ECM is beneficial for understanding the occurrence, invasion and metastasis of cancers. The high resemblance to ECM makes self-assembled peptide hydrogels as potent candidates to mimic tumor ECM to recapitulate 3D tumor microenvironments [305]. In comparison with other hydrogels, the entangled nanofiber networks within peptide hydrogels guarantee the essential compositional complexity and heterogeneity of tumor microenvironments [306].

Until now, several peptide hydrogels such as RADA16-1 (Ac-N-RADARADARADARADA)-based sequence [307,308], EAK16-II (AEAEAKAKA EAEAKAK)-based sequence [278,309], h9e (FLIVI-GSII-GPGGDGGD)-based sequence [310], bQ13 (Ac-QQKFQFQQFEQEQQ-Am) [311], P11-I (CH_3CO -QQRQQQQEQQ-NH₂) and P11-II (CH_3CO -QQRFQWQFEEQQ-NH₂)-based sequences have been exploited to mimic 3D tumor microenvironments. Their design and detailed application have been reviewed elsewhere [306], so only a few examples would be illustrated here to decipher the cancer cell behaviors in 3D context and explore tumor progression.

i) Investigating cancer cell behavior

In tumors, cellular behaviors such as viable proliferation, growth, adhesion, migration and invasion are always associated with their surrounded environment. Modulating the biochemical and biophysical properties of peptide hydrogel provides a feasible method to modify the microenvironment to direct cell behaviors. Mi and colleagues evaluated the influence of self-assembled RADA16 hydrogel on the malignant

phenotype of MDA-MB-231 cell, using collagen I and Matrigel as control groups [307]. Compared to 3D collagen I and Matrigel scaffolds, self-assembled peptide hydrogel could effectively reduce the malignant phenotype of MDA-MB-231 and malignancy *in vivo*. Recently, PeptiGeI®Alpha1 (a commercial self-assembling peptide hydrogel) was introduced to remodel the microenvironment of breast tumor *in vitro* [312]. Breast cancer cells survived and proliferated in peptide hydrogel. Moreover, the key features such as hypoxia and invasion in solid tumors could be well recapitulated. MCF-7 and MDA-MB-231 cells representing different stages of tumors could survive and grow in this hydrogel, but they exhibited different cell behaviors. The former formed large spheroids that would proliferate over time, while the latter remained dispersed and formed irregular structures with the invasive feature. Heeschen, Mata, Loessner and co-workers developed a 3D hydrogel to recapitulate the behavior of pancreatic ductal adenocarcinoma (PDAC) *in vivo* (Fig. 20A) [313]. The self-assembled peptide hydrogel doped with ECM components enabled cell culture and drug testing. Comparing with current *in vitro* organoids, according to the proteomic analysis, the culture of PDAC in co-assembled scaffold improved the matrisome recapitulation. Moreover, co-assembled scaffold could more effectively reproduce the patient-specific drug response *in vivo* than other culture models. After the *ex vivo* culture and treated by gemcitabine/nab-paclitaxel (gemcitabine and nab-paclitaxel target cell cycle arrest in M and G2 phase in cell cycle, respectively), cells showed a higher proportion in G1 phase when cultured in peptide-ECM hydrogel scaffold, suggesting the enhanced resistance of tumors (Fig. 20B).

ii) Investigating Cell-Cell and Cell-ECM Interaction

In tumor tissues, cancer cells would reprogram stromal cells through physical or molecular cell interactions. The interplay between cancer cells and stromal cells builds a specific microenvironment to further modulate the malignant properties of cancer cells and promote cancer development [314]. As such, dissecting the cell-cell and cell-ECM interactions in 3D matrices provides the prognostic value and therapeutic target. A self-assembled hydrogel from FEFEFKFK peptide was fabricated to probe the cell-cell and cell-matrix interactions *in vitro* [315]. The biochemical and physical properties of 3D hydrogel could be well customized, which therefore provided the convenience to separately evaluate the influence of biochemical composition and mechanics of matrix on cell behaviors. For instance, the hydrogel exhibited the independent control on matrix stiffness and ECM functionalization. Through adjusting the peptide concentration, hydrogel stiffness could be tailored to match different demands such as normal breast (<1 kPa), breast tumor tissue (>1 kPa), and even higher to favor breast cancer cell viability. Meanwhile, the peptide hydrogels could be customized through adding relevant matrix components to mate target tissues to regulate cell morphology and organization. Moreover, peptide amphiphiles were proposed to co-assemble with ECM proteins to produce tunable microenvironments of ovarian cancer [316]. The co-assembled hydrogel supported the formation of tumor spheroids from single ovarian cancer cell to reach comparative sizes to those cultured in Matrigel. When co-culturing HUVECs and human mesenchymal stem cells (hMSCs) in co-assembled hydrogel scaffold, F-actin networks were found to surround the formed multicellular spheroids, suggesting that cell-cell interactions between different cell types played a role in increasing the spheroid size.

4. *In situ* peptide self-assembly

The preformed peptide nanomaterials based on *ex situ* self-assembly have been widely applied in drug carriers, functional nanomedicines, and tissue engineering, etc. However, the biological barriers during transportation, the suboptimized biodistribution of nanomedicines and tendency of accumulating in the liver and kidney result in suboptimal outcomes and safety concern during disease treatments [317]. In recent

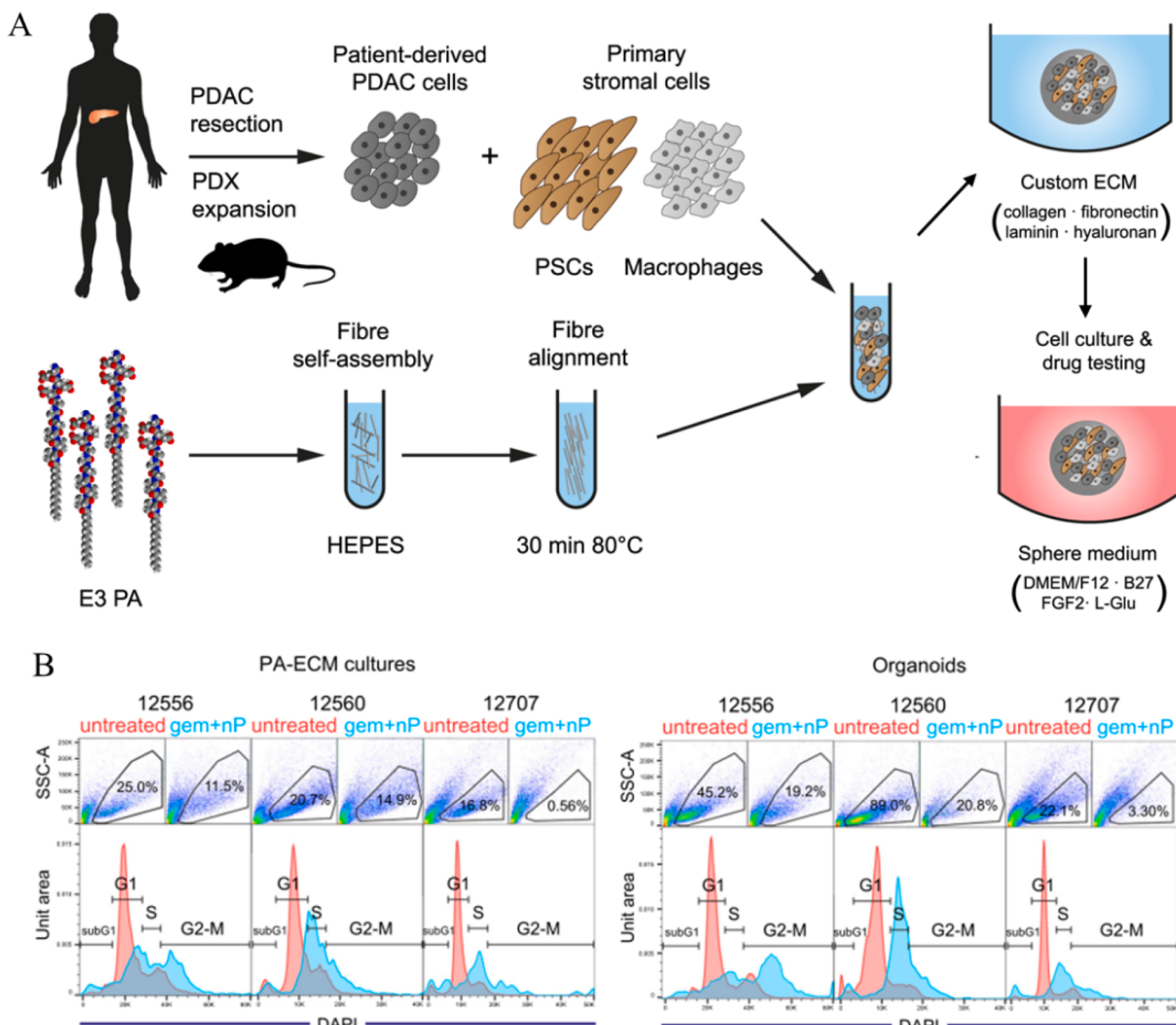


Fig. 20. (A) 3D cell culture of PDAC in co-assembled peptide-ECM to recapitulate the tumor biology. Patient-derived PDAC cells and stromal cells were co-cultured in peptide-ECM hydrogels for culture and drug testing. (B) Flow cytometry data showing the cell cycle arrest of different tumor cells cultured in peptide-ECM scaffold (left) and organoid (right) when untreated/treated with gemcitabine and nab-paclitaxel. Adapted with permission from Ref. [313]. Copyright 2021, Nature Publishing Group.

years, research has begun to focus on the *in situ* self-assembly using peptide/peptide-conjugates as building blocks to construct nanomaterials in living cells. The functional group can be incorporated into peptides at their termini, side chain, and as linkage within backbone (Fig. 21). Attributed to the specific pathological environments or highly level species in lesion location, the on-demand formation of nanomaterials *in vitro/in vivo* would result in certain biological effects, which could be utilized for disease imaging and therapy with high selectivity. These treatments mediated by *in situ* self-assembly show various advantages such as minimal drug resistance, high accumulation, reduced side effects to normal tissues and so on [318,319]. Notably, the strategy is expected to facilitate the drug penetration into deep tumors, because small molecules diffuse faster than their self-assemblies. Moreover, *in situ* formation of nanoparticles *in vitro/in vivo* increased the interaction between cells and nanomaterials. The imaging/therapeutic process generally includes three steps: 1) Initiation. The self-assembly event is commonly initiated by endogenous components in cells/tissues or exogenous stimuli; 2) Aggregation. The *in situ* self-assembly would result in the formation of certain nanoarchitectures at lesion sites. 3) Action. The self-assembled nanostructures exert the bioeffects.

4.1. Trigger module

To trigger the *in situ* self-assembly at where needed, certain pathological features such as low pH, high enzyme expression, high GSH, overexpressed receptors in relevant lesion sites have been considered [1,320]. As a consequence, the *in situ* peptide self-assembly is only/mainly initiated in pathological cells/tissues, facilitating the targeted imaging and therapy towards diseases. In this section, we briefly summarized the trigger module for *in situ* self-assembly and the structure design on peptides/peptide-conjugates. Some of recently reported *in situ* peptide self-assembled systems have been summarized in Table 2.

4.1.1. pH

Different tissues usually hold discrepant physiological environments due to their unique metabolisms. In contrast with the normal tissues with pH of ~7.4, for instance, weak acidity is usually detected in interstitial tumors with pH of 6.5–7.2. Aiming at the discrepancy in pHs, acidity-activatable drug delivery systems have been established via *ex situ* self-assembly strategy discussed above. Similar with the *ex situ* peptide self-assembly, ionizable amino acids and pH-sensitive linkers are usually introduced to create the building blocks for *in situ* peptide self-assembly. To circumvent the limited solid-tumor penetration of

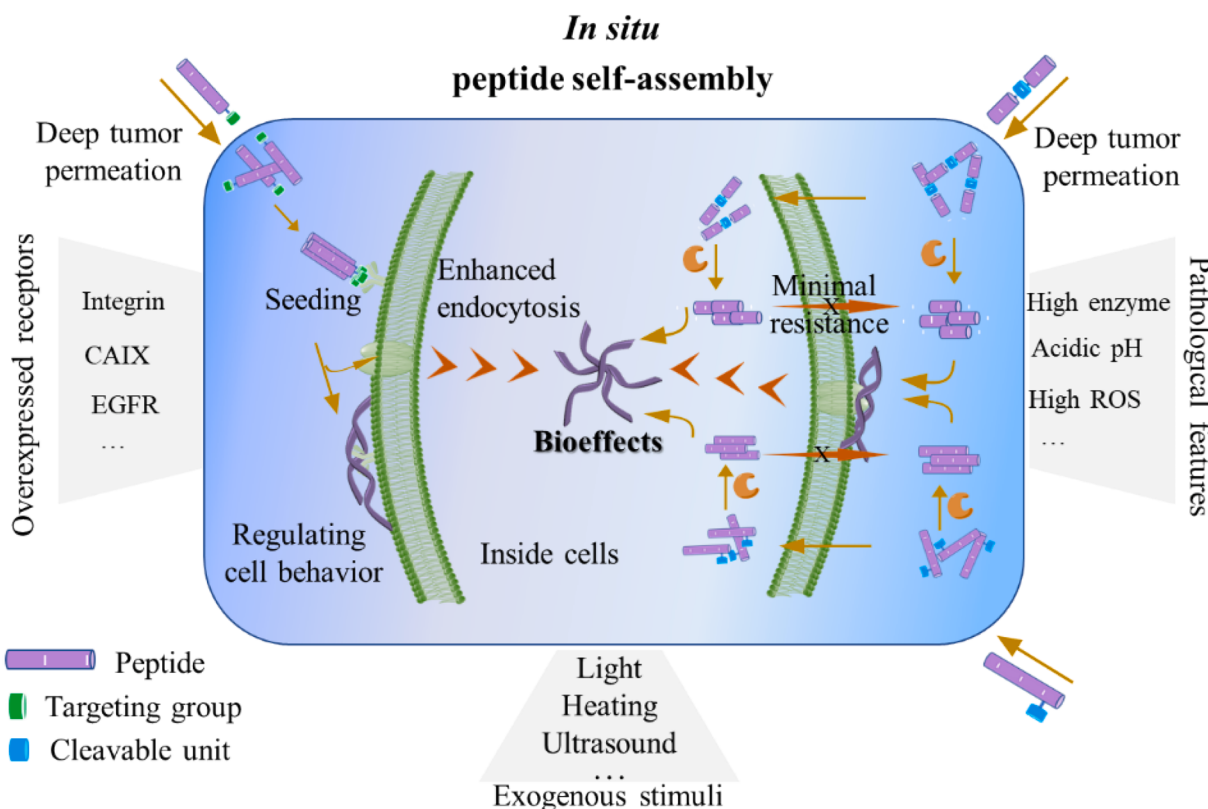


Fig. 21. Schematic illustration of peptide-based *in situ* self-assembly. Peptide formulation, trigger module, self-assembling process, and resultant bioeffects were illustrated. For one formulation, peptide is appended with targeting group to recognize overexpressed receptors and locates on cell surface. Then it acts as the “seed” and recruits more surrounding peptide for *in situ* self-assembly. Peptide self-assemblies can be located on cell surface to regulate cell behavior, or enter cells to elicit bioeffects. Comparing with individual molecules, the *in situ* formation of nanoparticles around cells enhanced endocytosis. For the other formulation, cleavable bond is incorporated into peptide backbone or side chain, which is cleaved by certain species inside cells or outside cells to initiate *in situ* self-assembly. The *in situ* formation of nanoparticles inside cells effectively retards drug efflux, which therefore minimizes drug resistance. Overall, aggregation/assembly induced retention (AIR) effect significantly increases the accumulation and retention of cargoes in the targeted cells/tissues.

nanomaterials, Wang's group designed a polymer-peptide conjugate (PT-K-CAA) that could undergo acid-induced self-assembly in tumor issues for cancer therapy (Fig. 22A) [321]. PT-K-CAA was designed by modifying a poly(β -thioester) backbone with a therapeutic KLAK peptide and a cell penetrating peptide of TAT. To endow this system with pH-sensitivity, KLAK segment was decorated with a pH-cleavable *cis*-aconitic anhydride (CAA) moiety to generate K-CAA. Owing to its molecular level size, PT-K-CAA chain could penetrate deeply into solid tumors, which thereafter responded to the weak acidity to initiate *in situ* self-assembly and recovered the therapeutic function of KLAK peptide (Fig. 22B). The *in situ* formation of nanoparticles in tumor improved drug internalization. As a result, the therapeutic outcomes were improved. Yamamoto and co-workers also exploited the pH-induced intracellular peptide self-assembly to kill cancer cells. The non-cytotoxic palmitoylated hexapeptide of C₁₆-VVAEE self-assembled into entangled nanofibers (hydrogel) in cancer cells and therefore displayed potential cytotoxicity. The cytotoxicity induced by *in situ* peptide self-assembly was correlated with intracellular pH values and showed remarkable anti-tumor activity towards acidic tumors [322]. Very recently, Han's group developed a chimeric peptide-conjugate that underwent pH-induced self-assembly *in vivo* to realize the synergistic PDT and PTT, as well as PA imaging (Fig. 22C) [323]. At physiological condition, the PEG and carboxylates within peptide residues increased the molecular hydrophilicity, which helped peptide-conjugate exist in a small size. At tumor extracellular acidic microenvironment, the protonation of carboxylates within peptide increased the hydrophobicity, leading to the formation larger nanoparticles (Fig. 22D). Thus the increase in size contributed to the improved cell internalization and tumor

accumulation of nanoparticles for better PDT, probably because large nanoparticles contain more monomers when compared to small nanoparticles. As a result, more monomers would be internalized when cells ingested the same number of nanoparticles. In the meanwhile, PDT-mediated cell death activated the caspase-3 enzyme, which cleaved DEVD peptide backbone and led to the aggregation of photosensitizer in apoptotic cells. The aggregated photosensitizer did not emit fluorescence or generate singlet oxygen, but showed higher photothermal feature for PTT. Meanwhile, the aggregation of photosensitizer enhanced the PA signal, which could be used to image the apoptotic cell and evaluate the therapeutic response.

4.1.2. Enzyme

Enzyme is one of most widely exploited pharmacological components to trigger the *in situ* self-assembly of peptides and their derivatives in cells and tissues [324]. Achievement of enzyme-responsive peptide self-assembly *in vivo* lies in the incorporation of chemical moieties that are sensitive to enzymes. According to the design principles, two routes have been formulated. The first is that the self-assembling precursors are prepared by modifying peptide units with certain blocking groups to inhibit the self-assembly outside the cells/tissues. After reaching the targeted sites, enzymes remove the blocking groups from their non-assembled precursors, leading to enzyme-instructed peptide self-assembly *in situ*. Xu and co-workers first reported the esterase-instructed intracellular self-assembly of functional peptides to regulate cell death [325]. C₁₀H₇CH₂C(O)-Phe-Phe-NHCH₂CH₂OH as a self-assembling building block was introduced, which was connected with butyric diacid *via* a cleavable ester bond for the enzymatic target. The

Table 2*In situ* peptide self-assembly triggered by different modalities for biomedical application.

Sequence	Trigger module	Formed morphology	Feature	Application	Refs
CGGG(K(CAA)LAK(CAA)LAK(CAA)) ₂ -poly(β-thioester)-CYGRKKRRQRRR (CAA: <i>cis</i> -aconitic anhydride)	pH	Nanoparticle	Achieving the deep-penetration of drugs for enhanced therapy	Tumor therapy	[321]
C ₁₆ -VVAEEE	pH	Entangled nanofiber	Noncytotoxic free peptide self-assembling into cytotoxic nanofibers for anti-tumor	Tumor therapy	[322]
C ₁₀ H ₇ CH ₂ C(O)-FF-NHCH ₂ CH ₂ OH	Esterase	Nanofiber/hydrogel	Noncytotoxic peptide self-assembling into cytotoxic nanofiber in cancer cell	Tumor therapy	[325]
NapFFK(NBD)pY (pY: L-phosphotyrosine)	Alkaline phosphatase (ALP)	Nanofiber/hydrogel	Providing a convenient approach to study the self-assembly of small molecules inside cells	Imaging the enzyme-triggered self-assembly	[326]
NBD-(^D NaI)- ^D F ^D F ^D pY (^D pY: D-phosphotyrosine)	ALP	Nanofibril	Spatiotemporally profiling the ALP activities in live cell	To understand reversible phosphorylation-dephosphorylation in extracellular domains	[327]
NBD-FFpYK(TPP)	ALP	Nanoscale assemblies	Enzyme-induced <i>in situ</i> self-assembly and mitochondrial targeting	Selectively killing cancer cells without drug resistance	[328]
NBD- ^D F ^D F ^D pY ^D (Me ₂)	ALP	Nanofiber	Targeting the immunosuppressive tumors <i>in vivo</i>	Selectively inhibiting bone tumors	[329]
NBD-LLLpY (1Lp); NBD-lllpY (1Dp)	ALP	Forming micelles and then converting into nanoribbons	Accumulating in cell nuclei and likely interacting with histone proteins in nuclei	Selectively killing osteosarcoma cells	[330]
(KLAKLAK) ₂ -K(pY)Y	ALP	Nanoparticle and co-assembly with ALP into larger assembly	Inducing cell membrane phase separation with improved drug internalization	Tumor therapy	[331]
C16-E4Y	Tyrosine kinase	Nanofiber	Inducing endoplasmic reticulum stress that caused apoptotic cell death	Tumor therapy	[332]
N-palmitoyl-GGGHG PLGLARK-CONH ₂	MMP-7	Nanofiber/hydrogel	The formation of hydrogel inside the cells to exert vital stress on the cancer cells	Tumor therapy	[333]
AVPIAQKDEVDKLVFFAEC(Cy)G	Caspase-3/7	Fibrous superstructures	Recognizing the X-linked inhibitor of apoptosis protein (XIAP) to activate caspase-3/7	Drug delivery and cancer imaging	[334]
BQA-GFFF	ROS	Nanofiber/hydrogel	The selective formation of fluorescent assemblies in malignant cells	Tumor imaging	[336]
BQA-GFFF	ROS	Nanofiber network	<i>In situ</i> formation of nanofibril network at inflammatory loci capable of mimicking the NETs to inhibit MRSE infection	Combating bacterial infection	[337]
N ₃ -quinazolinone-FFG	H ₂ S	Nanofiber/hydrogel	Detecting H ₂ S production and distribution in different sub-cellular organelles	H ₂ S-mediated cell imaging	[338]
ICG-PEP-c(RGD)fk (PEP: GSH-responsive FF dipeptide)	GSH	Nanofiber	Targeting glioma, strong tissue penetration and a long functional time in tumors	Enhanced PTT and potential theranostic	[339]
E3C16E6 and ER-EVM ^{SeO}	GSH	twisted nanofibrils and flat nanoribbons	<i>In situ</i> self-sorting and simultaneous targeting of endoplasmic reticulum and Golgi apparatus	Cancer therapy	[340]
NBD-GFFpY-ss-ERGD	ALP and GSH	Nanoparticle and then nanofiber	Enhancing therapeutic selectivity towards cancer cells	Potential tumor therapy	[341]
CPT-C ₅ -GNNNQNY-RGD	Integrin α _v β ₃	Nanocluster/nanofiber	Addressing the poor solubility and cell penetration of CPT	Augmenting PDC cell-entry efficiency	[342]
Pyrene-FFK (acetazolamide)K(TPP)	Carbonic anhydrase IX (CAIX)	Fibrous aggregate	Charge-reversal at the lysosome	Disrupting the lysosomal membrane and inducing cellular apoptosis	[343]
TPE-SKDEEWHK NNFPLSPNTYYEDQG KRRFFRRK	PD-L1	Dense nanofibers	Blocking the PD1/PD-L1 axis and reversing the immunosuppressive TME	Cancer therapy	[344]
Rhodamine-FFYEGK(Van)	Negatively charged lipid membrane D-Ala-D-Ala	Nanoaggregates	High antibacterial activity, cytocompatibility, and cost-effectiveness	Antimicrobial therapy	[345]
NBD-GFFpYHWYGYTPQNVI	ALP and EGFR-targeting	Polymorphic fibrils	Significantly increased fluorescence signal at the MRSA infected site	Imaging MRSA-infected myositis and lungs in mice	[346]
poly(β-thioester) modified with CGGG(KLAKLAK) ₂ , CYGRKKRRQRRR and ICG	Near-Infrared Laser (NIR)	Nanoparticle	Enabling artificial control on cancer cell membrane components	Cancer cell membrane engineering	[347]
PEG-tk-(P18)-D(KLAKLAK) ₂	Ultrasound (US)	Nanoparticle	Deep tissue penetration and NIR laser guided <i>in situ</i> self-assembly for improved drug accumulation in tumor	Deep tumor therapy	[348]
			Deep penetration of small drug molecules and US-induced cascade effect for synergistic cellular internalization	Orthotopic pancreatic cancer therapy	[349]

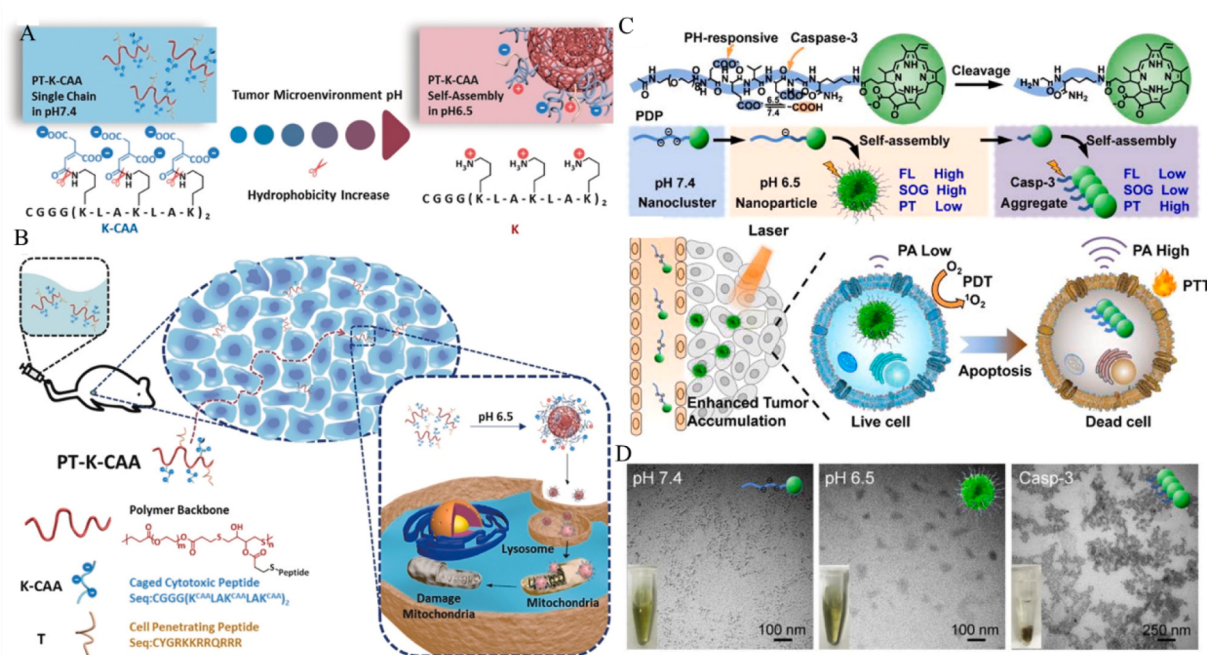


Fig. 22. (A) pH-induced hydrolysis of PT-K-CAA leading to the *in situ* self-assembly to form nanoparticles. (B) Schematic diagram of the improved deep-penetration of free PT-K-CAA into tumor, and pH-mediated self-assembly in tumor tissue to form nanoparticles for high drug internalization and mitochondrial damage. Reproduced with permission from Ref. [321]. Copyright 2019, Wiley-VCH. (C) The structure and schematic illustration of chimeric peptide that underwent pH- and Casp-3 induced sequential self-assembly *in vivo* to realize the synergistic PDT and PTT, and PA imaging. (D) TEM images of PT-K-CAA at different pHs and in presence of Casp-3. Adapted with permission from Ref. [323]. Copyright 2022 Elsevier.

precursor failed to self-assemble in normal cells but aggregated into nanofibers and hydrogelation in HeLa cells to induce the cell death. Along with the design criteria, they pioneered a series of soluble phosphorylated peptide precursors. In their design, phosphorylation on peptide residues to create phosphorous ester was exploited to construct soluble precursors, which were dephosphorylated by overexpressed alkaline phosphatase (ALP) in tumor cells and actualized the intracellular self-assembly to regulate cell behaviors [326–330]. Recently, Wang's group synthesized a phosphopeptide (Kyp), which contained an anticancer (KLA_nLAK)₂ peptide and a phosphoric acid-containing tyrosine (Fig. 23A) [331]. Once encountering ALP, Kyp was dephosphorylated and co-assembled with ALP *in situ* to form nanocomplex on cell membrane, leading to the phase separation of protein-lipid. Using giant plasma membrane vesicle (GPMVs) as a model cell, the separation of lipid and protein was visually evaluated. Comparing with the homogeneous and symmetrical distribution of red signal (from Dil introduced to mark lipid) and green signal (from FITC used to label ALP) on the GPMV membrane, incomplete green fluorescence was observed after the Kyp treatment (Fig. 23B). The dissociation of lipid and protein was also observed in HeLa cells (Fig. 23C). The increase in membrane permeability resulted in improved drugs internalization for enhanced mitochondrial apoptosis. Different from the dephosphorylation-induced intracellular self-assembly, Maruyama's group proposed a phosphorylation strategy to trigger *in situ* peptide self-assembly for cancer therapy (Fig. 23D, E) [332]. Induced by overexpressed tyrosine kinase in cancer cells, a tyrosine-containing C16-E4Y transformed into phosphorylated C16-E4pY, which self-assembled into nanofibers (Fig. 23F) and induced endoplasmic reticulum (ER) stress to trigger cell apoptosis.

Apart from the strategy of using enzymes to detach the steric blocks to initiate *in situ* peptide self-assembly, the other route is designing enzyme-cleavable peptide substrates. One typical example is incorporating matrix metalloproteinases (MMPs)-sensitive peptide sequences to construct the precursors. N-palmitoyl-GGGHGPLGLARK-CONH₂ was selected by Maruyama's group because of its sensitivity against MMP-7 [333], which hydrolyzed the precursor to generate peptide gelator.

Inside cancer cells, the molecular gelator self-assembled into nanofibers to impair cellular function. Caspase, a kind of protease enzyme that plays an imperative role in cell apoptosis, is also a common target for cancer treatment. Xu, Wang, Zhao and co-workers designed a multi-functional peptide of AVPIAQK-DEVD-KLVFFAEC(X)G, which could be used for cancer imaging/therapy by incorporating different groups (X, representing the imaging/chemotherapeutic agent) [334]. Peptide precursor containing AVPIAQK specifically recognized the overexpressed X-linked inhibitor of apoptosis protein (XIAP), which activated the downstream caspase-3/7 to target the DEVD linker. The formed nanostructures self-assembled from residual KLVFFAEC(X)G *in vivo* significantly improved the retention of functional imaging/chemotherapeutic agents in tumor tissue.

4.1.3. Oxidative/reducible substance

High level ROS in pathological lesions bestows ROS as an important endogenous stimulus to trigger and control the peptide self-assembly *in situ*. To endow the self-assembling precursors with ROS-sensitivity, ROS-cleavable moieties such as thiol-ether bond, thiol-ketal bond, selenoether bond, ferrocene, phenylboronic acid/ester and oligo-proline are generally incorporated into peptides [335]. ROS-mediated oxidation reaction modulates the hydrophobicity of precursors and thereby regulates their aggregating propensity. Huang and co-workers reported a ROS-induced supramolecular self-assembly strategy to image cancer cells [336]. The precursor consisted of a GGFF tetrapeptide and a quinazolinone derivative (BQA) that was modified with an aryl boronate immovable linker. It failed to self-assemble in solution. ROS-induced oxidation detached the boronate group and facilitated the formation of intramolecular hydrogen bond inside malignant cells. The intramolecular hydrogen bond planarized BQA-peptide, which self-assembled and generated a fluorophore once above a critical concentration to identify cancer cells. They further used this strategy to mimic the neutrophil extracellular traps (NETs) to combat methicillin-resistant staphylococcus epidermidis (MRSE) infection [337]. The *in situ* formation of nanofibril network efficiently trapped MRSE, which prevented

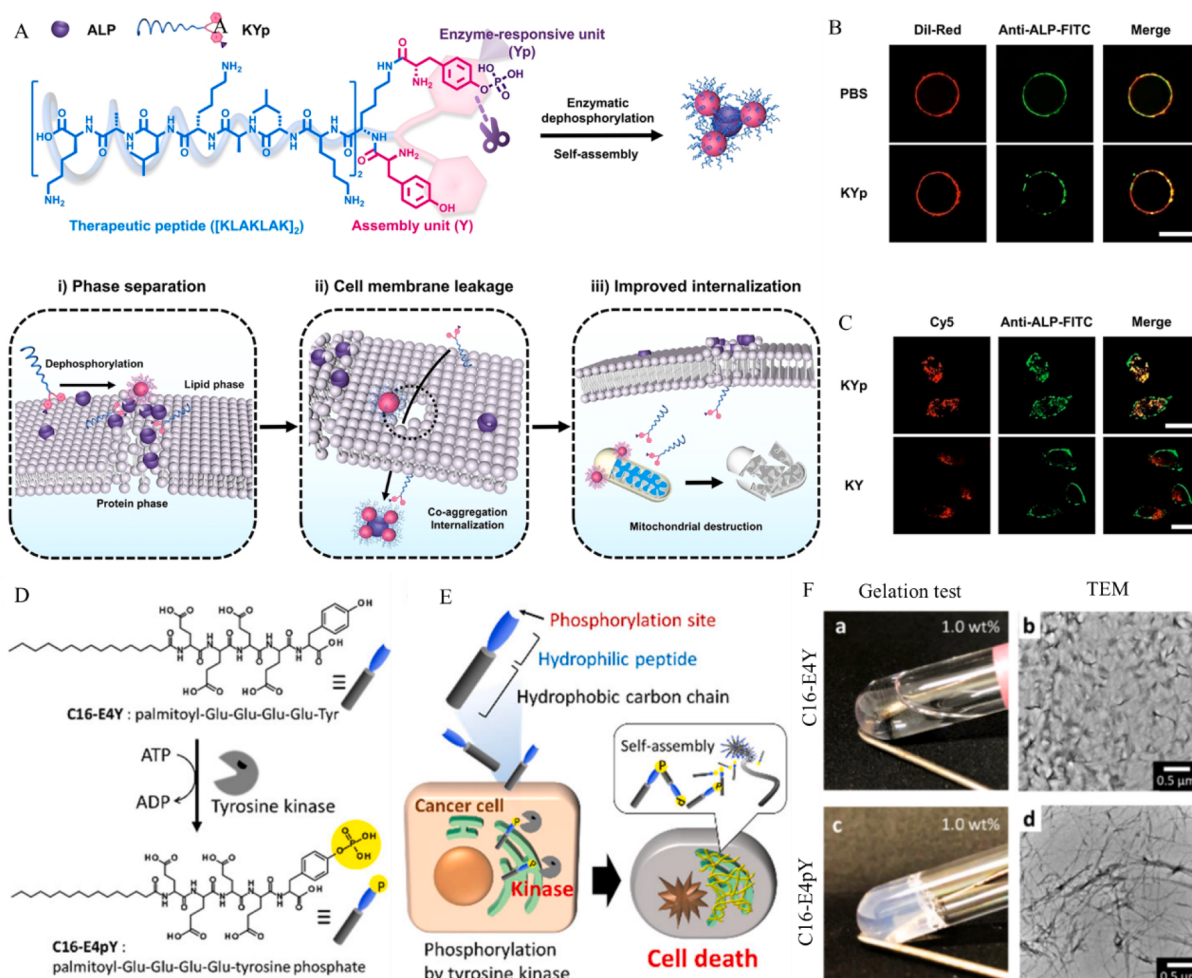


Fig. 23. (A) Peptide structure of KYp and its ALP-induced self-assembly on the surface of cell membrane, which resulted in phase separation, membrane leakage and improved drug internalization. (B) CLSM images of GPMVs treated with or without KYp. (C) CLSM images of Hela cells with Cy5-KYp and Cy5-KY treatments, respectively. Adapted with permission from Ref. [331]. Copyright 2021, Wiley-VCH. (D) Molecular structures of C16-E4Y and C16-E4pY. (E) Schematic illustration of phosphorylation-induced intracellular self-assembly for selectively killing tyrosine kinase overexpressed cancer cells. (F) Tyrosine kinase induced self-assembly and gelation. (a, c) Photos of C16-E4Y solution in PBS and resultant phosphorylated C16-E4pY hydrogel. (b, d) TEM images of corresponding peptide solutions. Adapted with permission from Ref. [332]. Copyright 2022, American Chemical Society.

them from aggressive dissemination.

Recently, reducing agents such as H₂S and GSH have been introduced to regulate peptide self-assembly *in situ*. A tri-peptide of FFG equipped with an azido-quinazolinone derivative was designed [338]. In the presence of H₂S, the reduction reaction converted the azido group to an amine, facilitating the formation of intramolecular hydrogen bond. As a result, formed hydrogen bond planarized the self-assembling molecules and thereafter promoted the supramolecular self-assembly. Disulfide linkage bearing peptide and peptide-conjugate can response GSH, and GSH-induced *in situ* self-assembly were proposed [339,340]. For example, Yu and co-workers designed different GSH-responsive peptides, which initiated *in situ* self-assembly and exhibited the self-sorting feature for simultaneous organelle targeting [340]. E₃C₁₆E₆ and EVM^{SeO}, the structures of which were shown in Fig. 24A, underwent GSH-induced reduction in cancer cells. The disulfide bond cleavage and selenoxide reduction led to the self-assembly of E₃C₁₆E₆ and EVM^{SeO}, respectively. The liberated thiol groups from disulfide bond could react with cysteine-rich proteins from Golgi apparatus to realize Golgi-targeting. Equipping EVM^{SeO} with *p*-toluene sulfonamide (Ts) unit endowed Ts-EVM^{SeO} with endoplasmic reticulum (ER) targeting. Even mixing the peptides of in one system and incubated with GSH, the SIM images showed separated green and red signals under the merged channels (Fig. 24 B, C), suggesting the self-sorting feature of nanofibrils

self-assembled from $E_3C_{16}E_6$ and EVM^{SeO} .

Beside the mono-trigger for *in situ* peptide self-assembly, Yang's group used ALP and GSH to tailor the tandem peptide self-assembly in liver cancer cells [341]. In liver cancer cells that possess high content of ALP and GSH, ALP induced peptide self-assembly into nanoparticles, which further transformed into nanofibers due to the high GSH. Comparing with individual molecules, the *in situ* formation of nanoparticles around cells showed more efficient cellular uptake. Inside cells, the transformation from nanospheres into nanofibers improved the retention time owing to their larger size of nanofibers. Owing to the tandem self-assembly strategy, peptide exhibited the improved cellular uptake in liver cancer cells, which therefore exhibited the selective growth inhibition of liver cancer cells.

4.1.4. Receptor

As we know, abnormal cells and tissues would generally over-express different receptors, and certain peptide sequences or functional moieties can recognize these receptors through receptor-ligand interactions. With this foundation, peptide ligands and targeted groups can be integrated into peptide nano-systems, which can be captured by cancer cells/tissues and act as the “seeds” to recruit more individual peptides for *in situ* self-assembly. For example, Wang’s group used the integrin receptor-mediated *in situ* self-assembly to improve the cell-entry efficiency of

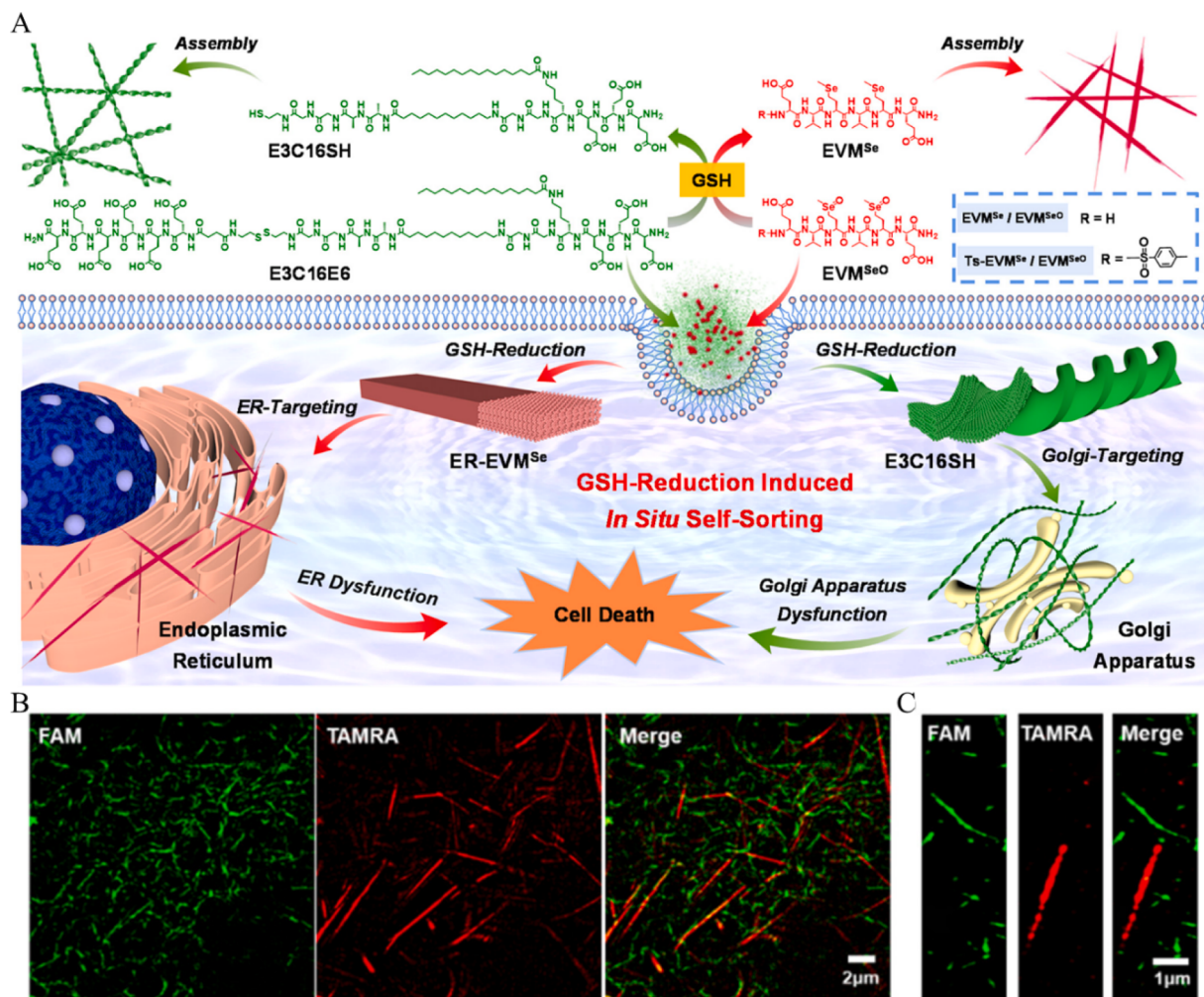


Fig. 24. (A) Illustration of GSH-mediated *in situ* self-assembly of E₃C₁₆E₆ and EVM^{SeO} and their targeting toward ER and Golgi apparatus. (B, C) SIM images of mixed E₃C₁₆E₆ (containing FAM-E₃C₁₆E₆) and EVM^{SeO} (containing TAMRA-EVM^{SeO}) after the 24 h GSH co-cubulation. The separated green and red nanofibrils indicated the GSH-induced self-sorting assembly of two peptides. The fluorescence of FAM (green) and TAMRA (Red) was collected under channels I and II, respectively. Adapted with permission from Ref. [340]. Copyright 2022, American Chemical Society.

therapeutic drugs for cancer therapy [342]. To mitigate the poor water-solubility of CPT drug, CPT was modified by an RGD tripeptide and a self-assembling GNNNQNY sequence. The yielded peptide-drug conjugate could be recognized by integrin-overexpressed tumor cells and recruited pure peptide molecules (without drugs) for co-assembly. *In situ* formation of nanoparticles improved the cell-entry efficiency of individual CPT-peptide. This strategy raised the maximum drug tolerance dose in breast and bladder xenografted mice models and therefore increased the therapeutic efficacy. Recently, Ryu and colleagues reported a carbonic Anhydrase IX (CAIX)-induced peptide self-assembly *in vitro* [343]. In ECM, the peptide amphiphile (Pep-AT) containing CAIX-targeting moiety (Fig. 25A) recognized the CAIX and improved the local concentration, thereafter self-assembling into fibrous nanoaggregates on the surface of CAIX overexpressed HeLa cells (Fig. 25B). Through CAIX-mediated endocytosis, the negative nanofibers reversed their charge in acidic lysosome, which further disturbed membrane integrity for cancer cell apoptosis. The proposed mechanism was illustrated in Fig. 25C.

Multimodal therapy combining immune checkpoint blockade and reversing immunosuppressive TME is capable of improving anti-tumor immunity, but the suitable dose and administrating order of individual agents remain elusive. To address these issues, researchers have proposed “all-in-one” drugs, which integrates different agents in one system. But the synergy among multiple agents is not well solved. By an “*in vivo* *in situ* screening” strategy, Wang and co-workers obtained a

totipotent “all-in-one” peptide (TAP) of TPE-SKDEEWHKNNFPLSPNTYYEDQG, which showed the multiple functions of PD-L1-induced self-assembly, blocking PD-1/PD-L1 axis, interfering the formation of Rbm38-eIF4E complex, and activating p53 (Fig. 25D) [344]. Once recruited by PD-L1 protein, TAP would rapidly self-assemble into dense nanofibers on the tumor cell membrane surface (Fig. 25E), which therefore blocked the PD1/PD-L1 axis.

4.1.5. Others

Beside using disease-relevant biomarkers as internal stimuli, inherent structure features of bio-membranes can also act as the target to manipulate *in situ* peptide self-assembly. Shen and co-workers found a cationic octapeptide of KRRFFRRK (termed as FF8) interacted with the negative lipid membrane and therefore self-assembled into nanofibers [345]. The *in situ* formation of nanofibers on the bacterial membrane led to the breakage of lipid membrane and pore formation, which caused continuous membrane leakage and bacterial death. Capitalizing on the targeting binding of vancomycin (Van) toward D-Ala-D-Ala in Gram-positive bacterial cell walls, Liu *et al.* developed fluorescent- and isotopic-labelled probe (Rho-FF-Van) that self-assembled on the Gram-positive bacteria surface for infection imaging [346]. Rho-FF-Van targeted the bacterial walls and located on their surfaces, which further recruited the surrounding Rho-FF-Van molecules for self-assembly. The formed nano-assemblies emitted a strong fluorescence at the infected

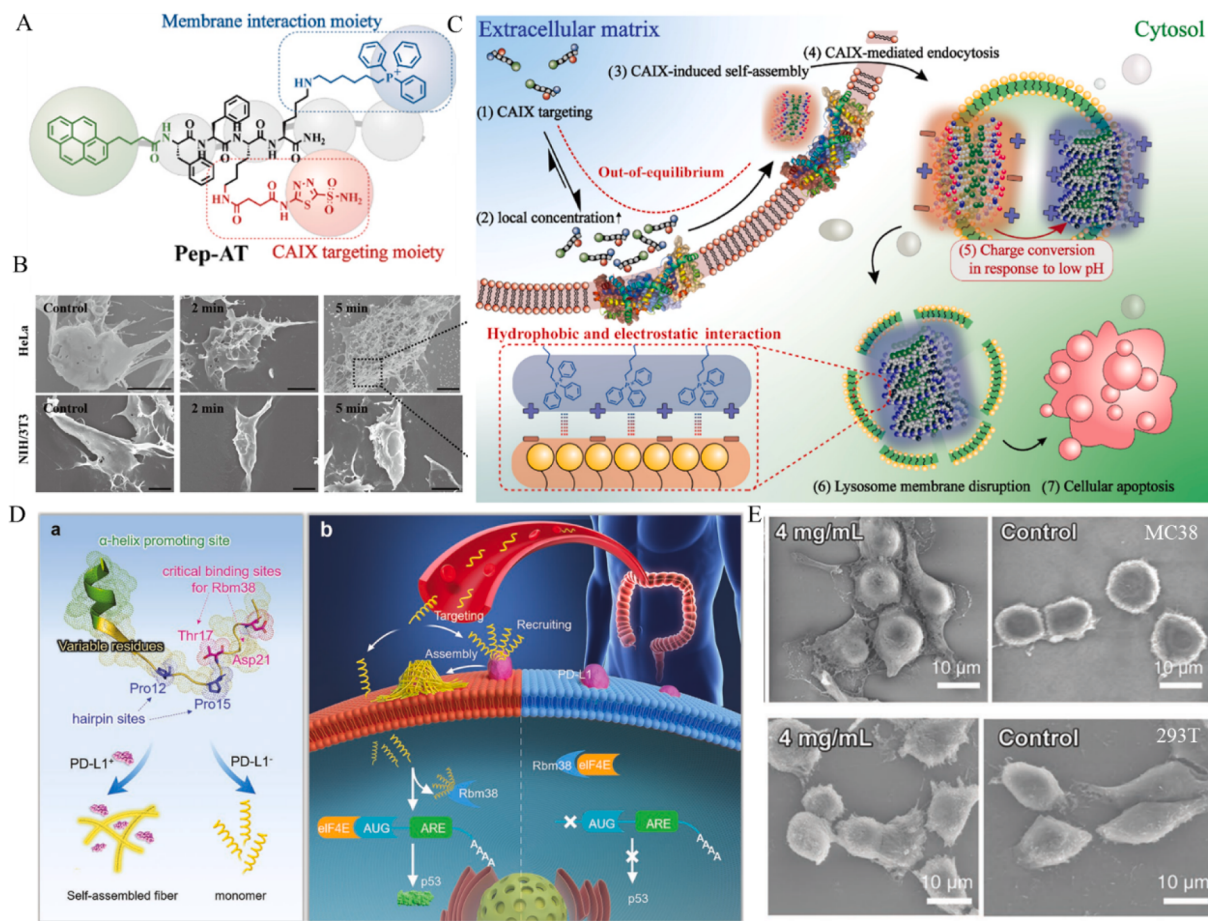


Fig. 25. (A) The chemical structure of Pep-AT. (B) Representative SEM images of HeLa and NIH/3T3 after treatment with Pep-AT. The formation of nanofiber was observed in HeLa cell that overexpressed CAIX. (C) Scheme of CAIX-mediated targeting, peptide self-assembly and endocytosis, and the charge conversion of negative nanofiber in acidic lysosome to disturb membrane integrity for cellular apoptosis. Adapted with permission from Ref. [343]. Copyright 2022, American Chemical Society. (D) Structural design of TAP and the proposed anti-tumor mechanism. (a) TAP contains an α -helix promoting domain, PD-L1 and Rbm38 targeting domains, and harpin binding region. Once encountering PD-L1, TAP could be recruited by PD-L1 and rapidly aggregate into nanofibers; (b) Proposed mechanisms of TAP-mediated ICB and reversing immunosuppressive TME. In detail, TAP adopted an α -helix secondary structure and actively targeted tumor cells during the circulation. Once recruited by PD-L1 protein, TAP rapidly self-assembled into dense nanofibers on tumor cell surface to block the PD1/PD-L1 axis. Meanwhile, the α -helical TAP facilitated its membrane penetration into the cytoplasm to target Rbm38 protein. This could prevent the recognition of Rbm38 toward eIF4E protein and therefore upregulated p53 protein expression. But in un-engineered tumors, the effective expression of PD-L1 would suppress T cell activity, and Rbm38 targeted eIF4E in the cytoplasm and thereby inhibited p53 protein expression. (E) SEM images of MC38 cells with high PD-L1 expression and 293 T cells with low PD-L1 expression after cultured with and without TAP. Adapted with permission from Ref. [344]. Copyright 2023, Wiley-VCH.

site. Once radiolabeled with iodine-125, Rho-FF-Van could also provide strong radioactive signal for dual fluorescent and radionuclide imaging.

Very recently, Hu, Yang and co-workers used the *in situ* peptide self-assembly to engineer cancer cell membranes [347]. Three phosphopeptides (pY1, pY2, and pY3) with difference in just one phosphorylated tyrosine were elaborated with ALP-regulated and epidermal growth factor receptor (EGFR)-targeting self-assembly (Fig. 26A, B). By comparison, pY1 showed the fastest dephosphorylation reaction and the strongest affinity with EGFR to mediate *in situ* peptide self-assembly for cancer cell membrane modification. After the incubation of pY1 with Dil (a common dye for membrane staining) for 1 h, HeLa cells showed an annular fluorescence feature of nitrobenzoxadiazole (NBD) and Dil (Fig. 26C), indicating the membrane-binding property of resultant nanoassemblies. Meanwhile, the time-dependent increase of fluorescent signal was also observed surrounding cell membranes, further indicating the membrane-located self-assembly of pY1 (Fig. 26D). Using a co-assembly strategy, other protein and peptide could be located on cancer cell membranes.

The triggering sources for *in situ* self-assembly mainly depend on the endogenous species, which are not always specific for the pathology and may cause the improper response. For example, some enzymes and

receptors are overexpressed by tumor sites, but they are also detected in the normal tissues. Furthermore, these contents are also varying in different cancer types. As a consequence, directing the *in situ* self-assembly by exogenous stimuli may be an alternative strategy. Exogenous stimuli bring the merit of good manipulation, ensuring the self-assembly in the desirable sites. Wang's group used the near-infrared laser to induce the *in situ* self-assembly of polymer-peptide conjugate (PPCs) for treating deep tumors [348]. PPC contained three segments of thermoresponsive poly(β -thioester) as the backbone, therapeutic peptide and a NIR molecule. Small-sized PPC molecule penetrated deeply into the tumor interior at normal body temperature, and then self-assembled into spherical nanoparticles due to NIR irradiation-induced temperature elevation. The *in situ* formation of nanoparticles enhanced the intratumoral accumulation and benefited for the access of therapeutic peptide into cells for mitochondrial membrane dysfunction. Moreover, ultrasound was also exploited by their group to guide *in situ* peptide self-assembly [349]. Ultrasound-activated cascade reaction resulted in *in situ* generation of nanoparticles. Meanwhile, ultrasound increased the permeability of cell membrane. The synergism of *in situ* nanoparticle formation and increased membrane permeability contributed to the high drug internalization efficiency of KLAK peptide, which

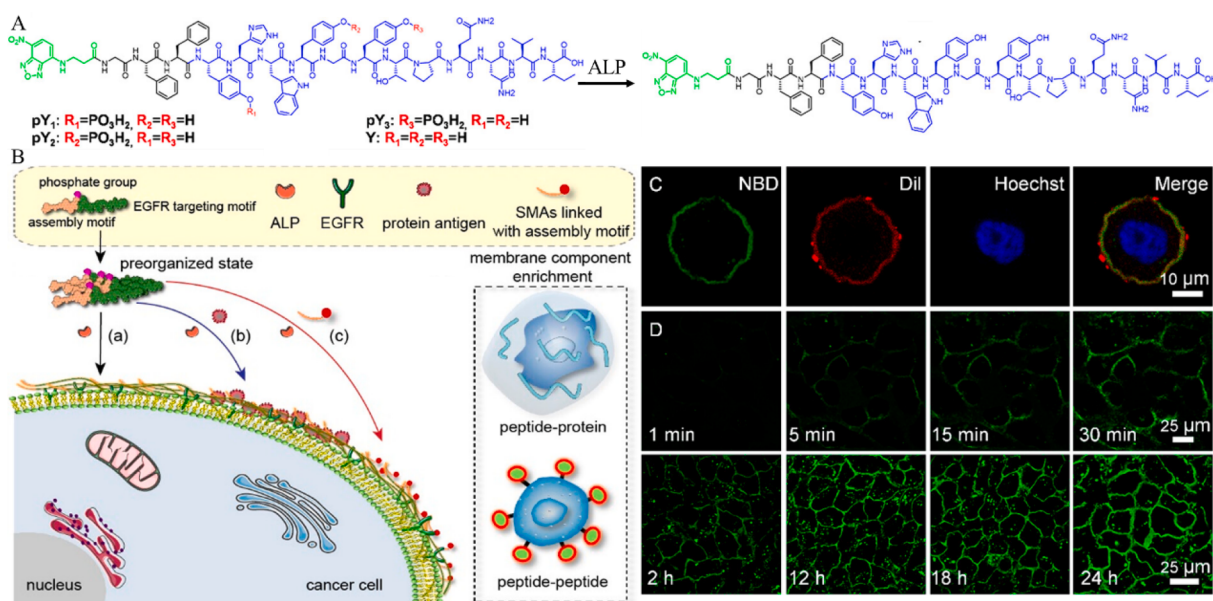


Fig. 26. (A) Molecular structure of phosphopeptides and their phosphorylation by ALP. (B) Illustration of enzyme-instructed self-assembly (EISA)/enzyme-instructed peptide co-assembly and EGFR targeting for cancer cell membrane modification. Membrane-engineered outcomes from the co-assembly of peptide + protein as well as peptide + peptide were inserted. (C) CLSM images of HeLa after the incubation with pY1 and Dil for 1 h. (D) CLSM images of HeLa cells after the incubation with pY1 for different times. Adapted with permission from Ref. [347]. Copyright 2023, American Chemical Society.

thus induced mitochondrial disruption and cancer cell apoptosis.

4.2. Applications of *in situ* peptide self-assembly

Self-assembly plays an important role in biological systems. For instance, the reversible self-assembly of cytoskeletal proteins allows cellular motility [350]. The networks self-assembled from cytoskeletal proteins modulate a myriad of biological processes such as cell migration, endocytic vesicle movement, as well as the intercellular transport of certain viral pathogens and bacteria [13]. Inspired by these findings, researchers capitalize on the intracellular peptide self-assembly to modulate cell behaviors for disease treatments. Generally, disease treatments contain three aspects: diagnosis, therapy, and combination of diagnosis and therapy. Accordingly, the biomedical applications of *in situ* peptide self-assembly were introduced and summarized in these three parts.

4.2.1. Imaging

The pathological biomarkers afford a considerable number of probabilities for disease diagnosis. However, direct measurement on some biomarkers remains challenging. *In situ* peptide self-assembly plays an important role in disease imaging/diagnosis. Noteworthy, this strategy displays the advantages over *ex situ* self-assembly, because the enhanced permeation into deep tumor and long-time retention of imaging agents could improve the signal-to-noise (S/N) ratio and image the eye-invisible tiny lesions. As such, several types of imaging strategies such as magnetic resonance imaging [351–353], PA imaging [354], and AIE-mediated imaging [355] have been developed relying on *in situ* peptide self-assembly. In this part, we will discuss the cancer and bacterial imaging mediated by *in situ* peptide self-assembly.

4.2.1.1. Cancer imaging. Nie, Wang and co-workers constructed a peptide-based near-infrared probe, which could be cleaved by FAP- α and self-assembled into nanofibers on the CAF surface [356]. The *in situ* self-assembly effectively enhanced the accumulation and retention of peptide nanoprobe around CAFs. After 48 h administration, a 5.5-fold fluorescence enhancement was detected in the tumor, in comparison to the control group without self-assembly. Meanwhile, the signal

intensity in tumor tissue was over 4- and 5-fold higher than that in the liver and kidney, respectively, indicating the perfect capability for tumor imaging. To address the issues of poor specificity and narrow imaging window for current fluorescence probes, Li and co-workers reported a bioactivated *in vivo* assembly (BIVA) strategy, which was applied to construct an optical probe that owned preferable tumor accumulation and extended imaging window [357]. mPEG-GPAKLVFFGC(IR₇₈₃)GRGD achieved the long circulation and active targeting. Then, FAP- α enzyme cleaved the GPA peptide on tumor cell surface, and residual AKLVFFGC(IR₇₈₃)GRGD self-assembled into nanofibers around the tumor cells. The assembly-induced metabolic stability amplified the tumor boundary, contributing to a delayed imaging window (8–96 h) with high S/N contrast (>9 folds). Collectively, the BIVA probe realized the precise imaging on small orthotopic pancreatic tumors with size less than 2 mm *in vivo*. To address inevitable photobleaching property of common fluorescent probes, Wang, Xu and co-workers reported a target reaction-induced aggregation peptide (TRAP) system, which underwent *in situ* self-assembly on cell membrane and achieved prolonged and stable imaging towards bladder cancer [358]. As shown in Fig. 27A, the probe contained a targeting peptide (TP) that recognized overexpressed CD44v6 on bladder cancer, and a self-assembling motif of RAP that could react with TP by click chemistry. After the specific recognition of TP on bladder cancer, RAP was added to react with TP on bladder cancer, yielding TRAP monomer for *in situ* peptide self-assembly. The formation of supramolecular nanofibers and further nanonetworks ignited photostable fluorescent signal for precise fluorescent imaging for human bladder cancer (Fig. 27B). Using CD44v6-positive RT112 as cell model, the recognition capability of TRAP was identified from the strong and long-term fluorescence signal on cell surface (Fig. 27C). Moreover, TRAP could effectively distinguish the tumor boundaries (Fig. 27D), showing the clinical potential in imaging-guided surgery for bladder cancer.

Monitoring the content/activity of overexpressed components in lesions provides another route for disease diagnosis. Zhong and co-workers conjugated a coumarin dye (Cou) to a short self-assembling peptide that was pre-modified with a hydrophilic ALP-responsive group [359]. Triggered by ALP, Cou-peptide actuated the EISA at a low peptide concentration, accompanying with the monomer-excimer

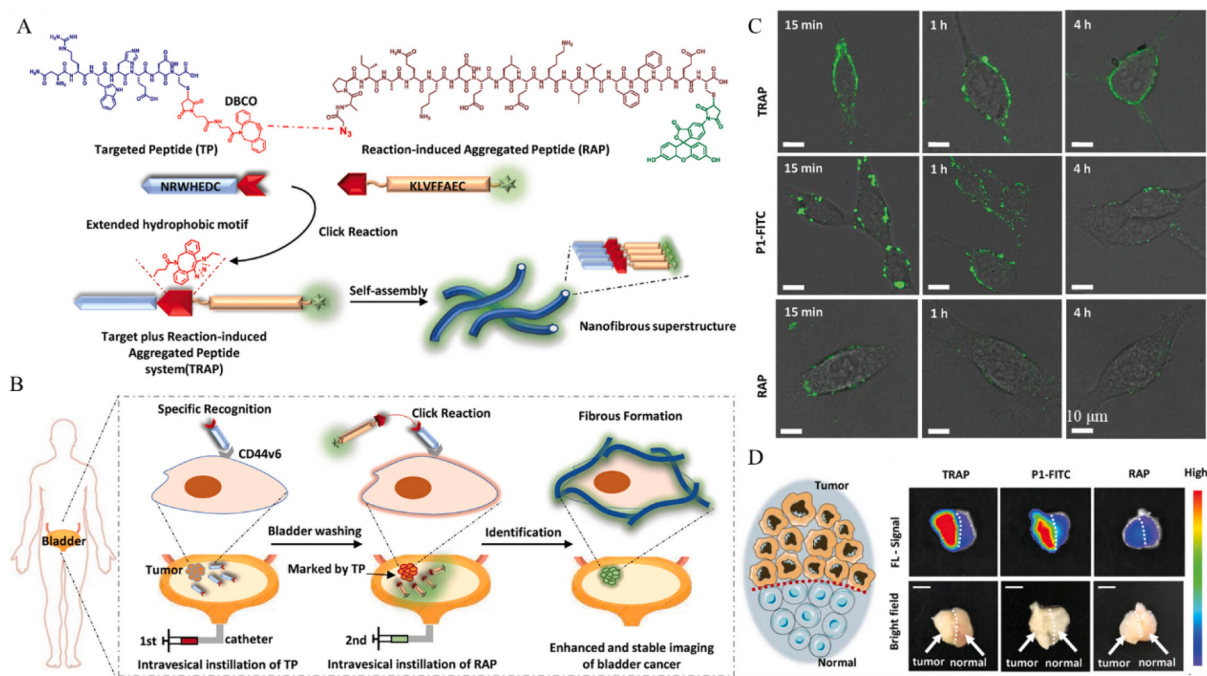


Fig. 27. (A) The molecular structure of TP, RAP and illustration of constructing TRAP system. (B) Schematic illustration of TRAP system for enhanced and stable bladder cancer imaging. TP specifically recognized CD44v6 overexpressed in bladder cancer. It was further captured by added RAP to form TRAP via click reaction on bladder cancer. Then, the TRAP monomer self-assembled into supramolecular nanofibers for bladder cancer imaging. (C) CLSM images of RT112 cells treated with different formulations for 0.25, 1, and 4 h, respectively. (D) Diagram of tumor tissue and fluorescence imaging of tumor boundary treated with different formulations. Scale bars: 2 mm. Adapted with permission from Ref. [358]. Copyright 2023, Wiley-VCH.

transition of Cou to generate luminescent nanofibers in living cells. After the co-culture of HeLa + H8 (human cervical epithelial cell, corresponding normal cell line of HeLa) as well as HepG2 + LO2 (human hepatocyte cell, corresponding normal cell line of HepG2) and treated with *p*YD, excimer PL was mainly detected in both cancerous HeLa and HepG2 cells, because of their high levels of endogenous ALP. Moreover, the PL intensity of excimer gradually increased in the tumor region after intravenous injection with *p*YD, suggesting the continuous transformation of *p*YD into luminescent nanofibers in mice. Therefore, the resultant fluorescent nanofibers could image ALP-overexpressed cancers through recording ALP activity. Additionally, the *in situ* peptide self-assembly can be used to monitor the instant therapeutic effect through fluorescent imaging. Rao's group screened a bio-orthogonal cyclization reaction to regulate the self-assembly of a fluorescent peptide, which could image the caspase-3/7 activity and therefore reflect the chemotherapeutic outcomes in human tumor xenograft mouse model [360]. Caspase-3/7 triggered-DEVD detachment and intracellular thiol-mediated disulfide reduction induced the intramolecular cyclization. The yielded macrocycle unit self-assembled into nanoaggregates *in situ*, leading to the enhanced retention of nanoprobe in apoptotic tumor cells and ignited fluorescence signal. The fluorescence intensity determined by enzyme activity *in vivo* reflected the chemotherapy-mediated tumor response.

Because their molecular aggregation leads to the fluorescent "turn-on", AIE-type chromophores show the unique advantages in self-assembled nanoplatforms for imaging. The AIEgen-peptide conjugates show no fluorescence emission in their single-molecule state. Once undergoing the aggregation/self-assembly, they emit strong fluorescence signal due to the restricted intramolecular rotation and prohibited energy dissipation in their aggregated state. Zhan and co-workers introduced an AIE molecule of tetraphenylethylene (TPE) to the N-terminus of Phe-Asp-Gly-Glu-Ala (FDGEA) peptide [361]. After the recognition of DGEA sequence towards the $\alpha_2\beta_1$ integrin of cancer cells, the self-assembly of TPE-FDGEA induced the aggregation of TPE molecule, facilitating the targeted fluorescent imaging on $\alpha_2\beta_1$ integrin

overexpressed cancer cells. Beside the binding-induced aggregation, another strategy is cleavage-induced self-assembly, of which cleavable bonds are exploited to connect the AIE molecules to functional peptides to construct AIE-based imaging systems. A peptide-AIEgen conjugate probe was proposed to image the pancreatic cancer cells, in which TPE molecule was covalently linked to an RGD peptide via an FAP- α -cleavable motif [362]. The probe exhibited fluorescence "turn-on" after the specific cleavage by FAP- α on pancreatic tumor cells. The *in situ* formed nanofibers could effectively accumulate in tumor cells for long-term fluorescent imaging.

4.2.1.2. Bacterial imaging. Apart from directly imaging cancer cells, *in situ* peptide self-assembly also shows their potentials for bacterial detections. Wang's group reported a class of chlorophyll-peptide conjugates for *in situ* bacterial infection imaging [363,364]. As an example, Ppa-PLGVRG-Van containing three moieties of Ppa as a signal molecule, an enzyme-cleavable PLGVRG linker, and a D-Ala-D-Ala-targeting ligand (Fig. 28A), was designed as a PA probe to diagnose bacterial infection [364]. Ppa-PLGVRG-Van specifically targeted the Gram-positive bacteria due to the recognition of Van to D-Ala-D-Ala on bacterial membrane. In the presence of overexpressed gelatinase, Ppa-PLGVRG-Van was cleaved to generate hydrophobic Ppa-PLG for *in situ* self-assembly. The formation of fibrous nanostructures increased the heat conversion efficiency, and the PA signal was also enhanced to image the gelatinase-positive bacteria *in vivo*. According to 3D reconstruction of bacterial myositis recorded by MSOT 128 multispectral optoacoustic tomography, bacteria-infected sites displayed significantly higher PA signal, showing the high detection ability towards Gram-positive, gelatinase-positive bacteria (Fig. 28B).

Using an AIEgen group as the fluorescent signal molecule, ALP-catalyzed *in situ* self-assembly strategy has been introduced to detect the ALP activity in bacteria (Fig. 28C) [365]. As shown in Fig. 28D, the probe could effectively distinguish high-ALP expressing *E. coli* from controlled *S. aureus*. In the presence of L-phenylalanine (an inhibitor of ALP), the probe fluorescence could not turn on, suggested that the

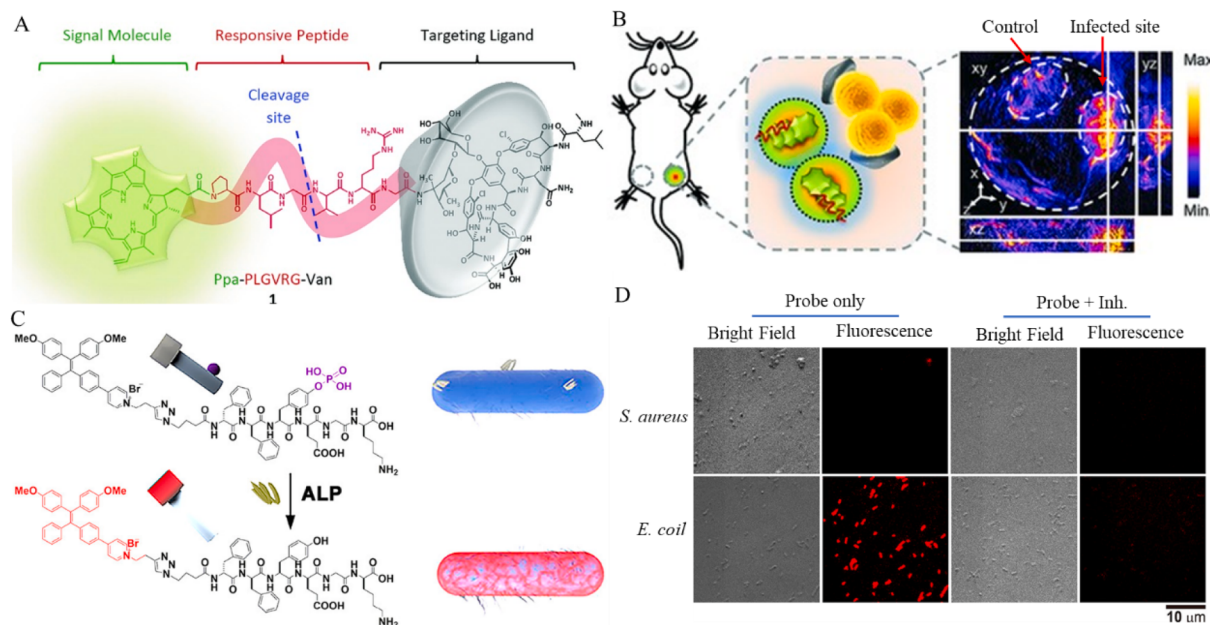


Fig. 28. (A) The chemical structure of Ppa-PLGVRG-Van. (B) Illustration of *in vivo* self-assembly of Ppa-PLGVRG-Van for bacterial infection detection based on PA imaging. 3D reconstruction of bacterial myositis after i.v. injection of Ppa-PLGVRG-Van was shown. Adapted with permission from Ref. [364]. Copyright 2016, Wiley-VCH. (C) ALP-induced peptide self-assembly to detect the ALP activity in bacteria due to the turn-on fluorescent signal. (D) CLSM images of *S. aureus* and *E. coli* incubated with probe for 4 h in the presence/absence of L-phenylalanine (an inhibitor of ALP). Adapted with permission from Ref. [365]. Copyright 2020, American Chemical Society.

fluorescent recovery was dependent on its dephosphorylation. With no need for tedious washing steps, the self-assembling probe showed the clear advantages over commercial ALP kits. In a recent study, the relationships among molecular structure of probe, self-assembly ability and imaging of ALP activity were illustrated [366]. To ensure the luminescent efficiency of TPE-peptide to ALP, the distance between TPE and self-assembling peptide unit should be less than five glycines. It was found that the self-assembly ability of TPE-peptide probe determined the sensitivity of probe to ALP and the strength of corresponding luminescence signal. Furthermore, co-assembly of AIEgen-peptide with a non-AIEgen-capped peptide has been found to enhance the luminescent output of AIEgen-peptide for imaging.

4.2.2. Therapy

4.2.2.1. Tumor therapy. The formation of peptide-based nanomaterials in the intracellular/pericellular space can selectively inhibit the cellular metabolic activity, hinder cell communication, induce cell apoptosis, and so on. As depicted above, peptide amphiphiles could spontaneously self-assemble into nanomaterials once exceeding a critical concentration. Jeena and co-workers achieved the peptide self-assembly inside living cells to regulate the biological functions [367]. A mitochondria-targeting moiety of triphenyl phosphonium delivered the modified phenylalanine dipeptide (Mito-FF) into mitochondria. After reaching the critical aggregation concentration, Mito-FF self-assembled into the fibrous nanostructure *in situ*, which induced mitochondria damage by disrupting their membrane integrity and caused cell apoptosis. Recently, intracellular self-assembly of Tyr-containing peptide was exploited to combat drug-resistant melanoma [368]. A tripeptide of Phe-Phe-Tyr (FFY) was intracellularly oxidized by tyrosinase and *in situ* self-assembled into nanoparticles, which interfered the tubulin assembly to induce severe G2/M arrest and mitochondrial dysfunction for cell apoptosis. With no need for chemotherapeutic drug, tyrosinase-regulated intracellular tripeptide self-assembly reduced 87.4 % tumor volume in drug-resistant melanoma.

Apart from traditional chemotherapy, *in situ* self-assembly have been developed in other therapeutic modalities. Liang and colleagues

designed a porphyrin derivative of Ac-DEVDD-TPP, which underwent apoptosis-amplified assembly to construct porphyrin nanofibers with enhanced PDT efficiency for oral squamous cell carcinoma (OSCC) therapy (Fig. 29A) [369]. When encountering caspase-3, Ac-DEVDD-TPP was cleaved and converted to D-TPP that aggregated into porphyrin nanofibers. Giving a laser irradiation, self-assembled porphyrin nanofibers generated more ${}^1\text{O}_2$ to induce cell apoptosis and pyroptosis, which further activated caspase-3 to amplify the self-assembly of D-TPP and ${}^1\text{O}_2$ generation. Comparing to the scrambled Ac-DEDVD-TPP peptide, Ac-DEVDD-TPP afforded the highest caspase-3 level and exhibited the largest tumor suppression both in subcutaneous and orthotopic oral tumor models (Fig. 29B). Zhang's group designed an Asp-Phe-Tyr (DFY) tripeptide to execute cancer immunotherapy (Fig. 29C) [370]. In melanoma cells with high-expressed tyrosinase, DFY initiated self-assembly and further underwent tyrosinase-catalyzed polymerization. The formed quinone-rich intermediates arrested tumor-specific proteins via Michael addition and formed antigen-loaded microfibers. Antigen-presenting cells (APCs) could effectively engulf the antigen-loaded microfibers and release antigen to boost immune effect. Wang's group reported a bispecific self-assembling antiCD3-G7-RGD peptide for cancer immunotherapy (Fig. 29D) [371]. The peptide molecule targeted the CD3 receptor and recruited surrounding peptides for the self-assembly to activate T-cell. Then the activated T-cell recognized the $\alpha\beta_3$ receptor protein on cancer cell membrane, resulting in T cell-mediated cancer cell cytotoxicity. The green fluorescence of NBD could be detected in positive groups of MCF-7 (Fig. 29E) and T cell (Fig. 29F), suggesting the specific targeting and recognition. The effective recognition of activated T cells to integrin overexpressed tumor cells was also verified by SEM. Aiming at the high ALP level and PD-L1 in 4 T1 cells, Yang's group combining the ALP-instructed self-assembly with PD-L1-induced self-assembly to realize the effective construction of peptide nanomaterials around PD-L1 on 4 T1 cell membrane surface, which led to the partial denaturation of PD-L1 and sequestering its functions. Furthermore, the endocytosis of PD-L1 into cells resulted in further degradation *via* the proteasome pathway in the cytoplasm, which effectively reactivated the effector T cells for cancer immunotherapy [372].

Recently, *in situ* peptide self-assembly has been utilized to sensitize

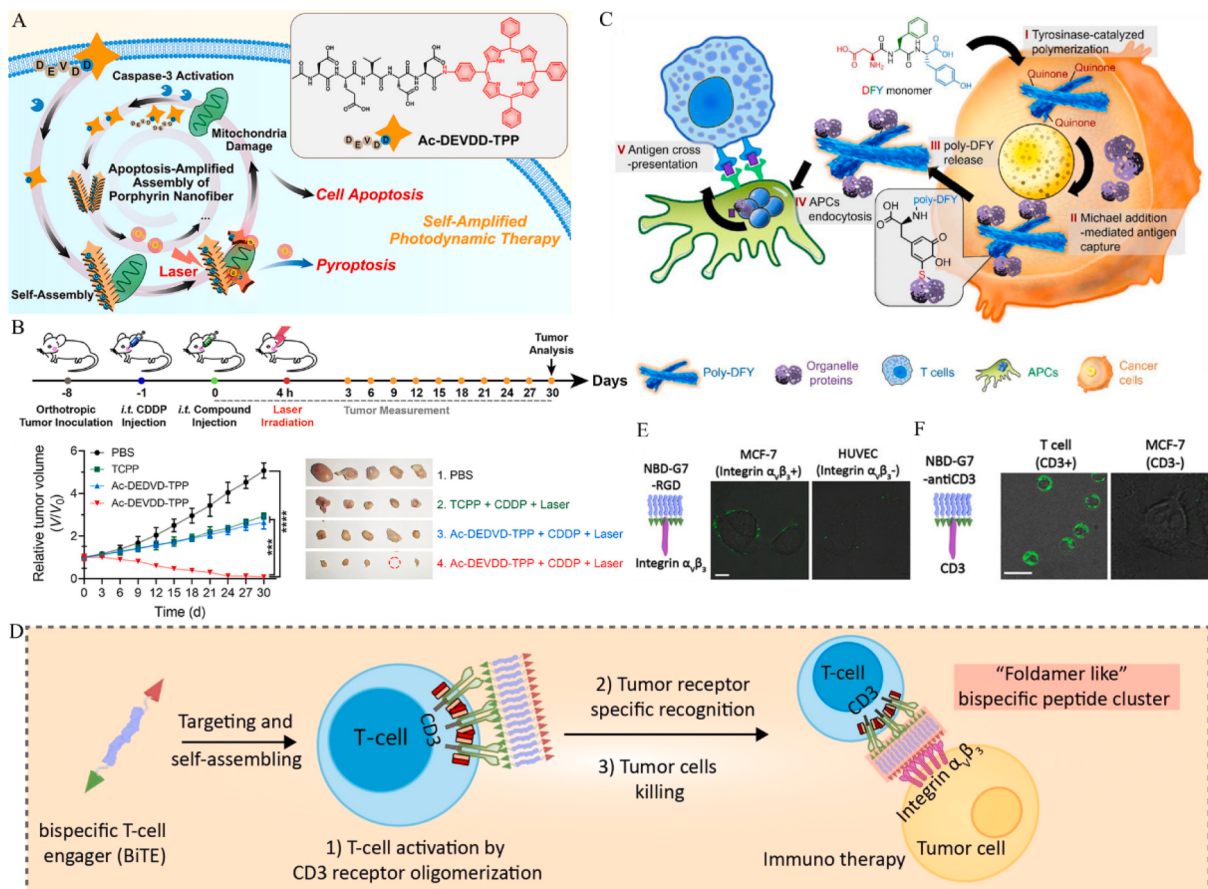


Fig. 29. (A) Scheme of the circle of Ac-DEVDD-TPP initiating apoptosis-amplified assembly to construct porphyrin nanofibers and generated more ${}^1\text{O}_2$ to induce cell apoptosis and pyroptosis. (B) Relative tumor volumes and tumor photos of SCC7 tumor bearing mice after various treatments. Reproduced with permission from Ref. [369]. Copyright 2023, American Chemical Society. (C) Schematic illustration of DFY-mediated self-assembly in tyrosinase high-expressed melanoma cells to achieve cancer immunotherapy. Reproduced with permission from Ref. [370]. Copyright 2021, American Chemical Society. (D) The *in situ* self-assembly of peptide containing CD3 and integrin $\alpha_v\beta_3$ dual targeting sequences to induce T cell-mediated cytotoxicity of $\alpha_v\beta_3$ overexpressed tumor cells. (E) CLSM images of MCF-7 (positive integrin $\alpha_v\beta_3$ expression) and HUVEC (negative integrin $\alpha_v\beta_3$ expression) treated with NBD-G7-RGD. (F) CLSM images of T cell and MCF-7 (control group) treated with NBD-G7-antiCD3. Scale bar: 10 μm . Adapted with permission from Ref. [371]. Copyright 2022 Wiley-VCH.

the traditional therapy strategy. Liu's group used the *in situ* EISA strategy to regulate the self-assembly of Nap-G^{DFD}FpYSV to selectively elevate the sensitivity of ALP-high-expressing cancer cells to γ -rays for enhanced radiotherapy [373]. Comparing with the control group of pre-fabricated nanofibers formed by same peptide in solution, nanofibers formed by *in-situ* EISA greatly improved the radiosensitivity of ALP-overexpressed cancer cells to γ -rays. The improved radiosensitivity was ascribed to that the *in situ* peptide self-assembly facilitated the selective accumulation of histone deacetylases inhibitor (HDACI) containing nanofibers in cancer cells, which accelerated DNA damage, trapped cells in the G1 phase and activated apoptosis. To address the problem that chemotherapy usually fails to treat the renal cell carcinoma (RCC) because of the intrinsic drug resistance, *in situ* peptide self-assembly occurring on the cancer cell membrane was exploited to sensitize the chemotherapy of RCC [374]. The first peptide chain (P1) containing RCC-targeted group was seeded on the RCC membrane surface due to the specific recognition. Then the second peptide (P2) was added to react with P1 to form a self-assembled building block, which self-aggregated into the superstructure on cell membrane to perturb membrane integrity/permeability. Because of the improved drug endocytosis, the IC₅₀ was reduced by nearly 3.5-fold and the tumor growth inhibition rate of xenografted mice was improved 3.2-fold compared with that treated with free DOX.

4.2.2.2. Antimicrobial therapy. The *in situ* peptide self-assembly has also

been applied to regulate the bacterial growth [375,376]. In this regard, some therapeutic strategies used for tumors can be applied for antimicrobial therapy since the pathogen infection sites show the similar physiological features with tumor tissues, such as the low pH value, elevated enzyme concentration and so on. Xu's group migrated the EISA strategy generally used for cancer therapy to combat the bacterial growth [377]. A phosphorylated peptide with structure of C₁₀H₁₈CH₂C(O)-L-Phe-L-Phe-Tyr-(PO(OH)₂) was designed, which suffered from the cleavage by the overexpressed ALP in *E. coli* to detach the phosphate residue for intracellular self-assembly and bacteria inhibition. Wang's group developed skin-like silk fibroin wound dressings in which the antibacterial GAGAGSGPLGVRLVFF (KLAKLAK)₂ (GPLK) peptide and epidermal growth factor (EGF) were loaded [378]. After reaching the site of bacterial infection, the over-secreted gelatinase cleaved PLGVRL and the residual VRGLVFF(KLAKLAK)₂ was liberated from the silk fibroin (SF) film, which self-assembled into nanofibers *in situ* to realize long-term accumulation and achieve effective anti-bacteria. Because of the on-demand release of antibacterial peptides at where needed, smart SF-based wound dressings also reduced the toxicity to normal tissues. In another example, an antimicrobial peptide WRWRWY was designed for wound healing via *in situ* enzyme-induced self-assembly [379]. WRWRWY underwent tyrosinase-triggered oxidation *in vivo* to generate mWRWRWY, which further self-assembled into mWRWRWY nanoparticles with effective antimicrobial effect (Fig. 30A). According to Live/Dead staining assay toward *E. coli* and *S. aureus*, mWRWRWY

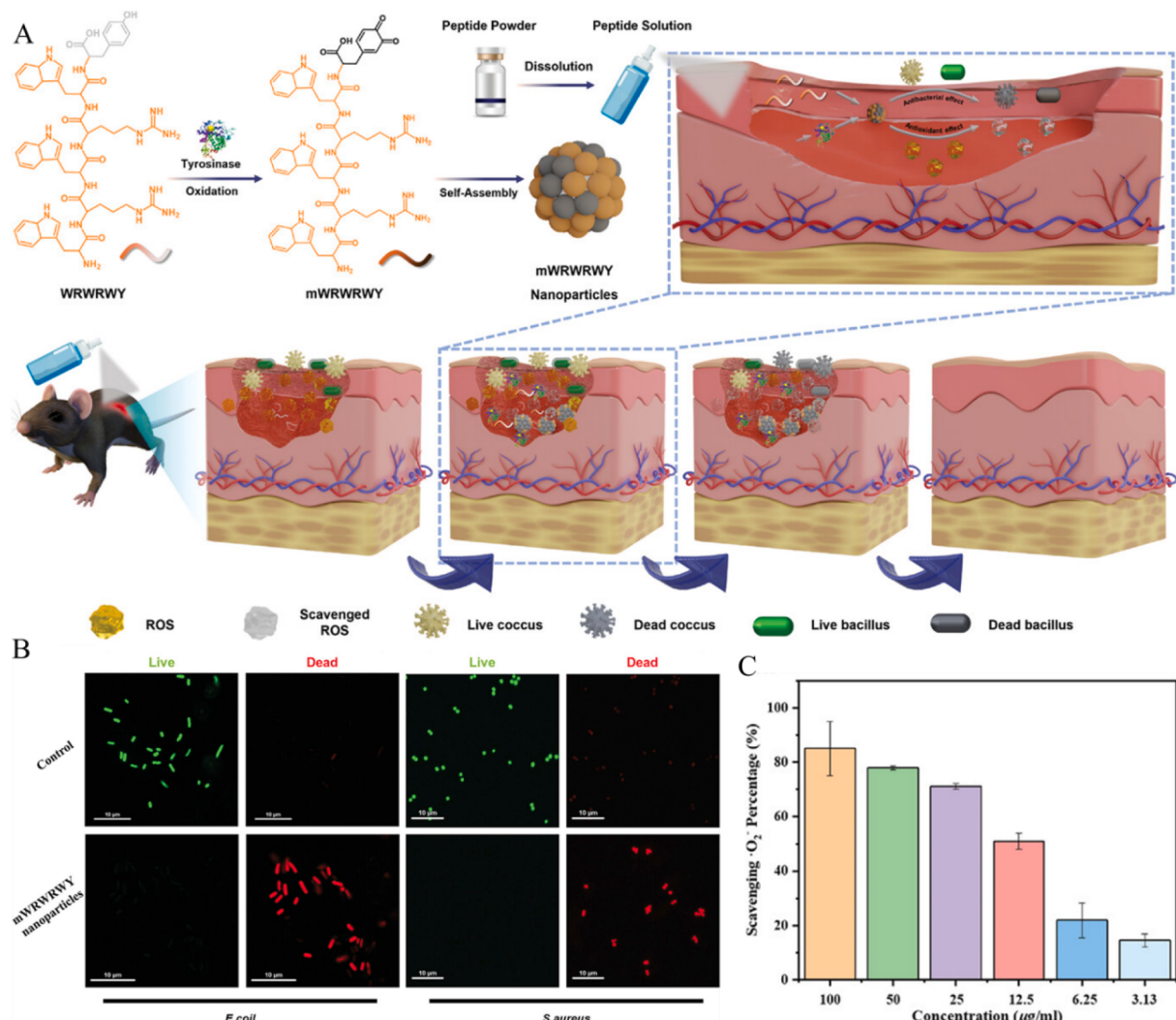


Fig. 30. (A) The chemical structure of WRWRWY and its illustration to form *m*WRWRWY nanoparticles via *in situ* tyrosinase-induced self-assembly for wound healing. (B) CLSM images of *E. coli* and *S. aureus* with treatment of *m*WRWRWY nanoparticles for 24 h. (C) Scavenging percentage of different concentrations of *m*WRWRWY nanoparticles towards O_2^- . Adapted with permission from Ref. [379]. Copyright 2023, Wiley-VCH.

nanopeptides excellent antimicrobial activity (Fig. 30B). Moreover, the self-assembled *m*WRWRWY nanoparticles showed ROS scavenging activities (Fig. 30C). Due to the good stability, antibacterial activity, and antioxidant potential, self-assembled *m*WRWRWY effectively promoted wound healing. Liu's group synthesized an AIEgen-peptide conjugate, which initiated the *in situ* self-assembly on the surface of Gram-positive bacteria for diagnosis and treatment of bacterial infection [380]. To effectively bind the Gram-positive bacteria, vancomycin was appended to the side chain of peptide due to its recognition on the D-Ala-D-Ala dipeptide in the bacteria wall. The "seed-induced" *in situ* self-assembly facilitated the AIE effect of luminogen for fluorescent image and simultaneously enhanced ROS generation for bacterial killing.

4.2.3. Imaging and therapy

4.2.3.1. Imaging-guided cancer surgery and chemotherapy. The turn-on fluorescent signal switched by the *in situ* self-assembly has been applied for disease diagnosis and disease-related species detection discussed above, which also provides the foundation for imaging-guided cancer surgery (FIGCS). To realize the FIGCS, a NIR-peptide precursor of RGDRDDRDPPLGGLFFC (Cy) was designed (Fig. 31A), which underwent the enzyme-induced *in situ* self-assembly and facilitated the fluorescent imaging of RCC for surgery-mediated tumor elimination

[381]. The NIR-peptide probe was specifically captured by $\alpha_v\beta_3$ integrin and selectively cleaved by MMP-2/9 to generate the probe residue in the tumor lesions (Fig. 31B). The *in vivo* self-assembly of probe residue into nanofibers exhibited the tumor-specific excretion-retarded (TER) effect in the kidney, contributing to a high S/N ratio in orthotopic RCC mice. Specially, the TER effect allowed for the precise identification of eye-visible tiny tumors with diameter less than 1 mm. As a result, this strategy enabled the complete tumor elimination and therefore significantly mitigated the post-surgical recurrence. In contrast with cleavage-initiated self-assembly, another strategy of driving AIEgens close for self-assembly was developed for FIGCS [382]. A peptide-AIEgen probe of MPA-Ph-R-FFGYSAYPDSVPMMMS was designed to selectively target the EphA2 receptor overexpressed cancer cells, and self-assembling FFG enabled the close of AIEgen molecules for aggregation in EphA2 cluster, leading to the improved restriction of AIEgens to generate bright fluorescence for imaging EphA2 cluster. In a peritoneal carcinomatosis-bearing mouse model, the probe achieved a high fluorescent output with a S/N ratio of ~ 13.4 , suggesting a rather high imaging function.

Liu, Guo, Ye and co-workers exploited the *in situ* self-assembly strategy to regulate peptide-based cisplatin prodrug (P-CyPt) for imaging-guided therapy *in vivo* (Fig. 31C) [383]. Triggered by extracellular ALP, P-CyPt dephosphorylated and self-assembled into Pt^{IV} NPs *in situ* for enhanced uptake. When encountering intracellular GSH, self-

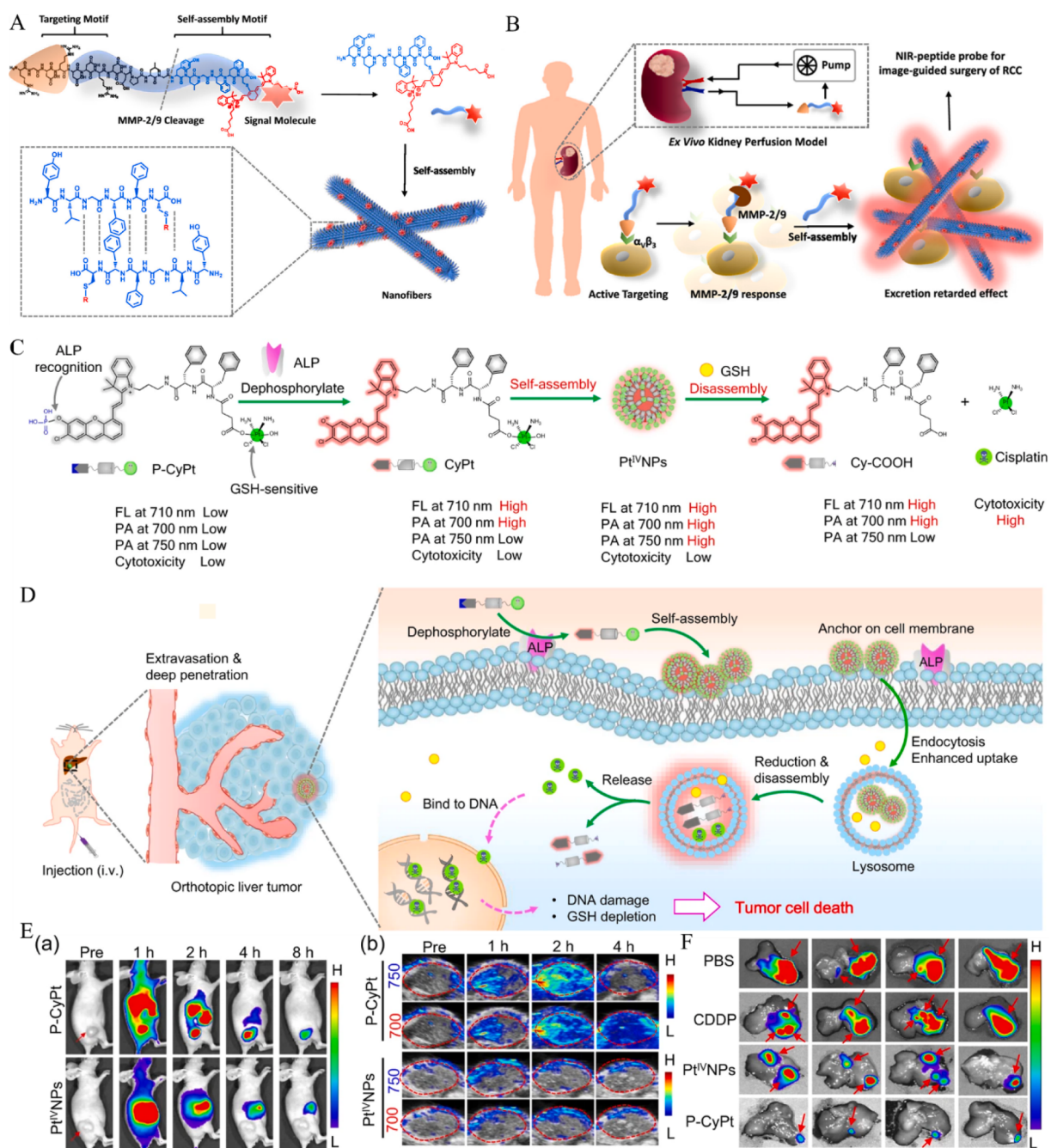


Fig. 31. (A) Peptide structure and the MMP-2/9-induced *in situ* self-assembly into nanofibers. (B) Schematic illustration of $\alpha_v\beta_3$ mediated targeting, MMP-2/9-induced self-assembly *in vivo* for image-guided surgery of RCC. Reproduced with permission from Ref. [381]. Copyright 2020, American Chemical Society. (C) Structure of P-CyPt that suffered from ALP-triggered dephosphorylation and *in situ* self-assembly into Pt^{IV}NPs, followed by GSH-induced dissociation and the release of cisplatin and Cy-COOH for therapy and imaging. (D) Proposed mechanism of successive *in situ* self-assembly and disassociation of P-CyPt for FL and PA imaging-guided chemotherapy to cure orthotopic liver tumors. (E) Time-dependent FL imaging (a) and dual PA imaging (b) of HeLa tumors after injected with P-CyPt or Pt^{IV}NPs. (F) Ex vivo BL images of resected livers after 15 d treatment. Tumor nodules in the liver were marked by red arrows. Adapted with permission from Ref. [383]. Copyright 2023, The Author(s).

assembled Pt^{IV} NPs dissociated and rapidly released cisplatin in tumor cells (Fig. 31D). In the meanwhile, P-CyPt activated fluorescence signal at 710 nm and dual PA signals at 700 and 750 nm *in vivo* (Fig. 31E), permitting highly-sensitive and spatially-resolved delineation of tumor foci. Imaging-guided treatment of P-CyPt for orthotopic HepG2/Luc liver tumors was evaluated. Bioluminescence (BL) images indicated that the tumor volumes treated by P-CyPt were obviously smaller than other groups (Fig. 31F).

4.2.3.2. Theranostic. By delicate molecular design, cancer theranostic is achievable by *in situ* peptide self-assembly. Wang's group designed two peptide-cyanine conjugates with the potential of fluorescent imaging and PTT (Fig. 32A) [384]. First, internalized peptide-cyanine conjugates (P-1Cy and P-2Cy) targeted the X-linked inhibitor of apoptosis protein (XIAP) inside cells and thereafter activated caspase-3/7. Both P-1Cy and P-2Cy responded to caspase-3/7 and yielded the self-assembling unit *in vivo*. For P-1Cy, the residual Pr-1Cy with a single cyanine could only aggregate into a loose column with undefined structure because of the too far distance between two cyanine molecules, which emitted NIR

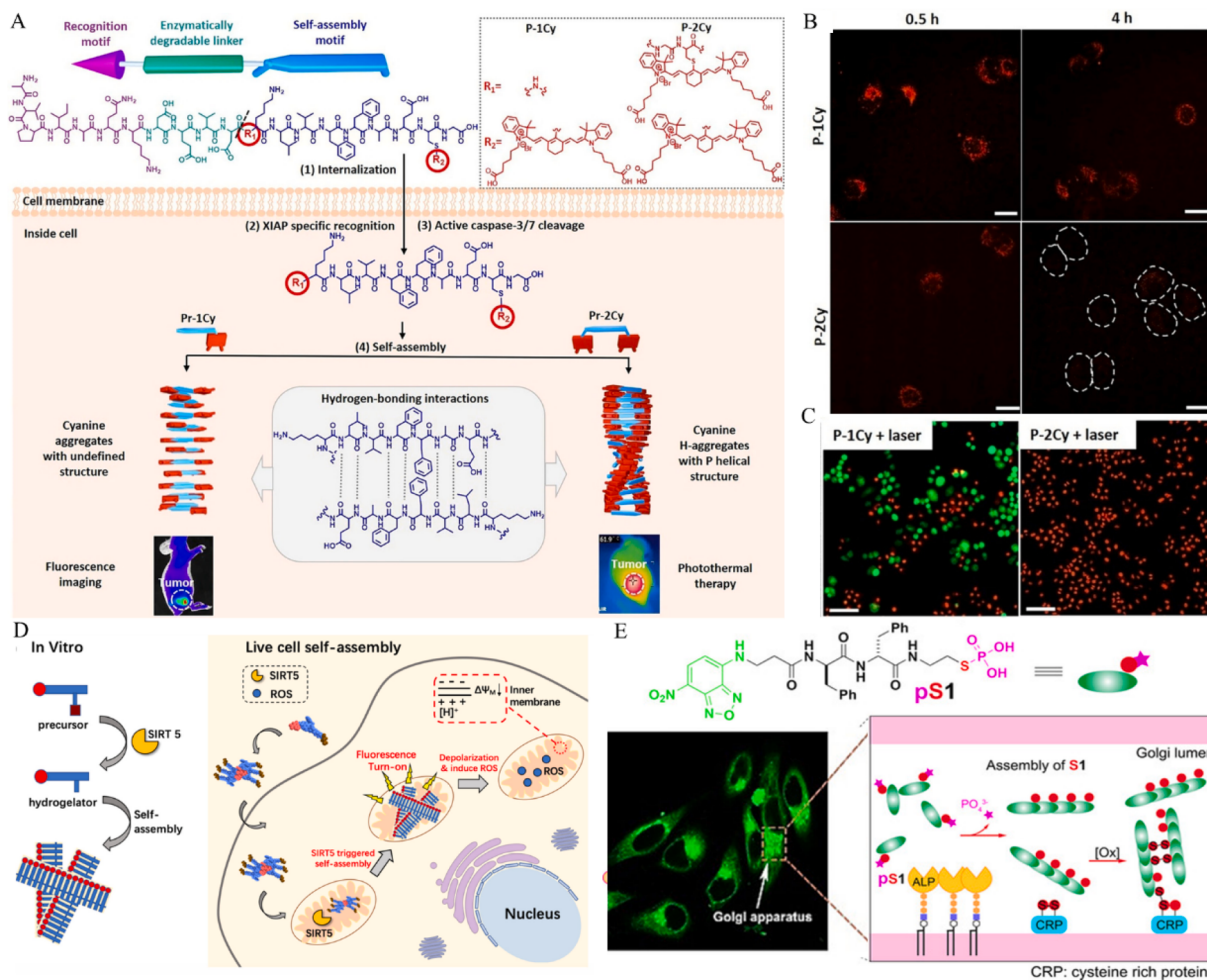


Fig. 32. (A) The chemical structure of two peptide-cyanine conjugates, which underwent enzyme-induced cleavage and *in vivo* self-assembly for fluorescent imaging (P-1Cy) and PTT (P-2Cy). (B) Confocal images of H460 cells after incubated with P-1Cy and P-2Cy for different times. (C) Live/dead staining of H460 cells treated with P-1Cy and P-2Cy. Adapted with permission from Ref. [384]. Copyright 2021, Wiley-VCH. (D) SIRT5-induced intra-mitochondrial self-assembly for SIRT5 imaging and potential antitumor. Reproduced with permission from Ref. [386]. Copyright 2020, American Chemical Society. (E) Chemical structure of NBD-thiophosphopeptide and its dephosphorylation to generate a self-assembling thiopeptide, which targeted and accumulated at the Golgi apparatus for imaging Golgi and killing cancer cells. Adapted with permission from Ref. [387]. Copyright 2021, Wiley-VCH.

fluorescence for tumor imaging. The imaging function was confirmed by the strong red fluorescence in XIAP high-expressed H460 cells (Fig. 32B). As for P-2Cy after caspase-3/7 cleavage, the released Pr-2Cy with two cyanines self-assembled into a P-helical column with H-aggregates. Self-assembled P-helical column showed good photothermal property, which effectively killed the H460 cells under laser radiation (Fig. 32C). To address the issues that the variant expression of enzymes in different cancers may lead to undesirable theranostic outcomes for some enzyme-mediated assembly, Shi and co-workers focused on the broad features of high GSH content and low pH in tumor tissues. A GSH and pH dual-responsive system was established by connecting a NIR agent of Cy7 to disulfide-containing peptide to realize the tumor theranostic [385]. The synergism of acidic pH and reductive GSH activated the intermolecular condensation of theranostic probe to generate an amphiphilic cyclic dimer, which aggregated into uniform nanoparticles with improved accumulation and retention in cancer cells. As a consequence, this strategy remarkably improved the NIR/PA imaging and PTT of tumors *in vivo*.

To achieve the suborganelle-confined supramolecular self-assembly, Yang and co-workers developed a mitochondria-localized enzyme of SIRT5 to regulate peptide self-assembly in mitochondria (Fig. 32D) [386]. Succinylated peptide precursors converted to self-assembling units via SIRT5 catalysis and formed supramolecular nanofibers in

living cells. The occurrence of self-assembly increased the hydrophobicity to elicit the bright fluorescence of NBD. Based on this, they achieved the SIRT5 imaging in living cells. Moreover, SIRT5-mediated peptide self-assembly could result in mitochondrial membrane potential depolarization and promote ROS production. It could also boost the activities of different chemotherapeutic drugs. Xu's group used the enzyme-induced *in situ* self-assembly to target golgi apparatus for selective imaging and therapy (Fig. 32E) [387]. The enzyme-induced rapid dephosphorylation of NBD-thiophosphopeptide generated a self-assembling thiopeptide, which targeted and accumulated at the Golgi apparatus for imaging Golgi and killing cancer cells.

5. Combination of *ex situ* and *in situ* peptide self-assembly

Nanoparticle-based drug systems have been well demonstrated with advantages in pharmacokinetics and drug accumulation at lesion sites. Recently, more and more studies show that the geometrical size and shape of nanomedicines also influence their bioactivities and pharmacokinetics [388]. For instance, nanomedicines with different sizes exhibit varying extravasation behavior. Their transvascular and interstitial penetrating efficiency are also discrepant. In general, small-size nanomaterials can effectively permeate into solid tumors, but their retention time at tumor sites was reduced when compared to the larger

nanomaterials [389]. Meanwhile, nanoparticles with rod-like and fibrous structures show improved blood circulation and preferable cellular association in compared with their sphere-shaped counterparts, because spherical nanostructures are more readily captured by immune cells. Overall, it is difficult to obtain the optimized outcomes when administrating nanomedicines with unchangeable morphology. To circumvent these dilemma, morphology-adaptable nanomedicines have been developed to overcome the physiological delivering barriers and simultaneously optimize pharmokinetics [390,391]. To fabricate morphology-adaptable nanomedicines, the strategy of combining *ex situ* with *in situ* self-assembly provides the possibility. Specifically, the *ex situ* peptide self-assembly is applied for constructing nanoarchitectures for cargo delivery, and *in situ* self-assembly further induces the morphological reconstruction, so as to achieve the demanded biological effects (Fig. 33). Some of recently reported systems relying on the combination of *ex situ* and *in situ* peptide self-assembly have been summarized in Table 3.

5.1. Morphological adaption for cancer treatments

The morphology of nanoparticles would strongly affect their *in vivo* behavior. To optimize the therapeutic/imaging outcomes of cancers, several strategies have been proposed to reconstitute the morphology of nano-assemblies. Herein, the combined applications of *ex situ* and *in situ* self-assembly were presented according to the induced mechanism that triggers the morphological transformation of self-assembled peptides.

5.1.1. pH-induced morphology transformation

pH-induced transformation is one of the most developed strategies to reshape self-assembled peptides for biomedical applications [392,393]. Han and co-workers designed a tumor acidity-responsive PpIX-peptide with adaptable self-assembled morphology for PDT [394]. PpIX-Ahx-AEAEAK(DMA)AK(DMA)AEAEAK(DMA)AK(DMA) self-assembled into spherical nanoparticles *via ex situ* peptide self-assembly, which transformed into the rod-like nanoparticles in acidic tumor tissues, resulted

from the detachment of acidity-responsive DMA groups. The *in situ* formation of rod-like nanoparticles accelerated drug internalization into tumor cells and prolonged the accumulation in tumor tissue for PDT. Yan, Hest and co-workers have also developed acid-activatable transmorphic peptide-porphyrin (PWG) nanoparticles for improved PDT (Fig. 34A) [395]. At the physiological condition of pH 7.4, PWG self-assembled into spherical nanoparticles. In the acidic tumor environment, PWG underwent the protonation and the self-assembled nanospheres transformed into nanofibers. Notably, the re-assembled nanofibers exhibited the enhanced $^{1}\text{O}_2$ generation. According to *in vivo* fluorescent experiments in Fig. 34B, red fluorescence was detected after 8 h post injection and reached a maximum at 72 h, which was presumably ascribed to the nanoparticle-associated effect in tumor tissue. The fluorescent signal remained strong up to 168 h in the tumor. The superior retention behavior of nanomedicines at tumor sites was benefited from the *in situ* transformation of nanospheres to fibrils, therefore improving the PDT efficiency. Different from the transformation from spherical nanoparticles into nanofibers, recently, self-assembled peptide nanofibers with pH-induced further aggregation were developed for cancer theranostic [396]. A PEGylated porphyrin-peptide conjugate (PHHPEG₆) with pH-sensitivity self-assembled into small nanofibers in aqueous solution, with fast tumor accumulation and long-term tumor retention. In the acidic tumor microenvironment, small nanofibers formed large aggregates, resulting in enhanced $^{1}\text{O}_2$ generation and prolonged tumor retention for PDT (Fig. 34C). After the intravenous injection of PHHPEG₆ nanofibers in mice, strong fluorescence was observed at the tumor site. After PDT, moreover, fluorescent intensity at the tumor site increased continuously from 48 h to 72 h (Fig. 34D), resulting from the release and diffusion of PHHPEG₆ nanofibers that were induced by the necrosis and apoptosis of tumor cells. The fluorescence rapidly disappeared 120 h, accompanying with the formation of thick scabs at the tumor sites. The abnormal increase of fluorescence and following rapid disappearance after PDT were associated with necrosis and apoptosis of tumor cells, showing the prognostic capacity and assessing treatment efficacy.

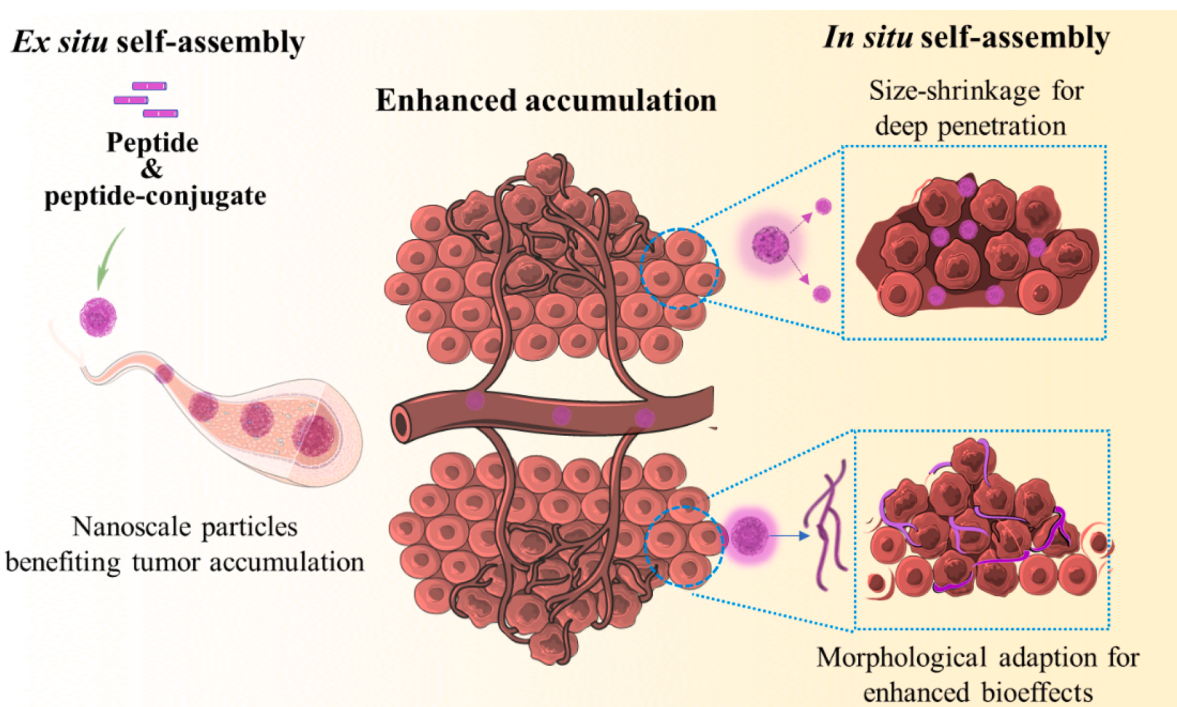


Fig. 33. Schematic illustration of combining *ex situ* and *in situ* peptide self-assembly for disease treatments. In detail, the *ex situ* peptide self-assembly is applied for constructing nanoarchitectures for cargo delivery, and *in situ* peptide self-assembly triggered by certain stimuli further induces the morphological transformation of prefabricated nanoarchitectures to achieve the demanded biological effects.

Table 3The combination of *ex situ* and *in situ* peptide self-assembly for morphology-adaptable biomedical application.

Sequence	Trigger module	Morphology transformation	Feature	Application	Ref
PpIX-Ahx-AEAEAK(DMA)AK(DMA) AEAEAK(DMA)AK(DMA)	pH	Nanosphere to rodlike nanoparticle	Accelerating drug internalization into tumor cells and prolonging the accumulation in tumor tissue	Enhanced PDT for cancer	[394]
GW-porphyrin-WG	pH	Nanosphere to nanofiber	Enhancing singlet oxygen generation	Enhanced PDT for cancer	[395]
FF-Amp-FF and Ce6-FF-Amp-FF	pH	Superhelix to nanoparticle	Prolonging circulation in the animal body and improved accumulation at tumor site	Enhanced PDT for cancer	[397]
FFPPF, FFPFF-CPT and FFPFF-indocyanine	pH	Superhelix to nanoparticle	Facilitating the improved penetration and accumulation at tumor site	Combinatorial chemo-photodynamic therapy	[398]
CPT-LVFFGFLG-PEG-RGD	Cathepsin B	Nanosphere to nanofiber	Improving the tumor-specific accumulation of drug	Tumor therapy and suppressing tumor recurrence	[406,407]
HA-MSDOX-KLA	MMP	Nanosphere to nanofiber	The formation of nanofiber inside cells to inhibit drug efflux and improve the intracellular drug retention	Overcome the MDR in cancer therapy	[408]
C ₁₆ -K(TPE)-GGGH-GFLGK-PEG ₈	Cathepsin B	Nanosphere to nanofiber	Residual CTGP reassembling with DOX into nanofibers on the cell membrane to restrict DOX efflux and encapsulate cells	Overcome the MDR in cancer therapy	[409]
Nap-ffk(GDYKDDDK)-NBD	Enterokinase	Micelle to nanofiber	Enzymatic reassembly of peptide for targeting mitochondria	Targeted drug delivery	[411]
Fmoc-A(2NI)IE or IR780-A(2NI)VE	Nitroreductase	Nanofiber to Nanoparticle	High accumulation and deep penetration into solid tumors for efficient fluorescence imaging	Imaging hypoxic tumor cells	[412]
Bis-pyrene-K-FFVLK-CREKA-FFVLK-DGR	Targeted fibrin and integrin unit	Nanosphere to nanofiber	Mimicking the natural fibronectin (FN) fibrillogenesis	Tumor therapy	[413]
Bis-pyrene-KLVFFK-GGDGR-YIGSR	Integrins and LN receptors	Nanosphere to nanofiber	<i>In situ</i> construction of an artificial extracellular matrix (AECM)	Inhibition of tumor invasion and metastasis	[414]
Bis-pyrene-KLVFF-VNTANST	Vimentin	Nanosphere to nanofiber	<i>In situ</i> formation of fibrous networks to block vimentin skeletonization	Inhibiting the migration and invasion of tumor cells	[415]
Bis-pyrene-FFVLKAHKHVHHVPVRL	CD105	Nanosphere to nanofiber	Blocking endothelial cells and cancer stem cells	Suppressing metastasis of renal cancer	[416]
Bis-pyrene-FFVLK-HSDVHK	Integrin $\alpha_v\beta_3$	Nanosphere to nanofiber	Blocking the activity of endothelial cells and inhibiting angiogenesis	Angiogenesis inhibition	[418]
Bis-Pyrene-KLVFF-PCAIWF	VEGFR	Nanosphere to nanofiber	Decreasing the activation of the downstream pathway for inhibiting the migration of endothelial cells and the angiogenesis	Anti-angiogenesis	[419]
Bis-pyrene-FFVLK(OEG-CREKA)-His ₆	Microthrombus	Nanosphere to nanofiber	The laminin-like fibrous network to capture red blood cells etc., and forming occlusion specifically in the tumor blood vessels	Precise embolization to inhibit the tumor growth	[420]
Bis-pyrene-FFVLK-YCDGFYACYMDV	HER2	Nanosphere to nanofiber	Inhibiting the HER2 dimer formation and therefore blocking the expression of proliferation and survival genes in the nucleus	Tumor therapy	[421]
Bis-pyrene-KLVFF-SWTLYTPSGQSK	N-cadherin	Nanosphere to nanofiber	Blocking the N-cadherin to inhibit cancer cell migration	Inhibiting the tumor metastasis	[417]
Bis-pyrene-FFVLK-RPL	NRP-1	Nanosphere to nanofiber	The formation of fibrous network trapping NRP-1 to alleviate the formation of choroidal neovascularization	Inhibiting angiogenesis	[423]
Lauric acid-FFVLK-HSDVHK	Integrin $\alpha_v\beta_3$, VEGFR2 and NRP-1	Nanosphere to nanofiber	Effective anti-angiogenesis with 97.7 times lower dose than bevacizumab	Inhibiting more receptors for anti-angiogenesis	[424]
Bis-pyrene-FFVLK-AHKHVHHVPVRL	CD105	Nanosphere to nanofiber	Mimicking the morphology transformation of platelets, initiating the coagulation process by peptide-based nanomaterials in blood vessels	Tumor therapy	[425]
Poly(vinyl alcohol) coupled by CGGGKLVFF-tk-PEG and CGGG(KLAKLAK) ₂	ROS	Nanoparticles to fibrous nanostructures	Enhanced destructiveness to mitochondria	Tumor therapy	[426]
PEG-tk-(P18)-LVFF-(KLAKLAK) ₂	Photo irradiation at 730 nm / 685 nm	Nanosphere to nanofiber	Photothermal-promoted morphology transformation (PMT) strategy enhancing drug accumulation and maximizing their retention in the tumor site	Photoacoustic image and tumor therapy	[429]

Inspired by the finding that human protein β 2-microglobulin containing a proline residue undergoes the misfolding and subsequently self-assembles into amyloid fibrils because of the cis/trans amide isomerization of proline, Yu and colleagues incorporated proline into short peptides to manipulate morphology-adaptable peptide self-assembly via pH change [397,398]. Co-assembly of one pentapeptide (named as AmpF) and two derivatives modified with CPT (CPT-AmpF) and photosensitive indocyanine (IR820-AmpF) generated peptide nanomedicine (Fig. 34E), which showed super-helical nanoarchitecture in blood for the prolonged circulation and tumor retention. After reaching the acidic tumor microenvironment, superhelices transformed

into nanoparticles, facilitating the penetration and accumulation at tumor sites. The nanoparticles further re-formed superhelices in cytoplasm after entering cells, due to the neutral pH in cytoplasm. The morphology-adaptable nanomedicines improved the tumor accumulation, evidenced by the higher fluorescence signal of ACI nanomedicine (morphology-adaptable nanomedicine) than that of PCI nanomedicine (a control group with a morphology persistent to pH) (Fig. 34F). Compared with other treatments, the combinatorial chemo-photodynamic therapy significantly inhibited the tumor growth (Fig. 34G). Especially, the tumor volume of mice treated with ACI nanomedicine was smaller than that treated with PCI nanomedicine,

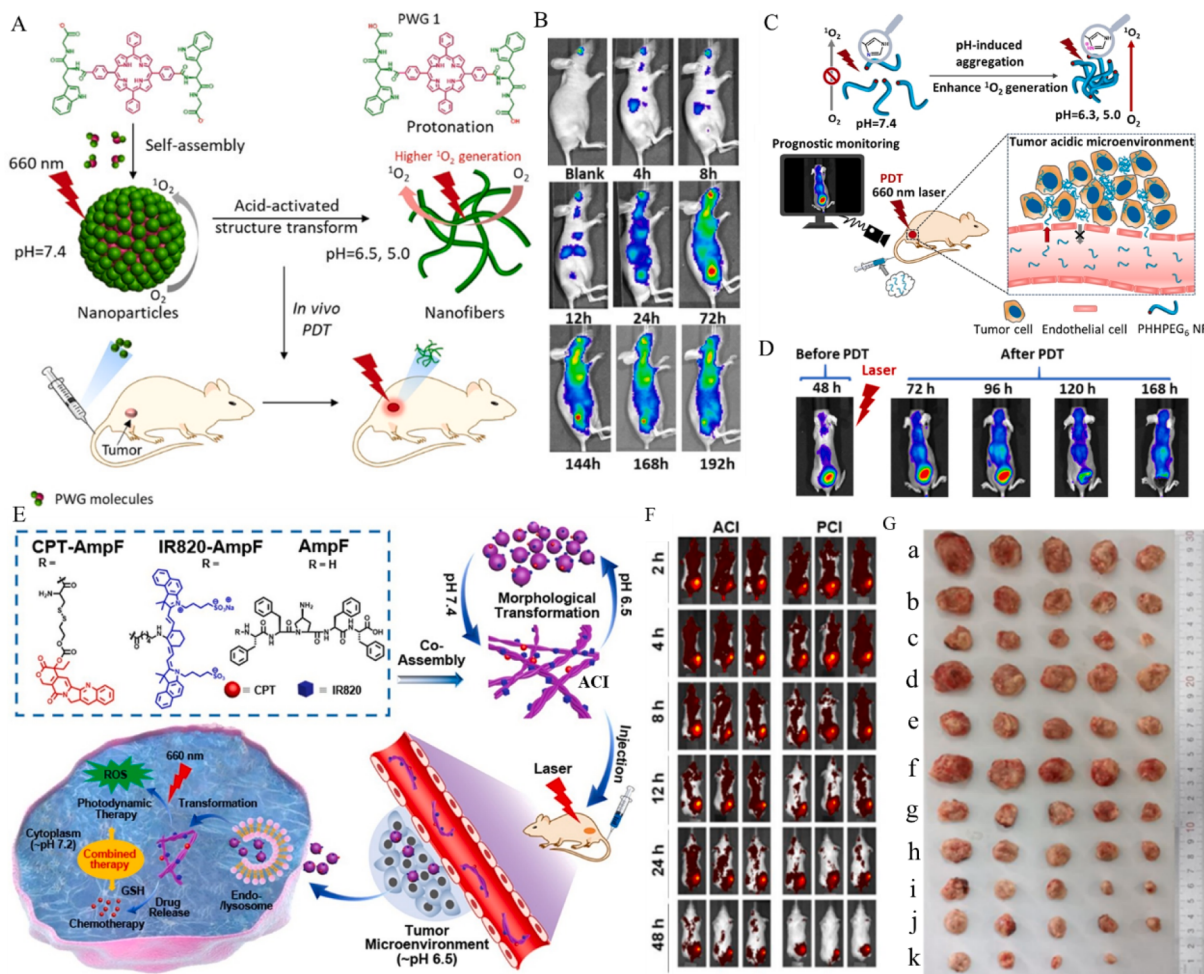


Fig. 34. (A) Acid-activatable morphological transformation of peptide-based nanomaterials from nanoparticles to nanofibers for higher $^1\text{O}_2$ generation. (B) In vivo imaging of MCF-7 tumor-bearing mice administrated PWG nanoparticles via intravenous injection for different time points. Adapted with permission from Ref. [395]. Copyright 2020, Wiley-VCH. (C) Illustration of pH-induced *in situ* aggregation of PHHPEG₆ nanofibers for prognostic monitoring and enhanced $^1\text{O}_2$ generation for PDT. (D) In vivo fluorescence images of 4 T1 tumor-bearing mice before and after PDT. Adapted with permission from Ref. [396]. Copyright 2022, Wiley-VCH. (E) Schematic illustration of morphology-adaptable peptide nanomedicines for combinatorial therapy of chemotherapy and PDT. (F) In vivo distribution of ACI and PCI nanomedicines in 4 T1 tumor-bearing mice at different time intervals. (G) Representative tumor images from mice treated with different modalities (a: PBS, b: free CPT, c: AC, d: free IR820-COOH + laser, e: free IR820-COOH + laser, f: AI, g: AI + laser, h: PCI, i: PCI + laser, j: ACI, k: ACI + laser). Adapted with permission from Ref. [398]. Copyright 2020 Elsevier.

indicating the advantage of morphology-adaptable nanomedicines [398].

5.1.2. Enzyme-induced morphology transformation

The overexpressed enzymes in cancers have also been well documented to regulate the *in situ* re-assembly of peptide-based nanoparticles to transform their morphologies for cancer therapy [399–405]. In an example, Wang's group used cathepsin B to *in situ* reorganize the self-assembled nanoparticles for enhanced cancer therapy [406]. The drug-peptide of CPT-LVFFGFLG-PEG-RGD (CPT-LFPR) was designed, which self-assembled into spherical nanoparticles for self-delivery. When encountering cathepsin B in tumor site, nanospheres detached the hydrophilic PEG-RGD shell and reorganized into fibrous nanostructures. The yielded fibrils acting as the "seeds" accelerated the *in situ* transformation of spherical nanoparticles into nanofibers, which served as the drug depot for sustained drug release to inhibit tumor growth. Similar with this idea, they further used this strategy to suppress tumor recurrence [407].

Morphology-adaptable nanomedicines have been documented to overcome the MDR. In light of the features of enhanced tumor accumulation for spherical nanomaterials and the prolonged intracellular

retention for fibrous counterparts, Zhang's group developed a "tumor-triggered morphological transformation" strategy to address the MDR [408]. A spherical nanomedicine was prefabricated from HA-MSDOX-KLA (HA: hyaluronic acid, MSDOX: MMP-cleavable CPLGLAGG peptide conjugated with DOX, KLA: proapoptotic (KLAKLAK)₂ peptide) based on the *ex situ* self-assembly. It exhibited the enhanced endocytosis by CD44 receptor-positive tumor cells due to HA-mediated tumor targeting. Upon encountering tumor overexpressed MMP, CPLGLAGG was cleaved, resulting in the re-assembly of released DOX-peptide into drug nanofibers. The formed nanofibers therefore inhibited drug efflux and improved intracellular drug retention. Comparing with that of free DOX, the antitumor efficacy of morphology-adaptable nanomedicine towards MCF-7/MDR showed apparent improvement, with a 6.1-fold and 4.5-fold enhancement *in vitro* and *in vivo*, respectively. Instead of eliciting morphological transformation inside cells, they further designed a transformable chimeric peptide to re-assemble on cell membrane surface to overcome tumor MDR [409]. In detail, the cell membrane-targeting and cathepsin B-responsive peptide of C₁₆-K(TPE)-GGGH-GFLGK-PEG₈ (CTGP) self-assembled into spherical nanoparticles and encapsulated DOX to yield CTGP@DOX. After the GFLG cleavage by pericellular overexpressed cathepsin B, CTGP@DOX was dissociated to

release DOX. Meanwhile, residual CTGP further co-assembled with DOX into nanofibers on the outer membrane to restrict DOX efflux and encapsulate cells. CTGP@DOX exhibited a much longer blood circulation time than free DOX, indicating the prolonged drug retention of nanofibers in tumor tissues. As a result, its *in vitro* anti-MDR ability toward drug-resistant MCF-7R cells was found to be 49-fold higher than that of free DOX. To conquer radio-resistance of cancer stem-like cells (CSCs), very recently, Liu's group reported a CAIX-induced *in situ* re-assembly on the CSC surface for cancer therapy (Fig. 35A,B) [410]. ABS-GFFK(Pt)YPLGLAG-PEG₁₀₀₀ (ABS: 4-(2-aminoethyl) benzenesulfonamide, a commercially available CAIX inhibitor) self-assembled into a spherical nanostructure (CA-Pt) (Fig. 35C) and reached the tumor tissue via EPR effect. MMP-2 induced CA-Pt dis-assembly and released ABS-GFFK(Pt)YPLG monomer for deep penetrability. After localizing on the surface of hypoxic CSCs, CAIX triggered the *in situ* self-assembly of ABS-GFFK(Pt)YPLG monomer to form nanofibers (Fig. 35D), which amplified the inhibitory efficacy of ABS towards CAIX and enhanced cellular uptake. In the meanwhile, the nanofibers anchored cell membrane could reduce the HIF-1 α expression and hydrogen proton production, which therefore induced the differentiation of hypoxic CSCs into non-CSCs. This morphology-adaptable strategy combining with therapeutic Pt could boost the radiotherapy (RT)-inducing DNA damage. Using a lung cancer mouse model, CA-Pt treatment could effectively help RT suppress tumor growth (Fig. 35E-G). It could also prevent tumor invasion and metastasis.

Because mitochondria play essential roles in many cellular processes such as metabolism and apoptosis, mitochondria-targeted treatment was proposed by Xu's group, who achieved the *in situ* re-assembly in mitochondria by integrating a peptide substrate of enterokinase (ENTK) with a self-assembling motif to produce precursors [411]. After being taken up by cells, the self-assembled micelles turned into nanofibers and located mainly at mitochondria due to the cleavage of peptide motif by enterokinase. The micelles self-assembled from precursors could deliver cargos into mitochondria, providing an example of targeting subcellular organelles for biomedical application. Besides the cancer therapy, Yu's group reported a noncanonical amino acid of 2-nitroimidazol-1-yl alanine (abbreviated as A(2NI)) and used it to create a nitroreductase

(NTR)-responsive supramolecular peptide probe for efficient hypoxia imaging *in vivo* [412]. In this nanoplateform, the nitroimidazole unit of A (2NI) could serve as the fluorescence quencher and locked the signal of fluorescent nanofibers. The overexpressed NTR in the hypoxia region reduced the nitro group into amino group, leading to morphology-transformation from nanofibers to nanoparticles and fluorescent "turn-on". The morphology-transformation allowed for the improved tumor accumulation and penetration of nanoprobes into solid tumors, facilitating efficiently imaging hypoxic tumor cells.

5.1.3. Receptor-induced morphology transformation

Inspired by the finding that the fibrillogenesis of laminin/fibronectin (FN) on cell surfaces through binding certain receptors can modulate the communication between cells and ECM, Wang's group pioneered a creative concept of "binding induced fibrogenesis" to regulate cell behaviors. In their design, the spherical nanoparticles are usually fabricated via *ex situ* peptide self-assembly, which can bind specific receptors on cancer cells and induce the *in situ* transformation from nanospheres to nanofibers. The formed fibrous networks can inhibit tumor growth, migration, invasion and metastasis [413–417], angiogenesis inhibition [418,419], precise embolization in tumor vessels [420], etc. For example, they used the "binding induced fibrogenesis" strategy to construct artificial fibrous FN *in vivo*, relying on the specific recognition between RGD tripeptide and overexpressed integrin receptors on cancer cell surfaces [413]. In the MDA-MB-231 tumor-bearing mouse model, they found that overexpressed integrin receptors induced the morphological transformation of spherical BP-K-FFVLK-CREKA-FFVLK-DGR peptide nanoparticles into FN-like fibrous structures. Interestingly, the artificial fibrous FN could inhibit the growth and migration of tumor cells. Along this line, they designed a transformable peptide nanoparticle to induce cancer cell death via arresting the HER2 signaling (Fig. 36A) [421]. Peptide of BP-FFVLK-YCDGFYACYMDV (TPM) consisting of three discrete functional domains was obtained, in which a bispyrene (BP) moiety with AIE property enabled the fluorescence reporting and acted as the hydrophobic core to induce the *ex situ* self-assembly, FFVLK was a reverse sequence of β -sheet-forming KLVFF peptide for self-assembly, and the residual YCDGFYACYMDV sequence

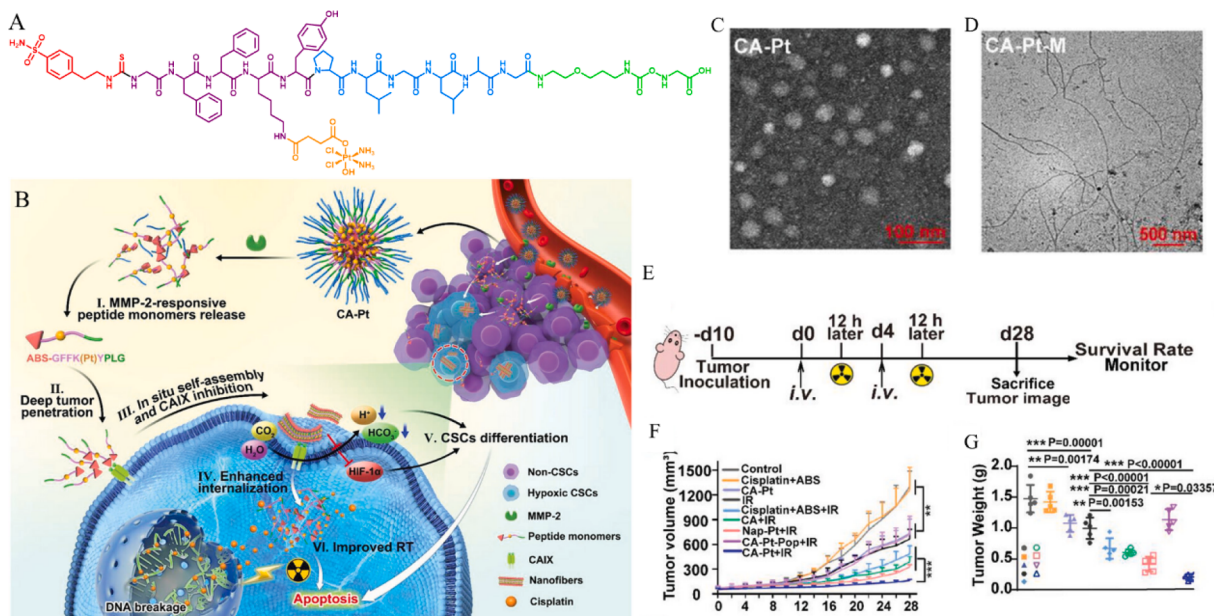


Fig. 35. (A) The chemical structure of ABS-GFFK(Pt)YPLGLAG-PEG₁₀₀₀. (B) Schematic illustration of the "monomer release-target accumulation-surface self-assembly" strategy to reverse CSC RT-resistance. This strategy allowed for deep tumor penetration, amplified CAIX inhibition, and enhanced drug internalization. (C, D) TEM images of CA-Pt nanomedicine before and after MMP-2 treatment. (E) Schematic diagram of tumor therapy schedule. (F) Tumor size of NCI-H1975-bearing BALB/c nude mice after the treatment with different formulations. (G) Weight of harvested tumors after different treatments. Adapted with permission from Ref. [410]. Copyright 2023, Wiley-VCH.

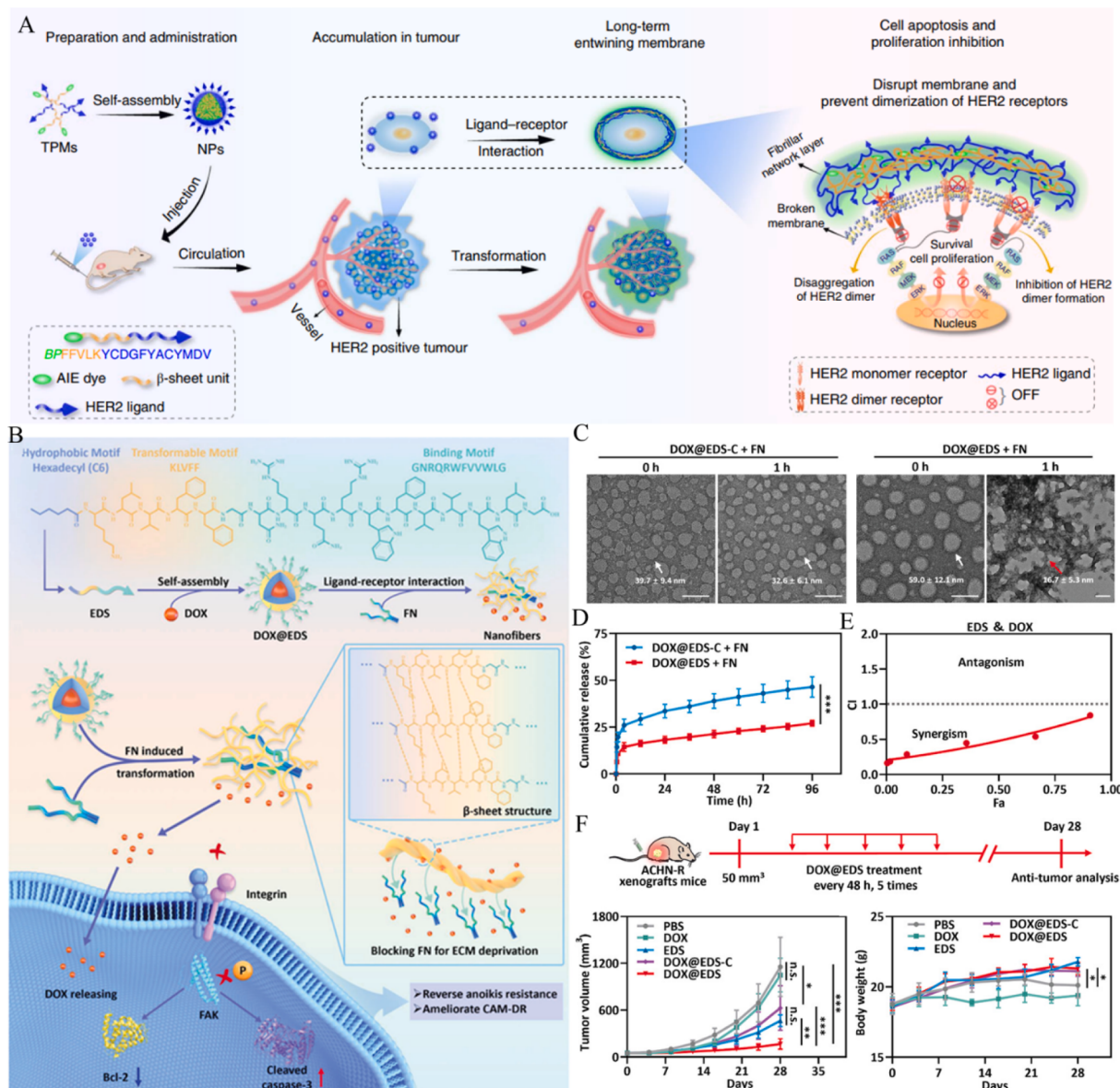


Fig. 36. (A) Schematic illustration of transformable peptide nanoparticles to arrest HER2 signalling for the cancer cell killing. Adapted with permission from Ref. [421]. Copyright 2020, Springer Nature (NC). (B) The structure of functional peptide, its self-assembly with DOX and re-assembly induced by FN, and the relevant of EDS. The formation of nanofibers long-term deprived ECM in tumor tissue and inhibited FAK-signaling to conquer the anoikis resistance and CAM-DR for synergistic anti-tumor. (C) TEM images of DOX@EDS and DOX@EDS-C (control group without morphological transformation) incubated with FN solution for different times. Scale bar: 100 nm. (D) Drug release curves of DOX@EDS and DOX@EDS-C incubated with FN solution. (E) Combinational index (CI) of EDS and DOX. (F) In vivo therapy of different formulations towards DOX-resistant ACHN-R cells-bearing mice, including therapeutic schedule, tumor volumes and body weight of treated mice. Adapted with permission from Ref. [422]. Copyright 2022, Wiley-VCH.

was proposed to target the HER2 that was overexpressed by breast cancers. Under the aqueous condition, TPMs self-assembled into spherical NPs that were preferentially accumulated at the tumor site. Once interacting with HER2 on tumor cell surfaces, spherical NPs transformed into the fibrillar network *in situ*, which inhibited the HER2 dimer formation and therefore blocked the expression of proliferating and survival genes in the nucleus. In another study, they further designed a bis-pyrene-KLVFF-VNTANST (BFV) to recognize vimentin, whose overexpression and improper self-assembly were related to tumor metastasis. Mediated by vimentin, self-assembled spherical BFV nano-peptide would *in situ* form fibrous networks to block vimentin skeletonection, therefore inhibiting the migration and invasion of tumor cells [415]. Recently, Wang and colleagues used the “binding induced fibrogenesis” strategy to construct ECM deprivation system (EDS) for suppressing RCC by conquering anoikis resistance and sensitizing

chemotherapy [422]. This was motivated by the phenomenon that FN directly regulates ECM-mediated anoikis resistance and cell adhesion-mediated drug resistance (CAM-DR). The structure of functional peptide was shown in Fig. 36B, which co-assembled with DOX and encapsulated it into the spherical inner. Based on the FN-mediated ligand-receptor interaction, spherical nanoparticle transformed into nanofibers (Fig. 36C). The re-assembled nanofibers could sequester FN and block the FN-mediated tumor-promoting signaling pathways for sustained ECM deprivation. Meanwhile, the reconstituted nanofibers acted as a drug depot for long-term drug release (Fig. 36D). ECM deprivation could conquer anoikis resistance and CAM-DR, and ultimately exerted synergistic therapy with DOX (Fig. 36E). In DOX-resistant ACHN cells (ACHN-R cells)-bearing mouse model, EDS effectively suppressed the growth of chemotherapy-resistance tumors (Fig. 36F).

Angiogenesis is usually associated with a variety of diseases such as

eye diseases and tumors, and anti-angiogenesis could be an effective route to cure these diseases. Overexpression of integrin $\alpha_v\beta_3$ on angiogenic tumor vasculature makes it an excellent target for disease treatment. Wang's group constructed a self-assembled BP-FFVLK-HSDVHK nanosphere with the ability of targeting integrin $\alpha_v\beta_3$ to inhibit angiogenesis [418]. Mediated by the binding of targeted HSDVHK peptide with integrin $\alpha_v\beta_3$, nanofibrous network was *in situ* formed and anchored on the surface of HUVECs, which inhibited their migration and angiogenesis. They further developed an antibody-like peptidic network (ALPN) to inhibit angiogenesis (Fig. 37A) [423]. The antibody-like peptide consisting of targeted RPL tripeptide and fibrillogenesis sequence of FFVLK could self-assemble into spherical nanoparticles (ALPN-NPs), which further targeted the angiogenesis-related

neuropilin-1 (NRP-1) and formed fibrous networks on the surface of endothelial cells (ECs). The fibrillogenesis trapped NRP-1 and blocked the normal signaling pathway of angiogenesis between VEGF and NRP-1, which alleviated the formation of choroidal neovascularization in rat eyes. According to the IHC staining and immunofluorescence staining on CD31 of choroidal neovascularization (CNV) area, ALPN-NPs group showed the similar inhibition on blood vessel formation (as indicated by red arrows and red circles) with the monoclonal antibody bevacizumab (Fig. 37B), but its dosage was 89.3 times lower than that of administrated bevacizumab. By adjusting the peptide composition, they further designed a peptide of lauric acid-FFVLK-HSDVHK [424]. The *in situ* fibrillogenesis on the membrane of neovascular endothelial cells could block multiple receptors such as integrin, VEGF receptor-2 and

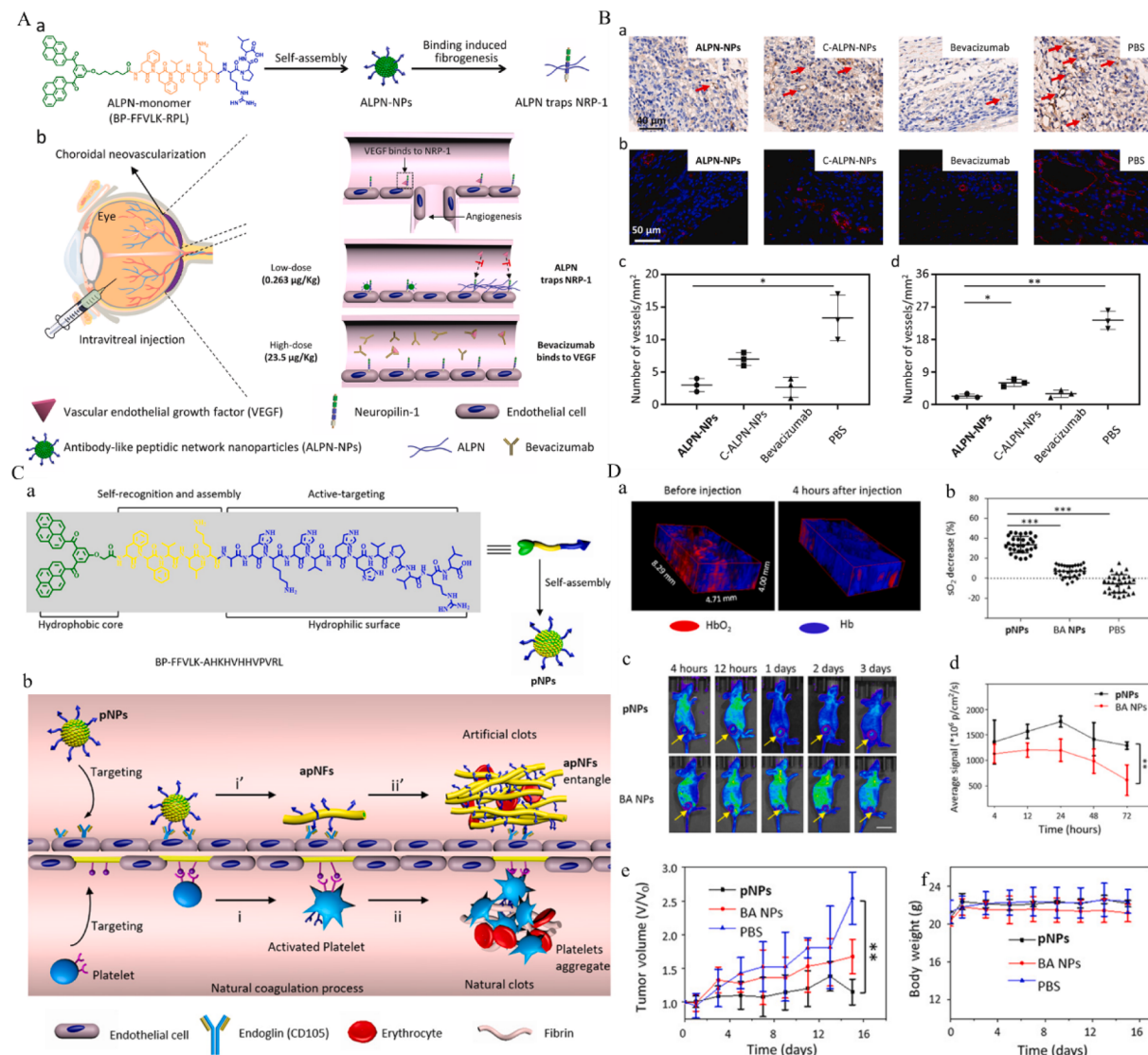


Fig. 37. (A) Peptide self-assembly, morphological transformation, and proposed mechanism of ALPN to inhibit angiogenesis. (a) The molecular structure of ALPN monomer, which self-assembled into spherical nanoparticles (ALPN-NPs) and underwent binding-induced fibrogenesis to trap NRP-1; (b) Schematic diagram of inhibiting angiogenesis-related CNV through blocking VEGF and NRP-1. The anti-angiogenesis mechanism of ALPN was trapping and blocking NRP-1 on the membrane of ECs, which was different from bevacizumab that bound to and blocked VEGF in ECM of ECs. (B) The anti-angiogenesis data of ALPN in a CNV rat model. (a, b) Immunohistochemistry staining and immunofluorescence images of CNV area in rats treated with different groups. Red arrows and red fluorescence signal indicated the new blood vessels; (c, d) vessel number statistics for corresponding groups of (a) and (b). Adapted with permission from Ref. [423]. Copyright 2021, Elsevier Ltd. (C) Illustration of receptor-mediated *in situ* peptide re-assembly to mimic the platelets for *in vivo* artificial coagulation. (a) Chemical structure of designed pNP monomer and its *ex situ* self-assembly into pNPs; (b) The proposed process of biomimetic and natural coagulation. (D) pNP-induced tumor thrombosis to inhibit MDA-MB-231 human breast growth. (a) Photoacoustic imaging on SO_2 in MDA-MB-231-xenografted tumor bearing BALB/c mice after pNP injection for 0 and 4 h; (b) Statistical analysis of SO_2 decrease [%] over time for different groups; (c, d) Time-dependent tumor volume curves and body weight curves after different treatments. Adapted with permission from Ref. [425]. Copyright 2020, The Authors.

neuropilin-1, which therefore achieved a highly efficient treatment of anti-angiogenesis, with 97.7 times lower dose than bevacizumab.

Originating from the significant role of platelets in regulating coagulation, Wang's group used the receptor-mediated *in situ* peptide re-assembly to mimic the platelets for *in vivo* artificial coagulation [425]. Functional peptide of BP-FFVLKAHKHVHHVPVRL was composed of three modules, i.e. hydrophobic bis-pyrenes (BP) for fluorescent imaging, FFVLK for self-assembly and morphological transformation, and AHKHVHHVPVRL that targeted to the endoglin (CD105) receptor (Fig. 37C). Because CD105 receptor was overexpressed by angiogenic endothelial cells in tumors, the self-assembled platelet-like nanoparticles (pNPs) could target the angiogenic endothelial cells via ligand-receptor recognition and thereafter re-assembled into activated platelet-like nanofibers. Then, the platelet-like nanofibers recruited surrounding fibers to form the artificial clots to inhibit the tumor growth. Compared with the decrease of blood oxygen saturation (sO_2) in PBS of -5.3% and NP group of 7.1% , the pNP treated group decreased significantly (33.8%), suggesting that the artificial clots effectively decreased the oxygen supply to tumors (Fig. 37D). Meanwhile, pNP-treated group showed much higher fluorescence signal in tumors than the control group, showing the long-time retention of pNPs in tumors. As a result, the pNP-treated group showed the smallest tumor volume in mice.

5.1.4. ROS-induced morphology transformation

Wang's group used endogenous ROS to induce the morphology transformation of self-assembled PPC for enhanced mitochondrial damage (Fig. 38A) [426]. Mitochondria-targeting therapeutic KLAK peptide and a self-assembling KLVFF segment conjugated with PEG through ROS-cleavable thioether were conjugated to the side group of poly(vinyl alcohol) backbone to generate PPC, which self-assembled into spherical nanoparticles and entered cancer cells to target the mitochondria. The over-generated ROS around mitochondria cleaved the thioether linker, facilitating the transformation of spherical

nanoparticles to fibrous nanostructures (Fig. 38B). The formed nanofibers with therapeutic KLAK peptide enhanced the interactions with mitochondria (Fig. 38C), which enhanced the accumulation in tumor tissue (Fig. 38D) and exhibited high antitumor efficacy (Fig. 38E). In another study, Yu and colleagues used the loaded PS to generate ROS to regulate peptide re-assembly for cancer therapy [427]. Methionine (Met, M) was incorporated to construct hexapeptide of EIMIME for oxidation-regulated self-assembly. Ce6 was introduced to connect with EIMIME to account for PDT and *in situ* Met-oxidation, which promoted morphological transition from primary nanofibers to nanospheres for deep tumor penetration.

5.1.5. Other species-induced morphology transformation

Apart from endogenous species, some exogenous stimuli such as light and heat have also been employed to regulate self-assembled morphology *in situ*. These exogenous stimuli share the feature of spatial and temporal precision. Wang, Zou and co-workers used light to induce peptide re-assembly from nanoparticles into nanofibers in living cells to regulate cell behavior [428]. 3-methylene-2-(quinolin-8-yl) isoindolin-1-one (MQIO) acting as a light-responsive unit was appended to a targeting peptide of SGFFVLK-RGD, and yielded MQIO-SGFFVLK-RGD self-assembled into nanospheres in solution (Fig. 39A). Given light irradiation, MQIO unit underwent molecular conformation change and molecular sliding, which therefore disrupted the primary hydrophilic/lipophilic balance (HLB) and resulted in the transformation from nanospheres to nanofibers. The light-triggered re-assembly in lysosomes induced cell death and improved the bioavailability of anti-cancer drugs. Moreover, Wang, et al. used light treatment to promote morphology transformation to improve the biological performance of drug molecules [429]. Peptide-conjugate was composed of a therapeutic (KLAKLAK)₂, a self-assembling KLVFF core, a GSH-cleavable disulfide bond connected with mPEG, and a photothermal/PA purpurin-18 (P18) molecule. With NIR illumination or heating that activated the photothermal effect of P18, the transformation rate from nanospheres to

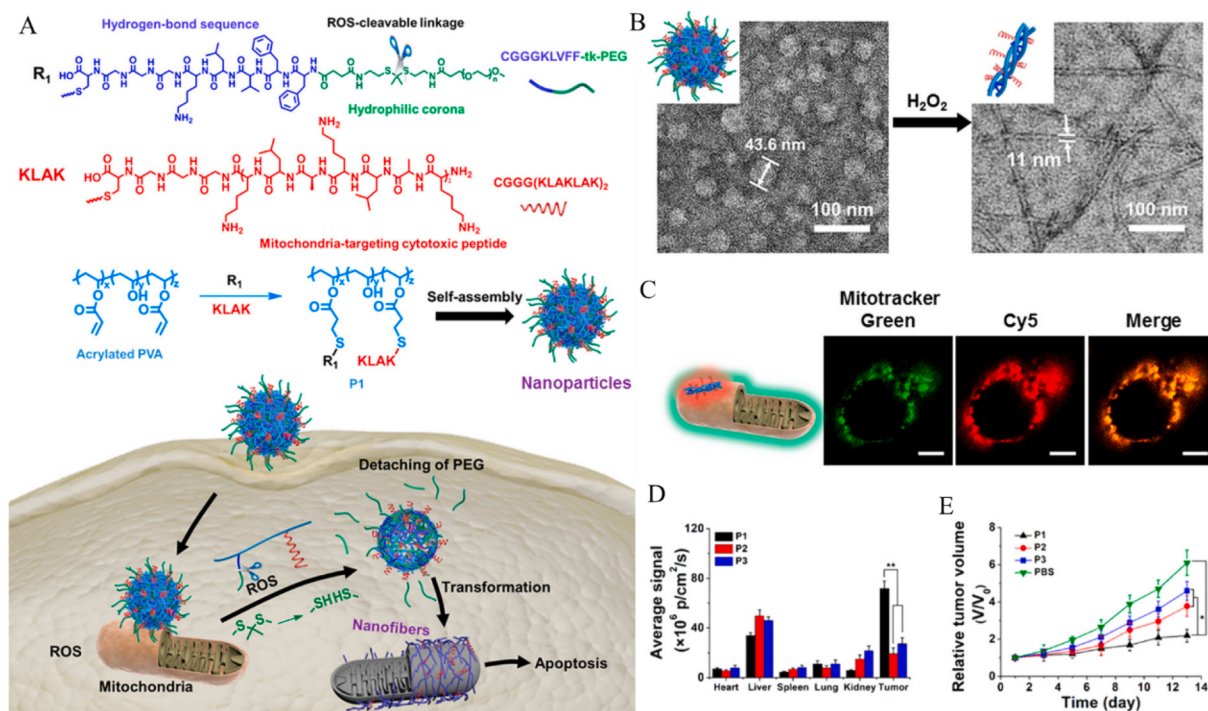


Fig. 38. (A) The structure of ROS-sensitive PPC and morphological transformation in mitochondria for apoptosis. (B) Representative TEM images of P1 nanoparticles before and after incubation with H_2O_2 . (C) CLSM images of HeLa cells treated with P1 and stained by Mitotracker (green, 488 nm) and Cy5 (red, 633 nm). Scale bar: 5 μ m. (D) Average fluorescence of tumor and major organs after 96 h post intravenous injection of Cy5-labeled PPC. (E) Relative tumor volumes of mice treated by self-assembled PPCs at different times. Adapted with permission from Ref. [426]. Copyright 2019, American Chemical Society.

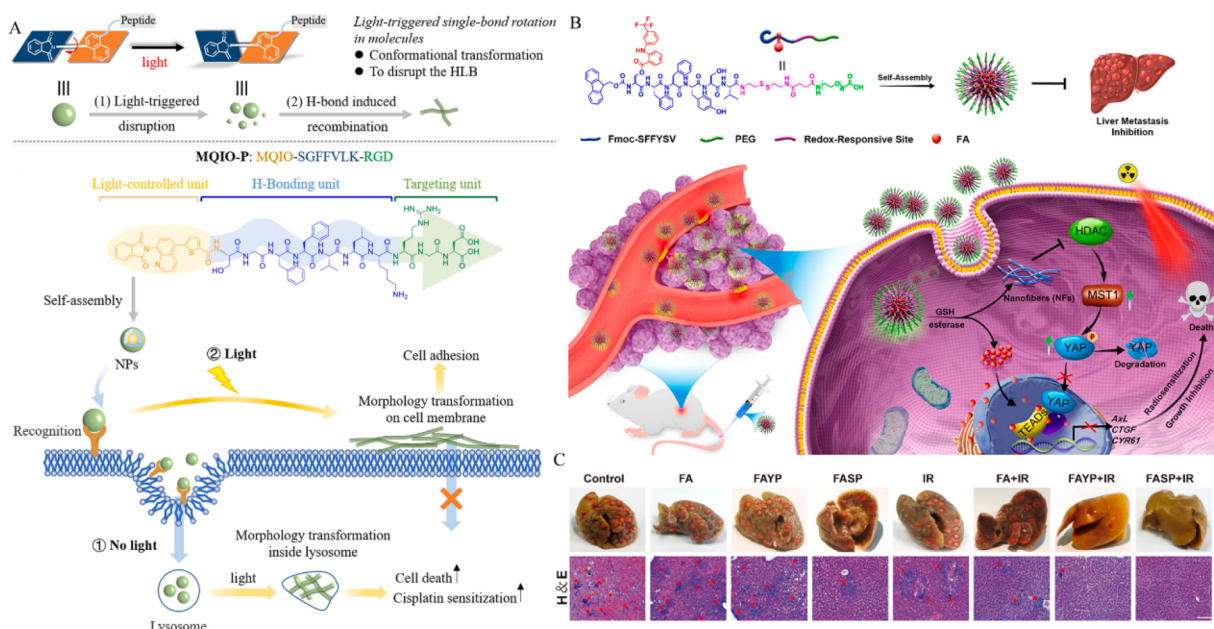


Fig. 39. (A) Molecular structure of MQIO-SGFFVLK-RGD and schematic illustration of light-triggered re-assembly driven by conformational change and hydrogel bond. The transformation process induced by light inside/outside cells and its relevant biological performance were illustrated. Reproduced with permission from Ref. [428]. Copyright 2022, American Chemical Society. (B) Molecular structure, *ex situ* self-assembly, and *in situ* transformation induced by dual-stimuli to activate Hippo pathway for inhibiting tumor growth and metastasis. (C) Photos of liver metastases and their corresponding H&E staining images treated with different groups. Representative metastatic nodules in the liver were marked by red circles and arrows. Adapted with permission from Ref. [430]. Copyright 2022, American Chemical Society.

nanofibers increased by ~4 times and the drug accumulation in tumor increased by ~2 times, resulting in enhanced anticancer capacity. Interestingly, the re-assembly process could be visualized through the advanced ratiometric photoacoustic (RPA) image, showing the potential of developing intelligent theranostic.

Apart from single-stimulus paradigm, the combination of double species has also been exploited to regulate the morphological transformation of peptide self-assemblies for cancer treatments. A self-deliverable nanomedicine from Fmoc-S(FA)FFYSV-SS-PEG₁₀₀₀ (abbreviated as FASP) was designed to targetedly activate Hippo pathway for cancer treatments [430]. FASP consisted of flufenamic acid (FA)-modified hydrophobic peptide, YSV, hydrophilic PEG, and esterase-responsive ester bond as well as GSH-responsive disulfide bond was incorporated (Fig. 39B). Stimulated by GSH and esterase in cancer cells, the transformation from inactive nanospheres to active nanofibers occurred, companying with the release of FA drug *in situ*. Free FA and YSV-containing nanofibers activated the maladjusted Hippo pathway through acting on the different targets. Moreover, the restoration of Hippo-pathway caused radio-sensitization. The liver metastasis of MDA-MB-231 cell bearing BALB/c nude mice was significantly reduced after treated by FASP NPs and FASP + IR (Fig. 39C). These resulted showed that the combination of hippo-pathway-targeted therapy and radiotherapy exhibited the antimetastatic ability against triple-negative breast cancer.

5.2. Morphological adaption for antimicrobial therapy

Beside the antitumor therapy, the combination of *ex situ* and *in situ* peptide self-assembly provides a new route to solve the bacterial infections. To bestow anti-bacterial agent with targeted accumulation and long-term retention in the infectious site, a polymer-peptide conjugate consisting of a chitosan backbone, an antibacterial peptide and a PEG-tethered enzyme-sensitive peptide was synthesized [431]. Polymer-peptide initially self-assembled into spherical nanoparticles with pegylated coronas. Once encountering the gelatinase secreted by bacteria, the nanoparticles detached the PEG coronas and transformed into

fibrous nanostructures, with the exposure of antimicrobial peptide to target bacterial membranes. Due to the *in situ* morphological transformation, self-assembling polymer-peptide achieved the enhanced accumulation and retention in infectious sites *in vivo*. Just for this, the “on-site transformation” model exhibited highly efficient antibacterial activity. Qin and co-workers introduced the charge reversal strategy to alleviate the undesirable hemolysis and toxicity of positive antimicrobial peptides, accompanying with morphological adaptation to improve *in vivo* bacterial ablation [432]. The ε-amino groups within C₁₆-A₃K₄-CONH₂ were acylated by DMA, and generated C₁₆-A₃K₄(DMA)-CONH₂ self-assembled into negative nanospheres to relieve protein adsorption and prolong blood circulation. After accessing into microbial infection sites, C₁₆-A₃K₄(DMA)-CONH₂ detached the DMA group to release the positive C₁₆-A₃K₄-CONH₂, which directly destroyed the bacterial membrane. At the same time, self-assembled nanospheres transformed into rod-like nanostructures with larger surface area, which improved the contact with bacterial membrane. Collectively, the acid-activated AMP nanotherapeutics exhibited desirable and broad-spectrum antimicrobial activities, as well as relieved hemolysis and cytotoxicity. Different from the transformation from spherical nanoparticles to nanofibers *in vivo*, very recently, Ma and co-workers reported morphology-adaptable peptide nano-assemblies from fibrous nanostructures to nanospheres to combat drug-resistant bacteria and biofilms [433]. At physiological pH, chimeric peptide of C₁₄-(HHHF)₄-HHHK (PEG₈)-QRKLAALKT-NH₂ self-assembled into biocompatible nanofibers, which thereafter transformed into smaller nanoparticles in acidic infection. This process would improve the penetration of nanopeptides into bacterial biofilms to kill drug-resistant bacteria through membrane damage (Fig. 40A). The live/dead staining of drug-resistant *P. aeruginosa* treated by peptide nano-assemblies was conducted at pH 5.0 and 7.4 (Fig. 40B), showing the pH-dependent antibacterial activity. *In vivo* fluorescence imaging of healthy and infected mice after intraperitoneal injection of nanopeptides indicated that size-transformable nano-assemblies could effectively remain in the infected site for a long time (Fig. 40C). The serum inflammatory factor analysis indicated nanopeptides relieved the level of cytokines (Fig. 40D). The *in vivo* assays in

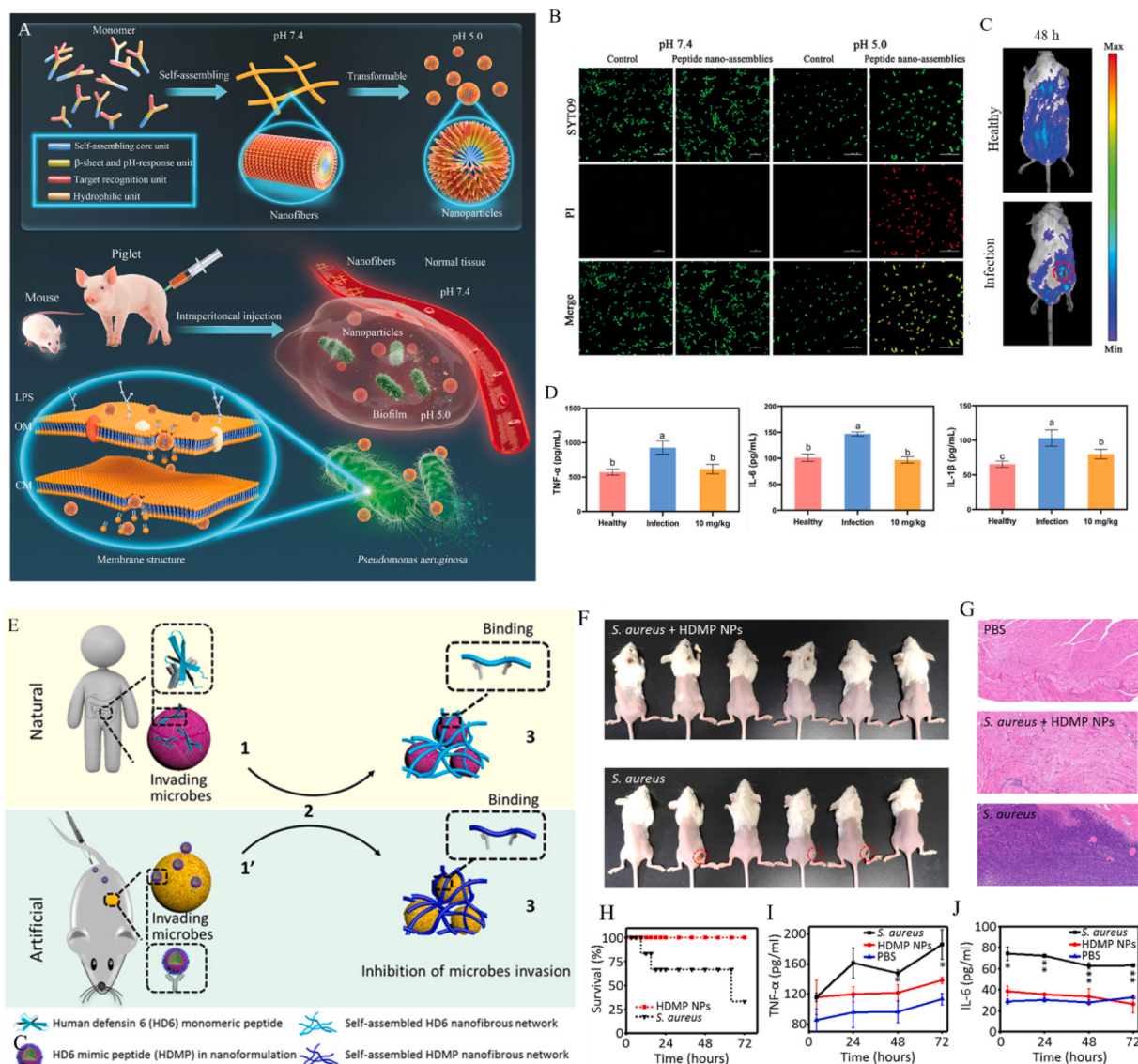


Fig. 40. (A) Schematic diagram of self-assembly of C₁₄-(HHHF)₄-HHHK(PEG₈)-QRKLAALKT-NH₂ and morphological transformation of nano-assemblies induced by pH, and antibacterial mechanism of killing drug-resistant *P. aeruginosa* by disrupting membrane. (B) Live/dead staining imaging of drug-resistant *P. aeruginosa* with nanopeptides at pH 5.0 and 7.4. (C) Fluorescence imaging of healthy and infected mice after intraperitoneally injecting nanopeptides. (D) Serum inflammatory factor (TNF-α, IL-6, and IL-1β) analysis of infected and healthy mice treated with PBS and nanopeptides. Adapted with permission from Ref. [433]. Copyright 2023, Wiley-VCH. (E) Schematic illustration of antimicrobial mechanisms of natural HD-6 and artificial HDMP. (F) Images of mice inoculated with *S. aureus* alone and HDMP NP-incubated *S. aureus*. (G) Corresponding H&E staining images of muscle tissue in mouse leg after treated with different formulations. (H) Survival curves of *S. aureus*-infected mice with/without HDMP NP treatment. (I) TNF-α and (J) IL-6 levels in mouse sera of different groups. Adapted with permission from Ref. [434]. Copyright 2020, The Authors.

mice and piglets indicated that the chimeric peptide nano-assemblies with size-adaption could effectively reduce bacterial load within biofilms.

The antimicrobial function of human defensin-6 (HD-6) is found to be ascribed to the formation of self-assembled entangled fibrous networks, which trap microbial pathogens and block their invasion rather than the direct killing of HD-6 toward microbials. Inspired by this finding, Wang's group designed a HD-6 mimic peptide of BP-KAAFF-RRLYLIGRR (HDMP) to inhibit bacterial invasion *in vivo* through the *in situ* peptide re-assembly (Fig. 40E) [434]. Peptide nanospheres (HDMP NP) targeted the bacteria through the recognition of RLYLIGRR peptide ligand towards the lipoteichoic acid (LTA) receptor, a unique constituent on Gram-positive bacteria surface. The ligand-receptor interaction induced the *in situ* adaptive transformation from nanospheres to nanofibrous network to inhibit microbial invasion. Three of six mice inoculated with *S. aureus* alone showed the abscess, but none

of the HDMP NP-incubated *S. aureus* group showed the sign of infection (Fig. 40F). The H&E staining images also indicated that bacterial infection was effectively inhibited by HDMP NP *in vivo* (Fig. 40G). What's more, the biomimetic antimicrobial strategy exhibited excellent biosafety with a survival rate of 100 % for *S. aureus* infected mice (Fig. 40H). It also reduced the amount of TNF-α and IL-6 in mice, indicating that sepsis was effectively inhibited (Fig. 40I, J).

5.3. Morphological adaption for other diseases

Apart from the imaging and therapy in cancers and bacterial infections, morphological adaption based on peptide self-assembly has also shown promising applications in the diagnosis and treatment of other diseases. For example, Wang, *et al.* introduced the Smart Peptide deFeNse (SPIN) web technique to trap immunoglobulin E (IgE) for allergic rhinitis (AR) therapy (Fig. 41A) [435]. Self-assembled BP-K

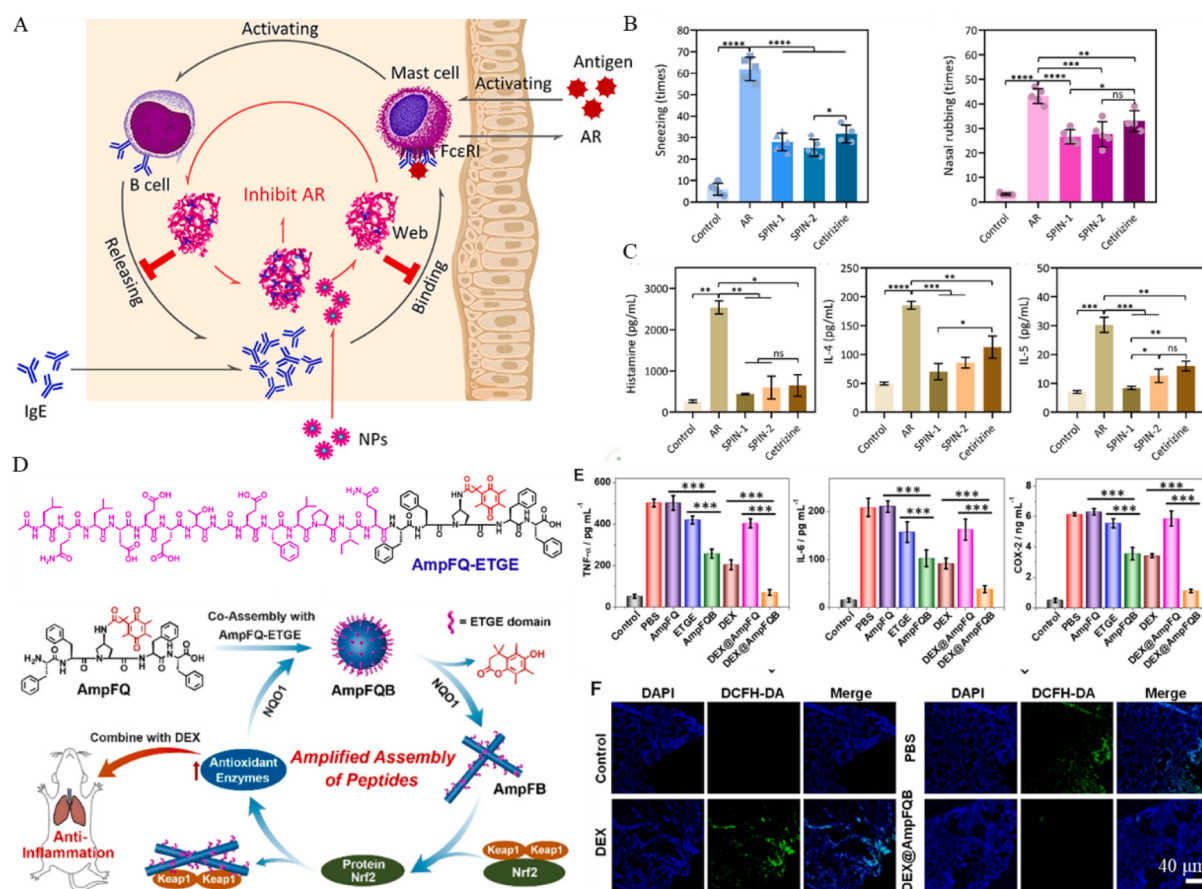


Fig. 41. (A) Schematic illustration of morphological transformation from NPs to SPIN web to trap IgE against AR in the nasal mucosa. Detailedly, peptidic NPs would transform into IgE-SPIN web once encountering IgE and settling in the nasal mucosa for a long time, which therefore prevented IgE from recognizing and binding its high-affinity receptor of Fc ϵ RI on mast cell surface to inhibit AR. (B) Counts of sneezing (Left) and nasal rubbing (Right) of mice in different groups on the 33 d. (C) Amount of histamine (Left), IL-4 (Middle), and IL-5 (Right) in the serum of each group on 34 d. Adapted with permission from Ref. [435]. Copyright 2022, American Chemical Society. (D) Peptide structures and their self-amplifying assembly to up-regulate the NQO1 expression. (E) Proinflammatory cytokines of TNF- α , IL-6, and COX-2 in mice with various treatments. (F) CLSM images of lung tissues (stained with DCFH-DA) dissected from injured mice treated with different formulations. Adapted with permission from Ref. [436]. Copyright 2022, American Chemical Society.

FFVLK-SILPVDAKDWIEGEG (SPIN-1) and BP-K-FFVLK-HPEYAVSVLL (SPIN-2) with different IgE-targeting sequences were able to trap IgE and transformed their morphology from nanoparticle to entangled nanofiber web. This process prevented IgE from binding with mast cells and inhibited mast cells to release inflammatory factors for AR. SPIN-1 and SPIN-2 effectively alleviated symptoms of rhinitis (Fig. 41B) and inflammatory factors (Fig. 41C) in AR model Balb/c mice, even better than cetirizine (a first-line clinical drug). Yu's group proposed a strategy of self-amplifying peptide assembly for inflammatory treatment, which involved in the *in situ* re-assembly of peptide to achieve this biologic function [436]. Co-assemble of a quinone propionic acid (QPA)-containing peptide (AmpFQ) and its derivative (AmpFQ-ETGE) resulted in the formation of spherical nanoparticle (AmpFQB) (Fig. 41D). Inside the cells, the enzyme of NAD(P)H quinone dehydrogenase 1 (NQO1) detached the QPA moiety, and residual peptide re-assembled into nanofibrils. Protein ligand of ETGE locating on nanofibril surface targeted the protein Kelch ECH-associated protein 1 (Keap1). This process led to the dissociation of Nrf2-Keap1 complex and activated protein Nrf2 (nuclear factor erythroid 2-related factor 2), which upregulated antioxidant enzymes for anti-inflammation and facilitated NQO1 expression for self-amplifying. The *in vivo* anti-inflammatory assay on acute lung injury indicated that this self-amplifying nanoplatform could enhance the anti-inflammation of dexamethasone (DEX) via downregulating proinflammatory cytokines of TNF- α , IL-6, and COX-2 (Fig. 41E) and alleviating ROS generation (Fig. 41F). Jokerst's group reported a peptide-

conjugate to selectively image and inhibit SARS-CoV-2-infected cells [437]. The amphiphilic peptide-conjugate containing five functional domains self-assembled into loose nanoparticles in aqueous solution, with positively charged surface and weak fluorescence. After the cleavage by the main protease (M^{pro}) in SARS-CoV-2, loose nanoparticles detached the hydrophilic hexamolyarginine and increased the hydrophobicity. The enhanced self-assembly behavior driven the re-assembly of residual peptide-conjugate into smaller nanoparticles with strong fluorescence for selective imaging. Meanwhile, the formation of smaller nanoparticles inside mitochondria could also selectively inhibit the growth of SARS-CoV-2-infected cells.

6. Summary and outlook

Integrating the advantages of peptides with molecular self-assembly, this review has summarized recent research that utilize peptide self-assembly to afford functional nanomaterials for biomedical applications. Herein, peptide self-assembly has been discussed from the perspectives of *ex situ* and *in situ*. We first present the *ex situ* peptide self-assembly to construct functional biomaterials. The pre-fabricated nanostructures applied as cargo delivery carriers, self-deliverable nanomedicines and tissue engineering are discussed. Capitalizing on the multifunction of peptides and EPR effects resulted from nanomaterials, these nanoplatforms are achievable of targeted delivery and smart release of various agents, which remarkably elevate the outcomes

of imaging and therapy. In parallel, the superiorities of self-assembled peptide hydrogels used for drug control release, 3D cell culture and remodeling tumor microenvironments are also discussed in the first section.

To replenish the functionalities of *ex situ* peptide self-assemblies in biomedical field, in the second section, “*in situ* peptide self-assembly” has been highlighted. As an alternative modality, the “*in situ* peptide self-assembly” mainly focuses on the direct construction of nanomaterials in living cells instead of in solution. Apart from the general trigger modalities that are manipulated by physiological and pathological environments (eg: pH, enzyme, redox, and receptor), biological effects elicited by “*in situ* peptide self-assembly” have been illustrated and extended to guide disease imaging and therapy. In this regard, “*in situ* self-assembly” holds the following merits. 1) AIR effect optimizes the cargo biodistribution, avoids the premature release, minimizes the drug resistance and reduces the accumulation of nanomedicines in liver and kidney. 2) The strategy allows the cargo penetration into deep tumors, which advances the imaging and therapy. 3) The direct construction of biomaterials *in vivo* allows for emulating the dynamic organization of functional species and investigating their sophisticated biological functions.

The morphological properties strongly affect the *in vivo* nanoparticle behavior, and it is generally difficult to obtain the optimized outcomes for nanomedicine with a constant shape and size. Morphology-adaptable nanoplatforms show the promising to maximize the benefits of different morphologies. In the third part, the strategy of *ex situ* combining with *in situ* peptide self-assembly was summarized. The *ex situ* self-assembly realized the construction of peptide nanoarchitectures for drug delivery, and *in situ* self-assembly deformed the morphology of nanoarchitectures in living subjects to achieve needed functions. The relevant biological effects triggered by peptide-based re-assembly were illustrated.

Notably, the inexhaustible sequence structures and discovering functions of peptides impart peptide self-assembly as a versatile toolbox to provide versatile biomaterials. Furthermore, self-assembly guided biological evolution in nature evokes continuous thought and will consequently arouse infinite possibilities. With these foundations, the development of peptide self-assembly can be further boosted. To robustly push the peptide self-assembly, several fundamental challenges should be considered.

First, the structure–activity relationships of peptides should be established not only at the molecular level, but also at the supramolecular level. The supramolecular elements such as the secondary conformation (eg: α -helix, β -sheet, random coil and their ratio) and aggregated state (morphology, size) that are related with the activity/function of peptide self-assemblies should be considered and compared. To evaluate their bioactivities at a supramolecular level, the batch-to-batch inconsistencies in drug content and degradation rate of different nanomedicines would be taken into account.

Second, the homogeneity and biostability of peptide self-assemblies are generally unclear, especially in *in vivo*. As we know, the self-assembly process is predominantly driven by thermodynamics (hydrogen-bonding, π - π stacking, electrostatic, hydrophobic, and van der Waals interactions), contributing to the formation of nanomaterials with certain size and shape. But not all the individual peptides transform into nanomaterials. The fate of these unassembled peptides and their influence on the overall outcomes are ignored. On the other hand, the thermodynamics is affected by various kinetic parameters such as pH, temperature, counter-ion, concentration, and other species. Kinetic factor-induced disassembly or self-assembly may occur prematurely in living cells, which result in the inaccuracy or even failure of disease diagnosis and therapy. More attention could be paid to the dynamic process of peptide self-assembly *in vivo*, and AIEgens may be a promising candidate for monitoring the dynamic process.

Third, anisotropic peptide self-assembly has not been well addressed. In human body, many bio-functions and even tumorigenesis are

associated with oriented arrangement of cells or ECM fibrils. As such, creating anisotropic peptide self-assemblies is very promising. Through designing peptide structures and controlling over the self-assembling process, peptide materials could be endowed with microscale and macroscale order, which can guide cell alignment to form certain tissue/organs, and recapitulate tumor microenvironment for cancer research.

Forth, the detailed interaction between peptide self-assemblies and organisms is not well understood. Given the tremendous potential of cryo-TEM and NMR in revealing the interaction information, exploring such techniques to study their interactions will accelerate the clinical implementations of peptide self-assembly.

Fifth, self-assembled peptide nanomaterials have been well exploited in treating cancers. But the efficacy of nanomedicines in cancer research has received controversy in recent years. On the one hand, some researchers questioned that the real role of EPR effect, and proposed that active transcytosis may contribute to the entry of nanodrugs into solid tumors. This should be considered in the future design criteria to develop new cancer nanomedicines. To improve the drug accumulation, functional peptides such as targeting peptides and stimulus-sensitive peptides could be rationally integrated into self-assembling nanosystems. On the other hand, the clinical efficacy of most nanomedicines is not desirable. Material scientists (chemists) should work together closely with pharmaceutical scientists and clinicians to design, evaluate and translate nanomedicines for clinical tumor therapy. Furthermore, the applications in the diagnosis and treatment of other diseases are less reported. Possibly, the continuous enrichment of peptide libraries and the optimization of self-assembling strategies can broaden their applications for more diseases such as nervous disease, non-bacterial inflammation, eye disease, nephropathy, obesity and liver fibrosis.

Conflicts of interest

There are no conflicts to declare.

Declaration of competing interest

The authors declare that they have no known competing financial interests or personal relationships that could have appeared to influence the work reported in this paper.

Data availability

Data will be made available on request.

Acknowledgements

This work was financially supported by the National Natural Science Foundation of China (52273313), the Natural Science Foundation of Hubei province of China (2022CFB466), Knowledge Innovation Program of Wuhan-Basic Research (20230202010150), and Fundamental Research Funds for the Central Universities, South-Central Minzu University (CZY22005).

References

- [1] S. Chagri, D.Y.W. Ng, T. Weil, Designing bioresponsive nanomaterials for intracellular self-assembly, Nat. Rev. Chem. 6 (2022) 320–338, <https://doi.org/10.1038/s41570-022-00373-x>.
- [2] F. Nie, K.Z. Wang, D. Yan, Supramolecular glasses with color-tunable circularly polarized afterglow through evaporation-induced self-assembly of chiral metal-organic complexes, Nat. Commun. 14 (2023) 1654, <https://doi.org/10.1038/s41467-023-37331-0>.
- [3] Z. Sun, R. Liu, T. Su, H. Huang, K. Kawamoto, R. Liang, B. Liu, M. Zhong, A. Alexander-Katz, C.A. Ross, J.A. Johnson, Emergence of layered nanoscale mesh networks through intrinsic molecular confinement self-assembly, Nat. Nanotechnol. 18 (2023) 273–280, <https://doi.org/10.1038/s41565-022-01293-z>.
- [4] Y. Xiao, G. Tian, W. Li, Y. Xie, B. Jiang, C. Tian, D. Zhao, H. Fu, Molecule Self-Assembly Synthesis of Porous Few-Layer Carbon Nitride for Highly Efficient

- Photoredox Catalysis, *J. Am. Chem. Soc.* 141 (2019) 2508–2515, <https://doi.org/10.1021/jacs.8b12428>.
- [5] J. Han, H. Gong, X. Ren, X. Yan, Supramolecular nanozymes based on peptide self-assembly for biomimetic catalysis, *Nano Today*. 41 (2021), 101295, <https://doi.org/10.1016/j.nantod.2021.101295>.
- [6] Y. Lou, B. Zhang, X. Ye, Z.-G. Wang, Self-assembly of the de novo designed peptides to produce supramolecular catalysts with built-in enzyme-like active sites: a review of structure–activity relationship, *Mater. Today Nano*. 21 (2023), 100302, <https://doi.org/10.1016/j.mtnano.2023.100302>.
- [7] P. Ding, L. Wu, Z. Lin, C. Lou, M. Tang, X. Guo, H. Guo, Y. Wang, H. Yu, Molecular Self-Assembled Ether-Based Polyrotaxane Solid Electrolyte for Lithium Metal Batteries, *J. Am. Chem. Soc.* 145 (2023) 1548–1556, <https://doi.org/10.1021/jacs.2c06512>.
- [8] Q. Cheng, H. Chen, F. Yang, Z. Chen, W. Chen, H. Yang, Y. Shen, X.M. Ou, Y. Wu, Y. Li, Y. Li, Molecular Self-Assembly Regulated Dopant-Free Hole Transport Materials for Efficient and Stable n-i-p Perovskite Solar Cells and Scalable Modules, *Angew. Chemie - Int. Ed.* 61 (2022) e202210613.
- [9] Y. Sasaki, R. Kubota, T. Minami, Molecular self-assembled chemosensors and their arrays, *Coord. Chem. Rev.* 429 (2021), 213607, <https://doi.org/10.1016/j.ccr.2020.213607>.
- [10] E. Froimchuk, S.T. Carey, C. Edwards, C.M. Jewell, Self-Assembly as a Molecular Strategy to Improve Immunotherapy, *Acc. Chem. Res.* 53 (2020) 2534–2545, <https://doi.org/10.1021/acs.accounts.0c00438>.
- [11] P.-P. He, X.-D. Li, L. Wang, H. Wang, Bispyrene-Based Self-Assembled Nanomaterials. In Vivo Self-Assembly, Transformation, and Biomedical Effects, *Acc. Chem. Res.* 52 (2019) 367–378, <https://doi.org/10.1021/acs.accounts.8b00398>.
- [12] Z. Lyu, L. Ding, A. Tintaru, L. Peng, Self-Assembling Supramolecular Dendrimers for Biomedical Applications: Lessons Learned from Poly(amidoamine) Dendrimers, *Acc. Chem. Res.* 53 (2020) 2936–2949, <https://doi.org/10.1021/acs.accounts.0c00589>.
- [13] A. Levin, T.A. Hakala, L. Schnaider, G.J.L. Bernardes, E. Gazit, T.P.J. Knowles, Biomimetic peptide self-assembly for functional materials, *Nat. Rev. Chem.* 4 (2020) 615–634, <https://doi.org/10.1038/s41570-020-0215-y>.
- [14] M.J. Webber, E.T. Pashuck, (Macro)molecular self-assembly for hydrogel drug delivery, *Adv. Drug Deliv. Rev.* 172 (2021) 275–295, <https://doi.org/10.1016/j.addr.2021.01.006>.
- [15] T.O. Mason, U. Shimanovich, Fibrous Protein Self-Assembly in Biomimetic Materials, *Adv. Mater.* 30 (2018) 1706462, <https://doi.org/10.1002/adma.201706462>.
- [16] S. Saad, D.F. Jarosz, Protein self-assembly: A new frontier in cell signaling, *Curr. Opin. Cell Biol.* 69 (2021) 62–69, <https://doi.org/10.1016/j.ceb.2020.12.013>.
- [17] L. He, J. Mu, O. Gang, X. Chen, Rationally Programming Nanomaterials with DNA for Biomedical Applications, *Adv. Sci.* 8 (2021) 2003775, <https://doi.org/10.1002/advs.202003775>.
- [18] J. Lu, P. Hu, L. Cao, Z. Wei, F. Xiao, Z. Chen, Y. Li, L. Tian, Genetically Encoded and Biologically Produced All-DNA Nanomedicine Based on One-Pot Assembly of DNA Dendrimers for Targeted Gene Regulation, *Angew. Chemie Int. Ed.* 60 (2021) 5377–5385, <https://doi.org/10.1002/anie.202012916>.
- [19] Z. Di, X. Yi, L. Li, Protease-Triggered, Spatially Controlled DNA Assembly in Apoptotic Cells for Early Evaluation of Therapeutic Efficacy, *J. Am. Chem. Soc.* 145 (2023) 7931–7940, <https://doi.org/10.1021/jacs.2c13214>.
- [20] S.-Y. Qin, M.-Y. Peng, L. Rong, B. Li, S.-B. Wang, S.-X. Cheng, R.-X. Zhuo, X.-Z. Zhang, Self-defensive nano-assemblies from camptothecin-based antitumor drugs, *Regen. Biomater.* 2 (2015) 159–166, <https://doi.org/10.1093/rb/rbv011>.
- [21] H.-T. Feng, J.W.Y. Lam, B.Z. Tang, Self-assembly of AIEgens, *Coord. Chem. Rev.* 406 (2020), 213142, <https://doi.org/10.1016/j.jccr.2019.213142>.
- [22] H. Wang, Z. Feng, B. Xu, Bioinspired assembly of small molecules in cell milieu, *Chem. Soc. Rev.* 46 (2017) 2421–2436, <https://doi.org/10.1039/C6CS00656F>.
- [23] S.-Y. Qin, Y.-J. Cheng, Z.-W. Jiang, Y.-H. Ma, A.-Q. Zhang, Morphology control of self-deliverable nanodrug with enhanced anticancer efficiency, *Colloids Surfaces B Biointerfaces*. 165 (2018) 345–354, <https://doi.org/10.1016/j.colsurfb.2018.02.054>.
- [24] Y. Wang, K. Xia, L. Wang, M. Wu, X. Sang, K. Wan, X. Zhang, X. Liu, G. Wei, Peptide-Engineered Fluorescent Nanomaterials: Structure Design, Function Tailoring, and Biomedical Applications, *Small* 17 (2021) 2005578, <https://doi.org/10.1002/smll.202005578>.
- [25] C. Zhang, W. Wu, R. Li, W. Qiu, Z. Zhuang, S. Cheng, X. Zhang, Peptide-Based Multifunctional Nanomaterials for Tumor Imaging and Therapy, *Adv. Funct. Mater.* 28 (2018) 1804492, <https://doi.org/10.1002/adfm.201804492>.
- [26] D. Wang, X. Zhang, H. Li, Y. Luan, G. Wei, J. Wang, Anticancer Properties of Lipidated Peptide Drug Supramolecular Self-Assemblies with Enhanced Stability, *ACS Appl. Bio Mater.* 2 (2019) 5995–6003, <https://doi.org/10.1021/acsabm.9b00913>.
- [27] K. Li, C.-J. Liu, X.-Z. Zhang, Multifunctional peptides for tumor therapy, *Adv. Drug Deliv. Rev.* 160 (2020) 36–51, <https://doi.org/10.1016/j.addr.2020.10.009>.
- [28] W. Lin, Y. Yang, Y. Lei, F. An, L. Sun, Y. Qin, L. Zhang, Self-Assembly of an Antitumor Dipeptide Induced Near-Infrared Fluorescence and Improved Stability for Theranostic Applications, *ACS Appl. Mater. Interfaces*. 13 (2021) 32799–32809, <https://doi.org/10.1021/acsami.1c07983>.
- [29] C. Karavasili, D.G. Fatouros, Self-assembling peptides as vectors for local drug delivery and tissue engineering applications, *Adv. Drug Deliv. Rev.* 174 (2021) 387–405, <https://doi.org/10.1016/j.addr.2021.04.024>.
- [30] Z.-Y. Qiao, Y.-X. Lin, W.-J. Lai, C.-Y. Hou, Y. Wang, S.-L. Qiao, D. Zhang, Q.-J. Fang, H. Wang, A General Strategy for Facile Synthesis and In Situ Screening of Self-Assembled Polymer-Peptide Nanomaterials, *Adv. Mater.* 28 (2016) 1859–1867, <https://doi.org/10.1002/adma.201504564>.
- [31] P.-P. Yang, Y.-J. Li, Y. Cao, L. Zhang, J.-Q. Wang, Z. Lai, K. Zhang, D. Shorty, W. Xiao, H. Cao, L. Wang, H. Wang, R. Liu, K.S. Lam, Rapid discovery of self-assembling peptides with one-bead one-compound peptide library, *Nat. Commun.* 12 (2021) 4494, <https://doi.org/10.1038/s41467-021-24597-5>.
- [32] L. Rong, S.-Y. Qin, C. Zhang, Y.-J. Cheng, J. Feng, S.-B. Wang, X.-Z. Zhang, Biomedical applications of functional peptides in nano-systems, *Mater. Today Chem.* 9 (2018) 91–102, <https://doi.org/10.1016/j.mtchem.2018.06.001>.
- [33] M.R. Ghadiri, J.R. Granja, R.A. Milligan, D.E. McRee, N. Khazanovich, Self-assembling organic nanotubes based on a cyclic peptide architecture, *Nature*. 366 (1993) 324–327, <https://doi.org/10.1038/366324a0>.
- [34] S. Zhang, T. Holmes, C. Lockshin, A. Rich, Spontaneous assembly of a self-complementary oligopeptide to form a stable macroscopic membrane, *Proc. Natl. Acad. Sci.* 90 (1993) 3334–3338, <https://doi.org/10.1073/pnas.90.8.3334>.
- [35] G.-B. Qi, Y.-J. Gao, L. Wang, H. Wang, Self-Assembled Peptide-Based Nanomaterials for Biomedical Imaging and Therapy, *Adv. Mater.* 30 (2018) 1703444, <https://doi.org/10.1002/adma.201703444>.
- [36] L. Li, Z. Qiao, L. Wang, H. Wang, Programmable Construction of Peptide-Based Materials in Living Subjects: From Modular Design and Morphological Control to Theranostics, *Adv. Mater.* 31 (2019) 1804971, <https://doi.org/10.1002/adma.201804971>.
- [37] Y. Wang, J. Weng, X. Wen, Y. Hu, D. Ye, Recent advances in stimuli-responsive in situ self-assembly of small molecule probes for in vivo imaging of enzymatic activity, *Biomater. Sci.* 9 (2021) 406–421, <https://doi.org/10.1039/DOBM00895H>.
- [38] J. Li, Y. Kuang, J. Shi, J. Zhou, J.E. Medina, R. Zhou, D. Yuan, C. Yang, H. Wang, Z. Yang, J. Liu, D.M. Dinulescu, B. Xu, Enzyme-Instructed Intracellular Molecular Self-Assembly to Boost Activity of Cisplatin against Drug-Resistant Ovarian Cancer Cells, *Angew. Chemie Int. Ed.* 54 (2015) 13307–13311, <https://doi.org/10.1002/anie.201507157>.
- [39] J. Gao, J. Zhan, Z. Yang, Enzyme-Instructed Self-Assembly (EISA) and Hydrogelation of Peptides, *Adv. Mater.* 32 (2020) 1805798, <https://doi.org/10.1002/adma.201805798>.
- [40] D. Zhu, H. Kong, Z. Sun, Y. Xu, P. Han, Y. Xi, G. Wei, Recent advance in tailoring the structure and functions of self-assembled peptide nanomaterials for biomedical applications, *Coord. Chem. Rev.* 494 (2023), 215374, <https://doi.org/10.1016/j.ccr.2023.215374>.
- [41] E. De Santis, M.G. Ryadnov, Peptide self-assembly for nanomaterials: the old new kid on the block, *Chem. Soc. Rev.* 44 (2015) 8288–8300, <https://doi.org/10.1039/CSCS00470E>.
- [42] N.J. Sinha, M.G. Langenstein, D.J. Pochan, C.J. Kloxin, J.G. Saven, Peptide Design and Self-Assembly into Targeted Nanostructure and Functional Materials, *Chem. Rev.* 121 (2021) 13915–13935, <https://doi.org/10.1021/acs.chemrev.1c00712>.
- [43] F. Sheehan, D. Sementa, A. Jain, M. Kumar, M. Tayarani-Najjaran, D. Kroiss, R. V. Ulijn, Peptide-Based Supramolecular Systems Chemistry, *Chem. Rev.* 121 (2021) 13869–13914, <https://doi.org/10.1021/acs.chemrev.1c00089>.
- [44] H. Wang, Z. Feng, B. Xu, Assemblies of Peptides in a Complex Environment and their Applications, *Angew. Chemie Int. Ed.* 58 (2019) 10423–10432, <https://doi.org/10.1002/anie.201814552>.
- [45] Y. Deng, W. Zhan, G. Liang, Intracellular Self-Assembly of Peptide Conjugates for Tumor Imaging and Therapy, *Adv. Healthc. Mater.* 10 (2021) 2001211, <https://doi.org/10.1002/adhm.202001211>.
- [46] M. Dergham, S. Lin, J. Geng, Supramolecular Self-Assembly in Living Cells, *Angew. Chemie Int. Ed.* 61 (2022) e2021142.
- [47] J. Wang, K. Liu, R. Xing, X. Yan, Peptide self-assembly: thermodynamics and kinetics, *Chem. Soc. Rev.* 45 (2016) 5589–5604, <https://doi.org/10.1039/C6CS00176A>.
- [48] S. Li, W. Zhang, H. Xue, R. Xing, X. Yan, Tumor microenvironment-oriented adaptive nanodrugs based on peptide self-assembly, *Chem. Sci.* 11 (2020) 8644–8656, <https://doi.org/10.1039/DOSC02937H>.
- [49] C. Yuan, A. Levin, W. Chen, R. Xing, Q. Zou, T.W. Herling, P.K. Challa, T.P. J. Knowles, X. Yan, Nucleation and Growth of Amino Acid and Peptide Supramolecular Polymers through Liquid-Liquid Phase Separation, *Angew. Chemie Int. Ed.* 58 (2019) 18116–18123, <https://doi.org/10.1002/anie.201911782>.
- [50] P. Zhou, R. Xing, Q. Li, J. Li, C. Yuan, X. Yan, Steering Phase-Separated Droplets to Control Fibrillar Network Evolution of Supramolecular Peptide Hydrogels, *Matter.* 6 (2023) 1–19, <https://doi.org/10.2139/ssrn.4287839>.
- [51] J. Wang, K. Liu, L. Yan, A. Wang, S. Bai, X. Yan, Trace Solvent as a Predominant Factor To Tune Dipeptide Self-Assembly, *ACS Nano.* 10 (2016) 2138–2143, <https://doi.org/10.1021/acsnano.5b06567>.
- [52] Y. Jiang, Y. Zhao, A.-Q. Zhang, X. Lei, S.-Y. Qin, Solvent-tailored ordered self-assembly of oligopeptide amphiphiles to create an anisotropic meso-matrix, *Chem. Commun.* 57 (2021) 6181–6184, <https://doi.org/10.1039/D1CC02034J>.
- [53] S. Vauthay, S. Santosso, H. Gong, N. Watson, S. Zhang, Molecular self-assembly of surfactant-like peptides to form nanotubes and nanovesicles, *Proc. Natl. Acad. Sci.* 99 (2002) 5355–5360, <https://doi.org/10.1073/pnas.072089599>.
- [54] J. Li, J. Wang, Y. Zhao, P. Zhou, J. Carter, Z. Li, T.A. Waigh, J.R. Lu, H. Xu, Surfactant-like peptides: From molecular design to controllable self-assembly with applications, *Coord. Chem. Rev.* 421 (2020), 213418, <https://doi.org/10.1016/j.ccr.2020.213418>.
- [55] J.D. Hartgerink, E. Beniash, S.I. Stupp, Self-Assembly and Mineralization of Peptide-Amphiphile Nanofibers, *Science* (80-.). 294 (2001) 1684–1688. <https://doi.org/10.1126/science.1063187>.

- [56] M.P. Hendricks, K. Sato, L.C. Palmer, S.I. Stupp, Supramolecular Assembly of Peptide Amphiphiles, *Acc. Chem. Res.* 50 (2017) 2440–2448, <https://doi.org/10.1021/acs.accounts.7b00297>.
- [57] S.Y. Qin, W.Q. Ding, Z.W. Jiang, X. Lei, A.Q. Zhang, Directing an oligopeptide amphiphile into an aligned nanofiber matrix for elucidating molecular structures, *Chem. Commun.* 55 (2019) 1659–1662, <https://doi.org/10.1039/c8cc09548e>.
- [58] W.-Q. Ding, H. Liu, S.-Y. Qin, Y. Jiang, X. Lei, A.-Q. Zhang, A Lyotropic Liquid Crystal from a Flexible Oligopeptide Amphiphile in Dimethyl Sulfoxide, *ACS Appl. Bio Mater.* 3 (2020) 8989–8996, <https://doi.org/10.1021/acsabm.0c01231>.
- [59] S.Y. Qin, Y. Jiang, H. Sun, H. Liu, A.Q. Zhang, X. Lei, Measurement of Residual Dipolar Couplings of Organic Molecules in Multiple Solvent Systems Using a Liquid-Crystalline-Based Medium, *Angew. Chemie - Int. Ed.* 59 (2020) 17097–17103, <https://doi.org/10.1002/anie.202007243>.
- [60] Y. Lin, J. Li, S.-Y. Qin, H. Sun, Y.-L. Yang, A. Navarro-Vázquez, X. Lei, Programmable alignment media from self-assembled oligopeptide amphiphiles for the measurement of independent sets of residual dipolar couplings in organic solvents, *Chem. Sci.* 13 (2022) 5838–5845, <https://doi.org/10.1039/d2sc01057g>.
- [61] E. Gazit, A possible role for π -stacking in the self-assembly of amyloid fibrils, *FASEB J.* 16 (2002) 77–83, <https://doi.org/10.1096/fj.01-0442hyp>.
- [62] I.W. Hamley, Self-Assembly, Bioactivity, and Nanomaterials Applications of Peptide Conjugates with Bulky Aromatic Terminal Groups, *ACS Appl. Bio Mater.* 6 (2023) 384–409, <https://doi.org/10.1021/acsabm.2c01041>.
- [63] Y. Wang, Q. Geng, Y. Zhang, L. Adler-Abramovich, X. Fan, D. Mei, E. Gazit, K. Tao, Fmoc-diphenylalanine gelating nanoarchitectonics: A simplistic peptide self-assembly to meet complex applications, *J. Colloid Interface Sci.* 636 (2023) 113–133, <https://doi.org/10.1016/j.jcis.2022.12.166>.
- [64] Y. Zhang, H. Gu, Z. Yang, B. Xu, Supramolecular Hydrogels Respond to Ligand-Receptor Interaction, *J. Am. Chem. Soc.* 125 (2003) 13680–13681, <https://doi.org/10.1021/ja036817k>.
- [65] V. Jayawarna, M. Ali, T.A. Jowitt, A.F. Miller, A. Saiani, J.E. Gough, R.V. Ulijn, Nanostructured Hydrogels for Three-Dimensional Cell Culture Through Self-Assembly of Fluorenylmethoxycarbonyl-Dipeptides, *Adv. Mater.* 18 (2006) 611–614, <https://doi.org/10.1002/adma.200501522>.
- [66] A. Mahler, M. Rechter, S. Cohen, E. Gazit, Rigid, Self-Assembled Hydrogel Composed of a Modified Aromatic Dipeptide, *Adv. Mater.* 18 (2006) 1365–1370, <https://doi.org/10.1002/adma.200501765>.
- [67] M.M. Pérez-Madrigal, A.M. Gil, J. Casanovas, A.I. Jiménez, L.P. Macor, C. Alemany, Self-assembly pathways in a triphenylalanine peptide capped with aromatic groups, *Colloids Surfaces B Biointerfaces* 216 (2022), 112522, <https://doi.org/10.1016/j.colsurfb.2022.112522>.
- [68] S.-Y. Qin, H.-F. Jiang, M.-Y. Peng, Q. Lei, R.-X. Zhuo, X.-Z. Zhang, Adjustable nanofibers self-assembled from an irregular conformational peptide amphiphile, *Polym. Chem.* 6 (2015) 519–524, <https://doi.org/10.1039/C4PY01237B>.
- [69] T. Kim, J. Hong, J. Kim, J. Cho, Y. Kim, Two-Dimensional Peptide Assembly via Arene-Perfluoroarene Interactions for Proliferation and Differentiation of Myoblasts, *J. Am. Chem. Soc.* (2023), <https://doi.org/10.1021/jacs.2c10938>.
- [70] H. Yokoi, T. Kinoshita, S. Zhang, Dynamic reassembly of peptide RADA16 nanofiber scaffold, *Proc. Natl. Acad. Sci.* 102 (2005) 8414–8419, <https://doi.org/10.1073/pnas.0407843102>.
- [71] K.L. Niece, J.D. Hartgerink, J.J.J.M. Donners, S.I. Stupp, Self-Assembly Combining Two Bioactive Peptide-Amphiphile Molecules into Nanofibers by Electrostatic Attraction, *J. Am. Chem. Soc.* 125 (2003) 7146–7147, <https://doi.org/10.1021/ja028215r>.
- [72] S. Ramachandran, P. Flynn, Y. Tseng, Y.B. Yu, Electrostatically Controlled Hydrogelation of Oligopeptides and Protein Entrapment, *Chem. Mater.* 17 (2005) 6583–6588, <https://doi.org/10.1021/cm0513076>.
- [73] X.D. Xu, C.S. Chen, B. Lu, S.X. Cheng, X.Z. Zhang, R.X. Zhuo, Coassembly of oppositely charged short peptides into Well-Defined supramolecular hydrogels, *J. Phys. Chem. B* 114 (2010) 2365–2372, <https://doi.org/10.1021/jp9102417>.
- [74] J.C. Stendahl, M.S. Rao, M.O. Guler, S.I. Stupp, Intermolecular Forces in the Self-Assembly of Peptide Amphiphile Nanofibers, *Adv. Funct. Mater.* 16 (2006) 499–508, <https://doi.org/10.1002/adfm.200500161>.
- [75] O.-S. Lee, S.I. Stupp, G.C. Schatz, Atomistic Molecular Dynamics Simulations of Peptide Amphiphile Self-Assembly into Cylindrical Nanofibers, *J. Am. Chem. Soc.* 133 (2011) 3677–3683, <https://doi.org/10.1021/ja110966y>.
- [76] P. Teng, G.M. Gray, M. Zheng, S. Singh, X. Li, L. Wojtas, A. van der Vaart, J. Cai, Orthogonal Halogen-Bonding-Driven 3D Supramolecular Assembly of Right-Handed Synthetic Helical Peptides, *Angew. Chemie Int. Ed.* 58 (2019) 7778–7782, <https://doi.org/10.1002/anie.201903259>.
- [77] H. Wang, H. Wu, Y. Yi, K.-F. Xue, J.-F. Xu, H. Wang, Y. Zhao, X. Zhang, Self-Motivated Supramolecular Combination Chemotherapy for Overcoming Drug Resistance Based on Acid-Activated Competition of Host-Guest Interactions, *CCS Chem.* 3 (2021) 1413–1425, <https://doi.org/10.31635/ccschem.021.202100964>.
- [78] X. Yang, B. Wu, J. Zhou, H. Lu, H. Zhang, F. Huang, H. Wang, Controlling Intracellular Enzymatic Self-Assembly of Peptide by Host-Guest Complexation for Programming Cancer Cell Death, *Nano Lett.* 22 (2022) 7588–7596, <https://doi.org/10.1021/acs.nanolett.2c02612>.
- [79] S. Chen, Z. Li, C. Zhang, X. Wu, W. Wang, Q. Huang, W. Chen, J. Shi, D. Yuan, Cation- π Interaction Trigger Supramolecular Hydrogelation of Peptide Amphiphiles, *Small.* 19 (2023) 2301063, <https://doi.org/10.1002/smll.202301063>.
- [80] Z. Yu, A. Erbas, F. Tantakitti, L.C. Palmer, J.A. Jackman, M. Olvera de la Cruz, N.-J. Cho, S.I. Stupp, Co-assembly of Peptide Amphiphiles and Lipids into Supramolecular Nanostructures Driven by Anion- π Interactions, *J. Am. Chem. Soc.* 139 (2017) 7823–7830, <https://doi.org/10.1021/jacs.7b02058>.
- [81] T. John, S. Piantavigna, T.J.A. Dealey, B. Abel, H.J. Risselada, L.L. Martin, Lipid oxidation controls peptide self-assembly near membranes through a surface attraction mechanism, *Chem. Sci.* 14 (2023) 3730–3741, <https://doi.org/10.1039/D3SC00159H>.
- [82] A. van Teijlingen, M.C. Smith, T. Tuttle, Short Peptide Self-Assembly in the Martini Coarse-Grain Force Field Family, *Acc. Chem. Res.* 56 (2023) 644–654, <https://doi.org/10.1021/acs.accounts.2c00810>.
- [83] N. Bertrand, J. Wu, X. Xu, N. Kamaly, O.C. Farokhzad, Cancer nanotechnology: The impact of passive and active targeting in the era of modern cancer biology, *Adv. Drug Deliv. Rev.* 66 (2014) 2–25, <https://doi.org/10.1016/j.addr.2013.11.009>.
- [84] S. Sindhwan, A.M. Syed, J. Ngai, B.R. Kingston, L. Maiorino, J. Rothschild, P. MacMillan, Y. Zhang, N.U. Rajesh, T. Hoang, J.L.Y. Wu, S. Wilhelm, A. Zilman, S. Gadde, A. Sulaiman, B. Ouyang, Z. Lin, L. Wang, M. Egeblad, W.C.W. Chan, The entry of nanoparticles into solid tumours, *Nat. Mater.* 19 (2020) 566–575, <https://doi.org/10.1038/s41563-019-0566-2>.
- [85] J.N. Israelachvili, D.J. Mitchell, B.W. Ninham, Theory of self-assembly of hydrocarbon amphiphiles into micelles and bilayers, *J. Chem. Soc. Faraday Trans. 2* (72) (1976) 1525, <https://doi.org/10.1039/F29767201525>.
- [86] Y.-Y. Xie, X.-T. Qin, J. Zhang, M.-Y. Sun, F.-P. Wang, M. Huang, S.-R. Jia, W. Qi, Y. Wang, C. Zhong, Self-assembly of peptide nanofibers with chirality-encoded antimicrobial activity, *J. Colloid Interface Sci.* 622 (2022) 135–146, <https://doi.org/10.1016/j.jcis.2022.04.058>.
- [87] S. Xiang, X. Long, Q. Tu, J. Feng, X. Zhang, G. Feng, L. Lei, Self-assembled, hemin-functionalized peptide nanotubes: an innovative strategy for detecting glutathione and glucose molecules with peroxidase-like activity, *Nano Converg.* 10 (2023) 7, <https://doi.org/10.1186/s40580-023-00356-8>.
- [88] W. Yu, Y. Sun, W. Li, X. Guo, X. Liu, W. Wu, W. Yu, J. Wang, A. Shan, Self-Assembly of Antimicrobial Peptide-Based Micelles Breaks the Limitation of Trypsin, *ACS Appl. Mater. Interfaces.* 15 (2023) 494–510, <https://doi.org/10.1021/acsami.2c17941>.
- [89] Z. Yu, F. Tantakitti, L.C. Palmer, S.I. Stupp, Asymmetric Peptide Nanoribbons, *Nano Lett.* 16 (2016) 6967–6974, <https://doi.org/10.1021/acs.nanolett.6b03062>.
- [90] M. Wang, J. Wang, P. Zhou, J. Deng, Y. Zhao, Y. Sun, W. Yang, D. Wang, Z. Li, X. Hu, S.M. King, S.E. Rogers, H. Cox, T.A. Waigh, J. Yang, J.R. Lu, H. Xu, Nanoribbons self-assembled from short peptides demonstrate the formation of polar zippers between β -sheets, *Nat. Commun.* 9 (2018) 5118, <https://doi.org/10.1038/s41467-018-07583-2>.
- [91] V.B. Kumar, B. Ozguney, A. Vlachou, Y. Chen, E. Gazit, P. Tamamis, Peptide Self-Assembled Nanocarriers for Cancer Drug Delivery, *J. Phys. Chem. b.* 127 (2023) 1857–1871, <https://doi.org/10.1021/acs.jpcb.2c06751>.
- [92] Z. Zhang, S. Ai, Z. Yang, X. Li, Peptide-based supramolecular hydrogels for local drug delivery, *Adv. Drug Deliv. Rev.* 174 (2021) 482–503, <https://doi.org/10.1016/j.addr.2021.05.010>.
- [93] Y. Zhou, Q. Li, Y. Wu, X. Li, Y. Zhou, Z. Wang, H. Liang, F. Ding, S. Hong, N. F. Steinmetz, H. Cai, Molecularly Stimuli-Responsive Self-Assembled Peptide Nanoparticles for Targeted Imaging and Therapy, *ACS Nano.* 17 (2023) 8004–8025, <https://doi.org/10.1021/acsnano.3c01452>.
- [94] R. Hadianamrei, X. Zhao, Current state of the art in peptide-based gene delivery, *J. Control. Release.* 343 (2022) 600–619, <https://doi.org/10.1016/j.jconrel.2022.02.010>.
- [95] S. Urundur, M.O. Sullivan, Peptide-Based Vectors: A Biomolecular Engineering Strategy for Gene Delivery, *Annu. Rev. Chem. Biomol. Eng.* 14 (2023) 243–264, <https://doi.org/10.1146/annurev-chembioeng-101121-070232>.
- [96] Z. Gong, X. Liu, J. Dong, W. Zhang, Y. Jiang, J. Zhang, W. Feng, K. Chen, J. Bai, Transition from vesicles to nanofibres in the enzymatic self-assemblies of an amphiphilic peptide as an antitumour drug carrier, *Nanoscale.* 11 (2019) 15479–15486, <https://doi.org/10.1039/C9NR02874A>.
- [97] Z. Gong, X. Liu, J. Wu, X. Li, Z. Tang, Y. Deng, X. Sun, K. Chen, Z. Gao, J. Bai, pH-triggered morphological change in a self-assembling amphiphilic peptide used as an antitumor drug carrier, *Nanotechnology.* 31 (2020), 165601, <https://doi.org/10.1088/1361-6528/ab667c>.
- [98] Z. Li, Y. Zhu, J.B. Matson, pH-Responsive Self-Assembling Peptide-Based Biomaterials: Designs and Applications, *ACS Appl. Bio Mater.* 5 (2022) 4635–4651, <https://doi.org/10.1021/acsabm.2c00188>.
- [99] J. Liang, W.-L. Wu, X.-D. Xu, R.-X. Zhuo, X.-Z. Zhang, pH Responsive micelle self-assembled from a new amphiphilic peptide as anti-tumor drug carrier, *Colloids Surfaces B Biointerfaces.* 114 (2014) 398–403, <https://doi.org/10.1016/j.colsurfb.2013.10.037>.
- [100] M. Xuan, J. Liang, J. Li, W. Wu, Multi-functional lipopeptide micelles as a vehicle for curcumin delivery, *Colloids Surfaces A Physicochem. Eng. Asp.* 616 (2021), 126208, <https://doi.org/10.1016/j.colsurfa.2021.126208>.
- [101] Y. Lai, P. Zhao, Z. Zhang, B. Li, J. Wu, An effective peptide cargo carrier for the delivery of cisplatin in ovarian cancer cells, *Dye. Pigment.* 143 (2017) 342–347, <https://doi.org/10.1016/j.dyepig.2017.04.025>.
- [102] S. Soukasene, D.J. Toft, T.J. Moyer, H. Lu, H.-K. Lee, S.M. Standley, V.L. Cryns, S. I. Stupp, Antitumor Activity of Peptide Amphiphile Nanofiber-Encapsulated Camptothecin, *ACS Nano.* 5 (2011) 9113–9121, <https://doi.org/10.1021/nn023343z>.
- [103] T. Xu, C. Liang, D. Zheng, X. Yan, Y. Chen, Y. Chen, X. Li, Y. Shi, L. Wang, Z. Yang, Nuclear delivery of dual anticancer drug-based nanomedicine constructed by cisplatin-induced peptide self-assembly, *Nanoscale.* 12 (2020) 15275–15282, <https://doi.org/10.1039/D0NR00143K>.

- [104] Q. Wang, X. Hou, J. Gao, C. Ren, Q. Guo, H. Fan, J. Liu, W. Zhang, J. Liu, A coassembled peptide hydrogel boosts the radiosensitization of cisplatin, *Chem. Commun.* 56 (2020) 13017–13020, <https://doi.org/10.1039/D0CC05184E>.
- [105] J. Liu, C. Wu, G. Dai, F. Feng, Y. Chi, K. Xu, W. Zhong, Molecular self-assembly of a tyroservatide-derived octapeptide and hydroxycamptothecin for enhanced therapeutic efficacy, *Nanoscale*. 13 (2021) 5094–5102, <https://doi.org/10.1039/D0NR08741F>.
- [106] X. Yin, Z. Chen, Y. Chen, Y. Xie, B. Xiong, H. Jiang, J. Zhu, Lipidated gemini peptide amphiphiles with enhanced loading capacity and cell membrane affinity for drug delivery, *Colloids Surfaces B Biointerfaces*. 195 (2020), 111271, <https://doi.org/10.1016/j.colsurfb.2020.111271>.
- [107] M. Zorko, S. Jones, Ü. Langel, Cell-penetrating peptides in protein mimicry and cancer therapeutics, *Adv. Drug Deliv. Rev.* 180 (2022), 114044, <https://doi.org/10.1016/j.addr.2021.114044>.
- [108] H. Cheng, R.-R. Zheng, G.-L. Fan, J.-H. Fan, L.-P. Zhao, X.-Y. Jiang, B. Yang, X.-Y. Yu, S.-Y. Li, X.-Z. Zhang, Mitochondria and plasma membrane dual-targeted chimeric peptide for single-agent synergistic photodynamic therapy, *Biomaterials*. 188 (2019) 1–11, <https://doi.org/10.1016/j.biomater.2018.10.005>.
- [109] M. Cao, S. Lu, N. Wang, H. Xu, H. Cox, R. Li, T. Waigh, Y. Han, Y. Wang, J.R. Lu, Enzyme-Triggered Morphological Transition of Peptide Nanostructures for Tumor-Targeted Drug Delivery and Enhanced Cancer Therapy, *ACS Appl. Mater. Interfaces*. 11 (2019) 16357–16366, <https://doi.org/10.1021/acsmami.9b03519>.
- [110] T. Ji, Y. Ding, Y. Zhao, J. Wang, H. Qin, X. Liu, J. Lang, R. Zhao, Y. Zhang, J. Shi, N. Tao, Z. Qin, G. Nie, Peptide Assembly Integration of Fibroblast-Targeting and Cell-Penetration Features for Enhanced Antitumor Drug Delivery, *Adv. Mater.* 27 (2015) 1865–1873, <https://doi.org/10.1002/adma.201404715>.
- [111] X. Jiang, X. Fan, W. Xu, C. Zhao, H. Wu, R. Zhang, G. Wu, Self-assembled peptide nanoparticles responsive to multiple tumor microenvironment triggers provide highly efficient targeted delivery and release of antitumor drug, *J. Control. Release*. 316 (2019) 196–207, <https://doi.org/10.1016/j.jconrel.2019.10.031>.
- [112] Y. Shi, P.A. Summers, M.K. Kuimova, H.S. Azevedo, Unravelling the Enzymatic Degradation Mechanism of Supramolecular Peptide Nanofibers and Its Correlation with Their Internal Viscosity, *Nano Lett.* 20 (2020) 7375–7381, <https://doi.org/10.1021/acs.nanolett.0c02781>.
- [113] J. Yang, X. Yu, J.-I. Song, Q. Song, S.C.L. Hall, G. Yu, S. Perrier, Aggregation-Induced Emission Featured Supramolecular Tubisomes for Imaging-Guided Drug Delivery, *Angew. Chem. Int. Ed.* 61 (2022) e202115208.
- [114] J. Chen, P. Zhang, C. Wu, Q. Yao, R. Cha, Y. Gao, Reductase-Labile Peptidic Supramolecular Hydrogels Aided in Oral Delivery of Probiotics, *ACS Appl. Mater. Interfaces*. 15 (2023) 31214–31223, <https://doi.org/10.1021/acsmami.3c04408>.
- [115] Y. Cai, C. Zheng, F. Xiong, W. Ran, Y. Zhai, H.H. Zhu, H. Wang, Y. Li, P. Zhang, Recent Progress in the Design and Application of Supramolecular Peptide Hydrogels in Cancer Therapy, *Adv. Healthc. Mater.* 10 (2021) 2001239, <https://doi.org/10.1002/adhm.202001239>.
- [116] A. Altunbas, S.J. Lee, S.A. Rajasekaran, J.P. Schneider, D.J. Pochan, Encapsulation of curcumin in self-assembling peptide hydrogels as injectable drug delivery vehicles, *Biomaterials*. 32 (2011) 5906–5914, <https://doi.org/10.1016/j.biomat.2011.04.069>.
- [117] X.-D. Xu, L. Liang, C.-S. Chen, B. Lu, N. Wang, F.-G. Jiang, X.-Z. Zhang, R.-X. Zhuo, Peptide Hydrogel as an Intraocular Drug Delivery System for Inhibition of Postoperative Scarring Formation, *ACS Appl. Mater. Interfaces*. 2 (2010) 2663–2671, <https://doi.org/10.1021/am100484c>.
- [118] R.W. Chakroun, A. Sneider, C.F. Anderson, F. Wang, P. Wu, D. Wirtz, H. Cui, Supramolecular Design of Unsymmetric Reverse Bolaamphiphiles for Cell-Sensitive Hydrogel Degradation and Drug Release, *Angew. Chemie Int. Ed.* 59 (2020) 4434–4442, <https://doi.org/10.1002/anie.201913087>.
- [119] W. Zhang, Q. Chen, F. Wu, J. Dai, D. Ding, J. Wu, X. Lou, F. Xia, Peptide-based nanomaterials for gene therapy, *Nanoscale Adv.* 3 (2021) 302–310, <https://doi.org/10.1039/D0NA00899K>.
- [120] H.O. McCarthy, J. McCaffrey, C.M. McCrudden, A. Zholobenko, A.A. Ali, J. W. McBride, A.S. Massey, S. Pentlavalli, K.-H. Chen, G. Cole, S.P. Loughran, N. J. Dunne, R.F. Donnelly, V.L. Kett, T. Robson, Development and characterization of self-assembling nanoparticles using a bio-inspired amphipathic peptide for gene delivery, *J. Control. Release*. 189 (2014) 141–149, <https://doi.org/10.1016/j.jconrel.2014.06.048>.
- [121] W. Qu, S.-Y. Qin, Y. Kuang, R.-X. Zhuo, X.-Z. Zhang, Peptide-based vectors mediated by avidin–biotin interaction for tumor targeted gene delivery, *J. Mater. Chem. b*, 1 (2013) 2147, <https://doi.org/10.1039/c3tb00226h>.
- [122] W. Qu, S.-Y. Qin, S. Ren, X.-J. Jiang, R.-X. Zhuo, X.-Z. Zhang, Peptide-Based Vector of VEGF Plasmid for Efficient Gene Delivery in Vitro and Vessel Formation in Vivo, *Bioconjug. Chem.* 24 (2013) 960–967, <https://doi.org/10.1021/bc300677n>.
- [123] H.Y. Wang, J.X. Chen, Y.X. Sun, J.Z. Deng, C. Li, X.Z. Zhang, R.X. Zhuo, Construction of cell penetrating peptide vectors with N-terminal stearylated nuclear localization signal for targeted delivery of DNA into the cell nuclei, *J. Control. Release*. 155 (2011) 26–33, <https://doi.org/10.1016/j.jconrel.2010.12.009>.
- [124] J. Yang, Q. Lei, K. Han, Y.-H. Gong, S. Chen, H. Cheng, S.-X. Cheng, R.-X. Zhuo, X.-Z. Zhang, Reduction-sensitive polypeptides incorporated with nuclear localization signal sequences for enhanced gene delivery, *J. Mater. Chem.* 22 (2012) 13591, <https://doi.org/10.1039/c2jm32223d>.
- [125] Y. Cheng, C. Sun, R. Liu, J. Yang, J. Dai, T. Zhai, X. Lou, F. Xia, A Multifunctional Peptide-Conjugated AIIGen for Efficient and Sequential Targeted Gene Delivery into the Nucleus, *Angew. Chemie Int. Ed.* 58 (2019) 5049–5053, <https://doi.org/10.1002/anie.201901527>.
- [126] M. Li, S. Schlesiger, S.K. Knauer, C. Schmuck, A Tailor-Made Specific Anion-Binding Motif in the Side Chain Transforms a Tetrapeptide into an Efficient Vector for Gene Delivery, *Angew. Chemie Int. Ed.* 54 (2015) 2941–2944, <https://doi.org/10.1002/anie.201410429>.
- [127] M. Li, M. Ehlers, S. Schlesiger, E. Zellermann, S.K. Knauer, C. Schmuck, Incorporation of a Non-Natural Arginine Analogue into a Cyclic Peptide Leads to Formation of Positively Charged Nanofibers Capable of Gene Transfection, *Angew. Chemie Int. Ed.* 55 (2016) 598–601, <https://doi.org/10.1002/anie.201508714>.
- [128] L.-P. Wu, D. Ahmadvand, J. Su, A. Hall, X. Tan, Z.S. Farhangrazi, S.M. Moghimi, Crossing the blood-brain-barrier with nanoligand drug carriers self-assembled from a phage display peptide, *Nat. Commun.* 10 (2019) 4635, <https://doi.org/10.1038/s41467-019-12554-2>.
- [129] L. Tang, R. Zhang, Y. Wang, X. Zhang, Y. Yang, B. Zhao, L. Yang, A simple self-assembly nanomicelle based on brain tumor-targeting peptide-mediated siRNA delivery for glioma immunotherapy via intranasal administration, *Acta Biomater.* 155 (2023) 521–537, <https://doi.org/10.1016/j.actbio.2022.11.013>.
- [130] J.X. Chen, H.Y. Wang, C. Li, K. Han, X.Z. Zhang, R.X. Zhuo, Construction of surfactant-like tetra-tail amphiphilic peptide with RGD ligand for encapsulation of porphyrin for photodynamic therapy, *Biomaterials*. 32 (2011) 1678–1684, <https://doi.org/10.1016/j.biomaterials.2010.10.047>.
- [131] J. Wu, Y. Liu, M. Cao, N. Zheng, H. Ma, X. Ye, N. Yang, Z. Liu, W. Liao, L. Sun, Cancer-Responsive Multifunctional Nanoplatform Based on Peptide Self-Assembly for Highly Efficient Combined Cancer Therapy by Alleviating Hypoxia and Improving the Immunosuppressive Microenvironment, *ACS Appl. Mater. Interfaces*. 15 (2023) 5667–5678, <https://doi.org/10.1021/acsmami.2c20388>.
- [132] K. Liu, R. Xing, Q. Zou, G. Ma, H. Möhwald, X. Yan, Simple Peptide-Tuned Self-Assembly of Photosensitizers towards Anticancer Photodynamic Therapy, *Angew. Chemie Int. Ed.* 55 (2016) 3036–3039, <https://doi.org/10.1002/anie.201509810>.
- [133] J. Li, A. Wang, L. Zhao, Q. Dong, M. Wang, H. Xu, X. Yan, S. Bai, Self-Assembly of Monomeric Hydrophobic Photosensitizers with Short Peptides Forming Photodynamic Nanoparticles with Real-Time Tracking Property and without the Need of Release in Vivo, *ACS Appl. Mater. Interfaces*. 10 (2018) 28420–28427, <https://doi.org/10.1021/acsmami.8b00993>.
- [134] S. Li, Q. Zou, Y. Li, C. Yuan, R. Xing, X. Yan, Smart Peptide-Based Supramolecular Photodynamic Metallo-Nanodrugs Designed by Multicomponent Coordination Self-Assembly, *J. Am. Chem. Soc.* 140 (2018) 10794–10802, <https://doi.org/10.1021/jacs.8b04912>.
- [135] H. Zhu, H. Wang, B. Shi, L. Shangguan, W. Tong, G. Yu, Z. Mao, F. Huang, Supramolecular peptide constructed by molecular Lego allowing programmable self-assembly for photodynamic therapy, *Nat. Commun.* 10 (2019) 2412, <https://doi.org/10.1038/s41467-019-10385-9>.
- [136] Q. Zou, M. Abbas, L. Zhao, S. Li, G. Shen, X. Yan, Biological Photothermal Nanodots Based on Self-Assembly of Peptide-Porphyrin Conjugates for Antitumor Therapy, *J. Am. Chem. Soc.* 139 (2017) 1921–1927, <https://doi.org/10.1021/jacs.6b11382>.
- [137] R. Chang, Q. Zou, L. Zhao, Y. Liu, R. Xing, X. Yan, Amino-Acid-Encoded Supramolecular Photothermal Nanomedicine for Enhanced Cancer Therapy, *Adv. Mater.* 34 (2022) 2200139, <https://doi.org/10.1002/adma.202200139>.
- [138] S.-Y. Qin, Y.-J. Cheng, Q. Lei, A.-Q. Zhang, X.-Z. Zhang, Combinational strategy for high-performance cancer chemotherapy, *Biomaterials*. 171 (2018) 178–197, <https://doi.org/10.1016/j.biomaterials.2018.04.027>.
- [139] Y.-J. Cheng, J.-J. Hu, S.-Y. Qin, A.-Q. Zhang, X.-Z. Zhang, Recent advances in functional mesoporous silica-based nanoplatforms for combinational photo-chemotherapy of cancer, *Biomaterials*. 232 (2020), 119738, <https://doi.org/10.1016/j.biomaterials.2019.119738>.
- [140] K. Han, S. Chen, W.-H. Chen, Q. Lei, Y. Liu, R.-X. Zhuo, X.-Z. Zhang, Synergistic gene and drug tumor therapy using a chimeric peptide, *Biomaterials*. 34 (2013) 4680–4689, <https://doi.org/10.1016/j.biomaterials.2013.03.010>.
- [141] K. Han, Q. Lei, H.Z. Jia, S.B. Wang, W.N. Yin, W.H. Chen, S.X. Cheng, X.Z. Zhang, A tumor targeted chimeric peptide for synergistic endosomal escape and therapy by dual-stage light manipulation, *Adv. Funct. Mater.* 25 (2015) 1248–1257, <https://doi.org/10.1002/adfm.201403190>.
- [142] J. Yang, J. Dai, Q. Wang, Y. Cheng, J. Guo, Z. Zhao, Y. Hong, X. Lou, F. Xia, Tumor-Triggered Disassembly of a Multiple-Agent-Therapy Probe for Efficient Cellular Internalization, *Angew. Chemie Int. Ed.* 59 (2020) 20405–20410, <https://doi.org/10.1002/anie.2020009196>.
- [143] J. Dai, J. Hu, X. Dong, B. Chen, X. Dong, R. Liu, F. Xia, X. Lou, Deep Downregulation of PD-L1 by Caged Peptide-Conjugated AIIGen/miR-140 Nanoparticles for Enhanced Immunotherapy, *Angew. Chem. Int. Ed. Engl.* 61 (2022) e202117798.
- [144] C. Karavasili, D.A. Andreadis, O.L. Katsamenis, E. Panteris, P. Anastasiadou, Z. Kakazanis, V. Zoumpourlis, C.K. Markopoulou, S. Koutsopoulos, I. S. Vizirianakis, D.G. Fatouros, Synergistic Antitumor Potency of a Self-Assembling Peptide Hydrogel for the Local Co-delivery of Doxorubicin and Curcumin in the Treatment of Head and Neck Cancer, *Mol. Pharm.* 16 (2019) 2326–2341, <https://doi.org/10.1021/acs.molpharmaceut.8b01221>.
- [145] S. Liu, M. Zhao, Y. Zhou, L. Li, C. Wang, Y. Yuan, L. Li, G. Liao, W. Bresette, Y. Chen, J. Cheng, Y. Lu, J. Liu, A self-assembling peptide hydrogel-based drug delivery platform to improve tissue repair after ischemia-reperfusion injury, *Acta Biomater.* 103 (2020) 102–114, <https://doi.org/10.1016/j.actbio.2019.12.011>.
- [146] S.M. Coulter, S. Pentlavalli, L.K. Vora, Y. An, E.R. Cross, K. Peng, K. McAulay, R. Schweins, R.F. Donnelly, H.O. McCarthy, G. Laverty, Enzyme-Triggered l- α /d-Peptide Hydrogels as a Long-Acting Injectable Platform for Systemic Delivery of HIV/AIDS Drugs, *Adv. Healthc. Mater.* 12 (2023) e2203198.

- [147] H. Liu, X. Bi, Y. Wu, M. Pan, X. Ma, L. Mo, J. Wang, X. Li, Cationic self-assembled peptide-based molecular hydrogels for extended oral drug delivery, *Acta Biomater.* 131 (2021) 162–171, <https://doi.org/10.1016/j.actbio.2021.06.027>.
- [148] Y. Li, H. Liang, C. Zhang, Y. Qiu, D. Wang, H. Wang, A. Chen, C. Hong, L. Wang, H. Wang, B. Hu, Ophthalmic Solution of Smart Supramolecular Peptides to Capture Semaphorin 4D against Diabetic Retinopathy, *Adv. Sci.* 10 (2023) 2203351, <https://doi.org/10.1002/advs.202203351>.
- [149] S. Alam, J.J. Panda, T.K. Mukherjee, V.S. Chauhan, Short peptide based nanotubes capable of effective curcumin delivery for treating drug resistant malaria, *J. Nanobiotechnology.* 14 (2016) 26, <https://doi.org/10.1186/s12951-016-0179-8>.
- [150] M. Li, M. Wang, L. Li, L. Zhang, B. Ma, W. Wang, A composite peptide-supramolecular microneedle system for melanoma immunotherapy, *Nano Res.* 16 (2023) 5335–5345, <https://doi.org/10.1007/s12274-022-5236-z>.
- [151] L. Zhang, Y. Tian, M. Li, M. Wang, S. Wu, Z. Jiang, Q. Wang, W. Wang, Peptide nano ‘head-grafting’ for SDT-facilitated immune checkpoints blocking, *Chem. Sci.* 13 (2022) 14052–14062, <https://doi.org/10.1039/d2sc02728c>.
- [152] S.Y. Qin, A.Q. Zhang, S.X. Cheng, L. Rong, X.Z. Zhang, Drug self-delivery systems for cancer therapy, *Biomaterials.* 112 (2017) 234–247, <https://doi.org/10.1016/j.biomat.2016.10.016>.
- [153] L.H. Liu, X.Z. Zhang, Carrier-free nanomedicines for cancer treatment, *Prog. Mater. Sci.* 125 (2022), 100919, <https://doi.org/10.1016/j.pmatsci.2021.100919>.
- [154] Y. Zhong, Y. Cen, L. Xu, S. Li, H. Cheng, Recent Progress in Carrier-Free Nanomedicine for Tumor Phototherapy, *Adv. Healthc. Mater.* 12 (2023) e2202307.
- [155] H.-H. Han, H. Tian, Y. Zang, A.C. Sedgwick, J. Li, J.L. Sessler, X.-P. He, T. D. James, Small-molecule fluorescence-based probes for interrogating major organ diseases, *Chem. Soc. Rev.* 50 (2021) 9391–9429, <https://doi.org/10.1039/DOCS01183E>.
- [156] Z. Fan, L. Sun, Y. Huang, Y. Wang, M. Zhang, Bioinspired fluorescent dipeptide nanoparticles for targeted cancer cell imaging and real-time monitoring of drug release, *Nat. Nanotechnol.* 11 (2016) 388–394, <https://doi.org/10.1038/nano.2015.312>.
- [157] W.-Q. Ding, S.-Y. Qin, Y.-J. Cheng, Y.-H. Ma, A.-Q. Zhang, Novel oligopeptide nanoprobe for targeted cancer cell imaging, *RSC Adv.* 8 (2018) 30887–30893, <https://doi.org/10.1039/C8RA06034G>.
- [158] J. Kong, J. Zhang, Y. Wang, W. Qi, H. Rao, L. Hu, R. Su, Z. He, Bioinspired pH-Sensitive Fluorescent Peptidyl Nanoparticles for Cell Imaging, *ACS Appl. Mater. Interfaces.* 12 (2020) 4212–4220, <https://doi.org/10.1021/acsmami.9b17866>.
- [159] S. Sivagnanam, K. Das, M. Basak, T. Mahata, A. Stewart, B. Maity, P. Das, Self-assembled dipeptide based fluorescent nanoparticles as a platform for developing cellular imaging probes and targeted drug delivery chaperones, *Nanoscale Adv.* 4 (2022) 1694–1706, <https://doi.org/10.1039/dina00885d>.
- [160] Y. Wang, Y. Lei, J. Wang, H. Yang, L. Sun, Tetrapeptide self-assembled multicolor fluorescent nanoparticles for bioimaging applications, *Chinese Chem. Lett.* 34 (2023), 107915, <https://doi.org/10.1016/j.cclet.2022.107915>.
- [161] J. Kong, Y. Wang, W. Qi, R. Su, Z. He, Photo- and Aromatic Stacking-Induced Green Emissive Peptidyl Nanoparticles for Cell Imaging and Monitoring of Nucleic Acid Delivery, *ACS Appl. Mater. Interfaces.* 11 (2019) 15401–15410, <https://doi.org/10.1021/acsmami.9b03945>.
- [162] J. Kong, J. Zhang, Y. Wang, W. Qi, M. Huang, R. Su, Z. He, Bioinspired Fluorescent Peptidyl Nanoparticles with Rainbow Colors, *ACS Appl. Mater. Interfaces.* 12 (2020) 31830–31841, <https://doi.org/10.1021/acsmami.0c08259>.
- [163] J. Kong, S. Zhao, X. Han, W. Li, J. Zhang, Y. Wang, X. Shen, Y. Xia, Z. Li, Quantitative Ratiometric Biosensors Based on Fluorescent Ferrocene-Modified Histidine Dipeptide Nanoassemblies, *Anal. Chem.* 95 (2023) 5053–5060, <https://doi.org/10.1021/acs.analchem.2c05609>.
- [164] Z. Fan, Y. Chang, C. Cui, L. Sun, D.H. Wang, Z. Pan, M. Zhang, Near infrared fluorescent peptide nanoparticles for enhancing esophageal cancer therapeutic efficacy, *Nat. Commun.* 9 (2018) 2605, <https://doi.org/10.1038/s41467-018-04763-y>.
- [165] Y. Chen, A.A. Orr, K. Tao, Z. Wang, A. Ruggiero, L.J.W. Shimon, L. Schnaider, A. Goodall, S. Rencus-Lazar, S. Gilead, I. Slutsky, P. Tamamis, Z. Tan, E. Gazit, High-Efficiency Fluorescence through Bioinspired Supramolecular Self-Assembly, *ACS Nano.* 14 (2020) 2798–2807, <https://doi.org/10.1021/acsnano.9b10024>.
- [166] K. Tao, Z. Fan, L. Sun, P. Makam, Z. Tian, M. Ruegger, S. Shaham-Niv, D. Hansford, R. Aizen, Z. Pan, S. Galster, J. Ma, F. Yuan, M. Si, S. Qu, M. Zhang, E. Gazit, J. Li, Quantum confined peptide assemblies with tunable visible to near-infrared spectral range, *Nat. Commun.* 9 (2018) 3217, <https://doi.org/10.1038/s41467-018-05568-9>.
- [167] Y. Zhao, T. Ji, H. Wang, S. Li, Y. Zhao, G. Nie, Self-assembled peptide nanoparticles as tumor microenvironment activatable probes for tumor targeting and imaging, *J. Control. Release.* 177 (2014) 11–19, <https://doi.org/10.1016/j.jconrel.2013.12.037>.
- [168] X. Duan, G. Zhang, S. Ji, Y. Zhang, J. Li, H. Ou, Z. Gao, G. Feng, D. Ding, Activatable Persistent Luminescence from Porphyrin Derivatives and Supramolecular Probes with Imaging-Modality Transformable Characteristics for Improved Biological Applications, *Angew. Chemie Int. Ed.* 61 (2022) e202116174.
- [169] C.-S. Chen, X.-D. Xu, Y. Wang, J. Yang, H.-Z. Jia, H. Cheng, C.-C. Chu, R.-X. Zhuo, X.-Z. Zhang, A Peptide Nanofibrous Indicator for Eye-Detectable Cancer Cell Identification, *Small.* 9 (2013) 920–926, <https://doi.org/10.1002/smll.201201928>.
- [170] J.-Q. Feng, D.-K. Shi, W.-Q. Ding, Y.-J. Cheng, S.-Y. Qin, A.-Q. Zhang, A Self-Assembled Nanoindicator from Alizarin Red S-Borono-Peptide for Potential Imaging of Cellular Copper(II) Ions, *ACS Biomater. Sci. Eng.* 7 (2021) 3361–3369, <https://doi.org/10.1021/acsbiomaterials.1c00457>.
- [171] Q. Wen, Y. Zhang, C. Li, S. Ling, X. Yang, G. Chen, Y. Yang, Q. Wang, NIR-II Fluorescent Self-Assembled Peptide Nanochain for Ultrasensitive Detection of Peritoneal Metastasis, *Angew. Chemie Int. Ed.* 58 (2019) 11001–11006, <https://doi.org/10.1002/anie.201905643>.
- [172] S.M. Standley, D.J. Toft, H. Cheng, S. Soukasene, J. Chen, S.M. Raja, V. Band, H. Band, V.L. Cryns, S.I. Stupp, Induction of Cancer Cell Death by Self-assembling Nanostructures Incorporating a Cytotoxic Peptide, *Cancer Res.* 70 (2010) 3020–3026, <https://doi.org/10.1158/0008-5472.CAN-09-3267>.
- [173] D.J. Toft, T.J. Moyer, S.M. Standley, Y. Ruff, A. Ugolkov, S.I. Stupp, V.L. Cryns, Coassembled Cytotoxic and Pegylated Peptide Amphiphiles Form Filamentous Nanostructures with Potent Antitumor Activity in Models of Breast Cancer, *ACS Nano.* 6 (2012) 7956–7965, <https://doi.org/10.1021/nn302503s>.
- [174] S.-Y. Qin, M.-Y. Peng, L. Rong, H.-Z. Jia, S. Chen, S.-X. Cheng, J. Feng, X.-Z. Zhang, An innovative pre-targeting strategy for tumor cell specific imaging and therapy, *Nanoscale.* 7 (2015) 14786–14793, <https://doi.org/10.1039/C5NR03862F>.
- [175] K. Han, Q. Lei, S.-B. Wang, J.-J. Hu, W.-X. Qiu, J.-Y. Zhu, W.-N. Yin, X. Luo, X.-Z. Zhang, Dual-Stage-Light-Guided Tumor Inhibition by Mitochondria-Targeted Photodynamic Therapy, *Adv. Funct. Mater.* 25 (2015) 2961–2971, <https://doi.org/10.1002/adfm.201500590>.
- [176] S. Chen, J.-X. Fan, X.-H. Liu, M.-K. Zhang, F. Liu, X. Zeng, G.-P. Yan, X.-Z. Zhang, A self-delivery system based on an amphiphilic proapoptotic peptide for tumor targeting therapy, *J. Mater. Chem. b.* 7 (2019) 778–785, <https://doi.org/10.1039/C8TB02945H>.
- [177] P. Pei, L. Chen, R. Fan, X.-R. Zhou, S. Feng, H. Liu, Q. Guo, H. Yin, Q. Zhang, F. Sun, L. Peng, P. Wei, C. He, R. Qiao, Z. Wang, S.-Z. Luo, Computer-Aided Design of Lasso-like Self-Assembling Anticancer Peptides with Multiple Functions for Targeted Self-Delivery and Cancer Treatments, *ACS Nano.* 16 (2022) 13783–13799, <https://doi.org/10.1021/acsnano.2c01014>.
- [178] Q. Xu, R. Lu, Z.-F. Zhu, J.-Q. Lv, L.-J. Wang, W. Zhang, J.-W. Hu, J. Meng, G. Lin, Z. Yao, Effects of tyrosine residue on histone acetylation in lung carcinoma cells, *Int. J. Cancer.* 128 (2011) 460–472, <https://doi.org/10.1002/ijc.25346>.
- [179] L. Shi, R. Ma, R. Lu, Q. Xu, Z. Zhu, L. Wang, C. Zhou, X. Li, H. Zhang, Z. Yao, Reversal effect of tyrosine residue (YSV) tripeptide on multi-drug resistance in resistant human hepatocellular carcinoma cell line BEL-7402/5-FU, *Cancer Lett.* 269 (2008) 101–110, <https://doi.org/10.1016/j.canlet.2008.04.033>.
- [180] Z. Zhang, L. Shi, C. Wu, Y. Su, J. Qian, H. Deng, X. Zhu, Construction of a Supramolecular Drug-Drug Delivery System for Non-Small-Cell Lung Cancer Therapy, *ACS Appl. Mater. Interfaces.* 9 (2017) 29505–29514, <https://doi.org/10.1021/acsmami.7b07565>.
- [181] C. Ren, Z. Wang, X. Zhang, J. Gao, Y. Gao, Y. Zhang, J. Liu, C. Yang, J. Liu, Construction of all-in-one peptide nanomedicine with photoacoustic imaging guided mild hyperthermia for enhanced cancer chemotherapy, *Chem. Eng. J.* 405 (2021), 127008, <https://doi.org/10.1016/j.cej.2020.127008>.
- [182] G. Li, B. Sun, Y. Li, C. Luo, Z. He, J. Sun, Small-Molecule Prodrug Nanoassemblies: An Emerging Nanoplatform for Anticancer Drug Delivery, *Small.* 17 (2021) 2101460, <https://doi.org/10.1002/smll.202101460>.
- [183] J. Wang, S. Hu, W. Mao, J. Xiang, Z. Zhou, X. Liu, J. Tang, Y. Shen, Assemblies of Peptide-Cytotoxin Conjugates for Tumor-Homing Chemotherapy, *Adv. Funct. Mater.* 29 (2019) 1807446, <https://doi.org/10.1002/adfm.201807446>.
- [184] Z. Chen, P. Zhang, A.G. Cheetham, J.H. Moon, J.W. Moxley, Y. Lin, H. Cui, Controlled release of free doxorubicin from peptide-drug conjugates by drug loading, *J. Control. Release.* 191 (2014) 123–130, <https://doi.org/10.1016/j.jconrel.2014.05.051>.
- [185] M.K. Shim, J. Park, H.Y. Yoon, S. Lee, W. Um, J.-H. Kim, S.-W. Kang, J.-W. Seo, S.-W. Hyun, J.H. Park, Y. Byun, I.C. Kwon, K. Kim, Carrier-free nanoparticles of cathepsin B-cleavable peptide-conjugated doxorubicin prodrug for cancer targeting therapy, *J. Control. Release.* 294 (2019) 376–389, <https://doi.org/10.1016/j.jconrel.2018.11.032>.
- [186] S. Zhang, X. Hu, D. Mang, T. Sasaki, Y. Zhang, Self-delivery of N-hydroxylethyl peptide assemblies to the cytosol inducing endoplasmic reticulum dilation in cancer cells, *Chem. Commun.* 55 (2019) 7474–7477, <https://doi.org/10.1039/C9CC03460A>.
- [187] C. Ren, Y. Gao, Y. Guan, Z. Wang, L. Yang, J. Gao, H. Fan, J. Liu, Carrier-Free Supramolecular Hydrogel Composed of Dual Drugs for Conquering Drug Resistance, *ACS Appl. Mater. Interfaces.* 11 (2019) 33706–33715, <https://doi.org/10.1021/acsmami.9b12530>.
- [188] R. Lin, A.G. Cheetham, P. Zhang, Y. Lin, H. Cui, Supramolecular filaments containing a fixed 41% paclitaxel loading, *Chem. Commun.* 49 (2013) 4968, <https://doi.org/10.1039/c3cc41896k>.
- [189] H. Xu, T. Wang, C. Yang, X. Li, G. Liu, Z. Yang, P.K. Singh, S. Krishnan, D. Ding, Supramolecular Nanofibers of Curcumin for Highly Amplified Radiosensitization of Colorectal Cancers to Ionizing Radiation, *Adv. Funct. Mater.* 28 (2018) 1707140, <https://doi.org/10.1002/adfm.201707140>.
- [190] Y. Ma, P. He, X. Tian, G. Liu, X. Zeng, G. Pan, Mussel-Derived, Cancer-Targeting Peptide as pH-Sensitive Prodrug Nanocarrier, *ACS Appl. Mater. Interfaces.* 11 (2019) 23948–23956, <https://doi.org/10.1021/acsmami.9b09031>.
- [191] A.G. Cheetham, P. Zhang, Y. Lin, L.L. Lock, H. Cui, Supramolecular Nanostructures Formed by Anticancer Drug Assembly, *J. Am. Chem. Soc.* 135 (2013) 2907–2910, <https://doi.org/10.1021/ja3115983>.
- [192] M. Peng, S. Qin, H. Jia, D. Zheng, L. Rong, X. Zhang, Self-delivery of a peptide-based prodrug for tumor-targeting therapy, *Nano Res.* 9 (2016) 663–673, <https://doi.org/10.1007/s12274-015-0945-1>.

- [193] R.W. Chakroun, F. Wang, R. Lin, Y. Wang, H. Su, D. Pompa, H. Cui, Fine-Tuning the Linear Release Rate of Paclitaxel-Bearing Supramolecular Filament Hydrogels through Molecular Engineering, *ACS Nano*. 13 (2019) 7780–7790, <https://doi.org/10.1021/acsnano.9b01689>.
- [194] K. Han, W.Y. Zhang, J. Zhang, Q. Lei, S.B. Wang, J.W. Liu, X.Z. Zhang, H.Y. Han, Acidity-Triggered Tumor-Targeted Chimeric Peptide for Enhanced Intra-Nuclear Photodynamic Therapy, *Adv. Funct. Mater.* 26 (2016) 4351–4361, <https://doi.org/10.1002/adfm.201600170>.
- [195] L.-H. Liu, W.-X. Qiu, Y.-H. Zhang, B. Li, C. Zhang, F. Gao, L. Zhang, X.-Z. Zhang, A Charge Reversible Self-Delivery Chimeric Peptide with Cell Membrane-Targeting Properties for Enhanced Photodynamic Therapy, *Adv. Funct. Mater.* 27 (2017) 1700220, <https://doi.org/10.1002/adfm.201700220>.
- [196] P.-L. Chen, S.-L. Peng, L.-T. Wu, M.-M. Fan, P. Wang, L.-H. Liu, Amphiphilic tumor-targeting chimeric peptide-based drug self-delivery nanomicelles for overcoming drug resistance in cancer by synergistic chemo-photodynamic therapy, *J. Mater. Sci.* 55 (2020) 15288–15298, <https://doi.org/10.1007/s10853-020-05084-6>.
- [197] H.-J. Cho, S.-J. Park, W.H. Jung, Y. Cho, D.J. Ahn, Y.-S. Lee, S. Kim, Injectable Single-Component Peptide Depot: Autonomously Rechargeable Tumor Photosensitization for Repeated Photodynamic Therapy, *ACS Nano*. 14 (2020) 15793–15805, <https://doi.org/10.1021/acsnano.0c06681>.
- [198] C. Zhang, M. Xu, S. He, J. Huang, C. Xu, K. Pu, Checkpoint Nano-PROTACs for Activatable Cancer Photo-Immunotherapy, *Adv. Mater.* 35 (2023) e2208553.
- [199] C. Zhang, S. He, Z. Zeng, P. Cheng, K. Pu, Smart Nano-PROTACs Reprogram Tumor Microenvironment for Activatable Photo-metabolic Cancer Immunotherapy, *Angew. Chemie - Int. Ed.* 61 (2022) e202114957.
- [200] S. Ma, S. Gu, J. Zhang, W. Qi, Z. Lin, W. Zhai, J. Zhan, Q. Li, Y. Cai, Y. Lu, Robust drug bioavailability and safety for rheumatoid arthritis therapy using D-amino acids-based supramolecular hydrogels, *Mater. Today Bio.* 15 (2022), 100296, <https://doi.org/10.1016/j.mtbio.2022.100296>.
- [201] P. Jia, X. Zhao, Y. Liu, M. Liu, Q. Zhang, S. Chen, H. Huang, Y. Jia, Y. Chang, Z. Han, Z. chao Han, Q. Li, Z. Guo, Z. Li., The RGD-modified self-assembling D-form peptide hydrogel enhances the therapeutic effects of mesenchymal stem cells (MSC) for hindlimb ischemia by promoting angiogenesis, *Chem. Eng. J.* (2022), <https://doi.org/10.1016/j.cej.2022.138004>.
- [202] Q. Guo, Y. Liu, Z. Wang, J. Zhang, G. Mu, W. Wang, J. Liu, Supramolecular nanofibers increase the efficacy of 10-hydroxycamptothecin by enhancing nuclear accumulation and depleting cellular ATP, *Acta Biomater.* 122 (2021) 343–353, <https://doi.org/10.1016/j.actbio.2020.12.052>.
- [203] F. Wang, H. Su, R. Lin, R.W. Chakroun, M.K. Monroe, Z. Wang, M. Porter, H. Cui, Supramolecular Tubustecan Hydrogel as Chemotherapeutic Carrier to Improve Tumor Penetration and Local Treatment Efficacy, *ACS Nano*. 14 (2020) 10083–10094, <https://doi.org/10.1021/acsnano.0c03286>.
- [204] S.Y. Qin, J. Feng, L. Rong, H.Z. Jia, S. Chen, X.J. Liu, G.F. Luo, R.X. Zhuo, X. Z. Zhang, Theranostic GO-based nanohybrid for tumor induced imaging and potential combinational tumor therapy, *Small.* 10 (2014) 599–608, <https://doi.org/10.1002/smll.201301613>.
- [205] L. Rong, Q. Lei, X. Zhang, Recent advances on peptide-based theranostic nanomaterials, *View.* 1 (2020) 20200050, <https://doi.org/10.1002/VIW.20200050>.
- [206] S.-Y. Li, L.-H. Liu, H.-Z. Jia, W.-X. Qiu, L. Rong, H. Cheng, X.-Z. Zhang, A pH-responsive prodrug for real-time drug release monitoring and targeted cancer therapy, *Chem. Commun.* 50 (2014) 11852–11855, <https://doi.org/10.1039/C4CC05008H>.
- [207] S.Y. Li, L.H. Liu, L. Rong, W.X. Qiu, H.Z. Jia, B. Li, F. Li, X.Z. Zhang, A dual-FRET-based versatile prodrug for real-time drug release monitoring and in situ therapeutic efficacy evaluation, *Adv. Funct. Mater.* 25 (2015) 7317–7326, <https://doi.org/10.1002/adfm.201503262>.
- [208] H. Su, Y. Cui, F. Wang, W. Zhang, C. Zhang, R. Wang, H. Cui, Theranostic supramolecular polymers formed by the self-assembly of a metal-chelating prodrug, *Biomater. Sci.* 9 (2021) 463–470, <https://doi.org/10.1039/D0BM00827C>.
- [209] W. Ma, S. Sha, P. Chen, M. Yu, J. Chen, C. Huang, B. Yu, Y. Liu, L. Liu, Z. Yu, A Cell Membrane-Targeting Self-Delivery Chimeric Peptide for Enhanced Photodynamic Therapy and In Situ Therapeutic Feedback, *Adv. Healthc. Mater.* 9 (2020) 1901100, <https://doi.org/10.1002/adhm.201901100>.
- [210] H. Zhang, K. Liu, S. Li, X. Xin, S. Yuan, G. Ma, X. Yan, Self-Assembled Minimalist Multifunctional Theranostic Nanoplatform for Magnetic Resonance Imaging-Guided Tumor Photodynamic Therapy, *ACS Nano*. 12 (2018) 8266–8276, <https://doi.org/10.1021/acsnano.8b03529>.
- [211] L. Liu, J. Zhang, R. An, Q. Xue, X. Cheng, Y. Hu, Z. Huang, L. Wu, W. Zeng, Y. Miao, J. Li, Y. Zhou, H. Chen, H. Liu, D. Ye, Smart Nanosensitizers for Activatable Sono-Photodynamic Immunotherapy of Tumors by Redox-Controlled Disassembly, *Angew. Chemie Int. Ed.* 62 (2023) e202217055.
- [212] W. Li, F. Separovic, N.M. O'Brien-Simpson, J.D. Wade, Chemically modified and conjugated antimicrobial peptides against superbugs, *Chem. Soc. Rev.* 50 (2021) 4932–4973, <https://doi.org/10.1039/D0CS01026J>.
- [213] A.S. Veiga, C. Sinthuvanich, D. Gaspar, H.G. Franquelim, M.A.R.B. Castanho, J. P. Schneider, Arginine-rich self-assembling peptides as potent antibacterial gels, *Biomaterials.* 33 (2012) 8907–8916, <https://doi.org/10.1016/j.biomaterials.2012.08.046>.
- [214] M. Abbas, M. Ovais, A. Atiq, T.M. Ansari, R. Xing, E. Spruijt, X. Yan, Tailoring supramolecular short peptide nanomaterials for antibacterial applications, *Coord. Chem. Rev.* 460 (2022), 214481, <https://doi.org/10.1016/j.ccr.2022.214481>.
- [215] L. Lombardi, Y. Shi, A. Falanga, E. Galdiero, E. De Alteris, G. Franci, I. Chourpa, H.S. Azevedo, S. Galdiero, Enhancing the Potency of Antimicrobial Peptides through Molecular Engineering and Self-Assembly, *Biomacromolecules.* 20 (2019) 1362–1374, <https://doi.org/10.1021/acs.biomac.8b01740>.
- [216] Y. Jiang, Y. Chen, Z. Song, Z. Tan, J. Cheng, Recent advances in design of antimicrobial peptides and polyptides toward clinical translation, *Adv. Drug Deliv. Rev.* 170 (2021) 261–280, <https://doi.org/10.1016/j.addr.2020.12.016>.
- [217] C. Chen, F. Pan, S. Zhang, J. Hu, M. Cao, J. Wang, H. Xu, X. Zhao, J.R. Lu, Antibacterial Activities of Short Designer Peptides: a Link between Propensity for Nanostructuring and Capacity for Membrane Destabilization, *Biomacromolecules.* 11 (2010) 402–411, <https://doi.org/10.1021/bm901130u>.
- [218] C. Chen, G. Li, X. Cui, J. Chen, Q. Yu, C. Zong, Y. Zhao, M. Xu, S. Zhou, H. Xu, Mechanistic Investigation of a Self-Assembling Peptide against *Escherichia coli*, *Langmuir*. 36 (2020) 9800–9809, <https://doi.org/10.1021/acs.langmuir.0c01311>.
- [219] S. Chou, H. Guo, F.G. Zingl, S. Zhang, J. Toska, B. Xu, Y. Chen, P. Chen, M.K. Waldor, W. Zhao, J.J. Mekalanos, X. Mou, Synthetic peptides that form nanostructured micelles have potent antibiotic and antibiofilm activity against polymicrobial infections, *Proc. Natl. Acad. Sci.* 120 (2023) e2219679120. <https://doi.org/10.1073/pnas>.
- [220] N. Rodrigues de Almeida, Y. Han, J. Perez, S. Kirkpatrick, Y. Wang, M. C. Sheridan, Design, Synthesis, and Nanostructure-Dependent Antibacterial Activity of Cationic Peptide Amphiphiles, *ACS Appl. Mater. Interfaces.* 11 (2019) 2790–2801, <https://doi.org/10.1021/acsami.8b17808>.
- [221] Z. Lai, Q. Jian, G. Li, C. Shao, Y. Zhu, X. Yuan, H. Chen, A. Shan, Self-Assembling Peptide Dendron Nanoparticles with High Stability and a Multimodal Antimicrobial Mechanism of Action, *ACS Nano.* 15 (2021) 15824–15840, <https://doi.org/10.1021/acsnano.1c03301>.
- [222] J.S. Lin, L.A. Bekale, N. Molchanova, J.E. Nielsen, M. Wright, B. Bacacao, G. Diamond, H. Jenssen, P.L. Santa Maria, A.E. Barron, Anti-persister and Anti-biofilm Activity of Self-Assembled Antimicrobial Peptoid Ellipsoid Micelles, *ACS, Infect. Dis.* 8 (2022) 1823–1830, <https://doi.org/10.1021/acsinfecdis.2c00288>.
- [223] G. Zaldivar, J. Feng, L. Lizarraga, Y. Yu, L. de Campos, K.M.P. de Oliveira, K. H. Piepenbrink, M. Conda-Sheridan, M. Tagliazucchi, Conformal Electrodeposition of Antimicrobial Hydrogels Formed by Self-Assembled Peptide Amphiphiles, *Adv. Mater. Interfaces.* 10 (2023) 2300046, <https://doi.org/10.1002/admi.202300046>.
- [224] Y. Niu, S. Padhee, H. Wu, B. Bai, Q. Qiao, Y. Hu, L. Harrington, W.N. Burda, L. N. Shaw, C. Cao, J. Cai, Lipo- γ -APeptides as a New Class of Potent and Broad-Spectrum Antimicrobial Agents, *J. Med. Chem.* 55 (2012) 4003–4009, <https://doi.org/10.1021/jm300274p>.
- [225] H. Gong, M.-A. Sani, X. Hu, K. Fa, J.W. Hart, M. Liao, P. Hollowell, J. Carter, L. A. Clifton, M. Campana, P. Li, S.M. King, J.R.P. Webster, A. Maestro, S. Zhu, F. Separovic, T.A. Waigh, H. Xu, A.J. McBain, J.R. Lu, How do Self-Assembling Antimicrobial Lipopeptides Kill Bacteria? *ACS Appl. Mater. Interfaces.* 12 (2020) 55675–55687, <https://doi.org/10.1021/acsmi.0c17222>.
- [226] A.-N. Zhang, W. Wu, C. Zhang, Q.-Y. Wang, Z.-N. Zhuang, H. Cheng, X.-Z. Zhang, A versatile bacterial membrane-binding chimeric peptide with enhanced photodynamic antimicrobial activity, *J. Mater. Chem. b.* 7 (2019) 1087–1095, <https://doi.org/10.1039/C8TB03094D>.
- [227] R. Huang, Q.H. Yu, X. Di Yao, W.L. Liu, Y.J. Cheng, Y.H. Ma, A.Q. Zhang, S.Y. Qin, Self-Deliverable Peptide-Mediated and Reactive-Oxygen-Species-Amplified Therapeutic Nanoplatform for Highly Effective Bacterial Inhibition, *ACS Appl. Mater. Interfaces.* 14 (2022) 159–171, <https://doi.org/10.1021/acsami.1c17271>.
- [228] D.-Y. Zhang, R.-G. Cao, Y.-J. Cheng, W.-L. Liu, R. Huang, A.-Q. Zhang, S.-Y. Qin, Programming lipopeptide nanotherapeutics for tandem treatment of post-surgical infection and melanoma recurrence, *J. Control. Release.* 362 (2023) 565–576, <https://doi.org/10.1016/j.jconrel.2023.09.009>.
- [229] L. Chen, D. Yang, J. Feng, M. Zhang, Q. Qian, Y. Zhou, Switchable modulation of bacterial growth and biofilm formation based on supramolecular tripeptide amphiphiles, *J. Mater. Chem. b.* 7 (2019) 6420–6427, <https://doi.org/10.1039/C9TB00973F>.
- [230] J. Li, Z. Chen, M. Zhou, J. Jing, W. Li, Y. Wang, L. Wu, L. Wang, Y. Wang, M. Lee, Polyoxometalate-Driven Self-Assembly of Short Peptides into Multivalent Nanofibers with Enhanced Antibacterial Activity, *Angew. Chemie Int. Ed.* 55 (2016) 2592–2595, <https://doi.org/10.1002/anie.201511276>.
- [231] L. Schnaider, S. Brahmachari, N.W. Schmidt, B. Mensa, S. Shaham-Niv, D. Bychenko, L. Adler-Abramovich, L.J.W. Shimoni, S. Kolusheva, W.F. DeGrado, E. Gazit, Self-assembling dipeptide antibacterial nanostructures with membrane disrupting activity, *Nat. Commun.* 8 (2017) 1365, <https://doi.org/10.1038/s41467-017-01447-x>.
- [232] S.L. Porter, S.M. Coulter, S. Pentlavalli, T.P. Thompson, G. Laverty, Self-assembling diphenylalanine peptide nanotubes selectively eradicate bacterial biofilm infection, *Acta Biomater.* 77 (2018) 96–105, <https://doi.org/10.1016/j.actbio.2018.07.033>.
- [233] S.B. Rezende, K.G.N. Oshiro, N.G.O. Júnior, O.L. Franco, M.H. Cardoso, Advances on chemically modified antimicrobial peptides for generating peptide antibiotics, *Chem. Commun.* 57 (2021) 11578–11590, <https://doi.org/10.1039/D1CC03793E>.
- [234] N. Mukherjee, S. Ghosh, J. Sarkar, R. Roy, D. Nandi, S. Ghosh, Amyloid-Inspired Engineered Multidomain Amphiphilic Injectable Peptide Hydrogel—An Excellent Antibacterial, Angiogenic, and Biocompatible Wound Healing Material, *ACS Appl. Mater. Interfaces.* 15 (2023) 33457–33479, <https://doi.org/10.1021/acsmi.3c06599>.
- [235] J. Zhou, R. Cha, Z. Wu, C. Zhang, Y. He, H. Zhang, K. Liu, M.S. Fareed, Z. Wang, C. Yang, Y. Zhang, W. Yan, K. Wang, An injectable, natural peptide hydrogel with potent antimicrobial activity and excellent wound healing-promoting effects,

- Nano Today. 49 (2023), 101801, <https://doi.org/10.1016/j.nantod.2023.101801>.
- [236] H. Zhang, Z. Wu, J. Zhou, Z. Wang, C. Yang, P. Wang, M.S. Fareed, Y. He, J. Su, R. Cha, K. Wang, The Antimicrobial, Hemostatic, and Anti-Adhesion Effects of a Peptide Hydrogel Constructed by the All-*<scop>d</scop>*-Enantiomer of Antimicrobial Peptide Jelleine-1, *Adv. Healthc. Mater.* (2023) e2301612.
- [237] N. Chauhan, Y. Singh, Self-Assembled Fmoc-Arg-Phe-Phe Peptide Gels with Highly Potent Bactericidal Activities, *ACS Biomater. Sci. Eng.* 6 (2020) 5507–5518, <https://doi.org/10.1021/acsbiomaterials.0c00660>.
- [238] J. Wang, X.-Y. Chen, Y. Zhao, Y. Yang, W. Wang, C. Wu, B. Yang, Z. Zhang, L. Zhang, Y. Liu, X. Du, W. Li, L. Qiu, P. Jiang, X.-Z. Mou, Y.-Q. Li, pH-Switchable Antimicrobial Nanofiber Networks of Hydrogel Eradicate Biofilm and Rescue Stalled Healing in Chronic Wounds, *ACS Nano*. 13 (2019) 11686–11697, <https://doi.org/10.1021/acsnano.9b05608>.
- [239] J. Zhou, H. Zhang, M.S. Fareed, Y. He, Y. Lu, C. Yang, Z. Wang, J. Su, P. Wang, W. Yan, K. Wang, An Injectable Peptide Hydrogel Constructed of Natural Antimicrobial Peptide J-1 and ADP Shows Anti-Infection, Hemostasis, and Antiadhesion Efficacy, *ACS Nano*. 16 (2022) 7636–7650, <https://doi.org/10.1021/acsnano.1c11206>.
- [240] P. Zou, W.-T. Chen, T. Sun, Y. Gao, L.-L. Li, H. Wang, Recent advances: peptides and self-assembled peptide-nanosystems for antimicrobial therapy and diagnosis, *Biomater. Sci.* 8 (2020) 4975–4996, <https://doi.org/10.1039/d0bm00789g>.
- [241] T. Ge, X. Hu, M. Liao, F. Zhou, J.R. Lu, Recent advances in the development and application of peptide self-assemblies in infection control, *Curr. Opin. Colloid Interface Sci.* 68 (2023), 101745, <https://doi.org/10.1016/j.cocis.2023.101745>.
- [242] X. Xi, T. Ye, S. Wang, X. Na, J. Wang, S. Qing, X. Gao, C. Wang, F. Li, W. Wei, G. Ma, Self-healing microcapsules synergistically modulate immunization microenvironments for potent cancer vaccination, *Sci. Adv.* 6 (2020) eaay7735, <https://doi.org/10.1126/sciadv.aay7735>.
- [243] S. Yan, Z. Luo, Z. Li, Y. Wang, J. Tao, C. Gong, X. Liu, Improving Cancer Immunotherapy Outcomes Using Biomaterials, *Angew. Chemie Int. Ed.* 59 (2020) 17332–17343, <https://doi.org/10.1002/anie.2020002780>.
- [244] M. Skwarczynski, I. Toth, Peptide-based synthetic vaccines, *Chem. Sci.* 7 (2016) 842–854, <https://doi.org/10.1039/C5SC03892H>.
- [245] R. Chang, X. Yan, Supramolecular Immunotherapy of Cancer Based on the Self-Assembling Peptide Design, *Small Struct.* 1 (2020) 2000068, <https://doi.org/10.1002/sstr.202000068>.
- [246] J.S. Rudra, Y.F. Tian, J.P. Jung, J.H. Collier, A self-assembling peptide acting as an immune adjuvant, *Proc. Natl. Acad. Sci.* 107 (2010) 622–627, <https://doi.org/10.1073/pnas.0912124107>.
- [247] J.S. Rudra, T. Sun, K.C. Bird, M.D. Daniels, J.Z. Gasiorowski, A.S. Chong, J. H. Collier, Modulating Adaptive Immune Responses to Peptide Self-Assemblies, *ACS Nano*. 6 (2012) 1557–1564, <https://doi.org/10.1021/nm204530r>.
- [248] Z. Luo, Q. Wu, C. Yang, H. Wang, T. He, Y. Wang, Z. Wang, H. Chen, X. Li, C. Gong, Z. Yang, A Powerful CD8 + T-Cell Stimulating D-Tetra-Peptide Hydrogel as a Very Promising Vaccine Adjuvant, *Adv. Mater.* 29 (2017) 1601776, <https://doi.org/10.1002/adma.201601776>.
- [249] Y. Xu, Y. Wang, Q. Yang, Z. Liu, Z. Xiao, Z. Le, Z. Yang, C. Yang, A versatile supramolecular nanoadjuvant that activates NF-κB for cancer immunotherapy, *Theranostics*. 9 (2019) 3388–3397, <https://doi.org/10.7150/thno.34031>.
- [250] Z. Wang, Y. Wang, J. Gao, Y. Shi, Z. Yang, Self-Assembling Peptides for Vaccine Development and Antibody Production, in: *Handb. Macrocycl. Supramol. Assem.*, Springer Singapore, Singapore, 2020: pp. 1497–1517. https://doi.org/10.1007/978-981-15-2686-2_63.
- [251] Z. Wang, Y. Shang, Z. Tan, X. Li, G. Li, C. Ren, F. Wang, Z. Yang, J. Liu, A supramolecular protein chaperone for vaccine delivery, *Theranostics*. 10 (2020) 657–670, <https://doi.org/10.7150/thno.39132>.
- [252] X. Li, Y. Wang, Y. Zhang, C. Liang, Z. Zhang, Y. Chen, Z. Hu, Z. Yang, A. Supramolecular, “Trident” for Cancer Immunotherapy, *Adv. Funct. Mater.* 31 (2021) 2100729, <https://doi.org/10.1002/adfm.202100729>.
- [253] S. Jia, S. Ji, J. Zhao, Y. Lv, J. Wang, D. Sun, D. Ding, A Fluorinated Supramolecular Self-Assembled Peptide as Nanovaccine Adjuvant for Enhanced Cancer Vaccine Therapy, *Small Methods*. 7 (2023) 2201409, <https://doi.org/10.1002/smtd.202201409>.
- [254] G.M. Lynn, C. Sedlik, F. Baharom, Y. Zhu, R.A. Ramirez-Valdez, V.L. Coble, K. Tobin, S.R. Nichols, Y. Itzkowitz, N. Zaidi, J.M. Gammon, N.J. Blobel, J. Denizéau, P. de la Roche, B.J. Francica, B. Decker, M. Maciejewski, J. Cheung, H. Yamane, M.G. Smelkinson, J.R. Francica, R. Laga, J.D. Bernstock, L. W. Seymour, C.G. Drake, C.M. Jewell, O. Lantz, E. Piaggio, A.S. Ishizuka, R. A. Seder, Peptide-TLR-7/8a conjugate vaccines chemically programmed for nanoparticle self-assembly enhance CD8 T-cell immunity to tumor antigens, *Nat. Biotechnol.* 38 (2020) 320–332, <https://doi.org/10.1038/s41587-019-0390-x>.
- [255] T. Aiga, Y. Manabe, K. Ito, T. Chang, K. Kabayama, S. Ohshima, Y. Kometani, A. Miura, H. Furukawa, H. Inaba, K. Matsuuwa, K. Fukase, Immunological Evaluation of Co-Assembling a Lipidated Peptide Antigen and Lipophilic Adjuvants: Self-Adjuvanting Anti-Breast-Cancer Vaccine Candidates, *Angew. Chemie Int. Ed.* 59 (2020) 17705–17711, <https://doi.org/10.1002/anie.202007999>.
- [256] C.N. Fries, Y. Wu, S.H. Kelly, M. Wolf, N.L. Votaw, S. Zauscher, J.H. Collier, Controlled Lengthwise Assembly of Helical Peptide Nanofibers to Modulate CD8 + T-Cell Responses, *Adv. Mater.* 32 (2020) 2003310, <https://doi.org/10.1002/adma.202003310>.
- [257] X. Zottig, S. Al-Halifa, M. Côté-Cyr, C. Calzas, R. Le Goffic, C. Chevalier, D. Archambault, S. Bourgault, Self-assembled peptide nanorod vaccine confers protection against influenza A virus, *Biomaterials*. 269 (2021), 120672, <https://doi.org/10.1016/j.biomaterials.2021.120672>.
- [258] L. Shao, H. Yu, J. Song, S. Liu, G. Li, Pyrene-Based Self-Assembling Peptide for Ratiometric Detection of Heparin, *ChemBioChem*. 24 (2023) e202200652.
- [259] M.K. Monroe, H. Wang, C.F. Anderson, M. Qin, C.L. Thio, C. Flexner, H. Cui, Antiviral supramolecular polymeric hydrogels by self-assembly of tenofovir-bearing peptide amphiphiles, *Biomater. Sci.* 11 (2023) 489–498, <https://doi.org/10.1039/D2BM01649D>.
- [260] J. Deng, D. Lin, X. Ding, Y. Wang, Y. Hu, H. Shi, L. Chen, B. Chu, L. Lei, C. Wen, J. Wang, Z. Qian, X. Li, Multifunctional Supramolecular Filament Hydrogel Boosts Anti-Inflammatory Efficacy In Vitro and In Vivo, *Adv. Funct. Mater.* 32 (2022) 2109173, <https://doi.org/10.1002/adfm.202109173>.
- [261] L. Chen, J. Deng, A. Yu, Y. Hu, B. Jin, P. Du, J. Zhou, L. Lei, Y. Wang, S. Valkal, X. Li, Drug-peptide supramolecular hydrogel boosting transcorneal permeability and pharmacological activity via ligand-receptor interaction, *Bioact. Mater.* 10 (2022) 420–429, <https://doi.org/10.1016/j.bioactmat.2021.09.006>.
- [262] B. Li, Y. Huang, J. Bao, Z. Xu, X. Yan, Q. Zou, Supramolecular Nanoarchitectonics Based on Antagonist Peptide Self-Assembly for Treatment of Liver Fibrosis, *Small*. 23(04675 (2023) 1–7, <https://doi.org/10.1002/smll.202304675>.
- [263] Q. Han, S. Ai, Q. Hong, C. Zhang, Y. Song, X. Wang, X. Wang, S. Cui, Z. Li, H. Zhu, Z. Yang, X. Chen, G. Cai, A supramolecular hydrogel based on the combination of YIGSR and RGD enhances mesenchymal stem cells paracrine function via integrin α2β1 and PI3K/AKT signaling pathway for acute kidney injury therapy, *Chem. Eng. J.* 436 (2022), 135088, <https://doi.org/10.1016/j.cej.2022.135088>.
- [264] D. Liu, D. Fu, L. Zhang, L. Sun, Detection of amyloid-beta by Fmoc-KLVFF self-assembled fluorescent nanoparticles for Alzheimer’s disease diagnosis, *Chinese Chem. Lett.* 32 (2021) 1066–1070, <https://doi.org/10.1016/j.cclet.2020.09.009>.
- [265] Y. Huang, B. Zhang, L. Yuan, L. Liu, A signal amplification strategy based on peptide self-assembly for the identification of amyloid-β oligomer, *Sensors Actuators B Chem.* 335 (2021), 129697, <https://doi.org/10.1016/j.snb.2021.129697>.
- [266] B. Ren, Y. Tang, D. Zhang, Y. Liu, Y. Zhang, H. Chen, R. Hu, M. Zhang, J. Zheng, Conformational-specific self-assembled peptides as dual-mode, multi-target inhibitors and detectors for different amyloid proteins, *J. Mater. Chem. b.* 10 (2022) 1754–1762, <https://doi.org/10.1039/D1TB02775A>.
- [267] S. Zhang, S. Asghar, C. Zhu, J. Ye, L. Lin, L. Xu, Z. Hu, Z. Chen, F. Shao, Y. Xiao, Multifunctional nanorods based on self-assembly of biomimetic apolipoprotein E peptide for the treatment of Alzheimer’s disease, *J. Control. Release.* 335 (2021) 637–649, <https://doi.org/10.1016/j.jconrel.2021.05.044>.
- [268] Z. Liu, M. Ma, D. Yu, Y. Ren, X. Qu, Target-driven supramolecular self-assembly for selective amyloid-β photooxygenation against Alzheimer’s disease, *Chem. Sci.* 11 (2020) 11003–11008, <https://doi.org/10.1039/D0SC04984K>.
- [269] C. Zhu, T. Li, Z. Wang, Z. Li, J. Wei, H. Han, D. Yuan, M. Cai, J. Shi, MC1R Peptide Agonist Self-Assembles into a Hydrogel That Promotes Skin Pigmentation for Treating Vitiligo, *ACS Nano*. 17 (2023) 8723–8733, <https://doi.org/10.1021/acsnano.3c01960>.
- [270] F.-Y. Cao, W.-N. Yin, J.-X. Fan, L. Tao, S.-Y. Qin, R.-X. Zhuo, X.-Z. Zhang, Evaluating the Effects of Charged Oligopeptide Motifs Coupled with RGD on Osteogenic Differentiation of Mesenchymal Stem Cells, *ACS Appl. Mater. Interfaces*. 7 (2015) 6698–6705, <https://doi.org/10.1021/acsmami.5b00064>.
- [271] M. Yang, Z.-C. Zhang, F.-Z. Yuan, R.-H. Deng, X. Yan, F.-B. Mao, Y.-R. Chen, H. Lu, J.-K. Yu, An immunomodulatory polypeptide hydrogel for osteochondral defect repair, *Bioact. Mater.* 19 (2023) 678–689, <https://doi.org/10.1016/j.bioactmat.2022.05.008>.
- [272] T. Falcucci, M. Radke, J.K. Sahoo, O. Hasturk, D.L. Kaplan, *Biomaterials* Multifunctional silk vinyl sulfone-based hydrogel scaffolds for dynamic material-cell interactions, *Biomaterials*. 300 (2023), 122201, <https://doi.org/10.1016/j.biomaterials.2023.122201>.
- [273] Z. Hao, H. Li, Y. Wang, Y. Hu, T. Chen, S. Zhang, X. Guo, L. Cai, J. Li, Supramolecular Peptide Nanofiber Hydrogels for Bone Tissue Engineering: From Multihierarchical Fabrications to Comprehensive Applications, *Adv. Sci.* 9 (2022) e2103820.
- [274] V.P. Gray, C.D. Amelung, I.J. Duti, E.G. Lauderlilch, R.A. Letteri, K.J. Lampe, *Biomaterials* via peptide assembly: Design, characterization, and application in tissue engineering, *Acta Biomater.* 140 (2022) 43–75, <https://doi.org/10.1016/j.actbio.2021.10.030>.
- [275] W. Sun, D.A. Gregory, X. Zhao, Designed peptide amphiphiles as scaffolds for tissue engineering, *Adv. Colloid Interface Sci.* 314 (2023), 102866, <https://doi.org/10.1016/j.jcis.2023.102866>.
- [276] T. Guan, J. Li, C. Chen, Y. Liu, Self-Assembling Peptide-Based Hydrogels for Wound Tissue Repair, *Adv. Sci.* 9 (2022) e2104165.
- [277] X. Ding, H. Zhao, Y. Li, A.L. Lee, Z. Li, M. Fu, C. Li, Y.Y. Yang, P. Yuan, Synthetic peptide hydrogels as 3D scaffolds for tissue engineering, *Adv. Drug Deliv. Rev.* 160 (2020) 78–104, <https://doi.org/10.1016/j.addr.2020.10.005>.
- [278] Z. Luo, Y. Yue, Y. Zhang, X. Yuan, J. Gong, L. Wang, B. He, Z. Liu, Y. Sun, J. Liu, M. Hu, J. Zheng, Designer D-form self-assembling peptide nanofiber scaffolds for 3-dimensional cell cultures, *Biomaterials*. 34 (2013) 4902–4913, <https://doi.org/10.1016/j.biomaterials.2013.03.081>.
- [279] X. Fan, J. Zhan, X. Pan, X. Liao, W. Guo, P. Chen, H. Li, W. Feng, Y. Cai, M. Chen, Enzymatic self-assembly nanofibers anchoring mesenchymal stem cells induce cell spheroids and amplify paracrine function for myocardial infarction therapy, *Chem. Eng. J.* 436 (2022), 135224, <https://doi.org/10.1016/j.cej.2022.135224>.
- [280] Y. Xiang, H. Mao, S. Tong, C. Liu, R. Yan, L. Zhao, L. Zhu, C. Bao, A Facile and Versatile Approach to Construct Photoactivated Peptide Hydrogels by Regulating Electrostatic Repulsion, *ACS Nano*. 17 (2023) 5536–5547, <https://doi.org/10.1021/acsnano.2c10896>.
- [281] A.E.G. Baker, L.C. Bahlmann, R.Y. Tam, J.C. Liu, A.N. Ganesh, N. Mitrousis, R. Marcellus, M. Spears, J.M.S. Bartlett, D.W. Cescon, G.D. Bader, M.S. Shoichet,

- Benchmarking to the Gold Standard: Hyaluronan-Oxime Hydrogels Recapitulate Xenograft Models with In Vitro Breast Cancer Spheroid Culture, *Adv. Mater.* 31 (2019) 1901166, <https://doi.org/10.1002/adma.201901166>.
- [282] M.F. Gencoglu, L.E. Barney, C.L. Hall, E.A. Brooks, A.D. Schwartz, D.C. Corbett, K.R. Stevens, S.R. Peyton, Comparative Study of Multicellular Tumor Spheroid Formation Methods and Implications for Drug Screening, *ACS Biomater. Sci. Eng.* 4 (2018) 410–420, <https://doi.org/10.1021/acsbiomaterials.7b00069>.
- [283] L. Hill, J. Bruns, S.P. Zustiak, Hydrogel matrix presence and composition influence drug responses of encapsulated glioblastoma spheroids, *Acta Biomater.* 132 (2021) 437–447, <https://doi.org/10.1016/j.actbio.2021.05.005>.
- [284] N. Singh, K. Patel, A. Navalkar, P. Kadu, D. Datta, D. Chatterjee, S. Mukherjee, R. Shaw, N. Gahlot, A. Shaw, S. Jadhav, S.K. Maji, Amyloid fibril-based thixotropic hydrogels for modeling of tumor spheroids in vitro, *Biomaterials.* 295 (2023), 122032, <https://doi.org/10.1016/j.biomaterials.2023.122032>.
- [285] J.J. Fu, Y. Zhou, X.X. Shi, Y.J. Kang, Z.S. Lu, Y. Li, C.M. Li, L. Yu, Spontaneous formation of tumor spheroid on a hydrophilic filter paper for cancer stem cell enrichment, *Colloids Surfaces B Biointerfaces.* 174 (2019) 426–434, <https://doi.org/10.1016/j.colsurfb.2018.11.038>.
- [286] J. Antunes, V.M. Gaspar, L. Ferreira, M. Monteiro, R. Henrique, C. Jerónimo, J.F. Mano, In-air production of 3D co-culture tumor spheroid hydrogels for expedited drug screening, *Acta Biomater.* 94 (2019) 392–409, <https://doi.org/10.1016/j.actbio.2019.06.012>.
- [287] P.S. Thakuri, C. Liu, G.D. Luker, H. Tavana, Biomaterials-Based Approaches to Tumor Spheroid and Organoid Modeling, *Adv. Healthc. Mater.* 7 (2018) 1700980, <https://doi.org/10.1002/adhm.201700980>.
- [288] H. Jian, M. Wang, Q. Dong, J. Li, A. Wang, X. Li, P. Ren, S. Bai, Dipeptide Self-Assembled Hydrogels with Tunable Mechanical Properties and Degradability for 3D Bioprinting, *ACS Appl. Mater. Interfaces.* 11 (2019) 46419–46426, <https://doi.org/10.1021/acsmami.9b13905>.
- [289] S. Ai, H. Li, H. Zheng, J. Liu, J. Gao, J. Liu, Q. Chen, Z. Yang, A SupraGel for efficient production of cell spheroids, *Sci. China Mater.* 65 (2022) 1655–1661, <https://doi.org/10.1007/s40843-021-1951-x>.
- [290] W.K. Restu, S. Yamamoto, Y. Nishida, H. Ienaga, T. Aoi, T. Maruyama, Hydrogel formation by short D-peptide for cell-culture scaffolds, *Mater. Sci. Eng. c.* 111 (2020), 110746, <https://doi.org/10.1016/j.msec.2020.110746>.
- [291] T. Guan, J. Li, C. Chen, Y. Liu, Self-Assembling Peptide-Based Hydrogels for Wound Tissue Repair, *Adv. Sci.* 9 (2022) 2104165, <https://doi.org/10.1002/advs.202104165>.
- [292] Y. Hu, H. Shi, X. Ma, T. Xia, Y. Wu, L. Chen, Z. Ren, L. Lei, J. Jiang, J. Wang, X. Li, Highly stable fibronectin-mimetic-peptide-based supramolecular hydrogel to accelerate corneal wound healing, *Acta Biomater.* 159 (2023) 128–139, <https://doi.org/10.1016/j.actbio.2023.01.047>.
- [293] J. Yuan, Y. Wang, W. Yang, X. Li, K. Tao, W. He, J. Yan, Biomimetic peptide dynamic hydrogel inspired by humanized defensin nanonets as the wound-healing gel coating, *Chem. Eng. J.* 470 (2023), 144266, <https://doi.org/10.1016/j.cej.2023.144266>.
- [294] Z. Feng, Q. Su, C. Zhang, P. Huang, H. Song, A. Dong, D. Kong, W. Wang, Bioinspired Nanofibrous Glycopeptide Hydrogel Dressing for Accelerating Wound Healing: A Cytokine-Free, M2-Type Macrophage Polarization Approach, *Adv. Funct. Mater.* 30 (2020) 202006454, <https://doi.org/10.1002/adfm.202006454>.
- [295] B. Chu, J.-M. He, L.-L. Liu, C.-X. Wu, L.-L. You, X.-L. Li, S. Wang, C.-S. Chen, M. Tu, Proangiogenic Peptide Nanofiber Hydrogels for Wound Healing, *ACS Biomater. Sci. Eng.* 7 (2021) 1100–1110, <https://doi.org/10.1021/acsbiomaterials.0c01264>.
- [296] Y. Shang, H. Liu, R. Peng, C. Ren, X. Luo, C. Ma, Y. Gao, Z. Wang, J. Gao, J. Liu, Z. Yang, PDGF-mimicking supramolecular nanofibers for ionizing radiation-induced injury repair, *Chem. Eng. J.* 410 (2021), 128309, <https://doi.org/10.1016/j.cej.2020.128309>.
- [297] Y. Li, X. Cai, Z. Wang, Y. Han, C. Ren, L. Yang, Z. Wang, G. Mu, H. Jia, J. Liu, J. Liu, C. Yang, Bio-inspired supramolecular metallopeptide hydrogel promotes recovery from cutaneous wound, *Chem. Eng. J.* 455 (2023), 140848, <https://doi.org/10.1016/j.cej.2022.140848>.
- [298] Q. Xuan, F. Jiang, H. Dong, W. Zhang, F. Zhang, T. Ma, J. Zhuang, J. Yu, Y. Wang, H. Shen, C. Chen, P. Wang, Bioinspired Intrinsic Versatile Hydrogel Fabricated by Amyloidal Toxin Simulant-Based Nanofibrous Assemblies for Accelerated Diabetic Wound Healing, *Adv. Funct. Mater.* 31 (2021) 2106705, <https://doi.org/10.1002/adfm.202106705>.
- [299] K.A. Tran, P.P. Partyka, Y. Jin, J. Bouyer, I. Fischer, P.A. Galie, Vascularization of self-assembled peptide scaffolds for spinal cord injury repair, *Acta Biomater.* 104 (2020) 76–84, <https://doi.org/10.1016/j.actbio.2019.12.033>.
- [300] B. Sarkar, X. Ma, A. Agas, Z. Siddiqui, P. Iglesias-Montoro, P.K. Nguyen, K.K. Kim, J. Haorah, V.A. Kumar, In vivo neuroprotective effect of a self-assembled peptide hydrogel, *Chem. Eng. J.* 408 (2021), 127295, <https://doi.org/10.1016/j.cej.2020.127295>.
- [301] C. Zhang, Y. Shang, X. Chen, A.C. Midgley, Z. Wang, D. Zhu, J. Wu, P. Chen, L. Wu, X. Wang, K. Zhang, H. Wang, D. Kong, Z. Yang, Z. Li, X. Chen, Supramolecular Nanofibers Containing Arginine-Glycine-Aspartate (RGD) Peptides Boost Therapeutic Efficacy of Extracellular Vesicles in Kidney Repair, *ACS Nano.* 14 (2020) 12133–12147, <https://doi.org/10.1021/acsnano.0c05681>.
- [302] S. Song, J. Wang, Z. Cheng, Z. Yang, L. Shi, Z. Yu, Directional molecular sliding movement in peptide hydrogels accelerates cell proliferation, *Chem. Sci.* 11 (2020) 1383–1393, <https://doi.org/10.1039/C9SC05808G>.
- [303] F.R. Balkwill, M. Capasso, T. Hagemann, The tumor microenvironment at a glance, *J. Cell Sci.* 125 (2012) 5591–5596, <https://doi.org/10.1242/jcs.116392>.
- [304] D. Dasgupta, D. Pally, D.K. Saini, R. Bhat, A. Ghosh, Nanomotors Sense Local Physicochemical Heterogeneities in Tumor Microenvironments, *Angew. Chemie Int. Ed.* 59 (2020) 23690–23696, <https://doi.org/10.1002/anie.202008681>.
- [305] B. Blanco-Fernandez, V.M. Gaspar, E. Engel, J.F. Mano, Proteinaceous Hydrogels for Bioengineering Advanced 3D Tumor Models, *Adv. Sci.* 8 (2021) 2003129, <https://doi.org/10.1002/advs.202003129>.
- [306] Z. Yang, H. Xu, X. Zhao, Designer Self-Assembling Peptide Hydrogels to Engineer 3D Cell Microenvironments for Cell Constructs Formation and Precise Oncology Remodeling in Ovarian Cancer, *Adv. Sci.* 7 (2020) 1903718, <https://doi.org/10.1002/advs.201903718>.
- [307] K. Mi, G. Wang, Z. Liu, Z. Feng, B. Huang, X. Zhao, Influence of a Self-Assembling Peptide, RADA16, Compared with Collagen I and Matrigel on the Malignant Phenotype of Human Breast-Cancer Cells in 3D Cultures and in vivo, *Macromol. Biosci.* 9 (2009) 437–443, <https://doi.org/10.1002/mabi.200800262>.
- [308] N. Betriu, C. Semino, Development of a 3D Co-Culture System as a Cancer Model Using a Self-Assembling Peptide Scaffold, *Gels.* 4 (2018) 65, <https://doi.org/10.3390/gels4030065>.
- [309] F. Gelain, Z. Luo, S. Zhang, Self-Assembling Peptide EAK16 and RADA16 Nanofiber Scaffold Hydrogel, *Chem. Rev.* 120 (2020) 13434–13460, <https://doi.org/10.1021/cacsrev.0c00690>.
- [310] H. Huang, Y. Ding, X.S. Sun, T.A. Nguyen, Peptide Hydrogelation and Cell Encapsulation for 3D Culture of MCF-7 Breast Cancer Cells, *PLoS One.* 8 (2013) e59482.
- [311] K.M. Hainline, F. Gu, J.F. Handley, Y.F. Tian, Y. Wu, L. de Wet, D.J. Vander Giemd, J.H. Collier, Self-Assembling Peptide Gels for 3D Prostate Cancer Spheroid Culture, *Macromol. Biosci.* 19 (2019) 1800249. <https://doi.org/10.1002/mabi.201800249>.
- [312] H.C. Clough, M. O'Brien, X. Zhu, A.F. Miller, A. Saiani, O. Tsigkou, Neutrally charged self-assembling peptide hydrogel recapitulates in vitro mechanisms of breast cancer progression, *Mater. Sci. Eng. c.* 127 (2021), 112200, <https://doi.org/10.1016/j.ms.2021.112200>.
- [313] D. Osuna de la Peña, S.M.D. Trabulo, E. Collin, Y. Liu, S. Sharma, M. Tatari, D. Behrens, M. Erkan, R.T. Lawlor, A. Scarpa, C. Heeschen, A. Mata, D. Loessner, Bioengineered 3D models of human pancreatic cancer recapitulate in vivo tumour biology, *Nat. Commun.* 12 (2021) 5623, <https://doi.org/10.1038/s41467-021-25921-9>.
- [314] H. Zhan, B. Zhou, Y. Cheng, J. Xu, L. Wang, G. Zhang, S. Hu, Crosstalk between stromal cells and cancer cells in pancreatic cancer: New insights into stromal biology, *Cancer Lett.* 392 (2017) 83–93, <https://doi.org/10.1016/j.canlet.2017.01.041>.
- [315] J.C. Ashworth, J.L. Thompson, J.R. James, C.E. Slater, S. Pijuan-Galitó, K. Lis-Slimak, R.J. Holley, K.A. Meade, A. Thompson, K.P. Arkill, M. Tassieri, A. Wright, G. Farnie, C.L.R. Merry, Peptide gels of fully-defined composition and mechanics for probing cell-cell and cell-matrix interactions in vitro, *Matrix Biol.* 85–86 (2020) 15–33, <https://doi.org/10.1016/j.matbio.2019.06.009>.
- [316] C.I. Hedegaard, C. Redondo-Gómez, B.Y. Tan, K.W. Ng, D. Loessner, A. Mata, Peptide-protein coassembling matrices as a biomimetic 3D model of ovarian cancer, *Sci. Adv.* 6 (2020) eabb3298, <https://doi.org/10.1126/sciadv.eabb3298>.
- [317] M. Mamuti, R. Zheng, H.-W. An, H. Wang, In vivo self-assembled nanomedicine, *Nano Today.* 36 (2021), 101036, <https://doi.org/10.1016/j.nantod.2020.101036>.
- [318] X. Sun, X. Yang, Y. Chen, J. Sun, Z. He, S. Zhang, C. Luo, In situ self-assembled nanomedicines for cancer treatment, *Chem. Eng. J.* 466 (2023), 143365, <https://doi.org/10.1016/j.cej.2023.143365>.
- [319] J. Kim, S. Lee, Y. Kim, M. Choi, I. Lee, E. Kim, C.G. Yoon, K. Pu, H. Kang, J.S. Kim, In situ self-assembly for cancer therapy and imaging, *Nat. Rev. Mater.* 8 (2023) 710–725, <https://doi.org/10.1038/s41578-023-00589-3>.
- [320] X. Liang, Y. Zhang, J. Zhou, Z. Bu, J. Liu, K. Zhang, Tumor microenvironment-triggered intratumoral in situ construction of theranostic supramolecular self-assembly, *Coord. Chem. Rev.* 473 (2022), 214824, <https://doi.org/10.1016/j.ccr.2022.214824>.
- [321] Y. Cong, L. Ji, Y. Gao, F. Liu, D. Cheng, Z. Hu, Z. Qiao, H. Wang, Microenvironment-Induced In Situ Self-Assembly of Polymer-Peptide Conjugates That Attack Solid Tumors Deeply, *Angew. Chemie Int. Ed.* 58 (2019) 4632–4637, <https://doi.org/10.1002/anie.201900135>.
- [322] S. Yamamoto, K. Nishimura, K. Morita, S. Kanemitsu, Y. Nishida, T. Morimoto, T. Aoi, A. Tamura, T. Maruyama, Microenvironment pH-Induced Selective Cell Death for Potential Cancer Therapy Using Nanofibrous Self-Assembly of a Peptide Amphiphile, *Biomacromolecules.* 22 (2021) 2524–2531, <https://doi.org/10.1021/acsbiomac.1c00267>.
- [323] J. Zhang, Y. Mu, M. Xu, M.F. Foda, H. Han, Sequential assembled chimeric peptide for precise synergistic phototherapy and photoacoustic imaging of tumor apoptosis, *Chem. Eng. J.* 427 (2022), 130775, <https://doi.org/10.1016/j.cej.2021.130775>.
- [324] H. He, W. Tan, J. Guo, M. Yi, A.N. Shy, B. Xu, Enzymatic Noncovalent Synthesis, *Chem. Rev.* (2020), <https://doi.org/10.1021/acs.chemrev.0c00306>.
- [325] Z.M. Yang, K.M. Xu, Z.F. Guo, Z. Guo, B. Xu, Intracellular Enzymatic Formation of Nanofibers Results in Hydrogelation and Regulated Cell Death, *Adv. Mater.* 19 (2007) 3152–3156, <https://doi.org/10.1002/adma.200701971>.
- [326] Y. Gao, J. Shi, D. Yuan, B. Xu, Imaging enzyme-triggered self-assembly of small molecules inside live cells, *Nat. Commun.* 3 (2012) 1033, <https://doi.org/10.1038/ncomms2040>.
- [327] J. Zhou, X. Du, C. Berciu, H. He, J. Shi, D. Nicastro, B. Xu, Enzyme-Instructed Self-Assembly for Spatiotemporal Profiling of the Activities of Alkaline Phosphatases on Live Cells, *Chem.* 1 (2016) 246–263, <https://doi.org/10.1016/j.chempr.2016.07.003>.

- [328] H. Wang, Z. Feng, Y. Wang, R. Zhou, Z. Yang, B. Xu, Integrating Enzymatic Self-Assembly and Mitochondria Targeting for Selectively Killing Cancer Cells without Acquired Drug Resistance, *J. Am. Chem. Soc.* 138 (2016) 16046–16055, <https://doi.org/10.1021/jacs.6b09783>.
- [329] Z. Feng, X. Han, H. Wang, T. Tang, B. Xu, Enzyme-Instructed Peptide Assemblies Selectively Inhibit Bone Tumors, *Chem.* 5 (2019) 2442–2449, <https://doi.org/10.1016/j.chempr.2019.06.020>.
- [330] S. Liu, Q. Zhang, H. He, M. Yi, W. Tan, J. Guo, B. Xu, Intranuclear Nanoribbons for Selective Killing of Osteosarcoma Cells, *Angew. Chemie - Int. Ed.* 61 (2022) e202210568.
- [331] R. Guo, X. Zhang, P. Fan, B. Song, Z. Li, Z. Duan, Z. Qiao, H. Wang, In Vivo Self-Assembly Induced Cell Membrane Phase Separation for Improved Peptide Drug Internalization, *Angew. Chemie Int. Ed.* 60 (2021) 25128–25134, <https://doi.org/10.1002/anie.202111839>.
- [332] K. Morita, K. Nishimura, S. Yamamoto, N. Shimizu, T. Yashiro, R. Kawabata, T. Aoi, A. Tamura, T. Maruyama, In Situ Synthesis of an Anticancer Peptide Amphiphile Using Tyrosine Kinase Overexpressed in Cancer Cells, *JACS Au.* 2 (2022) 2023–2028, <https://doi.org/10.1021/jacsau.2c00301>.
- [333] A. Tanaka, Y. Fukuoka, Y. Morimoto, T. Honjo, D. Koda, M. Goto, T. Maruyama, Cancer cell death induced by the intracellular self-assembly of an enzyme-responsive supramolecular gelator, *J. Am. Chem. Soc.* 137 (2015) 770–775, <https://doi.org/10.1021/ja510156v>.
- [334] H.-W. An, L.-L. Li, Y. Wang, Z. Wang, D. Hou, Y.-X. Lin, S.-L. Qiao, M.-D. Wang, C. Yang, Y. Cong, Y. Ma, X.-X. Zhao, Q. Cai, W.-T. Chen, C.-Q. Lu, W. Xu, H. Wang, Y. Zhao, A tumour-selective cascade activatable self-detained system for drug delivery and cancer imaging, *Nat. Commun.* 10 (2019) 4861, <https://doi.org/10.1038/s41467-019-12848-5>.
- [335] B. Hu, Z. Lian, Z. Zhou, L. Shi, Z. Yu, Reactive Oxygen Species-Responsive Adaptable Self-Assembly of Peptides toward Advanced Biomaterials, *ACS Appl. Bio Mater.* 3 (2020) 5529–5551, <https://doi.org/10.1021/acsabm.0c00758>.
- [336] Z. Huang, Q. Yao, J. Chen, Y. Gao, Redox supramolecular self-assemblies nonlinearly enhance fluorescence to identify cancer cells, *Chem. Commun.* 54 (2018) 5385–5388, <https://doi.org/10.1039/C8CC02648C>.
- [337] Z. Huang, Y. Liu, L. Wang, A. Ali, Q. Yao, X. Jiang, Y. Gao, Supramolecular assemblies mimicking neutrophil extracellular traps for MRSE infection control, *Biomaterials.* 253 (2020), 120124, <https://doi.org/10.1016/j.biomaterials.2020.120124>.
- [338] S. Wei, X.-R. Zhou, Z. Huang, Q. Yao, Y. Gao, Hydrogen sulfide induced supramolecular self-assembly in living cells, *Chem. Commun.* 54 (2018) 9051–9054, <https://doi.org/10.1039/C8CC05174G>.
- [339] W. Song, X. Zhang, Y. Song, K. Fan, F. Shao, Y. Long, Y. Gao, W. Cai, X. Lan, Enhancing Photothermal Therapy Efficacy by In Situ Self-Assembly in Glioma, *ACS Appl. Mater. Interfaces.* 15 (2023) 57–66, <https://doi.org/10.1021/acsami.2c14413>.
- [340] X. Liu, M. Li, J. Liu, Y. Song, B. Hu, C. Wu, A.-A. Liu, H. Zhou, J. Long, L. Shi, Z. Yu, In Situ Self-Sorting Peptide Assemblies in Living Cells for Simultaneous Organelle Targeting, *J. Am. Chem. Soc.* 144 (2022) 9312–9323, <https://doi.org/10.1021/jacs.2c01025>.
- [341] J. Zhan, Y. Cai, S. He, L. Wang, Z. Yang, Tandem Molecular Self-Assembly in Liver Cancer Cells, *Angew. Chemie Int. Ed.* 57 (2018) 1813–1816, <https://doi.org/10.1002/anie.201710237>.
- [342] M.-D. Wang, D.-Y. Hou, G.-T. Lv, R.-X. Li, X.-J. Hu, Z.-J. Wang, N.-Y. Zhang, L. Yi, W.-H. Xu, H. Wang, Targeted in situ self-assembly augments peptide drug conjugate cell-entry efficiency, *Biomaterials.* 278 (2021), 121139, <https://doi.org/10.1016/j.biomaterials.2021.121139>.
- [343] D. Kim, S. Kim, G. Park, H. Choi, J.-H. Ryu, Spatiotemporal Self-Assembly of Peptide Amphiphiles by Carbonic Anhydrase IX-Targeting Induces Cancer-Lysosomal Membrane Disruption, *JACS Au.* 2 (2022) 2539–2547, <https://doi.org/10.1021/jacsau.2c00422>.
- [344] L. Zhang, Z. Jiang, X. Yang, Y. Qian, M. Wang, S. Wu, L. Li, F. Jia, Z. Wang, Z. Hu, M. Zhao, X. Tang, G. Li, H. Shang, X. Chen, W. Wang, A. Totipotent, “All-In-One” Peptide Sequentially Blocks Immune Checkpoint and Reverses the Immunosuppressive Tumor Microenvironment, *Adv. Mater.* 35 (2023) 2207330, <https://doi.org/10.1002/adma.202207330>.
- [345] Z. Shen, Z. Guo, L. Zhou, Y. Wang, J. Zhang, J. Hu, Y. Zhang, Biomembrane induced in situ self-assembly of peptide with enhanced antimicrobial activity, *Biomater. Sci.* 8 (2020) 2031–2039, <https://doi.org/10.1039/C9BM01785B>.
- [346] C. Yang, C. Ren, J. Zhou, J. Liu, Y. Zhang, F. Huang, D. Ding, B. Xu, J. Liu, Dual Fluorescent- and Isotopic-Labelled Self-Assembling Vancomycin for in vivo Imaging of Bacterial Infections, *Angew. Chemie Int. Ed.* 56 (2017) 2356–2360, <https://doi.org/10.1002/anie.201610926>.
- [347] Y. Ding, D. Zheng, L. Xie, X. Zhang, Z. Zhang, L. Wang, Z.-W. Hu, Z. Yang, Enzyme-Instructed Peptide Assembly Favored by Preorganization for Cancer Cell Membrane Engineering, *J. Am. Chem. Soc.* 145 (2023) 4366–4371, <https://doi.org/10.1021/jacs.2c11823>.
- [348] F.-H. Liu, Y. Cong, G.-B. Qi, L. Ji, Z.-Y. Qiao, H. Wang, Near-Infrared Laser-Driven in Situ Self-Assembly as a General Strategy for Deep Tumor Therapy, *Nano Lett.* 18 (2018) 6577–6584, <https://doi.org/10.1021/acs.nanolett.8b03174>.
- [349] D.-B. Cheng, X.-H. Zhang, Y. Chen, H. Chen, Z.-Y. Qiao, H. Wang, Ultrasound-Activated Cascade Effect for Synergistic Orthotopic Pancreatic Cancer Therapy, *Iscience.* 23 (2020), 101144, <https://doi.org/10.1016/j.isci.2020.101144>.
- [350] E. Granger, G. McNee, V. Allan, P. Woodman, The role of the cytoskeleton and molecular motors in endosomal dynamics, *Semin. Cell Dev. Biol.* 31 (2014) 20–29, <https://doi.org/10.1016/j.semcdb.2014.04.011>.
- [351] Y. Yuan, P. Raj, J. Zhang, S. Siddhanta, I. Barman, J.W.M. Bulte, Furin-Mediated Self-Assembly of Olsalazine Nanoparticles for Targeted Raman Imaging of Tumors, *Angew. Chemie Int. Ed.* 60 (2021) 3923–3927, <https://doi.org/10.1002/anie.202014839>.
- [352] D. Wang, D.-B. Cheng, L. Ji, L.-J. Niu, X.-H. Zhang, Y. Cong, R.-H. Cao, L. Zhou, F. Bai, Z.-Y. Qiao, H. Wang, Precise magnetic resonance imaging-guided sonodynamic therapy for drug-resistant bacterial deep infection, *Biomaterials.* 264 (2021), 120386, <https://doi.org/10.1016/j.biomaterials.2020.120386>.
- [353] L.-J. Luo, X.-M. Liu, X. Zhang, J. Liu, Y. Gao, T.-Y. Sun, L.-L. Li, Quantitative Detection of In Vivo Aggregation Degree for Enhanced M2 Macrophage MR Imaging, *Nano Lett.* 22 (2022) 1694–1702, <https://doi.org/10.1021/acs.nanolett.1c04711>.
- [354] X. Jin, Y. Fei, J. Ma, L.-L. Li, H. Wang, Photoacoustic probe of targeting intracellular *Staphylococcus aureus* infection with signal-enhanced by self-assembly, *Methods Enzymol.* (2021) 331–347, <https://doi.org/10.1016/bs.mie.2021.06.027>.
- [355] N.-Y. Zhang, X.-J. Hu, H.-W. An, J.-X. Liang, H. Wang, Programmable design and self assembly of peptide conjugated AIEngens for biomedical applications, *Biomaterials.* 287 (2022), 121655, <https://doi.org/10.1016/j.biomaterials.2022.121655>.
- [356] X. Zhao, L. Li, Y. Zhao, H. An, Q. Cai, J. Lang, X. Han, B. Peng, Y. Fei, H. Liu, H. Qin, G. Nie, H. Wang, In Situ Self-Assembled Nanofibers Precisely Target Cancer-Associated Fibroblasts for Improved Tumor Imaging, *Angew. Chemie Int. Ed.* 58 (2019) 15287–15294, <https://doi.org/10.1002/anie.201908185>.
- [357] H. Ren, X.-Z. Zeng, X.-X. Zhao, D. Hou, H. Yao, M. Yaseen, L. Zhao, W. Xu, H. Wang, L.-L. Li, A bioactivated in vivo assembly nanotechnology fabricated NIR probe for small pancreatic tumor intraoperative imaging, *Nat. Commun.* 13 (2022) 418, <https://doi.org/10.1038/s41467-021-27932-y>.
- [358] Z. Wang, C. Zhao, Y. Li, J. Wang, D. Hou, L. Wang, Y. Wang, X. Wang, X. Liu, H. Wang, W. Xu, Photostable Cascade Activatable Peptide Self-assembly on a Cancer Cell Membrane for High-Performance Identification of Human Bladder Cancer, *Adv. Mater.* 2210732 (2023) 1–9, <https://doi.org/10.1002/adma.202210732>.
- [359] Y. Zhong, J. Zhan, G. Xu, Y. Chen, Q. Qin, X. Liao, S. Ma, Z. Yang, Y. Cai, Enzyme-Instructed Self-Assembly Enabled Monomer-Excimer Transition to Construct Higher Ordered Luminescent Supramolecular Assembly for Activity-based Bioimaging, *Angew. Chemie Int. Ed.* 60 (2021) 8121–8129, <https://doi.org/10.1002/anie.202014278>.
- [360] D. Ye, A.J. Shuhendler, L. Cui, L. Tong, S.S. Tee, G. Tikhomirov, D.W. Felsher, J. Rao, Biosoorthogonal cyclization-mediated in situ self-assembly of small-molecule probes for imaging caspase activity in vivo, *Nat. Chem.* 6 (2014) 519–526, <https://doi.org/10.1038/nchem.1920>.
- [361] F.-K. Zhan, J.-C. Liu, B. Cheng, Y.-C. Liu, T.-S. Lai, H.-C. Lin, M.-Y. Yeh, Tumor targeting with DGEA peptide ligands: a new aromatic peptide amphiphile for imaging cancers, *Chem. Commun.* 55 (2019) 1060–1063, <https://doi.org/10.1039/C8CC08679F>.
- [362] S. Lu, X. Guo, F. Zhang, X. Li, M. Zou, L.-L. Li, Bioactivated in vivo assembly (BIVA) peptide-tetraphenylethylene (TPE) probe with controllable assembled nanostructure for cell imaging, *Chinese Chem. Lett.* 32 (2021) 1947–1952, <https://doi.org/10.1016/j.cclet.2021.01.007>.
- [363] Q. Cai, Y. Fei, L. Hu, Z. Huang, L.-L. Li, H. Wang, Chemotaxis-Instructed Intracellular *Staphylococcus aureus* Infection Detection by a Targeting and Self-Assembly Signal-Enhanced Photoacoustic Probe, *Nano Lett.* 18 (2018) 6229–6236, <https://doi.org/10.1021/acs.nanolett.8b02286>.
- [364] L.-L. Li, H.-L. Ma, G.-B. Qi, D. Zhang, F. Yu, Z. Hu, H. Wang, Pathological-Condition-Driven Construction of Supramolecular Nanoassemblies for Bacterial Infection Detection, *Adv. Mater.* 28 (2016) 254–262, <https://doi.org/10.1002/adma.201503437>.
- [365] X. Zhang, C. Ren, F. Hu, Y. Gao, Z. Wang, H. Li, J. Liu, B. Liu, C. Yang, Detection of Bacterial Alkaline Phosphatase Activity by Enzymatic In Situ Self-Assembly of the AIEngen-Peptide Conjugate, *Anal. Chem.* 92 (2020) 5185–5190, <https://doi.org/10.1021/acs.analchem.9b05704>.
- [366] L. Zhang, Y. Li, G. Mu, L. Yang, C. Ren, Z. Wang, Q. Guo, J. Liu, C. Yang, Structure of Self-assembled Peptide Determines the Activity of Aggregation-Induced Emission Luminogen-Peptide Conjugate for Detecting Alkaline Phosphatase, *Anal. Chem.* 94 (2022) 2236–2243, <https://doi.org/10.1021/acs.analchem.1c04936>.
- [367] M.T. Jeena, L. Palanikumar, E.M. Go, I. Kim, M.G. Kang, S. Lee, S. Park, H. Choi, C. Kim, S.-M. Jin, S.C. Bae, H.W. Rhee, E. Lee, S.K. Kwak, J.-H. Ryu, Mitochondria localization induced self-assembly of peptide amphiphiles for cellular dysfunction, *Nat. Commun.* 8 (2017) 26, <https://doi.org/10.1038/s41467-017-00047-z>.
- [368] M. Sun, C. Wang, M. Lv, Z. Fan, J. Du, Intracellular Self-Assembly of Peptides to Induce Apoptosis against Drug-Resistant Melanoma, *J. Am. Chem. Soc.* 144 (2022) 7337–7345, <https://doi.org/10.1021/jacs.2c00697>.
- [369] X. Liu, W. Zhan, G. Gao, Q. Jiang, X. Zhang, H. Zhang, X. Sun, W. Han, F.-G. Wu, G. Liang, Apoptosis-Amplified Assembly of Porphyrin Nanofiber Enhances Photodynamic Therapy of Oral Tumor, *J. Am. Chem. Soc.* 145 (2023) 7918–7930, <https://doi.org/10.1021/jacs.2c13189>.
- [370] Q.-L. Zhang, D. Zheng, X. Dong, P. Pan, S.-M. Zeng, F. Gao, S.-X. Cheng, X.-Z. Zhang, A Strategy Based on the Enzyme-Catalyzed Polymerization Reaction of Asp-Phe-Tyr Tripeptide for Cancer Immunotherapy, *J. Am. Chem. Soc.* 143 (2021) 5127–5140, <https://doi.org/10.1021/jacs.1c00945>.
- [371] M. Di Wang, G.T. Lv, H.W. An, N.Y. Zhang, H. Wang, In Situ Self-Assembly of Bispecific Peptide for Cancer Immunotherapy, *Angew. Chemie - Int. Ed.* 61 (2022) 1–7, <https://doi.org/10.1002/anie.202113649>.
- [372] Y. Wang, X. Li, D. Zheng, Y. Chen, Z. Zhang, Z. Yang, Selective Degradation of PD-L1 in Cancer Cells by Enzyme-Instructed Self-Assembly, *Adv. Funct. Mater.* 31 (2021) 2102505, <https://doi.org/10.1002/adfm.202102505>.

- [373] Y. Gao, J. Gao, G. Mu, Y. Zhang, F. Huang, W. Zhang, C. Ren, C. Yang, J. Liu, Selectively enhancing radiosensitivity of cancer cells via *in situ* enzyme-instructed peptide self-assembly, *Acta Pharm. Sin. B* 10 (2020) 2374–2383, <https://doi.org/10.1016/j.apsb.2020.07.022>.
- [374] Z. Wang, H.-W. An, D. Hou, M. Wang, X. Zeng, R. Zheng, L. Wang, K. Wang, H. Wang, W. Xu, Addressable Peptide Self-Assembly on the Cancer Cell Membrane for Sensitizing Chemotherapy of Renal Cell Carcinoma, *Adv. Mater.* 31 (2019) 1807175, <https://doi.org/10.1002/adma.201807175>.
- [375] J. Chen, P. Zhang, Y. Zhao, J. Zhao, X. Wu, R. Zhang, R. Cha, Q. Yao, Y. Gao, Nitroreductase-instructed supramolecular assemblies for microbiome regulation to enhance colorectal cancer treatments, *Sci. Adv.* 8 (2022) eadd2789, <https://doi.org/10.1126/sciadv.add2789>.
- [376] W. Zhan, G. Gao, Z. Liu, X. Liu, L. Xu, M. Wang, H.D. Xu, R. Tang, J. Cao, X. Sun, G. Liang, Enzymatic Self-Assembly of Adamantane-Peptide Conjugate for Combating Staphylococcus aureus Infection, *Adv. Healthc. Mater.* 2203283 (2023) 1–8, <https://doi.org/10.1002/adhm.202203283>.
- [377] Z. Yang, G. Liang, Z. Guo, B. Xu, Intracellular Hydrogelation of Small Molecules Inhibits Bacterial Growth, *Angew. Chemie Int. Ed.* 46 (2007) 8216–8219, <https://doi.org/10.1002/anie.200701697>.
- [378] X.-Y. Zhang, C. Liu, P.-S. Fan, X.-H. Zhang, D.-Y. Hou, J.-Q. Wang, H. Yang, H. Wang, Z.-Y. Qiao, Skin-like wound dressings with on-demand administration based on *in situ* peptide self-assembly for skin regeneration, *J. Mater. Chem. B* 10 (2022) 3624–3636, <https://doi.org/10.1039/D2TB00348A>.
- [379] R. Teng, Y. Yang, Z. Zhang, K. Yang, M. Sun, C. Li, Z. Fan, J. Du, *In Situ* Enzyme-Induced Self-Assembly of Antimicrobial-Antioxidative Peptides to Promote Wound Healing, *Adv. Funct. Mater.* 33 (2023) 2214454, <https://doi.org/10.1002/adfm.202214454>.
- [380] C. Yang, F. Hu, X. Zhang, C. Ren, F. Huang, J. Liu, Y. Zhang, L. Yang, Y. Gao, B. Liu, J. Liu, Combating bacterial infection by *in situ* self-assembly of AIEgen-peptide conjugate, *Biomaterials*. 244 (2020), 119972, <https://doi.org/10.1016/j.biomaterials.2020.119972>.
- [381] H.-W. An, D. Hou, R. Zheng, M.-D. Wang, X.-Z. Zeng, W.-Y. Xiao, T.-D. Yan, J.-Q. Wang, C.-H. Zhao, L.-M. Cheng, J.-M. Zhang, L. Wang, Z.-Q. Wang, H. Wang, W. Xu, A Near-Infrared Peptide Probe with Tumor-Specific Excretion-Retarded Effect for Image-Guided Surgery of Renal Cell Carcinoma, *ACS Nano*. 14 (2020) 927–936, <https://doi.org/10.1021/acsnano.9b08209>.
- [382] J. Gao, J. Li, D. Wei, H. Yang, Y. Duan, Y. Zhang, X. Gong, H. Wang, D. Ding, X. Wu, J. Chang, Enabling AIEgens close assembly in tumor-overexpressed protein cluster for boosted image-guided cancer surgery, *Sci. China Chem.* 63 (2020) 1694–1702, <https://doi.org/10.1007/s11426-020-9829-x>.
- [383] X. Wen, R. Zhang, Y. Hu, L. Wu, H. Bai, D. Song, Y. Wang, R. An, J. Weng, S. Zhang, R. Wang, L. Qiu, J. Lin, G. Gao, H. Liu, Z. Guo, D. Ye, Controlled sequential *in situ* self-assembly and disassembly of a fluorogenic cisplatin prodrug for cancer theranostics, *Nat. Commun.* 14 (2023) 800, <https://doi.org/10.1038/s41467-023-36469-1>.
- [384] R. Zheng, J. Yang, M. Mamuti, D. Hou, H. An, Y. Zhao, H. Wang, Controllable Self-Assembly of Peptide-Cyanine Conjugates *In Vivo* as Fine-Tunable Theranostics, *Angew. Chemie Int. Ed.* 60 (2021) 7809–7819, <https://doi.org/10.1002/anie.202015126>.
- [385] A. Wang, Q. Mao, M. Zhao, S. Ye, J. Fang, C. Cui, Y. Zhao, Y. Zhang, Y. Zhang, F. Zhou, H. Shi, pH/Reduction Dual Stimuli-Triggered Self-Assembly of NIR Theranostic Probes for Enhanced Dual-Modal Imaging and Photothermal Therapy of Tumors, *Anal. Chem.* 92 (2020) 16113–16121, <https://doi.org/10.1021/acs.analchem.0c03800>.
- [386] L. Yang, R. Peltier, M. Zhang, D. Song, H. Huang, G. Chen, Y. Chen, F. Zhou, Q. Hao, L. Bian, M. He, Z. Wang, Y. Hu, H. Sun, Desuccinylation-Triggered Peptide Self-Assembly: Live Cell Imaging of SIRT5 Activity and Mitochondrial Activity Modulation, *J. Am. Chem. Soc.* 142 (2020) 18150–18159, <https://doi.org/10.1021/jacs.0c08463>.
- [387] W. Tan, Q. Zhang, J. Wang, M. Yi, H. He, B. Xu, Enzymatic Assemblies of Thiophosphopeptides Instantly Target Golgi Apparatus and Selectively Kill Cancer Cells, *Angew. Chemie Int. Ed.* 60 (2021) 12796–12801, <https://doi.org/10.1002/anie.202012601>.
- [388] X. Li, E.C. Montague, A. Pollinzi, A. Loftis, T. Hoare, Design of Smart Size-, Surface-, and Shape-Switching Nanoparticles to Improve Therapeutic Efficacy, *Small*. 18 (2022) 1–29, <https://doi.org/10.1002/smll.202104632>.
- [389] Y. Wang, W. Zhen, X. Jiang, J. Li, Driving Forces Sorted *In Situ* Size-Increasing Strategy for Enhanced Tumor Imaging and Therapy, *Small Sci.* 2 (2022) 2100117, <https://doi.org/10.1002/smll.202100117>.
- [390] W. Jia, Y. Wang, R. Liu, X. Yu, H. Gao, Shape Transformable Strategies for Drug Delivery, *Adv. Funct. Mater.* 31 (2021) 2009765, <https://doi.org/10.1002/adfm.202009765>.
- [391] Y. Qin, F. Tong, W. Zhang, Y. Zhou, S. He, R. Xie, T. Lei, Y. Wang, S. Peng, Z. Li, J. Leong, H. Gao, L. Lu, Self-Delivered Supramolecular Nanomedicine with Transformable Shape for Ferrocene-Amplified Photodynamic Therapy of Breast Cancer and Bone Metastases, *Adv. Funct. Mater.* 31 (2021) 2104645, <https://doi.org/10.1002/adfm.202104645>.
- [392] M. Li, Z. Wang, X. Liu, N. Song, Y. Song, X. Shi, J. Liu, J. Liu, Z. Yu, Adaptable peptide-based therapeutics modulating tumor microenvironment for combinatorial radio-immunotherapy, *J. Control. Release*. 340 (2021) 35–47, <https://doi.org/10.1016/j.jconrel.2021.10.026>.
- [393] J. Yang, R. Zheng, M. Mamuti, D.-Y. Hou, Y.-D. Zhao, H.-W. An, H. Wang, Y. Zhao, Oncolytic peptide nanomachine circumvents chemo resistance of renal cell carcinoma, *Biomaterials*. 284 (2022), 121488, <https://doi.org/10.1016/j.biomaterials.2022.121488>.
- [394] K. Han, J. Zhang, W. Zhang, S. Wang, L. Xu, C. Zhang, X. Zhang, H. Han, Tumor-Triggered Geometrical Shape Switch of Chimeric Peptide for Enhanced *In Vivo* Tumor Internalization and Photodynamic Therapy, *ACS Nano*. 11 (2017) 3178–3188, <https://doi.org/10.1021/acsnano.7b00216>.
- [395] B. Sun, R. Chang, S. Cao, C. Yuan, L. Zhao, H. Yang, J. Li, X. Yan, J.C.M. Hest, Acid-Activatable Transmorphic Peptide-Based Nanomaterials for Photodynamic Therapy, *Angew. Chemie Int. Ed.* 59 (2020) 20582–20588, <https://doi.org/10.1002/anie.202008708>.
- [396] B. Sun, X. Guo, M. Feng, S. Cao, H. Yang, H. Wu, M.H.M.E. van Stevendaal, R.A.J. F. Oerlemans, J. Liang, Y. Ouyang, J.C.M. van Hest, Responsive Peptide Nanofibers with Theranostic and Prognostic Capacity, *Angew. Chemie Int. Ed.* 61 (2022) e202208732.
- [397] M. Li, Y. Ning, J. Chen, X. Duan, N. Song, D. Ding, X. Su, Z. Yu, Proline Isomerization-Regulated Tumor Microenvironment-Adaptable Self-Assembly of Peptides for Enhanced Therapeutic Efficacy, *Nano Lett.* 19 (2019) 7965–7976, <https://doi.org/10.1021/acs.nanolett.9b03136>.
- [398] Z. Cheng, Y. Cheng, Q. Chen, M. Li, J. Wang, H. Liu, M. Li, Y. Ning, Z. Yu, Y. Wang, H. Wang, Self-assembly of pentapeptides into morphology-adaptable nanomedicines for enhanced combinatorial chemo-photodynamic therapy, *Nano Today*. 33 (2020), 100878, <https://doi.org/10.1016/j.nantod.2020.100878>.
- [399] B. Jana, S. Jin, E.M. Go, Y. Cho, D. Kim, S. Kim, S.K. Kwak, J.-H. Ryu, Intralysosomal Peptide Assembly for the High Selectivity Index against Cancer, *J. Am. Chem. Soc.* 145 (2023) 18414–18431, <https://doi.org/10.1021/jacs.3c04467>.
- [400] Z. Gong, B. Zhou, X. Liu, J. Cao, Z. Hong, J. Wang, X. Sun, X. Yuan, H. Tan, H. Ji, J. Bai, Enzyme-Induced Transformable Peptide Nanocarriers with Enhanced Drug Permeability and Retention to Improve Tumor Nanotherapy Efficacy, *ACS Appl. Mater. Interfaces*. 13 (2021) 55913–55927, <https://doi.org/10.1021/acsmami.1c17917>.
- [401] T. Wang, Z. He, C.-S. Yuan, Z.-W. Deng, F. Li, X.-G. Chen, Y. Liu, MMP-responsive transformation nanomaterials with IAP antagonist to boost immune checkpoint therapy, *J. Control. Release*. 343 (2022) 765–776, <https://doi.org/10.1016/j.jconrel.2022.02.018>.
- [402] L. Wang, B. Fu, D.Y. Hou, Y.L. Lv, G. Yang, C. Li, J.C. Shen, B. Kong, L.B. Zheng, Y. Qiu, H.L. Wang, C. Liu, J.J. Zhang, S.Y. Bai, L.L. Li, H. Wang, W.H. Xu, PKM2 allosteric converter: A self-assembly peptide for suppressing renal cell carcinoma and sensitizing chemotherapy, *Biomaterials*. 296 (2023), 122060, <https://doi.org/10.1016/j.biomaterials.2023.122060>.
- [403] Y. Sun, B. Lyu, C. Yang, B. He, H. Zhang, X. Wang, Q. Zhang, W. Dai, An enzyme-responsive and transformable PD-L1 blocking peptide-photosensitizer conjugate enables efficient photothermal immunotherapy for breast cancer, *Bioact. Mater.* 22 (2023) 47–59, <https://doi.org/10.1016/j.bioactmat.2022.08.020>.
- [404] J. Cao, X. Liu, X. Yuan, F. Meng, X. Sun, L. Xu, H. Li, Y. Liu, Z. Hong, J. Bai, Enzyme-induced morphological transformation of self-assembled peptide nanovehicles potentiates intratumoral aggregation and inhibits tumour immunosuppression, *Chem. Eng. J.* 454 (2023), 140466, <https://doi.org/10.1016/j.cej.2022.140466>.
- [405] J. Cao, X. Yuan, X. Sun, F. Meng, H. Li, Z. Hong, Y. Liu, X. Zhai, J. Ma, S. Peng, Y. Zhou, X. Liu, J. Hao, J. Bai, Matrix Metalloproteinase-2-Induced Morphologic Transformation of Self-Assembled Peptide Nanocarriers Inhibits Tumor Growth and Metastasis, *ACS Mater. Lett.* 5 (2023) 900–908, <https://doi.org/10.1021/acsmaterialslett.2c01093>.
- [406] D.-B. Cheng, D. Wang, Y.-J. Gao, L. Wang, Z.-Y. Qiao, H. Wang, Autocatalytic Morphology Transformation Platform for Targeted Drug Accumulation, *J. Am. Chem. Soc.* 141 (2019) 4406–4414, <https://doi.org/10.1021/jacs.8b13512>.
- [407] D. Cheng, X. Zhang, Y. Gao, D. Wang, L. Wang, H. Chen, Z. Qiao, H. Wang, Site-Specific Construction of Long-Term Drug Depot for Suppression of Tumor Recurrence, *Small*. 15 (2019) 1901813, <https://doi.org/10.1002/smll.201901813>.
- [408] W.H. Chen, G.F. Luo, W.X. Qiu, Q. Lei, L.H. Liu, D.W. Zheng, S. Hong, S.X. Cheng, X.Z. Zhang, Tumor-Triggered Drug Release with Tumor-Targeted Accumulation and Elevated Drug Retention to Overcome Multidrug Resistance, *Chem. Mater.* 28 (2016) 6742–6752, <https://doi.org/10.1021/acs.chemmater.6b03236>.
- [409] C. Zhang, L.-H. Liu, W.-X. Qiu, Y.-H. Zhang, W. Song, L. Zhang, S.-B. Wang, X.-Z. Zhang, A Transformable Chimeric Peptide for Cell Encapsulation to Overcome Multidrug Resistance, *Small*. 14 (2018) 1703321, <https://doi.org/10.1002/smll.201703321>.
- [410] Q. Wang, H. Cao, X. Hou, D. Wang, Z. Wang, Y. Shang, S. Zhang, J. Liu, C. Ren, J. Liu, Cancer Stem-like Cells-Oriented Surface Self-Assembly to Conquer Radioresistance, *Adv. Mater.* 2302916 (2023) 1–13, <https://doi.org/10.1002/adma.202302916>.
- [411] H. He, J. Wang, H. Wang, N. Zhou, D. Yang, D.R. Green, B. Xu, Enzymatic Cleavage of Branched Peptides for Targeting Mitochondria, *J. Am. Chem. Soc.* 140 (2018) 1215–1218, <https://doi.org/10.1021/jacs.7b11582>.
- [412] B. Hu, N. Song, Y. Cao, M. Li, X. Liu, Z. Zhou, L. Shi, Z. Yu, Noncanonical Amino Acids for Hypoxia-Responsive Peptide Self-Assembly and Fluorescence, *J. Am. Chem. Soc.* 143 (2021) 13854–13864, <https://doi.org/10.1021/jacs.1c06435>.
- [413] P.-P. He, X.-D. Li, J.-Q. Fan, Y. Fan, P.-P. Yang, B.-N. Li, Y. Cong, C. Yang, K. Zhang, Z.-Q. Wang, D.-Y. Hou, H. Wang, L. Wang, Live Cells Process Exogenous Peptide as Fibronectin Fibrillogenesis *In Vivo*, *CCS Chem.* 2 (2020) 539–554, <https://doi.org/10.31635/ccschem.020.201900117>.
- [414] X.-X. Hu, P.-P. He, G.-B. Qi, Y.-J. Gao, Y.-X. Lin, C. Yang, P.-P. Yang, H. Hao, L. Wang, H. Wang, Transformable Nanomaterials as an Artificial Extracellular Matrix for Inhibiting Tumor Invasion and Metastasis, *ACS Nano*. 11 (2017) 4086–4096, <https://doi.org/10.1021/acsnano.7b00781>.
- [415] J.-Q. Fan, Y.-J. Li, Z.-J. Wei, Y. Fan, X.-D. Li, Z.-M. Chen, D.-Y. Hou, W.-Y. Xiao, M.-R. Ding, H. Wang, L. Wang, Binding-Induced Fibrillogenesis Peptides

- Recognize and Block Intracellular Vimentin Skeletonization against Breast Cancer, *Nano Lett.* 21 (2021) 6202–6210, <https://doi.org/10.1021/acs.nanolett.1c01950>.
- [416] L. Wang, Y. Lv, C. Li, G. Yang, B. Fu, Q. Peng, L. Jian, D. Hou, J. Wang, C. Zhao, P. Yang, K. Zhang, L. Wang, Z. Wang, H. Wang, W. Xu, Transformable Dual-Inhibition System Effectively Suppresses Renal Cancer Metastasis through Blocking Endothelial Cells and Cancer Stem Cells, *Small.* 16 (2020) 2004548, <https://doi.org/10.1002/smll.202004548>.
- [417] J. Fan, Y. Fan, Z. Wei, Y. Li, X. Li, L. Wang, H. Wang, Transformable peptide nanoparticles inhibit the migration of N-cadherin overexpressed cancer cells, *Chinese Chem. Lett.* 31 (2020) 1787–1791, <https://doi.org/10.1016/j.cclet.2020.03.065>.
- [418] Z. Chen, K. Zhang, J. Fan, Y. Fan, C. Yang, W. Tian, Y. Li, W. Li, J. Zhang, H. Wang, L. Wang, In situ construction of ligand nano-network to integrin $\alpha v\beta 3$ for angiogenesis inhibition, *Chinese Chem. Lett.* 31 (2020) 3107–3112, <https://doi.org/10.1016/j.cclet.2020.04.006>.
- [419] S. Wen, K. Zhang, Y. Li, J. Fan, C. Ziming, J. Zhang, H. Wang, L. Wang, A self-assembling peptide targeting VEGF receptors to inhibit angiogenesis, *Chinese Chem. Lett.* 31 (2020) 3153–3157, <https://doi.org/10.1016/j.cclet.2020.03.077>.
- [420] K. Zhang, P.-P. Yang, P.-P. He, S.-F. Wen, X.-R. Zou, Y. Fan, Z.-M. Chen, H. Cao, Z. Yang, K. Yue, X. Zhang, H. Zhang, L. Wang, H. Wang, Peptide-Based Nanoparticles Mimic Fibrillogenesis of Laminin in Tumor Vessels for Precise Embolization, *ACS Nano.* 14 (2020) 7170–7180, <https://doi.org/10.1021/acsnano.0c02110>.
- [421] L. Zhang, D. Jing, N. Jiang, T. Rojalin, C.M. Baehr, D. Zhang, W. Xiao, Y. Wu, Z. Cong, J.J. Li, Y. Li, L. Wang, K.S. Lam, Transformable peptide nanoparticles arrest HER2 signalling and cause cancer cell death in vivo, *Nat. Nanotechnol.* 15 (2020) 145–153, <https://doi.org/10.1038/s41565-019-0626-4>.
- [422] L. Wang, C. Li, J. Wang, G. Yang, Y. Lv, B. Fu, L. Jian, J. Ma, J. Yu, Z. Yang, P. Wu, G. Li, X. Liu, Z. Kang, Z. Wang, L. Wang, H. Wang, W. Xu, Transformable ECM Deprivation System Effectively Suppresses Renal Cell Carcinoma by Reversing Anoikis Resistance and Increasing Chemotherapy Sensitivity, *Adv. Mater.* 34 (2022) 2203518, <https://doi.org/10.1002/adma.202203518>.
- [423] K. Zhang, H. Zhang, X.-R. Zou, Y. Hu, D.-Y. Hou, J.-Q. Fan, C. Yang, Z.-M. Chen, S.-F. Wen, H. Cao, P.-P. Yang, L. Wang, An antibody-like peptidic network for anti-angiogenesis, *Biomaterials.* 275 (2021), 120900, <https://doi.org/10.1016/j.biomaterials.2021.120900>.
- [424] K. Zhang, H. Zhang, Y.-H. Gao, J.-Q. Wang, Y. Li, H. Cao, Y. Hu, L. Wang, A Monotargeting Peptidic Network Antibody Inhibits More Receptors for Anti-Angiogenesis, *ACS Nano.* 15 (2021) 13065–13076, <https://doi.org/10.1021/acsnano.1c02194>.
- [425] P.-P. Yang, K. Zhang, P.-P. He, Y. Fan, X.J. Gao, X. Gao, Z.-M. Chen, D.-Y. Hou, Y. Li, Y. Yi, D.-B. Cheng, J.-P. Zhang, L. Shi, X.-Z. Zhang, L. Wang, H. Wang, A biomimetic platelet based on assembling peptides initiates artificial coagulation, *Sci. Adv.* 6 (2020) eaaz4107, <https://doi.org/10.1126/sciadv.aaz4107>.
- [426] D.-B. Cheng, X.-H. Zhang, Y.-J. Gao, L. Ji, D. Hou, Z. Wang, W. Xu, Z.-Y. Qiao, H. Wang, Endogenous Reactive Oxygen Species-Triggered Morphology Transformation for Enhanced Cooperative Interaction with Mitochondria, *J. Am. Chem. Soc.* 141 (2019) 7235–7239, <https://doi.org/10.1021/jacs.8b07727>.
- [427] N. Song, Z. Zhou, Y. Song, M. Li, X. Yu, B. Hu, Z. Yu, In situ oxidation-regulated self-assembly of peptides into transformable scaffolds for cascade therapy, *Nano Today.* 38 (2021), 101198, <https://doi.org/10.1016/j.nantod.2021.101198>.
- [428] S. Sun, H.-W. Liang, H. Wang, Q. Zou, Light-Triggered Self-Assembly of Peptide Nanoparticles into Nanofibers in Living Cells through Molecular Conformation Changes and H-Bond Interactions, *ACS Nano.* 16 (2022) 18978–18989, <https://doi.org/10.1021/acsnano.2c07895>.
- [429] X.-H. Zhang, D.-B. Cheng, L. Ji, H.-W. An, D. Wang, Z.-X. Yang, H. Chen, Z.-Y. Qiao, H. Wang, Photothermal-Promoted Morphology Transformation in Vivo Monitored by Photoacoustic Imaging, *Nano Lett.* 20 (2020) 1286–1295, <https://doi.org/10.1021/acsnano.9b04752>.
- [430] Z. Wang, C. Yang, H. Zhang, Y. Gao, M. Xiao, Z. Wang, L. Yang, J. Zhang, C. Ren, J. Liu, In Situ Transformable Supramolecular Nanomedicine Targeted Activating Hippo Pathway for Triple-Negative Breast Cancer Growth and Metastasis Inhibition, *ACS Nano.* 16 (2022) 14644–14657, <https://doi.org/10.1021/acsnano.2c05263>.
- [431] G.-B. Qi, D. Zhang, F.-H. Liu, Z.-Y. Qiao, H. Wang, An “On-Site Transformation” Strategy for Treatment of Bacterial Infection, *Adv. Mater.* 29 (2017) 1703461, <https://doi.org/10.1002/adma.201703461>.
- [432] Q.-H. Yu, R. Huang, K.-Y. Wu, X.-L. Han, Y.-J. Cheng, W.-L. Liu, A.-Q. Zhang, S.-Y. Qin, Infection-activated lipopeptide nanotherapeutics with adaptable geometrical morphology for in vivo bacterial ablation, *Acta Biomater.* 154 (2022) 359–373, <https://doi.org/10.1016/j.actbio.2022.09.067>.
- [433] P. Tan, C. Wu, Q. Tang, T. Wang, C. Zhou, Y. Ding, H. Fu, S. Xu, Y. Feng, Y. Zhang, Q. Dai, X. Ma, pH-Triggered Size-Transformable and Bioactivity-Switchable Self-Assembling Chimeric Peptide Nanoassemblies for Combating Drug-Resistant Bacteria and Biofilms, *Adv. Mater.* 2210766 (2023) 1–16, <https://doi.org/10.1002/adma.202210766>.
- [434] Y. Fan, X.D. Li, P.P. He, X.X. Hu, K. Zhang, J.Q. Fan, P.P. Yang, H.Y. Zheng, W. Tian, Z.M. Chen, L. Ji, H. Wang, L. Wang, A biomimetic peptide recognizes and traps bacteria in vivo as human defensin-6, *Sci. Adv.* 6 (2020) eaaz4767, <https://doi.org/10.1126/sciadv.aaz4767>.
- [435] M.-R. Ding, Q.-L. Liang, H.-G. Xu, X.-D. Li, K. Zhang, Z.-J. Wei, Y.-H. Gao, Q.-S. Zhang, R. Huang, H. Yang, L. Wang, H. Wang, Smart Peptide Defense Web In Situ Connects for Continuous Interception of IgE against Allergic Rhinitis, *ACS Appl. Mater. Interfaces.* 14 (2022) 29639–29649, <https://doi.org/10.1021/acsmami.2c07092>.
- [436] Y. Song, M. Li, N. Song, X. Liu, G. Wu, H. Zhou, J. Long, L. Shi, Z. Yu, Self-Amplifying Assembly of Peptides in Macrophages for Enhanced Inflammatory Treatment, *J. Am. Chem. Soc.* 144 (2022) 6907–6917, <https://doi.org/10.1021/jacs.2c01323>.
- [437] Y. Cheng, A.E. Clark, J. Zhou, T. He, Y. Li, R.M. Borum, M.N. Creyer, M. Xu, Z. Jin, J. Zhou, W. Yim, Z. Wu, P. Fajtová, A.J. O'Donoghue, A.F. Carlin, J. V. Jokerst, Protease-Responsive Peptide-Conjugated Mitochondrial-Targeting AIEgens for Selective Imaging and Inhibition of SARS-CoV-2-Infected Cells, *ACS Nano.* 16 (2022) 12305–12317, <https://doi.org/10.1021/acsnano.2c03219>.